

NIST Technical Note 1455-1
February 2008 Revision

Performance of Home Smoke Alarms Analysis of the Response of Several Available Technologies in Residential Fire Settings

Richard W. Bukowski
Richard D. Peacock
Jason D. Averill
Thomas G. Cleary
Nelson P. Bryner
William D. Walton
Paul A. Reneke
Erica D. Kuligowski

Performance of Home Smoke Alarms

Analysis of the Response of Several Available Technologies in Residential Fire Settings

Richard W. Bukowski
Richard D. Peacock
Jason D. Averill
Thomas G. Cleary
Nelson P. Bryner
William D. Walton
Paul A. Reneke
Erica D. Kuligowski

*Fire Research Division
Building and Fire Research Laboratory*

February 2008



U.S. Department of Commerce
Donald L. Evans, Secretary

Technology Administration
Phillip J. Bond, Under Secretary for Technology

National Institute of Standards and Technology
Arden L. Bement, Jr., Director

Certain commercial entities, equipment, or materials may be identified in this document in order to describe an experimental procedure or concept adequately. Such identification is not intended to imply recommendation or endorsement by the National Institute of Standards and Technology, nor is it intended to imply that the entities, materials, or equipment are necessarily the best available for the purpose.

The policy of the National Institute of Standards and Technology is to use metric units of measurement in all its publications. In this document intended for the construction and building materials industries, however, in North America certain non-metric units are so widely used instead of metric units that it is more practical and less confusing to include certain measurement values in customary units only.

**National Institute of Standards and Technology Technical Note 1455-1
Natl. Inst. Stand. Technol. Tech. Note 1455-1, 396 pages (February 2008)
CODEN: NSPUE2**

U.S. GOVERNMENT PRINTING OFFICE
WASHINGTON: 2008

For sale by the Superintendent of Documents, U.S. Government Printing Office
Internet: bookstore.gpo.gov — Phone: (202) 512-1800 — Fax: (202) 512-2250
Mail: Stop SSOP, Washington, DC 20402-0001

Bibliographic Information

Abstract

This report presents the results of the project and provides details of the response of a range of residential smoke alarm technologies in a controlled laboratory test and in a series of real-scale tests conducted in two different residential structures. The data developed in this study include measurement of temperature and smoke obscuration in addition to gas concentrations for a range of fire scenarios and residences. The results are intended to provide both insight into siting and response characteristics of residential smoke alarms and a set of reference data for future enhancements to alarm technology based on fires from current materials and constructions.

Smoke alarms of either the ionization type or the photoelectric type consistently provide time for occupants to escape from most residential fires, although in some cases the escape time provided can be short. Consistent with prior findings, ionization type alarms provide somewhat better response to flaming fires than photoelectric alarms, and photoelectric alarms provide (often) considerably faster response to smoldering fires than ionization type alarms.

Escape times in this study were systematically shorter than those found in a similar study conducted in the 1970's. This is related to some combination of faster fire development times for today's products that provide the main fuel sources for fires, such as upholstered furniture and mattresses, different criteria for time to untenable conditions, and improved understanding of the speed and range of threats to tenability.

Keywords

detector sensitivity; fire tests; heat alarms; ionization alarms; photoelectric alarms; building fires; residential buildings; smoke alarms

Revision History

Since its initial publication in 2004, NIST TN 1455 has been scrutinized by fire research professionals and several inconsistencies have been identified. Analysis of noted inconsistencies has led to the identification of a number of errors in data and computations that impact the alarm performance assessment. These errors did not impact the major conclusions of the study. A description of each error and the corrective action taken for NIST Technical Note 1455-1 is given below.

- In earlier revisions of the report, the dual ion/photo alarms appeared to perform worse than individual photo or ion alarms because the dual-alarms were often located further from the fire source than the individual photo or ion alarms listed in tables 23, 24, 27 and 28. The affected tables and figures 206-208 have now been revised by removing the instances where a particular alarm type was not co-located. It is stressed that the individual alarm times reported in the appendix of the report have not been changed and remain available for direct comparison of the individual alarms and the dual ion/photo alarm in every case where these alarms were co-located. Specifically, the flaming chair fires in the two-story homes, test 28 was removed from the calculation of average alarm time for the dual or aspirated alarms since no alarms of these types were included in the test. For all other tests, alarm times for dual-alarms and aspirated alarms for placements other than every level were removed from the analysis since there were no alarms of these types co-located with individual ionization or photoelectric alarms. (February 2008)¹
- One disposable alarm in each of tests SDC10, SDC14, SDC22, and SDC28 was found to be connected with a reverse polarity. This caused the alarm time not to be properly recognized in the analysis. This has been corrected and resulted in a change to Tables 24 and 28. (February 2008)
- In the original report, the method NIST used to determine the detection time in the smoldering fire involving the 2-story house was in error. The results of the smoldering mattress test (test SDC 21) should not have been included in the analysis since the fire development did not allow enough alarms to respond by the time the test concluded. In addition, test SDC 14 was inadvertently excluded from the original analysis. Tables 11, 12, 23, 24, 27, 28, 30, and 32 were revised to correct these errors. (March 2006)
- Section 1.3.10 was corrected to define the format for the test data as comma-separated spreadsheet file. (November 2007).

¹Dates in parentheses indicate when the report was revised to correct the noted error.

- Table 11 was corrected to note that test SDC09 was conducted with the bedroom door closed. (November 2007)
- Appendix A Calculation of Times to Untenable Conditions. From test SDC30 to SDC41, the carbon monoxide (GASC_1) and carbon dioxide (GASC_3) data columns were switched for both ISO FED and NIST FED calculations. The corrective action was to switch the data columns to the proper position and recalculate the gas tenability values. Since tenability times for these tests are based on smoke obscuration (which occurred prior to reaching the gas tenability limit), no change in the report text resulted from this correction. (November 2007)
- Appendix A Calculated Alarm Times. From test SDC01 though SDC15, two sets of dual photo/ion alarms were not functioning properly and did not transmit alarms to the data acquisition system. They were subsequently coded as present but never reaching alarm. This had the effect of assignment of the end of test as a surrogate alarm time for each of the non-functioning alarms. The corrective action taken was the removal of all non-functioning dual photo/ion alarms from the Appendix A Calculated Alarm Times spreadsheets. Tables 13, 15, 21, 23, 24, 27, and 28 were revised. (November 2007)
- Gas analyzer concentrations. NIST Report of Test 4016, October 2001 and NIST Report of Test 4017, May 2002. Several carbon monoxide and carbon dioxide gas analyzers exhibited uncompensated baseline drifts that significantly impacted the gas species tenability limit calculations. The largest errors where observed in the first manufactured home test series (SDC01 -SDC15). The corrective action taken was to apply a baseline correction to all gas analyzers such that at the start of a test, carbon monoxide analyzers read zero, carbon dioxide read between 0.04 to 0.06 volume percent, and oxygen analyzers read 20.95 volume percent. After baseline adjustments, the times to untenable conditions in Appendix A were re-calculated. Tables 14, 27, and 28 were revised based on the re-calculated tenability times. (November 2007)
- Excessive gas analyzer noise - The following carbon monoxide gas analyzer data were excessively noisy indicating sampling or instrumentation malfunction:
 - SDC04 - GASA_1
 - SDC06 - GASA_1
 - SDC12 - GASA_1, GASC_1
 - SDC13 - GASC_1

The corrective action taken was that all of the excessively noisy gas data were not used in tenability calculations, thus the assessment of tenable conditions at these sampling locations is incomplete. Fortunately, there was always a gas sampling point closer to the fire that would be the likely location where the gas tenability limit would be reached first.

A single spurious data point was filtered out from SDC04 - GASC_1. Since tenability limits for these tests are based on smoke obscuration (which occurred prior to reaching the gas tenability limit), no change in the report text resulted from this correction. (November 2007)

- Smoke optical density meter drift - NIST Report of Test 4016, October 2001 and NIST Report of Test 4017, May 2002. The following smoke meter data were removed because of output signal drift that made the optical density measurement unreliable.

SDC01 - SMB_1, SMC_1, SMF_1
SDC02 - SME_4
SDC06 - SMD_4
SDC08 - SMD01
SDC11 - SMF_1
SDC34 - SMA_1
SDC35 - SMA_1
SDC37 - SMB_1, SMC_1
SDC38 - SMA_1
SDC41 - SMA_1

Only smoke meters SME_4 and SMD_4 affect the time to untenable conditions.

The corrective action taken was to re-calculate Appendix A Calculation of Times to Untenable Conditions. Tables 21, 27 and 28 were revised based on the re-calculated tenability times. (November 2007)

- The following smoke alarms were not functioning:

SDC09 - Pho1_B
SDC11 - Pho1_D
SDC36 - Ion1_C
SDC37 - Ion_1C
SDC38 - Ion_1C
SDC39 - Ion_1C
SDC41 - Ion1_D

This had the effect of assignment of the end of test as a surrogate alarm time for each of the non-functioning alarms. The corrective action taken was to remove these alarms from Appendix A Calculated Alarm Times. Tables 21, 23, 27, and 28 were revised based on the re-calculated tenability times. (November 2007)

- Appendix A Calculated Alarm Times. For tests SDC30, SDC31, SDC34, SDC35, and SDC41 location (E) was mislabeled as a bedroom. It should have been labeled as the living room. The corrective action taken was the proper label was assigned. Average time to alarm, and available egress times were updated and the values reported in tables 23 and 27 were corrected. (November 2007)
- Table 27 has been changed to reflect a correction of a rounding error and to add a footnote for the best-case scenario. (July 2004)

Contents

Revision History	v
Contents	ix
Figures and Tables	xiii
Executive Summary	xxiii
Acknowledgments	xxvii
1 Introduction	1
1.1 History	2
1.2 Concerns Raised	3
1.3 Organizing the Research Project	4
1.3.1 Evaluate the Performance of Current Smoke Alarm Technology	4
1.3.2 Test Conditions Representative of Current Fatal Residential Fires	5
1.3.3 Evaluate the Efficacy of Current Requirements for Number and Location of Smoke Alarms	6
1.3.4 Develop Standard Nuisance Alarm Sources to Be Included in the Test Program	7
1.3.5 Examine Other Fire Detection Technologies in Combination with Smoke Alarms	7
1.3.6 Obtain Data on the Potential for Improvements in Performance by New Technologies	8
1.3.7 Include Fuel Items That Incorporate Materials and Constructions Representative of Current Residential Furnishings	8
1.3.8 Fully Characterize Test Detectors and Alarms in a Consistent Manner to Facilitate Comparisons	8
1.3.9 Utilize Fire Models to Extend the Applicability of the Test Arrangements and Maximize the Test Instrumentation	8
1.3.10 Make All of the Data Collected as Widely Accessible as Possible	8
1.3.11 Provide Opportunities to Enhance Public Fire Safety Education	9
1.4 Project Oversight	9
2 Residential Fire Alarms, Sensor Response and Calibration in the FE/DE	11
2.1 Residential Alarms Included in the Study	11

2.2 The fire emulator/detector evaluator	12
2.3 Smoke Aerosols	14
2.4 Calibration of Smoke and CO alarms	18
2.5 Alarm Identification	24
2.6 Evaluation of Unmodified Alarm Response	28
2.7 Effect of Sensor Board Location on Response	47
2.8 Thresholds for Modified Alarms	62
3 Fire Source Test Scenarios and Geometries	65
3.1 Scenario Development	65
3.2 Material Selection	67
3.2.1 Upholstered Furniture	67
3.2.2 Mattress	69
3.2.3 Cooking Materials	69
3.3 Ignition Methodology	70
3.3.1 Flaming Ignition	70
3.3.2 Smoldering Ignition	71
3.3.3 Cooking Ignition	72
3.4 Test Geometry	72
3.4.1 Manufactured Home	72
3.4.2 Two-story Home	73
4 Fire Source Testing Instrumentation	77
4.1 Temperature	77
4.2 Sample Mass	82
4.3 Primary Gases – CO, CO ₂ , and O ₂	83
4.4 FTIR Gas Analysis	84
4.5 Optical Density	84
4.6 Smoke Properties	87
4.7 Smoke and CO Alarm Response	89
4.8 Sprinkler Response	90
4.9 Mechanical Heat Alarm Response	91
5 Fire Source Test Results and Calculations	93
5.1 Tests Conducted	93
5.2 Test Data	95
5.3 Calculation of Alarm Times	104
5.4 Calculation of Time to Untenable Conditions	119
5.4.1 Tenability Limits	119
5.4.2 Tenability Times	121
5.5 Assessment of Overall Alarm Performance	122
5.6 Aerosol Concentration and Size Measurements	124

5.6.1 Mass and Number Concentration	125
5.6.2 Particle Size Analysis	137
5.7 Measurement Uncertainty	147
6 Residential Smoke Alarm Nuisance Source Testing	149
6.1 Nuisance Scenario Tests	150
6.2 Instrumentation	150
6.2.1 Aerosol Instruments	151
6.2.2 Temperature and Humidity	153
6.2.3 Flow Velocity	153
6.2.4 Analog Output Photoelectric, Ionization and Sensors	154
6.3 Results	155
6.3.1 Toasting Scenarios	155
6.3.2 Frying Bacon	165
6.3.3 Frying Butter and Margarine	170
6.3.4 Frying Hamburgers	176
6.3.5 Deep-frying Tortillas and French-fried Potatoes	180
6.3.6 Broiled and Baked/Broiled Pizza	183
6.3.7 Broiling Hamburgers	187
6.3.8 Boiling Spaghetti Pasta	189
6.3.9 Candle Burning	193
6.3.10 Cigarette Smoking	194
6.4 Controlled Incipient Fire Sources	194
6.4.1 Cotton Smolder	195
6.4.2 Wood Smolder	199
6.4.3 Polyurethane Foam Smolder	201
6.5 FE/DE Emulation of Nuisance Sources	207
6.5.1 Cotton Wick Calibration	207
6.5.2 Cotton Smolder Smoke Fire Scenario	211
6.5.3 Wood Smolder Smoke Fire Scenario	211
6.5.4 Candle Flame Nuisance Scenario	220
6.5.5 Heated Margarine or Butter Nuisance Scenario	221
6.5.6 Toasting Bread Nuisance Scenario	221
7 Discussion	231
7.1 Smoke Alarm Activation Time	231
7.2 Tenability Times	236
7.3 Time Needed for Escape	236
7.3.1 Movement Speed	237
7.3.2 Premovement Activities	237
7.3.3 Escape Times	238
7.4 Smoke Alarm Performance	240

7.5 Other Alarm Technologies	246
7.5.1 Carbon Monoxide Alarms	247
7.5.2 Heat Alarms	247
7.5.3 Tell-tale Sprinklers	248
7.6 Comparison with Earlier Tests	248
7.7 Nuisance Alarms	251
8 Summary	253
9 Conclusions	259
10 References	261
Appendix A: Alarm Activation and Time to Untenable Conditions During Tests of Residential Smoke Alarms Included in the Study	A-1
Appendix B: FTIR Gas Measurement in Home Smoke Alarm Tests	B-1

Figures and Tables

Figures

Figure 1. Sample sensor test board used during tests of residential smoke alarms	11
Figure 2. Schematic of the FE/DE (all units in cm)	13
Figure 3. Propene smoke generator	14
Figure 4. Propene smoke calibration run	15
Figure 5. Smolder source, staged wick ignition device	15
Figure 6. Smolder smoke calibration run	16
Figure 7. Smolder smoke CO calibration run	16
Figure 8. UL grey smoke (smolder smoke) sensitivity limits and FE/DE data	17
Figure 9. UL black smoke sensitivity limits and corresponding FE/DE data	17
Figure 10. Alarm identification coding	24
Figure 11. Calibration runs for Ion-1 alarm	25
Figure 12. Calibration runs for Ion-3 alarm	25
Figure 13. Calibration runs for Ion-4 alarm	26
Figure 14. Calibration runs for Photo-1 alarm	26
Figure 15. Calibration runs for Photo-2 alarm	27
Figure 16. Calibration runs for ASP alarm	27
Figure 17. Calibration runs for CO alarms	28
Figure 18. Photo-1, eight wicks – 12 s delay, Disp 1 and Disp 7 alarms	30
Figure 19. Photo-1, 16 wicks – 12 s delay, Disp 1 and Disp 7 alarms	30
Figure 20. Photo-1, eight wicks – 12 s delay, Disp 1 and Disp 7 alarms	31
Figure 21. Photo-1, eight wicks – 30 s delay, Disp 4 and Disp 10 alarms	31
Figure 22. Photo-1, eight wicks – 12 s delay, Disp 37 and Disp 40 alarms	32
Figure 23. Photo-1, eight wicks, 12 s delay, Disp 46 and Disp 55 alarms	32
Figure 24. Photo-1, eight wicks – 12 s delay, Disp 52 and Disp 58 alarms	33
Figure 25. Photo-1, eight wicks – 12 s delay, Disp 61 and Disp 64 alarms	33
Figure 26. Photo-1, eight wicks – 12 s delay, Disp 10 and Disp 55 alarms	34
Figure 27. Photo-1, 16 wicks – 12 s delay, Disp 10 and Disp 55 alarms	34
Figure 28. Ion-1, three wicks - 30 s delay, Disp 11 and Disp 38 alarms	36
Figure 29. Ion-1, four wicks - 30 s delay, Disp 11 and Disp 38 alarms	36
Figure 30. Ion-1, four wicks - 30 s delay, Disp 2 and Disp 5 alarms	37
Figure 31. Ion-1, six wicks 12 s delay, Disp 2 and Disp 5 alarms	37
Figure 32. Ion-1, four wicks 30 s delay, Disp 8 and Disp 44 alarms	38
Figure 33. Ion-1, six wicks 12 s delay, Disp 8 and Disp 44 alarms	38
Figure 34. Ion-1, six wicks 12 s delay, Disp 41 and Disp 51 alarms	39
Figure 35. Ion-1, three wicks 12 s delay, Disp 53 and Disp 44 alarms	39
Figure 36. Ion-1, six wicks 12 s delay, Disp 60 and Disp 63 alarms	40

Figure 37. Ion-1, six wicks 12 s delay, Disp 57 and Disp 60 alarms	40
Figure 38. Ion-3, six wicks - 12 s delay, Disp 39 and Disp 48 alarms	41
Figure 39. Ion-3, four wicks - 30 s delay, Disp 39 and Disp 48 alarms	41
Figure 40. Ion-3, three wicks 30 s delay, Disp 39 and Disp 48 alarms	42
Figure 41. Ion-3, three wicks 30 s delay, Disp 39 and Disp 48 alarms	42
Figure 42. Ion-3, three wicks 30 s delay, Disp 3 and Disp 6 alarms	43
Figure 43. Ion-3, three wicks 30 s delay, Disp 9 and Disp 12 alarms	43
Figure 44. Ion-3, three wicks 30 s delay, Disp 30 and Disp 45 alarms	44
Figure 45. Ion-3, three wicks 30 s delay, Disp 54 and Disp 56 alarms	44
Figure 46. Ion-3, three wicks 30 s delay, Disp 59 and Disp 62 alarms	45
Figure 47. Ion-3, three wicks 30 s delay, Disp 53 and Disp 50 alarms	45
Figure 48. UL grey smoke (smolder smoke) sensitivity limits and FE/DE data	46
Figure 49. Test board layout	47
Figure 50. Axial velocity at a fan speed of 5 Hz	48
Figure 51. Axial velocity at a fan speed of 7 Hz	48
Figure 52. Axial velocity at a fan speed of 12 Hz	49
Figure 53. Ion-1 response, fan speed 5 Hz (see table 4)	50
Figure 54. Ion-1 response, fan speed 7 Hz	50
Figure 55. Ion-1 response, fan speed 12 Hz	51
Figure 56. Ion-1 response, fan speed 5 Hz - repeat test	51
Figure 57. Ion-1 response, fan speed 7 Hz - repeat test	52
Figure 58. Ion-1 response, fan speed 12 Hz - repeat test	52
Figure 59. Ion-3 response, fan speed 5 Hz	53
Figure 60. Ion-3 response, fan speed 7 Hz	53
Figure 61. Ion-3 response, fan speed 12 Hz	54
Figure 62. Ion-3 response, fan speed 5 Hz - repeat test	54
Figure 63. Ion-3 response, fan speed 7 Hz - repeat test	55
Figure 64. Ion-3 response, fan speed 12 Hz - repeat test	55
Figure 65. Ion-4 response, fan speed 5 Hz	56
Figure 66. Ion-4 response, fan speed 7 Hz	56
Figure 67. Ion-4 response, fan speed 12 Hz	57
Figure 68. Ion-4 response, fan speed 5 Hz - repeat test	57
Figure 69. Ion-4 response, fan speed 7 Hz - repeat test	58
Figure 70. Ion-4 response, fan speed 12 Hz - repeat test	58
Figure 71. Photo-3 response, fan speed 5 Hz	59
Figure 72. Photo-3 response, fan speed 7 Hz	59
Figure 73. Photo-3 response, fan speed 12 Hz	60
Figure 74. Photo-3 response, fan speed 5 Hz - repeat test	60
Figure 75. Photo-3 response, fan speed 7 Hz - repeat test	61
Figure 76. Photo-3 response, fan speed 7 Hz - repeat test	61
Figure 77. Measurements of upholstered chair used for smoldering experiments	67
Figure 78. Upholstered chair used for smoldering experiments	67

Figure 79. Measurements of upholstered chair used for flaming experiments	68
Figure 80. Upholstered chair used for flaming experiments	68
Figure 81. Mattress used for smoldering and flaming experiments	69
Figure 82. Corn oil used for kitchen cooking materials fire experiments	69
Figure 83. “Electric match” used for flaming ignitions	70
Figure 84. Location of “electric match” ignition source for flaming upholstered chair and mattress experiments	71
Figure 85. Rod used for smoldering ignitions	72
Figure 86. Heating ignition source with cooking oil	72
Figure 87. Layout of manufactured home used for test of smoke alarm performance	74
Figure 88. Layout of first floor of two-story home used for tests of smoke alarm performance	75
Figure 89. Layout of second floor of two-story home used for tests of smoke alarm performance	76
Figure 90. Sample instrumentation showing relative locations of temperature, primary gas analysis, smoke obscuration, and smoke alarm response measurements	77
Figure 91. Instrumentation in manufactured home during tests of smoke alarm performance	79
Figure 92. Instrumentation in first floor of two-story home during tests of smoke alarm performance	80
Figure 93. Instrumentation in second floor of two-story home during tests of smoke alarm performance	81
Figure 94. Example of mass loss measurement showing upholstered chair on load cell prior to one of the flaming ignition tests and load cell apparatus mounted beneath manufactured home	82
Figure 95. Optical density instrument designs	84
Figure 96. Smoke properties measurement showing collection lines (foreground) and smoke velocity measurement (background)	87
Figure 97. Calibration of residential ionization chamber	88
Figure 98. Measurement station showing several alarms arranged for testing	89
Figure 99. Measurement station showing unmodified smoke alarms arranged for testing	91
Figure 100. Mass loss of burning mattress during flaming ignition test of a mattress, test SDC05 (Note that the mass loss is averaged to minimize noise in the data. Thus, peak mass loss and initiation of suppression do not exactly coincide)	96
Figure 101. Gas temperatures from ceiling to floor in remote bedroom during a flaming ignition test of a mattress, test SDC05	97
Figure 102. Gas temperatures from ceiling to floor in main bedroom (ignition location) during a flaming ignition test of a mattress, test SDC05	98
Figure 103. Gas temperatures from ceiling to floor in hallway outside remote bedroom in a flaming ignition test of a mattress, test SDC05	99
Figure 104. Gas temperatures from ceiling to floor in hallway outside main bedroom in a flaming ignition test of a mattress, test SDC05	100
Figure 105. Gas temperatures from ceiling to floor in living area during a flaming ignition test of a mattress, test SDC05	101

Figure 106. Gas temperatures from ceiling to floor in front door hallway during a flaming ignition test of a mattress, test SDC05	102
Figure 107. Gas temperature in closed bedroom during a flaming ignition test of a mattress, test SDC05	103
Figure 108. Smoke obscuration at 20 mm and 900 mm below ceiling in remote bedroom during flaming ignition test of a mattress, test SDC05	105
Figure 109. Smoke obscuration at 20 mm and 900 mm below ceiling in main bedroom (ignition location) during flaming ignition test of a mattress, test SDC05	106
Figure 110. Smoke obscuration at 20 mm and 900 mm below ceiling in hallway outside remote bedroom during flaming ignition test of a mattress, test SDC05	107
Figure 111. Smoke obscuration at 20 mm and 900 mm below ceiling in hallway outside main bedroom during flaming ignition test of a mattress, test SDC05	108
Figure 112. Smoke obscuration at 20 mm and 900 mm below ceiling in living area during flaming ignition test of a mattress, test SDC05	109
Figure 113. Smoke obscuration at 20 mm and 900 mm below ceiling in front door hallway during flaming ignition test of a mattress, test SDC05	110
Figure 114. Smoke obscuration at 1520 mm below ceiling in closed bedroom during flaming ignition test of a mattress, test SDC05	111
Figure 115. Carbon monoxide concentration 900 mm below ceiling at four locations during a flaming ignition test of a mattress, test SDC05	112
Figure 116. Carbon dioxide concentration 900 mm below ceiling at four locations during a flaming ignition test of a mattress, test SDC05	113
Figure 117. Oxygen concentration 900 mm below ceiling at four locations during a flaming ignition test of a mattress, test SDC05	114
Figure 118. Measured output for several analog-modified smoke alarms in hallway outside main bedroom during a flaming ignition test of a mattress, test SDC05	115
Figure 119. Measured output for several analog-modified carbon monoxide alarms in hallway outside main bedroom during a flaming ignition test of a mattress, test SDC05	116
Figure 120. Measured output for a heat alarm in hallway outside main bedroom during a flaming ignition test of a mattress, test SDC05	117
Figure 121. Measured output for a tell-tale residential sprinkler in hallway outside main bedroom during a flaming ignition test of a mattress, test SDC05	118
Figure 122. Smoke properties for smoldering chair scenario SDC01	127
Figure 123. Smoke properties for flaming chair scenario SDC02	128
Figure 124. Smoke properties for smoldering mattress scenario SDC06	129
Figure 125. Smoke properties for flaming mattress scenario SDC07	129
Figure 126. Smoke properties for smoldering mattress scenario SDC08	130
Figure 127. Smoke properties for flaming chair scenario SDC10	131
Figure 128. Smoke properties for smoldering chair scenario SDC11	133
Figure 129. Smoke properties for cooking oil fire scenario SDC12	134
Figure 130. Smoke properties for cooking oil fire scenario SDC13	134
Figure 131. Smoke properties for smoldering mattress with burn room door closed SDC14 ..	135

Figure 132. Smoke properties for smoldering chair scenario SDC23	136
Figure 133. Smoke properties for cooking oil fire scenario SDC24	138
Figure 134. Smoke properties for flaming chair scenario SDC25	139
Figure 135. Smoke properties for flaming chair scenario SDC26	139
Figure 136. Smoke properties for smoldering chair scenario with air conditioning SDC27 ..	140
Figure 137. Cascade impactor results for flaming chair scenario SDC02	143
Figure 138. Cascade impactor results for flaming chair scenario SDC10	143
Figure 139. Cascade impactor results for cooking oil fire scenarios SDC12 and SDC13 ..	144
Figure 140. Cascade impactor results for smoldering chair fire scenarios SDC23 and SDC27	145
Figure 141. Schematic of the manufactured home for nuisance testing	151
Figure 142. Ion chamber schematic	152
Figure 143. Response of the ion chamber and MIC to cotton smolder smoke	152
Figure 144. Thermocouple and sampling line placement	153
Figure 145. Photo, Ion, CO and thermistor unit	154
Figure 146. Velocity and speed components for toasting bread nuisance source with and without forced ventilation	157
Figure 147. Toasting bread scenario - toaster on at t=0, off at 240 s. No forced flow	158
Figure 148. Toasting bread scenario – toaster on at t=0, off at 255 s. No forced flow, remote bedroom window open	160
Figure 149. Toasting bread scenario - toaster on at t=0, off at 255 s. Room fan turned on	161
Figure 150. Toasting bread scenario - toaster on at t=0, off at 270 s. Room fan turned on	162
Figure 151. Toasting frozen bagel scenario – toaster on at t=0, off at 300 s. Room fan turned off	163
Figure 152. Toasting frozen bagel scenario – toaster on at t=0, off at 300 s. Room fan turned on	164
Figure 153. Frying bacon scenario - cast-iron pan, LPG hot plate, no forced flow, burner lit at t=0, bacon in pan at 60 s	166
Figure 154. Frying bacon scenario - cast-iron pan, LPG hot plate, no forced flow, burner lit at t=0, bacon in pan at 60 s	167
Figure 155. Frying bacon scenario - aluminum pan, electric range, no forced flow, bacon in pan at 120 s	168
Figure 156. Frying bacon scenario - aluminum pan, electric range, floor fan on, bacon in pan at 120 s	169
Figure 157. Frying butter scenario - aluminum pan, electric range, floor fan off, butter in pan at t=0	171
Figure 158. Frying butter scenario - aluminum pan, electric range, floor fan off, butter in pan at t=0	172
Figure 159. Frying butter scenario - cast iron pan, electric range, floor fan off, butter in pan at t=0	173
Figure 160. Frying butter scenario - cast iron pan, electric range, floor fan on, butter in pan at t=0	174

Figure 161. Frying margarine scenario - cast iron pan, electric range, floor fan off, margarine in pan at t=0	175
Figure 162. Frying hamburgers - three hamburgers in non-stick frying pan, floor fan off. Hamburgers in pan at t=120 s	177
Figure 163. Frying hamburgers - three hamburgers in non-stick frying pan, floor fan on, living room window open. Hamburgers in pan at t=160 s	178
Figure 164. Frying hamburgers - three hamburgers in non-stick frying pan, floor fan on. Hamburgers in pan at t=150 s	179
Figure 165. Deep-frying Tortillas scenario - steel wok, LPG hotplate, floor fan off, first tortillas in pan at t=360 s	181
Figure 166. Deep-frying french fries scenario - steel wok, LPG hotplate, floor fan off, first french fries in pan at t=360 s	182
Figure 167. Broiling Pizza - one frozen pizza in oven set on broil, floor fan off. Oven on at t=0	183
Figure 168. Bake/ broil pizza - one frozen pizza in oven set on bake and pre-heated to 350 °F, then set to broil 630 s later. Floor fan was off. Pizza in at t=0	185
Figure 169. Bake/ broil pizza - one frozen pizza in oven set on bake and pre-heated to 350 °F, then set to broil 630 s later. Floor fan was on. Pizza in at t=0	186
Figure 170. Broiling hamburgers - four hamburgers in oven set on broil, floor fan off. Oven on at t=0	188
Figure 171. Broiling hamburgers - four hamburgers in oven set on broil, floor fan on. Oven on at t=0	189
Figure 172. Boiling spaghetti pasta - 1/3 package (150 g), floor fan off. Pasta placed in pot at t=360 s	190
Figure 173. Boiling spaghetti pasta - 2/3 package (300 g), floor fan off. Pasta placed in pot at t=450 s	191
Figure 174. Boiling spaghetti pasta - 1/2 package (225 g), lid on, floor fan off. Pasta placed in pot at t=480 s	192
Figure 175. Candles burning - four tea candles burning on electric range top area. Floor fan was off. Candles lit at t=0	193
Figure 176. Cigarette smoking - two smokers smoking one cigarette each in kitchen area. Floor fan was off. Cigarettes lit at t=0	195
Figure 177. Cigarette smoking – two smokers smoking one cigarette each in kitchen area. Floor fan was off. Cigarettes lit at t=0	196
Figure 178. Smoldering cotton wicks – eight sets of four wicks were ignited with a 12 s delay using the staged wick ignition device, located on the living room floor at the chair burn location. Fan was off. Ignition sequence started at t=30 s	197
Figure 179. Smoldering cotton wicks -eight sets of four wicks were ignited with a 12 s delay using the staged wick ignition device, located on the living room floor at the chair burn location. Fan was on. Ignition sequence started at t=30 s	198

Figure 180. Smoldering wood blocks - eight beech wood blocks on an electric hotplate, located on the living room floor at the chair burn location. Fan was off. Power to hotplate on at t=0	200
Figure 181. Smoldering wood blocks - eight beech wood blocks on an electric hotplate, located on the living room floor at the chair burn location. Fan was on. Power to hotplate on at t=0	201
Figure 182. Smoldering foam - A polyurethane foam block, located on the living room floor at the chair burn location and ignited with an electrically powered nichrome wire heater imbedded in the block. Fan was off. Power to igniter on at t=0. Sample flamed at 798 s	203
Figure 183. Smoldering foam - a polyurethane foam block, located on the living room floor at the chair burn location and ignited with an electrically powered nichrome wire heater imbedded in the block. Fan was off. Power to igniter on at t=0. Sample stopped smoldering	204
Figure 184. Smoldering foam - a polyurethane foam block, located on the living room floor at the chair burn location and ignited with an electrically powered nichrome wire heater imbedded in the block. Fan was on. Power to igniter on at t=0	205
Figure 185. Smoldering foam - a polyurethane foam block, located on the living room floor at the chair burn location and ignited with an electrically powered nichrome wire heater imbedded in the block. Fan was on. Power to igniter on at t=0	206
Figure 186. Photoelectric sensor response to cotton smolder smoke calibration test. A and B indicate repeated tests	208
Figure 187. Ionization sensor response to cotton smolder smoke calibration test. A and B indicate repeated tests	209
Figure 188. Electrochemical cell CO sensor response to cotton smolder smoke calibration test. A and B indicate repeated tests	210
Figure 189. Smoldering cotton fire scenario, fan speed 7 Hz	212
Figure 190. Smoldering cotton fire scenario, fan speed 7 Hz	213
Figure 191. Smoldering cotton fire scenario, fan speed 12Hz	214
Figure 192. Smoldering cotton fire scenario, fan speed 12 Hz	215
Figure 193. Smoldering wood fire scenario, fan speed 7 Hz	216
Figure 194. Smoldering wood fire scenario, fan speed 7 Hz	217
Figure 195. Smoldering wood fire scenario, fan speed 12 Hz	218
Figure 196. Smoldering wood fire scenario, fan speed 12 Hz	219
Figure 197. Candle flame , fan speed 7 Hz	220
Figure 198. Margarine heated in a pan , fan speed 7 Hz	222
Figure 199. Margarine heated in a pan, fan speed 7 Hz	223
Figure 200. Butter heated in a pan, fan speed 7 Hz	224
Figure 201. Bread in a toaster, fan speed 7 Hz	225
Figure 202. Bread in a toaster, fan speed 7 Hz	226
Figure 203. Bread in a toaster, fan speed 7 Hz	227
Figure 204. Bread in a toaster, fan speed 12 Hz	228

Figure 205. Bread in a toaster, fan speed 12 Hz	229
Figure 206. Average available egress time for several different alarm and fire types with alarms on every level for manufactured home tests	244
Figure 207. Average available egress time for several different alarm and fire types with alarms on every level + bedrooms for manufactured home tests	244
Figure 208. Average available egress time for several different alarm and fire types with alarms in every room for manufactured home tests	245
Figure 209. Test structure, sample interior room, and instrumentation in original 1975 Indiana Dunes Experiments	247

Tables

Table 1. Calibration of smoke and CO alarms	21
Table 2. Listed unmodified alarm sensitivities.	29
Table 3. MIC output and obscuration during tests of two ionization alarms	46
Table 4. Mean axial velocity 5 cm below ceiling	49
Table 5. Threshold criteria for modified alarms	62
Table 6. Top fire scenarios ranked by frequency of occurrence, 1992 – 1996	66
Table 7. Locations for temperature measurement in tests of smoke alarm response	78
Table 8. Locations for primary gas measurement in tests of smoke alarm response	83
Table 9. Locations for primary optical density measurements in tests of smoke alarm response	86
Table 10. Alarm and sprinkler locations in tests of smoke and CO alarm response	90
Table 11. Test conditions for tests conducted in a manufactured home	94
Table 12. Test Conditions for tests conducted in a two-story home	95
Table 13. Alarm Times for Several Smoke Alarms in Hallway Outside Main Bedroom During Flaming Ignition Test of a Mattress, Test SDC05	119
Table 14. Calculated tenability for a flaming ignition test of a mattress, test SDC05	122
Table 15. Activation times for several smoke alarms during a flaming ignition test of a mattress, test SDC05	123
Table 16. Activation times for several alternative technologies during a flaming ignition test of a mattress, test SDC05	124
Table 17. Cascade impactor results	141
Table 18. Estimated particle size from smoldering chair scenario	146
Table 19. Estimated particle size from flaming sources	147
Table 20. Estimated particle size from cooking oil fire scenario	147
Table 21. Variability for tenability time and alarm time during tests of residential smoke alarms (expressed as the ratio of standard uncertainty for replicate tests and the average value for these tests)	148
Table 22. Alarm sensitivity for photoelectric and ionization sensors	155

Table. 23. Average time to alarm (in seconds) for several smoke alarms and fire scenarios in a manufactured home	234
Table 24. Average time to alarm (in seconds) for several smoke alarms and fire scenarios in a two-story home	235
Table 25. Sample premovement activity time	238
Table 26. Estimates of required escape times for best and worst case scenarios	240
Table. 27. Available egress time (in seconds) for several different alarm technologies and fire scenarios in a manufactured home	242
Table 28. Available egress time (in seconds) for several different alarm technologies and fire scenarios in a two-story home	243
Table. 29. Activation time (in seconds) for several different fire detection technologies and fire scenarios in a manufactured home.	246
Table 30. Comparison of alarm times and times to untenable conditions for 1975 and current studies	248
Table 31. Comparison of tenability criteria used in the 1975 and current studies	248
Table 32. Comparison of fire growth rates in the 1975 and current studies	248

Executive Summary

According to estimates by the National Fire Protection Association and the U. S. Fire Administration, U. S. home usage of smoke alarms rose from less than 10 % in 1975 to at least 95 % in 2000, while the number of home fire deaths was cut nearly in half. Thus the home smoke alarm is credited as the greatest success story in fire safety in the last part of the 20th century, because it alone represented a highly effective fire safety technology with leverage on most of the fire death problem that went from only token usage to nearly universal usage in a remarkably short time. Other highly effective fire safety technologies either affect a smaller share of the fire death problem (e.g., child-resistant lighter, cigarette-resistant mattress or upholstered furniture) or have yet to see more than token usage (e.g., home fire sprinkler, reduced ignition-strength cigarette).

A seminal component that underpinned this success was the existence of a comprehensive, independent set of tests conducted in 1975-76 that clearly demonstrated the potential of smoke alarms to save lives. These were the so-called Indiana Dunes tests sponsored by The National Institute of Standards and Technology, NIST, (then the National Bureau of Standards) and conducted by Illinois Institute of Technology Research Institute and Underwriters Laboratories.

In the past few years questions were being raised about the efficacy of some smoke alarm technologies, whether the numbers and locations in homes still represented the optimum configuration, and if multi-sensor designs (as are becoming popular for commercial fire alarm systems) might perform better or produce fewer nuisance alarms. Some simply thought that it was time to reexamine the technology in light of its importance to public safety. To this end a consortium of four federal agencies and Underwriters Laboratories (with in-kind support from several others) funded this project.

The present work followed a design similar to that used in the Indiana Dunes tests. Tests were conducted in actual homes with representative sizes and floorplans, utilized actual furnishings and household items for fire sources, and tested actual smoke alarms currently sold in retail stores. Smoke alarm performance was quantified in terms of the escape time provided by groups of alarms installed in accordance with typical code provisions. While some of the smoke alarms were modified by their manufacturers to provide continuous, analog output from their sensors (which allowed the analysis of the performance of multi-sensors and decision algorithms) these were compared to identical models purchased from retail stores and included in all tests. Additionally a separate study of nuisance alarm sources was conducted because this was identified as an important issue in a prior study by the U.S. Consumer Product Safety Commission.

The fire emulator/detector evaluator (FE/DE) is a single-pass "wind tunnel" at NIST designed to reproduce all relevant conditions needed to assess the performance of spot-type particulate, thermal and gas sensor detectors or combination detectors. Specifically, the FE/DE allows for the control of the flow velocity, air temperature, gas species, and aerosol concentrations at a test section wherein detectors and sensors are exposed to these environmental conditions . Included in this report are complete data from tests conducted in the FE/DE apparatus and calibrations for all of the alarms and detectors used in this study. Calibration in the FE/DE of the alarms used in the current study showed that the sensitivity of the alarms was consistent with manufacturer ratings and, on average, of equivalent sensitivity to those used in the 1975 study. The average sensitivity measured for all alarms tested was $5.1\text{ \%}/\text{m} \pm 1\text{ \%}/\text{m}$ ($1.5\text{ \%}/\text{ft} \pm 0.4\text{ \%}/\text{ft}$). In the 1975 study, the average of all alarms tested was $6.3\text{ \%}/\text{m} \pm 2\text{ \%}/\text{m}$ ($1.9\text{ \%}/\text{ft} \pm 0.7\text{ \%}/\text{ft}$). While the average for the 1975 tests is higher, the uncertainty in the data overlaps.

An analysis of residential fire statistics was conducted for this study to identify the important fire scenarios that were included in the study. Flaming and smoldering upholstered furniture and mattresses account for the top four most deadly fire scenarios. Flaming cooking materials are involved more than five times more frequently than any other material. These scenarios included the top five ranked by number of deaths, and among the top ten ranked by frequency of occurrence.

Fire produces heat, smoke, and toxic gases, all of which can threaten human life. In these experiments environmental parameters that have an impact on human response were measured. Parameters include temperature rise, toxic gas production, and smoke obscuration. Aspects of these that can be measured directly include the gas temperature, mass loss of the burning item, species concentrations, including CO, CO₂, O₂, and other gases. Two different geometries of residential structures were used for the tests. The manufactured home geometry represented an array of residential layouts. The arrangement of the manufactured home was sufficiently generic as to represent an apartment, condominium, or small ranch house, in addition to a manufactured home, although it did include a sloped ceiling throughout the structure. The primary partitioning of the 84.7 m² (911 ft²) home consisted of three bedrooms, one full bathroom, one kitchen/dining area, one living room, and two hallways. The 139 m² (1495 ft²) two-story home was a brick-clad 3 bedroom home. The first floor consisted of a foyer, den, family room, kitchen, dining room, bathroom, and stairwell to the upstairs. The home did not have a basement. The 2-car garage was accessible from the first floor den. The second floor consisted of a stairwell to the downstairs, hallway, 2 bathrooms, and two smaller bedrooms and one master bedroom. A total of 36 tests were conducted in the two homes; 27 in the manufactured home, and 8 in the 2-story home.

The experimental design provided data on the performance of alarms in various installation arrangements. Groups of alarms were located in the room of fire origin, at least one bedroom, and in a central location on every level. Thus, by considering the alarm times of devices in various locations against tenability times for any test it was possible to determine the escape

time provided by various installation arrangements including every room, every level with or without every bedroom, and single detectors. Since both ionization and photoelectric types were included at each location the performance by sensor type was also quantified.

Smoke alarms of either type installed on every level generally provided the necessary escape time for different fire types and locations. Adding smoke alarms in bedrooms increased the escape time provided, especially for smoldering fires. These tests quantified an increased escape time for fires starting in the bedroom.

The results obtained were similar to those of the earlier work. Both common residential smoke alarm technologies (ionization and photoelectric) provided positive escape times in most fire scenarios with the ionization type reacting earlier to flaming fires and the photoelectric type reacting earlier to smoldering fires. The main difference from the earlier work is that the amount of escape time provided is consistently less. For example, average times to untenable conditions for flaming tests was 3 min compared to 17 min in the prior work. While some of this difference may be attributed to the tenability criteria used in the current study, it is also clear that fire growth in the current tests are significantly faster than in the earlier tests. For flaming fires, time to alarm activation and measurement of elevated temperatures in the room of fire origin support this faster fire growth observation. However, the smoldering fire scenarios are very difficult to reproduce experimentally and tenability times in the present study have an uncertainty (based upon one standard deviation) which overlaps the uncertainty from the 1975 study. Therefore, caution should be exhibited in drawing conclusions based upon comparisons of smoldering tenability times between the two studies. It is important to note that while both the 1975 study and the current study attempted to use a representative sample of available and important furnishings, each study included only a small fraction of those available in the marketplace. Still, this study is consistent with other recent studies of furniture and mattresses, even though there may be significant differences in the burning behavior between items of furniture.

Activation times for other fire detection technologies were also collected. As expected, CO alarms respond best to fires which produce considerable quantities of carbon monoxide during the combustion process, i.e., smoldering fire scenarios and the closed-door flaming mattress (which smoldered after the room of fire origin became oxygen limited). Tell-tell sprinklers and heat alarms responded to the flaming fire scenarios as well as to the smoldering fire scenarios after a transition to flaming combustion. Activation times of these devices support the current practice of use only in conjunction with smoke alarms.

Nuisance alarms in residential settings from typical cooking activities, smoking or candle flames are affected by the properties of the aerosol produced and its concentration, the location of an alarm relative to the source, and the air flow that transports smoke to an alarm. This is not surprising, as the same observations have been made in the fire tests here and other studies. This study provides a detailed set of data that can be used to address several issues involving nuisance alarms and reinforces current suggested practices. Clearly, the advice that alarms not be

installed close to cooking appliances if at all possible is valid. These results show that homeowners who are able to move the location of an alarm that frequently experiences nuisance alarms would do well to maximize its distance from cooking appliances while keeping it in the area to be protected. It was observed that ionization alarms had a propensity to alarm when exposed to nuisance aerosols produced in the early stages of some cooking activities, prior to noticeable smoke production. This phenomenon could be particularly vexing to homeowners who experience such nuisance alarms. Carbon monoxide electrochemical cells at all alarm locations gathered data on the level of carbon monoxide produced during the tests and transported to the alarms. These data in conjunction with the complete fire test series data could be used to verify combined smoke/CO alarm algorithms.

The FE/DE nuisance source tests captured salient features of some of the manufactured home tests. More work needs to be done to produce a set of tests and the performance criteria that covers a significant range of residential nuisance sources, and would assure a benefit in terms of nuisance alarm reduction. This work is part of ongoing research with the FE/DE at NIST. The nuisance alarm study also represents a wealth of data valuable in establishing (amazingly for the first time) test methods and criteria for what a smoke alarm should not respond to. Testing labs are examining NIST's unique FE/DE apparatus to replace the current, product specific test apparatus that do not allow multi-sensor devices to be evaluated.

The present work has produced an extensive database of documented data on typical residential fires. All data collected in the tests are available in electronic form (<http://smokealarm.nist.gov>) and are already being used by the smoke alarm industry to improve their products, by the product approval agencies to improve testing procedures, and by researchers to validate and improve fire models.

The present work has considerable potential for communicating important fire safety messages to the public. The material has been made freely available and NIST plans to produce examples and is willing to work with others wishing to do the same.

Acknowledgments

The authors gratefully acknowledge the efforts of the Fire Metrology Group and others, including D. Stroup, W. Twilley, J. Lee, G. Roadarmel, J. McElroy, M. Selepak, D. Weinert, M. Donnelly, M. Nyden, C. Davis, and L. DeLauter. G. Forney developed the web conversion for the test data. In addition, an in-kind contribution from the National Research Council-Canada measured toxicological species with FTIR within the manufactured home. The measurements were taken by Dr. J. Su and Dr. J. Kanabus-Kaminska.

The steering committee for the project included representatives from government and other organizations interested in the research. Their expertise provided direction throughout the project and insightful review of this report. Members of the committee included S. Coulberson, Centers for Disease Control and Prevention; J. Hall, National Fire Protection Association; A. Lee, U.S. Consumer Product Safety Commission (CPSC); R. McCarthy, U.S. Fire Administration (USFA); J. Milke, University of Maryland; M. Nealy, CPSC; J. Ottoson, USFA; I. Papier and P. Patty of Underwriters Laboratories Inc.; J. Su, National Research Council Canada; and E. Taylor, U.S. Department of Housing and Urban Development, Healthy Homes Initiative.

The home smoke alarm project was sponsored by the U.S. Consumer Product Safety Commission, Centers for Disease Control and Prevention, U.S. Fire Administration, and the U.S. Department of Housing and Urban Development, Healthy Homes Initiative, Underwriters Laboratories. The National Fire Protection Association (In-kind contribution), and National Research Council Canada, (In-kind contribution).

Performance of Home Smoke Alarms

Analysis of the Response of Several Available Technologies in Residential Fires²

Richard W. Bukowski, Richard D. Peacock, Jason D. Averill, Thomas G. Cleary, Nelson P. Bryner, William D. Walton, Paul A. Reneke, and Erica D. Kuligowski

Fire Research Division
Building and Fire Research Laboratory

1 Introduction

Smoke alarms are often the primary life safety strategy for occupants in the event of an unwanted residential fire. As the number of annual residential fire deaths (about 3000) far outpaces the number of commercial and industrial fire deaths (just over 100 in all non-residential structure fires) it is crucial to understand the level of safety provided by smoke alarms in the residential environment. In 1975, the Illinois Institute of Technology Research Institute (IITRI) and Underwriters Laboratories, Inc (UL), with funding from the National Bureau of Standards (NBS, now the National Institute of Standards and Technology (NIST)), evaluated the performance of commercially available smoke alarms in 76 residential fire experiments representative of the major fatal fire scenarios of the time, in actual homes scheduled for demolition. The purpose of the project, known as the Indiana Dunes Tests, was to evaluate the “requirements for fire alarms to protect residential occupancies.” [1] The tests became the basis for the siting and response characteristics of residential smoke alarms, worldwide.

Since 1975, however, the materials and construction of contents that represent the major combustible items in a typical residential structure have changed and the response characteristics of current smoke alarms have also changed as the technology matured. Thus, a systematic evaluation of current residential smoke alarm requirements is again considered necessary. The United States Consumer Product Safety Commission (CPSC), the United States Fire Administration (USFA), the Centers for Disease Control and Prevention (CDC), the United States Department of Housing and Urban Development (HUD), Underwriters Laboratories, Inc. (UL), the National Fire Protection Association (NFPA), and the National Research Council

²Certain commercial entities, equipment, or materials may be identified in this report in order to describe an experimental procedure or concept adequately. Such identification is not intended to imply recommendation or endorsement by the National Institute of Standards and Technology, nor is it intended to imply that the entities, materials, or equipment are necessarily the best available for the purpose.

Canada (NRCC), in conjunction with NIST's Building and Fire Research Laboratory (BFRL), have joined forces to evaluate the current state of residential smoke alarm requirements.

The overall purpose of the project is to determine how different types of fire alarms can respond to threatening residential fire settings in order to permit egress of typical occupant sets. The plan was to conduct real-scale tests of current smoke alarms and related technologies in actual homes with actual contents as fuels.

This report presents the results of the project and provides details of the response of a range of residential smoke alarm technologies in a controlled laboratory test and in a series of real-scale tests conducted in two different residential structures. The results are intended to provide both insight into siting and response characteristics of residential smoke alarms and a set of reference data for future enhancements to alarm technology based on fires from current materials and constructions.

1.1 History

As early as 1961 the potential of early warning of fire to reduce fatalities was recognized [2], however the costs associated with commercial detectors and alarm systems was prohibitive and such systems were found in fewer than 1 % of U.S. dwellings. In 1965 the first self-contained (so-called single-station) smoke alarms were developed but it was not until the battery-powered smoke alarm was marketed in 1969 that homeowners began to take notice.

Initial sales were slow due largely to costs near \$100 but interest by large, consumer products companies brought more efficient production and marketing to bear and costs declined. By 1975 prices had dropped below \$39.95 (which General Electric cited as a level that brought impulse buyers) and sales really began to accelerate.

At about this time the National Bureau of Standards (now NIST) was promoting building code requirements for the installation of smoke alarms in new and existing dwelling units. Research to develop minimum product performance standards was being conducted in cooperation with Underwriters Laboratories (UL) and installation requirements were proposed to the National Fire Protection Association (NFPA) Standard 74, Household Fire Warning Equipment.

Initially, the installation scheme was based on the McGuire and Ruscoe recommendations [2] but it was recognized that testing was needed to verify the adequacy of the number, sensitivity, and location of devices in typical homes. This led to the conduct of the so-called *Indiana Dunes Tests* [1] that pioneered the every-level smoke alarm requirement now found in nearly every building code in the world.

In the decade 1975-1985 smoke alarm sales were estimated in the 14 million per year range and (state and local) building codes were commonly amended to require smoke alarms at least in new residential construction. Many jurisdictions reported precipitous drops in residential fire fatalities, in many cases reaching zero [3]. This success inspired other jurisdictions to require smoke detectors in existing dwellings and programs to distribute free smoke alarms to the disadvantaged.

According to estimates by the National Fire Protection Association and the U. S. Fire Administration, U. S. home usage of smoke alarms rose from less than 10 % in 1975 to at least 95 % in 2000, while the number of home fire deaths was cut nearly in half. Thus the home smoke alarm is credited as the greatest success story in fire safety in the last part of the 20th century, because it alone represented a highly effective fire safety technology with leverage on most of the fire death problem that went from only token usage to nearly universal usage in a remarkably short time. Other highly effective fire safety technologies either affect a smaller share of the fire death problem (e.g., child-resistant lighter, cigarette-resistant mattress or upholstered furniture) or have yet to see more than token usage (e.g., home fire sprinkler, reduced ignition-strength cigarette).

1.2 Concerns Raised

In the early 1990s the U.S. Consumer Product Safety Commission (CPSC), in conjunction with the US Fire Administration, NFPA, NIST, and the Centers for Disease Control and Prevention undertook an extensive study called the National Smoke Detector Project. The objective was to examine who did and did not have detectors, how many were working (many were now more than 10 years old), and, if not working, why. Also included were consumer awareness issues, availability in economically disadvantaged households, and rates of testing and battery replacement [4].

While the results of the study were generally good there were areas for concern. Surveys of representative homes showed that most had working smoke detectors (since renamed smoke alarms) correctly installed. While a third of the smoke detectors did not work on initial test, half of these were made operational by restoring power (mostly installing a fresh battery). Homeowner interviews revealed that most of these were intentionally disconnected due to nuisance alarms, mostly from cooking. While there were some failures identified there were no large or systematic problems identified with detector designs or manufacturing practices that cast any doubt on their long term reliability.

In this period, reports surfaced that some privately funded testing had shown delayed response from smoke alarms using ionization-type sensors to smoldering fires. While detailed reports were never published in the open literature, these persistent reports were the cause of some concern. Given the significant public benefits resulting from smoke alarms in homes CPSC,

NIST, and others felt that it was time to make a new investment in research that would address these concerns directly and would examine ways to improve the protection provided while reducing nuisance alarms that were leading to disabling of the alarms.

1.3 Organizing the Research Project

Under the leadership of CPSC staff and with technical support from NIST, a series of public meetings were held to garner support for a new research program. Funding was provided by CPSC, USFA, HUD (Healthy Homes Initiative), CDC, and Underwriters Laboratories with additional support from NFPA, National Research Council of Canada, University of Maryland, and the US smoke alarm manufacturers to make this ambitious program possible. The level of resources allowed a broad program of research objectives to be identified. These were:

1. Evaluate the performance of current smoke-alarm technology.
2. Test conditions representative of current fatal residential fires.
3. Evaluate the efficacy of current requirements for number and location of smoke alarms.
4. Develop standard nuisance alarm sources to be included in the test program.
5. Examine other fire detection technologies in combination with smoke alarms (example: residential sprinkler and heat detectors).
6. Obtain data on the potential for improvements in performance by new technologies.
7. Include fuel items that incorporate materials and constructions representative of current residential furnishings.
8. Fully characterize test detectors and alarms in a consistent manner to facilitate comparisons.
9. Utilize fire models to extend the applicability of the test arrangements and maximize the test instrumentation.
10. Make all of the data collected as widely accessible as possible.
11. Provide opportunities to enhance public fire safety education.

The considerations made to address each of these objectives are discussed in the following sections.

1.3.1 Evaluate the Performance of Current Smoke Alarm Technology

Current technology includes two operating principles – the ionization-type sensor and the photoelectric (scattering) sensor. The major manufacturers produce both types representing unique designs that exhibit individual performance characteristics. Thus, the project included examples of current products containing each of the sensor designs so that the results would be representative of the full range of product performance expected.

In addition, representative electrical and mechanical heat detectors, and residential sprinklers were included in the test program to provide reference data on activation times. Also included were current residential carbon monoxide (CO) alarms employing two of the three sensor types found in commercial products (metal oxide and electrochemical cells). The biometric sensors were not included because they could not be modified for continuous, analog output. The CO alarms evaluated are specifically marketed as not being suitable as fire detectors, but rather are for detecting high levels of CO from malfunctioning or improper use of combustion appliances. However, they were included because they are increasingly being required in addition to smoke alarms and because they may be useful in improving performance and reducing nuisance alarms in conjunction with smoke alarms.

All prior studies had been done with ordinary alarm devices that operate on an alarm threshold basis – produce an alarm signal when some pre-determined alarm level is exceeded. This limits the ability to evaluate the change in performance from variations above or below the set threshold, and does not allow determination of performance of multiple sensors or of alarm algorithms. Thus it was decided to include devices that were modified (by their manufacturers) to produce a continuous, analog output signal from their sensor.

While greatly increasing the usefulness of the data such modification by the manufacturer raises the issue of whether the performance is representative of an unmodified commercial product. To address this the project employed two approaches:

- First, there were numerous unmodified devices of the identical model as the analog device that were purchased by NIST from local retail sources. These served as a comparison to the analog devices when characterized in NIST's fire emulator / detector evaluator (FE/DE) apparatus [5]. The FE/DE is a single-pass "wind tunnel" designed to reproduce all relevant conditions needed to assess the performance of spot-type particulate, thermal and gas sensor detectors or combination detectors.
- Second, these unmodified devices were used in every test in the room of fire origin.

1.3.2 Test Conditions Representative of Current Fatal Residential Fires

To ensure that the room sizes and arrangements, materials of construction, and ventilation conditions are representative of actual dwellings, all tests were conducted in real dwelling units. First, a manufactured home was procured and delivered to the NIST site for use in both fire tests and nuisance alarm tests. The floor plan selected was a three bedroom, two bath arrangement with a master suite at one end and the other bedrooms at the other end. This size and arrangement represents not only manufactured homes but also apartments and condominiums of about 100 m² (or about 1000 ft²).

A second test site, obtained through the Federal Emergency Management Agency (FEMA), was a three bedroom, two-story, brick home in Kinston, NC. The home was in an area impacted by a hurricane where the homes were purchased to be demolished and the owners relocated. While most homes in the area had flood damage, this one was on a higher elevation lot and had not been damaged. Floor plan drawings of both homes are provided in section 3.4.

Of key importance to the representativeness of the study was the selection of the test scenarios. These include the room of fire origin, ignition source and first item ignited, and the ventilation conditions that affect the fire development and combustion chemistry. Here we began with an NFPA analysis of the USFA's National Fire Incident Reporting System (NFIRS) data on fatal residential fires.

In addition to the scenarios themselves, the test matrix considered the need to perform sufficient replicates to allow estimates of experimental uncertainty and repeatability.

Finally the desire to run tests in a wide range of geometries (room sizes, materials, arrangements, and ventilation conditions) is limited by the costs of full-scale tests and available resources. Here the availability of computer fire models can provide a means to assess the potential impact of other geometries on smoke alarm performance. NIST's computational fluid dynamics (CFD) model, FDS, was used in advance of the tests to assist in planning and instrumentation and to provide quantification of modeling uncertainty. CFD models are now available to extrapolate the test results to other geometries of interest.

1.3.3 Evaluate the Efficacy of Current Requirements for Number and Location of Smoke Alarms.

Current U.S. model building codes contain requirements for smoke alarms in residential occupancies. These codes typically require smoke alarms on every level (story) outside sleeping areas and in all sleeping areas (bedrooms). Bedroom alarms are generally required only in newly constructed units. This requirement added in the mid-1990s based on the need for audibility with bedroom doors closed. Proposals to extend bedroom alarms to existing construction have lacked justification on life safety grounds compared to the significant expense.

The design of the experiments was meant to provide data on the performance of alarms in various installation arrangements. Groups of alarms were located in the room of fire origin, at least one bedroom, and in a central location on every level. Thus, by considering the alarm times of devices in various locations against tenability times for any test it was possible to determine the escape time provided by various installation arrangements including every room, every level with or without every bedroom, and single detectors. Since both ionization and photoelectric types were included at each location the performance by sensor type is also quantified.

The inclusion of analog sensors allowed the evaluation of performance changes resulting from variation in alarm threshold settings. The analysis in this report is based on typical alarm threshold settings. Data are also available to allow comparison at other threshold values.

1.3.4 Develop Standard Nuisance Alarm Sources to Be Included in the Test Program.

Smoke alarms are susceptible to alarming when exposed to non-fire aerosols. In residential settings, this typically involves cooking activities or transient, high humidity conditions (i.e., "shower steam"). The Smoke Detector Operability Survey [6] conducted by the U.S. Consumer Product Safety Commission reported that about one half of the 1012 respondents indicated they experienced nuisance alarms, with 80 % of those attributed to cooking activities, and an additional 6 % citing steam from bathrooms. Dust, and tobacco smoke are also mentioned sources. The survey also reported that of the alarms with missing or disconnected batteries, or disconnected AC power, more than one third of respondents indicated that power was removed due to nuisance alarms.

The objective of this research task was to develop a basis for standard residential nuisance source testing. The approach taken was to define a set of nuisance scenarios, replicate the events that cause nuisance alarms, and quantify the important variables that cause nuisance alarms. Translating the results to a set of nuisance source conditions reproducible in a suitable test-bed (i.e., a test room or the fire emulator/detector evaluator) would allow for more comprehensive detector performance testing. Preliminary tests were performed in the FE/DE with this in mind. Programming realistic and reproducible fire and nuisance conditions in the FE/DE is an ongoing research project at NIST.

1.3.5 Examine Other Fire Detection Technologies in Combination with Smoke Alarms

Prior studies have evaluated alternate detection technologies such as heat detectors [1] and metal oxide gas sensing [7] compared to and in combination with particulate smoke sensing. In the present study residential carbon monoxide alarms were included to evaluate their performance individually and in combination with smoke and heat sensing. By including these data, the use of multi-criteria algorithms to combine the signals from different sensors can be examined as opposed to the simple AND and OR logic of the past. Similar work has been performed by others [8, 9] for a broader range of sensor types but many of these are not commercially feasible, especially for the price-sensitive residential market.

Simple combinations of smoke sensors with CO and thermal signals were evaluated for performance against fires and nuisance sources. More complex algorithms were evaluated under a grant to University of Maryland and will be reported separately.

Residential fire sprinklers have increasingly been required in new, multiple dwelling units (apartments, condominiums, and some townhomes) and under the relevant standards include smoke alarms in the same number and locations as without sprinklers. While these sprinklers have been extensively evaluated and have an outstanding record of saving lives and property [10], there are no research programs that provide data on how the two systems work together.

Thus typical residential sprinklers were included in these tests to provide comparative data on activation times but the sprinklers were not connected to water as this would have interfered with the data on smoke alarm performance.

1.3.6 Obtain Data on the Potential for Improvements in Performance by New Technologies

Simple alarm times are not sufficient to identify potential performance improvements; so analog sensor data were recorded for both the fire performance and nuisance alarm testing. Additional instrumentation was selected and located to supplement the analog sensor data and allow better quantification of results. Examples include thermocouple measurements of temperatures and temperature gradients, smoke and gas species concentrations in several locations, and convective flow velocities in the ceiling layer at the level of the sensors.

1.3.7 Include Fuel Items That Incorporate Materials and Constructions Representative of Current Residential Furnishings

Fuel (combustible) items were selected as generically appropriate to the room of origin and fire scenario identified from NFIRS analysis and typical of materials and constructions in common use today. Specifically, upholstered chairs were used for living room fires and mattresses for bedroom fires that were purchased from local, retail sources. No modifications were made and no accelerants were used to enhance or retard the burning behavior of the items. Cooking oil used in kitchen fires was also a normal commercial product that was not modified in any way.

1.3.8 Fully Characterize Test Detectors and Alarms in a Consistent Manner to Facilitate Comparisons

All detectors (smoke, heat, and CO) were characterized in NIST's FE/DE apparatus [5] under similar conditions using an appropriate source. This allows direct calibration of all devices in a comparable way and a means to verify the performance of sensors in combination or utilizing algorithms that may be suggested by the results of this study.

1.3.9 Utilize Fire Models to Extend the Applicability of the Test Arrangements and Maximize the Test Instrumentation

Modeling, using NIST's CFAST and FDS models, was performed prior to testing to evaluate the impacts of the selected fuels and fire scenarios on the instrumentation and test structures and to assist in identifying the most appropriate instrument locations.

1.3.10 Make All of the Data Collected as Widely Accessible as Possible

Clearly the best method of (global) dissemination of the test data was to employ the Internet. Thus, a public web site was established (<http://smokealarm.nist.gov/>) on which the detailed results of tests were published as NIST Report of Tests [11, 12]. This publication vehicle exists as a means to quickly disseminate test data that is factual in nature – no observations or conclusions can be included. Thus the web site contains floor plans of the test sites showing instrument locations, details of the fuels and test conditions, and test data in electronic form. For

this we used the Fire Data Management System (FDMS) format [13] and comma-separated spreadsheet (.csv) files.

1.3.11 Provide Opportunities to Enhance Public Fire Safety Education

The information obtained in these tests will provide a basis for numerous public fire safety messages and will quantify the protection provided by residential smoke alarms. The project data will be used to show the reduction in protection resulting from one or more devices being nonfunctional as a motivation for testing and maintenance by the homeowner. Videos will be made available for use in public safety announcements and educational materials. A press day was held that resulted in stories carried on all the major news networks and on more than 75 local outlets from Maine to Hawaii.

1.4 Project Oversight

The project was initiated by NIST in October 2000 with a 24 month schedule for completion. A Project Steering Committee was established with representatives of each of the sponsoring organizations along with NFPA, the University of Maryland, and the National Research Council of Canada. In addition a larger mailing list of interested parties was organized by CPSC to whom copies of the quarterly reports were sent by email. Semi-annual meetings were held with the Steering committee and annual briefings were held for the larger group in order to keep communications open. However, in keeping with NIST policy, recommendations from either group were given every consideration but were not *a priori* considered binding on the NIST team.

2 Residential Fire Alarms, Sensor Response and Calibration in the FE/DE

2.1 Residential Alarms Included in the Study

Figure 1 shows one of the fire alarm sensor test boards used during the tests. Two classes of alarms were used in the test series, unmodified off-the-shelf smoke alarms and modified smoke and CO alarms that produce a continuous voltage signal in response to the sensor environment (such as smoke or CO concentrations, ambient pressure, humidity, and temperature). The unmodified alarms consisted of a photoelectric model and two ionization alarms corresponding to the modified models provided by the manufacturers. These alarms were purchased from retail establishments for use in this test series. The alarm response was verified by a single test in the FE/DE for at least 12 alarms of each type. The modified smoke and CO alarms were provided by their respective manufacturers. These represented three photoelectric type smoke alarms (one of which was of an aspirated design), three ionization type smoke alarms, and three CO alarms, two of which employed an electrochemical cell, and one which employed a tin oxide semiconductor (so-called Taguchi-type) sensor. Each alarm was assigned an arbitrary number for this report. A naming convention using the alarm type (i.e., Ion) and the arbitrary number is used throughout the report to identify individual alarms (i.e., Ion-1 identifies one particular model of the ionization alarms; additional identification details the location for each alarm in each test – see section 2.4). Calibration tests were performed on the modified smoke and CO alarms in order to develop voltage response curves for smoke and carbon monoxide gas exposures. The effects of local flow conditions and sensor test board location on the sensor response were examined in the FE/DE to quantify alarm response biasing due to a particular alarm's position on the test board in the test series. Details of these experiments are given below.



Figure 1. Sample sensor test board used during tests of residential smoke alarms

Essentially all residential smoke alarms sold in the United States are listed by Underwriters Laboratories Inc. and meet the requirements of test standard UL 217 [14]. From tests performed on a particular model of detector, a sensitivity value is derived from an average of smoke levels reached at alarm for repeated tests. This sensitivity is recorded on the back of the smoke detector along with a lower and upper range that defines the allowed variation in sensitivity for the particular model. Alarms are periodically checked during the manufacturing process in accordance with UL 217 to make sure the model type still alarms within its sensitivity range.

During the formulation of the research plan for the Home Smoke Alarm Project it was decided that modified smoke and CO alarms that provide a continuous signal would be used. The purpose for this decision was two-fold. First, using the voltage response curve, any single sensitivity (alarm point) can be specified for a particular alarm model or type of alarm. Therefore any range of sensitivities can be examined. Second, continuous sensor output is useful for experimental algorithm development; it lends itself to signal processing feature extraction, and multi-sensor/multi-criteria algorithm development. The time investment in the modification of the smoke alarms, and their individual calibrations required that they be re-used throughout the test series. In almost all cases, calibrations were re-checked after a test series was complete for alarms used in that series.

2.2 The fire emulator/detector evaluator

The fire emulator/detector evaluator (FE/DE) is a single-pass "wind tunnel" at NIST designed to reproduce all relevant conditions needed to assess the performance of spot-type particulate, thermal and gas sensor detectors or combination detectors. Specifically, the FE/DE allows for the control of the flow velocity, air temperature, gas species, and aerosol concentrations at a test section wherein detectors and sensors are exposed to these environmental conditions [5]. A schematic of the FE/DE is shown in figure 2.

Room air is drawn into the opening, and exhausted to a ventilation hood at the end of the duct. The air velocity at the test section is controlled over a range of flows between 0.02 m/s (4 ft/min) to over 2 m/s (400 ft/min) by means of the computer-controlled axial blower. Air is first propelled through the annular finned heating elements, then travels along the duct to the test section. The flow is conditioned before it reaches the test section by passing through a 0.1 m (4 in) long aluminum honeycomb with 5 mm rectangular openings. The goal is to provide a carefully controlled flow profile indicative of what would be experienced by a detector in a ceiling jet flow. A rectangular baffle plate covering 1/2 of the duct cross-section may be placed in the center of the duct 0.3 m (1 ft) upstream from the test section to produce velocity fluctuations similar to those observed in room flows. Additional information on flows during room tests is discussed in section 6.

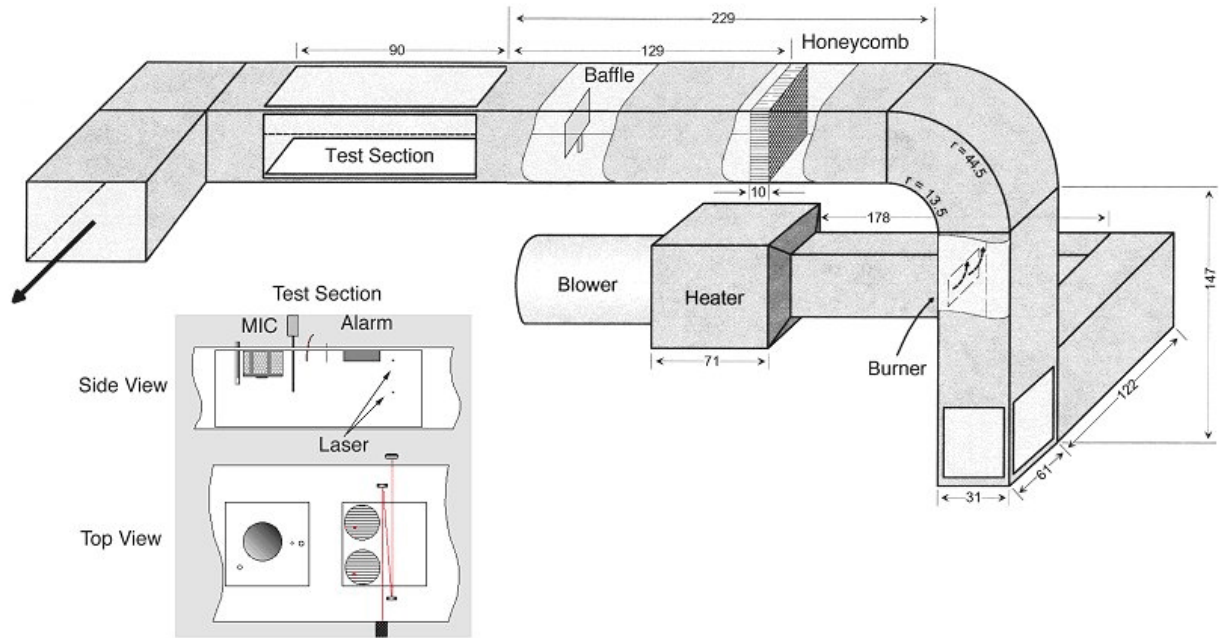


Figure 2. Schematic of the FE/DE (all units in cm)

Heat may be added to the flow by a series of 9 annular finned heating elements. Each element is rated at 5 kW for a total maximum heat input of 45 kW. Power to the heating elements is controlled by a feedback controller that receives set-point values from an input file and compares them to the air temperature upon exiting the heaters. A rate of temperature rise in airflow of 0.5 °C/s is achievable at the test section, up to maximum of about 80 °C. For the testing described in this report, this feature was not used; any temperature rise is attributed to the smoke source heat output. Air temperature at the test section is measured with a chromel-alumel thermocouple located 5 cm below the duct ceiling.

CO, CO₂, or other gas blends may be metered into the flow via electronic mass flow controllers. CO, and CO₂ gas concentrations at the test section are monitored by a dual gas non-dispersive infrared (NDIR) analyzer (Siemens Ultramat 22P CO/CO₂ analyzer). Various types of smokes and non-combustion aerosols may be introduced into the flow, including flaming soot, smolder smokes, dust, nebulized liquid mists, and cooking aerosols. Laser light transmission measurements across the duct at the test section are used to calculate the light extinction coefficient, optical density, or obscuration of the aerosol. Extinction coefficient or optical density is the typical "concentration" measurement of smoke. In this report though, obscuration expressed in terms of (percent per foot) will be used often as it is the industry standard measurement unit. A linearly polarized helium-neon laser at 632.8 nm wavelength coupled with a stabilizer utilizing a liquid crystal polarizer is the light source. This system maintains nearly constant laser intensity. The main beam is split and introduced at two heights: the center of the duct, and 5 cm below the top of the duct. Each light beam is reflected off two mirrors inside the

duct and directed at a photodetector placed on the opposite side of where the beam enters the duct. The total light transmission path length inside the duct is $1.52\text{ m} \pm 0.01\text{ m}$. The photodetector output voltage is linear with respect to the transmitted light intensity. The standard relative uncertainty due to random fluctuations in the output is 0.06 % of the measured light transmittance (light intensity divided by smoke-free initial light intensity). A measuring ionization chamber (MIC) is located in the test section to provide a reference chamber current measurement appropriate for characterizing ionization detectors. The chamber voltage potential was set at 18 V, the flow rate was set at 30 L/min and the chamber current was measured with a picoammeter that provides a proportional analog voltage. The picoammeter voltage output was calibrated with a precision current source (99.7746 pA at 20 °C) constructed from a weston standard cell and a 10 GΩ resistor. The clean air chamber output was typically $95\text{ pA} \pm 5\text{ pA}$ with a standard relative measurement uncertainty of 2 pA. Relative humidity was recorded with a capacitance-type humidity sensor (Oakton model WD-35612-10) with a stated measurement uncertainty of 2 %. Barometric pressure in the FE/DE laboratory was recorded by an electronic manometer (Druck model DPI 145) with the measurement uncertainty of 1 Pa.

2.3 Smoke Aerosols

The modified smoke alarms were calibrated against two smoke sources: a propene flame soot generator, and smoldering cotton wick smoke. Initially, all detectors were tested against each smoke source twice. Repeat calibration checks were performed with the cotton smolder smoke source.

The propene smoke generator provides black soot typical of flaming hydrocarbon or plastics fire smoke, figure 3. The propene smoke generator is directly attached to the FE/DE duct at the vertical riser section. The concentration of smoke is varied by changing the fuel flow of the burner, and opening or closing dampers allowing more or less flow from the burner to enter the duct. For the calibration runs performed in this study, the



Figure 3. Propene smoke generator.

burner fuel and air were incremented every 170 s in a series of 8 steps to produce steps in the soot concentration ending with a light transmittance value of approximately 0.7. The flat sections of the upper laser beam light transmission curve (spanning approximately 120 s) are compared to the detector signal over the same time interval. Figure 4 shows the light transmittance and MIC current output as a function of time for one of the test runs. The curves consist of a series of stepped outputs which were averaged to determine values for the calibration curves.

Smoldering cotton smoke is generated by a staged-wick-ignition device (figure 5) that ignites wicks by applying power to electrical heating wires in a prescribed computer-controlled sequence to affect a specific rate of smoke build-up at the test section. Eight groups of up to four individual wicks can be ignited in sequence to provide the controlled rate-of-rise in smoke concentration at the test section. The cotton smolder source is similar to the cotton smolder test fire 3 in EN 54 part 9 [8] and the UL standard [14]. Power is applied at 200 s intervals to each of the four sets of four wick igniters followed by 2 sets of 8 wick igniters to yield six steps in the smolder smoke concentration. Figure 6 shows the light transmittance and MIC current output as a function of time for one of the test runs, with the steady values used for calibration curves highlighted. The smoldering cotton smoke source was used to produce increasing levels of CO for calibrating the CO alarms as well. Figure 7 shows the CO and CO₂ volume fractions as a function of time for the same test.

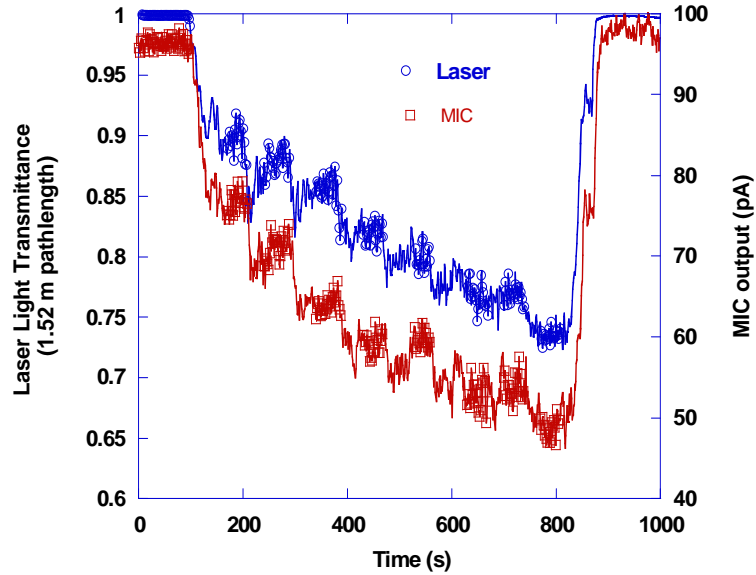


Figure 4. Propene smoke calibration run

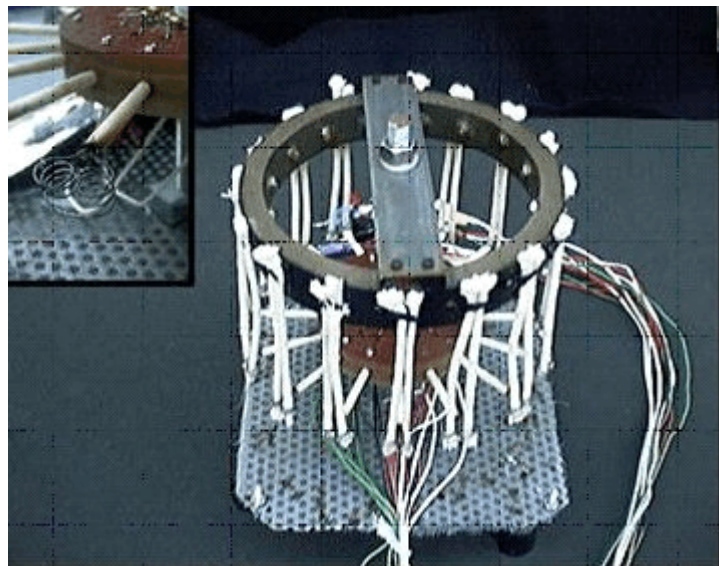


Figure 5. Smolder source, staged wick ignition device

Figure 6 shows the light transmittance and MIC current output as a function of time for one of the test runs, with the steady values used for calibration curves highlighted. The smoldering cotton smoke source was used to produce increasing levels of CO for calibrating the CO alarms as well. Figure 7 shows the CO and CO₂ volume fractions as a function of time for the same test.

Examining the relationship between the test smokes used here and those used in the UL standard [14] is important in order to establish the validity of computed alarm times from the smoke sensor voltage values recorded in the test series. The smolder smoke source is used to specify an alarm's sensitivity, thus establishing the relationship between the UL cotton wick aerosol and the cotton wick aerosol produced here is of primary concern. Direct comparison of the physical properties and size distribution of the test smokes was not within the scope of this study. However, the UL standard allows for alternate aerosol generation equipment so long as the relationship between the MIC and the light transmittance values fall within specified sensitivity test limits. This relationship fixes the obscuration range at ionization alarm levels, but not necessarily the obscuration range at photoelectric alarm levels for alternate aerosols.

The relationship for cotton smolder smoke is shown in figure 8. Along with the sensitivity test limits, results from 12 separate FE/DE tests (spanning a 6 month test interval) are shown, where the mean values over the steady time periods are plotted along with the corresponding standard deviations. It is seen that the FE/DE results fall within the UL cotton smolder smoke test limits down to light transmittance values of about 0.9, then deviate outside of those bounds for lesser light transmittance values. The observation that the FE/DE test results stay within the bounds down to a transmittance of 0.9 is significant because the sensitivity range for most residential ionization alarms falls within a transmittance range above 0.9 for the smolder smoke.

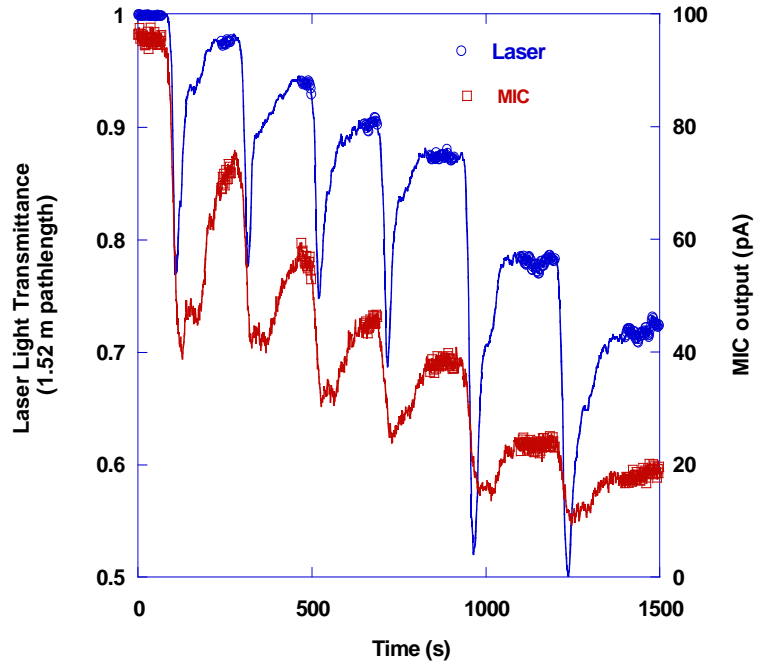


Figure 6. Smolder smoke calibration run

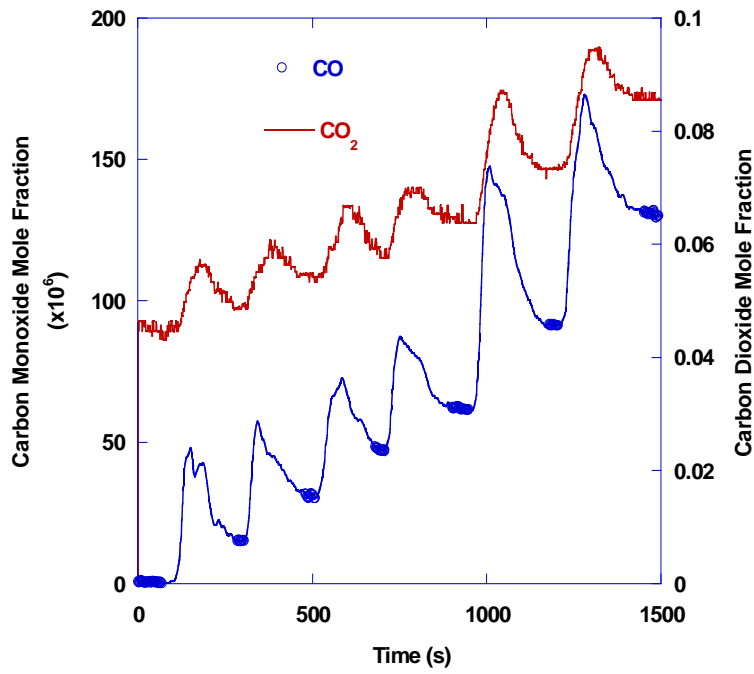


Figure 7. Smolder smoke CO calibration run

The FE/DE test results for the smolder smoke are shown in figure 9. The results are plotted for the same time intervals as the calibration run. The mean values and standard deviations are shown for each time interval. The results are compared to the UL cotton smolder smoke test limits. The FE/DE test results are shown to fall within the test limits for the first two time intervals, but deviate outside of the bounds for the remaining time intervals. The deviation occurs at lower transmittance values than the calibration run, indicating a lower sensitivity for the FE/DE test results.

Thus, within the range typical of ionization smoke alarms, the response is within the limits of the UL 217 test.

Residential photoelectric alarms typically alarm at transmittances greater than 0.84 in the UL test. While the FE/DE smoke deviates outside the MIC limits at a transmittance of about 0.9, this observation is not by itself a cause for concern.

The deviation between UL and FE/DE test smoke results at lower light transmittance values suggests a smoke size distribution difference between the two smolder smokes. Since the UL smoke box is a re-circulating system, it can take between 12 min to 17 min to reach a light transmittance value of 0.8. The FE/DE is an open, single-pass flow system and the smoke transport time for these calibration tests is on the order of 30 s. Therefore, potentially more smoke aging (i.e. coagulation growth of the smolder aerosol) can take place in the smoke box relative to the FE/DE. Assuming that fresh smolder smokes are identical in the smoke box and the FE/DE, additional coagulation growth in the smoke box will tend to increase light extinction while decreasing the MIC output for a fixed amount of smoke. This could explain MIC difference between the two sources at lower transmittances. The difference between relative levels of obscuration and light scattering of fresh and aged smolder smokes should be less pronounced. There are two reasons for this supposition. First, coagulation growth tends to incorporate the smallest particles into bigger particles. The smaller particles scatter little light, and contribute almost nothing to obscuration, thus they are not missed. Second, the growth of particles that scatter significant amounts of light will tend to

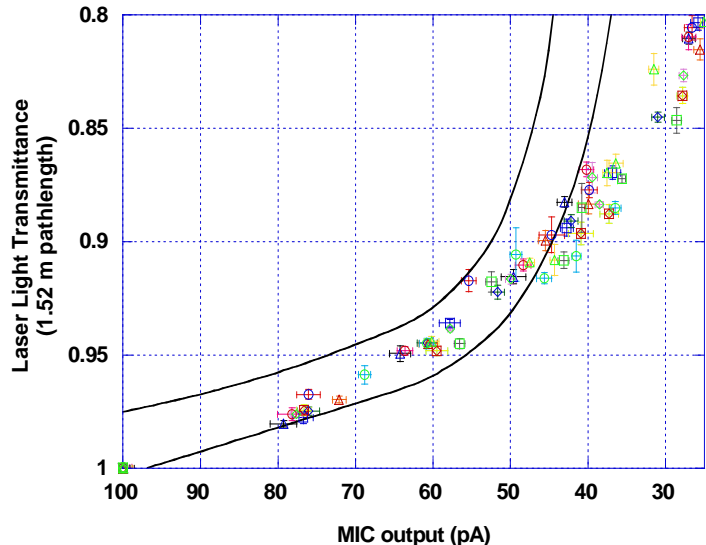


Figure 8. UL grey smoke (smolder smoke) sensitivity limits and FE/DE data

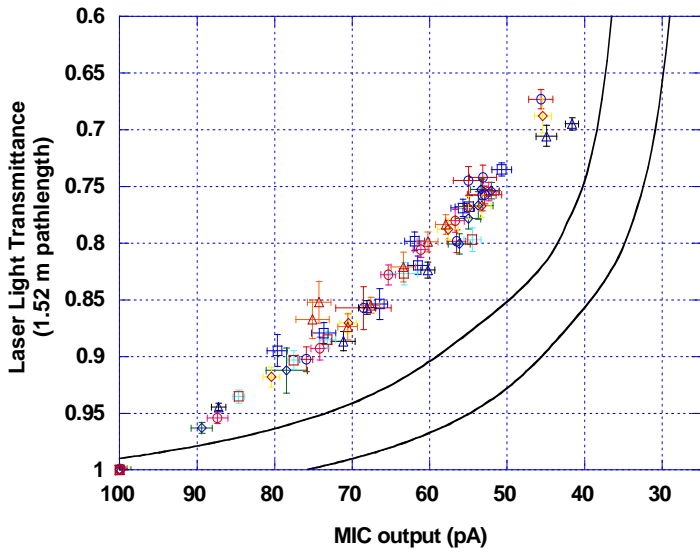


Figure 9. UL black smoke sensitivity limits and corresponding FE/DE data

increase the scattered light at the same rate the obscuration is increased since for the light colored smolder smoke scattering dominates the light extinction.

The relationship for black smoke is shown in figure 9. Along with the sensitivity test limits, results from 9 separate FE/DE tests are shown as well. It is seen that for the most part, the FE/DE results fall outside the UL black smoke test limits yielding lower transmittance values over the MIC output range, although the trend is the same. Although certainly related to the characteristics of the smoke, the reasons for the difference has not been studied.

2.4 Calibration of Smoke and CO alarms

Calibration details for each type of detector are described below, including alarm power requirements, data acquisition details, and observations on sensor range limits. While the data collection conditions were similar between the laboratory calibrations runs and field tests for the analog alarms, slight differences between alarm power, signal transmission noise environment, and amplifier characteristics could affect initial (clean air) sensor voltage readings, not to mention background environmental effects. It is important to account for these differences in some cases by shifting field test baselines.

The FE/DE uses a custom routine programmed with National Instrument's Labview software running on a Pentium PC computer. Analog data acquisition is performed with two AT-MIO/AI E series multifunction I/O boards. The modified alarm analog signals were digitized on a AT-MIO-16E-10 board configured for 8 differential inputs, with a voltage range of 0 V to 10 V. It has 12 bit resolution, and an offset error of ± 0.5 mV and a gain error of $\pm 0.01\%$ of reading. The input impedance of the programmable gain amplifier is $100\text{ G}\Omega$ in parallel with 50 pF with input and offset bias currents of $\pm 200\text{ pA}$ and 100 pA respectively. All floating signal sources (i.e. battery powered alarms) had their ground reference (negative terminal) tied to the board analog input ground.

For smoke alarms, typically two flaming soot and two smoldering smoke calibration runs were performed for each detector prior to field test use, followed by a single smoldering smoke calibration run after each use in a field test series. CO alarms were subjected to a single smoldering smoke calibration run prior to field tests with the smoldering smoke calibration re-run after a field test series. The calibration data for each detector is available [15]. The data fields for the smoke alarms consist of test time, air temperature, laser light transmittance from the upper laser beam, relative humidity in the duct, barometric pressure in the laboratory, MIC output, and alarm voltage signal. The continuous time data is segmented into time blocks with nominally steady smoke production to produce the steady values for calibration. Over these steady periods, the mean values of alarm voltage, MIC output, and laser light transmittance were computed and recorded along with the standard deviation. From the mean laser light output, the

extinction (m^{-1}), $k = \ln(I / I_0) / L_m$, where I is the light intensity, I_0 is the initial light intensity, and L_m is the path length in meters. Obscuration (%/ft),

$obs = \left(1 - \left(I/I_0\right)^{1/L_f}\right) \times 100$, where L_f is the path length in feet, were computed along with their standard deviation. The data fields for the ionization alarms include a dimensionless variable, Y , computed from the alarm voltage signal whose functional form was derived from ionization chamber theory [16, 17]. Y is defined as:

$$Y = \left(\frac{\Delta V}{V_O}\right) \left(\frac{2 - \Delta V/V_O}{1 - \Delta V/V_O} \right) \quad (1)$$

Since the ion chamber current is proportional to the ion alarm analog voltage (V), a simple substitution is made. V_O is the initial “clean air” chamber voltage and ΔV is ($V_O - V$). The benefit of converting the alarm output to the dimensionless variable Y is that it is a linear function of obscuration. Best fit lines through obscuration versus Y provides the calibration equation. These best fit lines are presented along with the calibration data, beginning in figure 11. During the re-calibration of detectors, the picoammeter used to measure the MIC chamber current ceased functioning and subsequently, only light extinction data are reported for re-calibration runs.

The data collected for the CO alarms include: CO and CO_2 analyzer voltage output, and the CO alarm voltage, (the MIC output is not included). The conversion factor between voltage and volume fraction for the CO analyzer is $93.0 (\text{volume fraction} \times 10^6)/\text{V}$, with a stated measurement uncertainty of 2.5×10^{-6} volume fraction. The conversion factor for the CO_2 analyzer is 7.48×10^{-3} (volume fraction)/V, with a stated measurement uncertainty of 4.0×10^{-5} volume fraction.

Ionization smoke alarm Ion-1: The analog output was provided by the alarm's application specific integrated circuit (ASIC) as a voltage signal proportional to the ion chamber current flow. 9.00 V was provided by a variable voltage DC power supply. Clean air voltage level was on the order of 6 V and the value decreased with increasing smoke level.

Ionization smoke alarm Ion-3: Similar to Ion-1, the analog voltage was provided by the alarm's application specific integrated circuit (ASIC) as a voltage signal proportional to the ion chamber current flow. 9.00 V was provided by a variable voltage DC power supply. Clean air voltage level was on the order of 4 V and the value decreased with increasing smoke level.

Ionization smoke alarm Ion-4: This alarm provided a digital signal that was transmitted to a multiplexing box that converted the digital signal to an analog voltage. The multiplexing box also provided the power to the detector. The clean air voltage level was nominally 0 V, with an increasing output in the presence of smoke. In order to compute Y values, a cutoff voltage of 2 V was specified and the voltage signal was transformed by the equation:

$$\text{New Signal} = 2 - \text{Old Signal} \quad (2)$$

With this transformation, new signal decreases with increasing smoke and equation (1) is used to compute Y . The 2 V cutoff voltage was chosen as an approximate upper limit for the output of the alarm.

Photoelectric smoke alarm Photo-1: This alarm was modified by adding a sample and hold IC and an amplifier to monitor and amplify the photo-detector signal. It needed a dual power supply of ± 9 V, which was provided by a series/parallel (6x2) arrangement of 1.5 volt AA size alkaline batteries. The nominal clean air voltage level was 0.2 V.

Photoelectric smoke alarm Photo-3: Identical to Ion-4, this alarm provided a digital signal that was transmitted to a multiplexing box that converted the digital signal to an analog voltage. The multiplexing box also provided the power to the detector. The clean air voltage level was nominally 0 V. The voltage output increased in the presence of smoke.

Photoelectric smoke alarm ASP-1: This alarm is a commercial design and already has the provision for an amplified analog voltage proportional to the photodetector signal. It has an integrated fan that aspirates room air through a special filter medium and into the sensing chamber periodically at a fixed time interval. While it has no smoke entry lag characteristics, its response was affected by the aspiration time interval (normally 30 s). It was powered at 12.0 V by a variable voltage DC power supply.

Carbon monoxide alarm CO-1: This alarm contained a semiconductor tin oxide CO sensor and provided a digital signal that was transmitted to a multiplexing box that converted the digital signal to an analog voltage. The multiplexing box also provided the power to the detector. As a consequence of its programming, this alarm did not produce any voltage change until the CO volume fraction was greater than 50×10^{-6} (as indicated on the unit's LED display). Calibrations for this alarm start at 50 (volume fraction $\times 10^6$).

Carbon monoxide alarm CO-2: This alarm contained a CO electrochemical cell, and provided an analog voltage proportional to the concentration of CO. These alarms were powered by a fresh alkaline 9 volt battery. The nominal clean air voltage level was 0.45 V.

Carbon monoxide alarm CO-3: This alarm contained a CO electrochemical cell, and provided an analog voltage proportional to the concentration of CO. 9.00 V was provided by a variable voltage DC power supply. Clean air voltage level was on the order of 0 V.

Representative calibration plots are show in figures 11 to 17 for each alarm type. A single smoldering test was used to specify a specific alarm's calibration used for particular test series.

The test series are identified as S1, S2 and S3 for the first manufactured homes series (tests 1 to 15), the two-story home (tests 20 to 28), and the second manufactured home series (tests 30 to 42) respectively. The alarm calibrations are listed in table 1.

Table 1. Calibration of smoke and CO alarms

Detector	Test Series ^a	m_0^b	m_1^b	R ^c
Aspirated-1- - -3	s1	-1.629	2.971	0.988
	s3	-1.392	2.064	0.999
Aspirated-1- - -5	s1	-1.512	2.568	0.996
	s2	-1.349	2	0.999
	s3	-1.672	2.144	0.985
Aspirated-1- - -6	s1	-1.276	1.846	0.996
	s2	-1.714	2.324	0.996
Aspirated-1- - -7	s1	-1.37	2.625	0.991
	s2	-1.598	3.021	0.994
	s3	-2.338	3.994	0.981
Aspirated-1- - -12	s1,s2	-1.727	2.998	0.999
CO-1- - -1	s1	-44.67	239.1	0.999
CO-1- - -2	s2	-0.733	109.1	0.98
CO-1- - -3	s2	-9.807	153.7	0.993
CO-1- - -4	s1	-4.379	129.8	0.999
CO-1- - -5	s1	-43.62	233.2	0.97
CO-1- - -6	s1	-19.05	100.7	0.991
	s3	1.61	114.1	0.986
CO-1- - -8	s1	-33.82	193	0.975
CO-1- - -9	s1	-22.58	180.9	0.997
	s3	24.76	153.4	0.958
CO-1- - -10	s2	-10.32	132.5	0.988
CO-1- - -14	s3	56.17	110	0.979
CO-1- - -16	s2,s3	27.5	132.2	0.969
CO-1- - -17	s2,s3	34.38	140	0.944
CO-2- - -1	s1	-45.93	109.4	0.995
CO-2- - -2	s1	-45.07	92.91	0.993
CO-2- - -3	s3	-59.45	117.6	0.999
CO-2- - -5	s1	-48.8	113.7	0.999
CO-2- - -6	s2	-57.92	115.2	0.999
	s3	-74.84	179.5	0.998
CO-2- - -8	s2	-52.18	119.9	0.999
	s3	-56.24	144.3	0.999
CO-2- - -9	s2	-58.96	137.9	0.998
	s3	-63.73	128.8	0.991
CO-2- - -11	s1	-50.37	104.25	0.997
CO-2- - -12	s2	-45.4	93.62	0.997
	s3	-48.92	98.93	0.997
CO-2- - -13	s2	-44.05	103.4	0.999
CO-3- - -1	s2	-6.924	166.1	0.999

Detector	Test Series ^a	m_0^{b}	m_1^{b}	R ^c
CO-3- - -2	s2	-2.237	165.7	0.999
CO-3- - -3	s2	-5.251	161.6	0.996
	s3	-2.551	165.4	0.997
CO-3- - -4	s1	-6.457	163.4	0.998
CO-3- - -5	s1	-6.232	170.8	0.999
CO-3- - -6	s1	-0.882	172.9	0.99
	s3	-1.96	173.8	0.999
CO-3- - -7	s2	-2.464	171.2	0.999
	s3	-2.58	168.8	0.995
CO-3- - -8	s1	-2.542	165.5	0.998
CO-3- - -10	s1	-2.954	165.7	0.998
CO-3- - -11	s3	-4.059	163.1	0.998
Ion-1- - -1	s1		2.151	0.998
Ion-1- - -2	s3		2.07	0.997
Ion-1- - -3	s2		1.789	0.995
Ion-1- - -4	s1		1.66	0.991
Ion-1- - -5	s2		2.164	0.998
	s3		1.827	0.994
Ion-1- - -6	s1		2.27	0.997
Ion-1- - -7	s1		1.685	0.987
Ion-1- - -8	s3		1.823	0.997
Ion-1- - -9	s2		1.93	0.999
	s3		1.863	0.992
Ion-1- - -10	s1		1.919	0.998
Ion-1- - -11	s1		2.093	0.997
	s3		2.095	0.999
Ion-3- - -1	s3		1.247	0.985
Ion-3- - -2	s3		1.197	0.988
Ion-3- - -3	s1		1.215	0.949
Ion-3- - -4	s2		1.558	0.998
Ion-3- - -6	s1		1.421	0.997
Ion-3- - -7	s2		1.001	0.998
	s3		1.007	0.999
Ion-3- - -9	s1		1.144	0.998
Ion-3- - -10	s1		0.984	0.999
Ion-3- - -11	s2		1.184	0.987
	s3		1.299	0.989
Ion-3- - -13	s1		1.147	0.995
Ion-3- - -17	s2		1.066	0.988
Ion-4- - -1 ^d	s1		1.462	0.996
	s3		1.506	0.998
Ion-4- - -2 ^d	s2		2.374	0.99
Ion-4- - -3 ^d	s1		1.463	0.992
Ion-4- - -4 ^d	s3		2.926	0.997
Ion-4- - -5 ^d	s1		1.806	0.953
Ion-4- - -6 ^d	s1		3.353	0.984
	s3		2.624	0.985
Ion-4- - -8 ^d	s1		2.562	0.997
Ion-4- - -9 ^d	s2		1.35	0.996

Detector	Test Series ^a	m_0 ^b	m_1 ^b	R ^c
	s3		1.222	0.998
Ion-4- - -10 ^d	s1		2.642	0.993
	s3		2.498	0.984
Ion-4- - -11 ^d	s2		1.832	0.996
Ion-4- - -12 ^d	s2		3.202	0.985
Photo-1- - -1	s1	-0.801	5.779	0.997
	s2	-2.351	7.755	0.997
	s3	-2.274	8.117	0.997
Photo-1- - -2	s1	-2.185	5.786	0.997
	s2	-3.761	8.383	0.994
	s3	-2.758	8.589	0.987
Photo-1- - -3	s1	-1.498	6.717	0.997
	s2,s3	-1.566	7.855	0.998
Photo-1- - -4	s1	-1.523	8.569	0.995
	s2	-0.0972	0.452	0.999
	s3	-2.569	14.15	0.996
Photo-1- - -5	s1	-1.963	6.882	0.996
Photo-1- - -6	s1	-1.56	9.248	0.997
	s2	-2.195	11.82	0.997
	s3	-2.154	12.67	0.997
Photo-3- - -1 ^d	s2	-1.724	11.03	0.999
	s3	-2.415	12.87	0.999
Photo-3- - -2 ^d	s2	-1.701	9.473	0.998
Photo-3- - -3 ^d	s1	-1.734	10.83	0.999
Photo-3- - -4 ^d	s1	-0.875	8.524	0.995
	s3	-2.408	11.2	0.998
Photo-3- - -5 ^d	s1	-2.096	11.563	0.999
Photo-3- - -6 ^d	s1	-1.421	9	0.999
	s3	-1.825	12.032	0.997
Photo-3- - -8 ^d	s1	-1.411	10.574	0.996
Photo-3- - -9 ^d	s1	-1.289	9.323	0.999
	s3	-1.532	10.124	0.998

a For the purposes of these calibrations, the test series is identified as s1 for tests 1-15, s2 for tests 20-28, and s3 for tests 30-41.

b $Obs_{ion} = m_1 Y$ (in %/ft), where Y is defined in eq. (1)

$Obs_{photo} = m_0 + m_1 V$ (in %/ft), where V is in volts

$X_{CO} = m_0 + m_1 V$ (in volume fraction x 10⁶), where V is in volts

c R is the square root of the coefficient of determination for the regression equation defined in note b.

d Alarms Photo-3 and Ion-4 are components of a single dual alarm.

Due to differences in power supply levels, data acquisition hardware, signal noise pickup, and other environmental effects, initial “clean air” voltage signals measured in the field tests usually deviated slightly from those observed in laboratory tests. In applying the calibration equations to test series data, differences in initial “clean air” values were handled in a consistent manner. First, an average initial value was obtained from the twenty recorded values preceding the start of the test (time = 0), typically 20 s of data. Second, adjustments were made using this initial

voltage. In the case of photoelectric and CO sensors, the difference between the calibration “clean air” value ($-m_0/m_1$) and the average initial value was added to the data to adjust for any offset. In the case of the ionization sensors, equation 1 was applied to the test data and using the initial “clean air” average as V_0 .

2.5 Alarm Identification

Throughout the report, each alarm is identified with a specific code that identifies the model of the alarm, the location the alarm was used in a test, and the specific sample of the alarm used (see figure 10). The code has the format ‘device type’ - ‘model’ - ‘alarm board location’ - ‘alarm board position’ - ‘alarm sample’ where ‘device type’ specifies the technology of the device, ‘model’ is a number which identifies a specific model of the type, ‘alarm board location’ is a letter code that specifies where in the structure the alarm was located for a specific test, ‘alarm board position’ is a number that specifies the location of the alarm on an alarm board in a particular test, and ‘alarm sample’ is a number which identifies a specific sample of an alarm. For example, Ion-1-A-3-8 describes a specific model of an ionization alarm (Ion-1) located on alarm sensor board ‘A’ at position 3 (-A-3) and it is identified as the eighth sample of that particular model alarm. Since the calibrations were not dependent upon a position in a test and these test locations were randomly varied throughout the test series to minimize systematic errors due to specific alarm placement, the ‘alarm board location’ and ‘alarm board position’ are left blank in table 1. Appendix A includes full identification for every alarm in each of the tests.

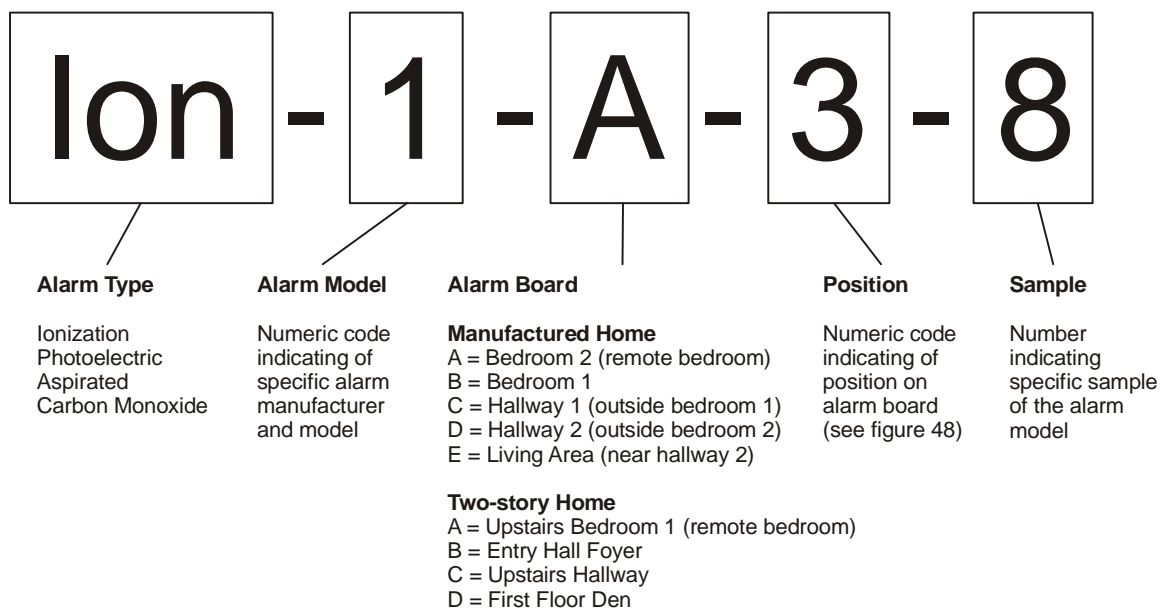


Figure 10. Alarm identification coding

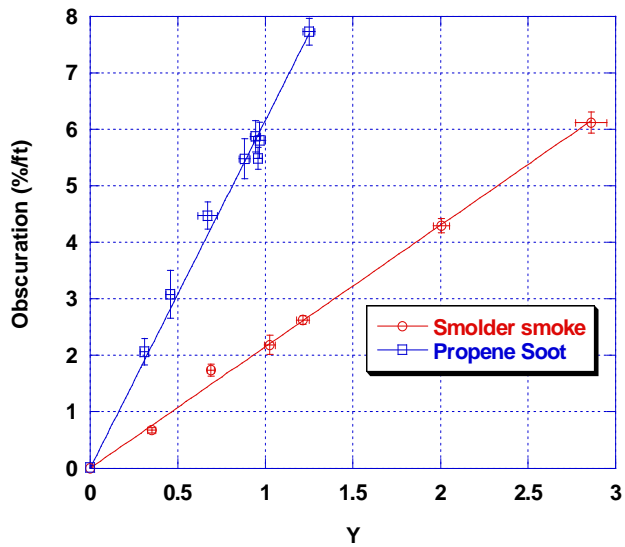


Figure 11. Calibration runs for Ion-1 alarm

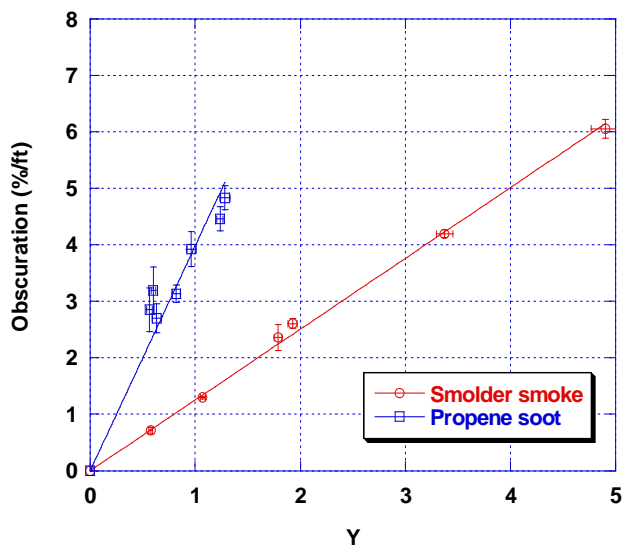


Figure 12. Calibration runs for Ion-3 alarm

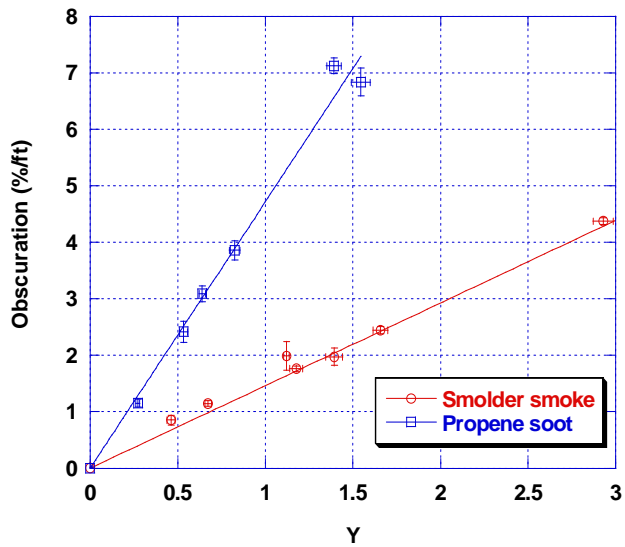


Figure 13. Calibration runs for Ion-4 alarm

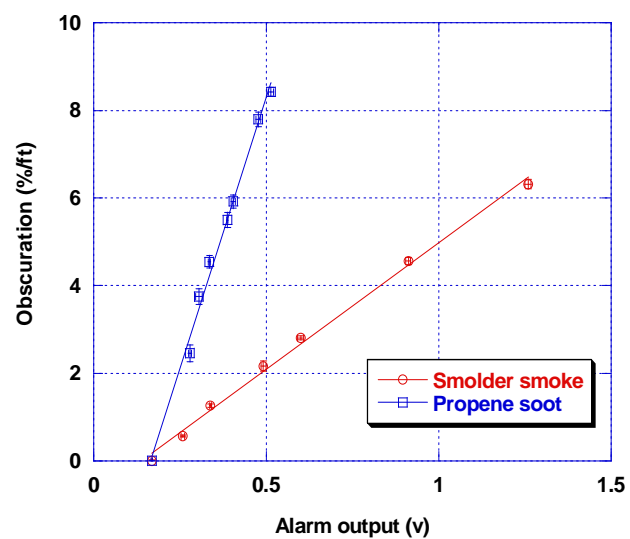


Figure 14. Calibration runs for Photo-1 alarm

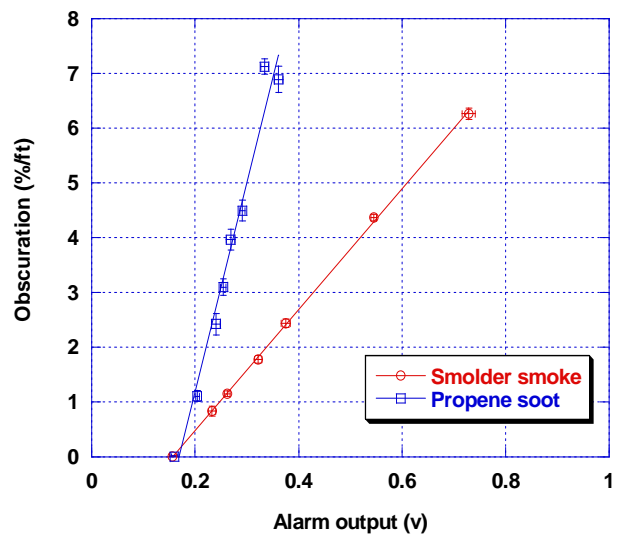


Figure 15. Calibration runs for Photo-2 alarm

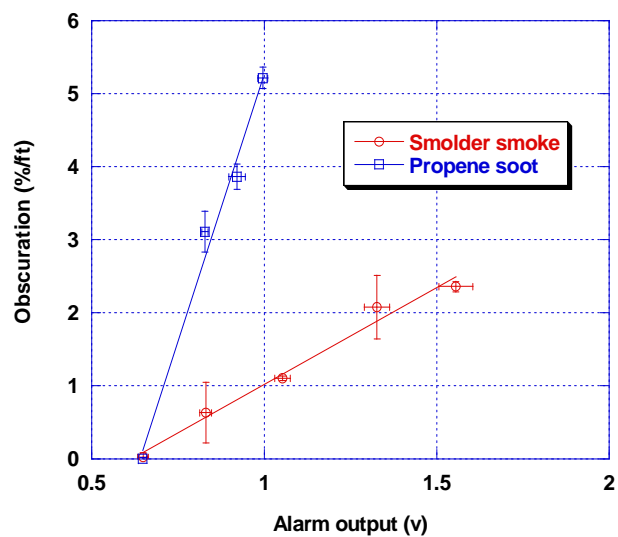


Figure 16. Calibration runs for ASP alarm

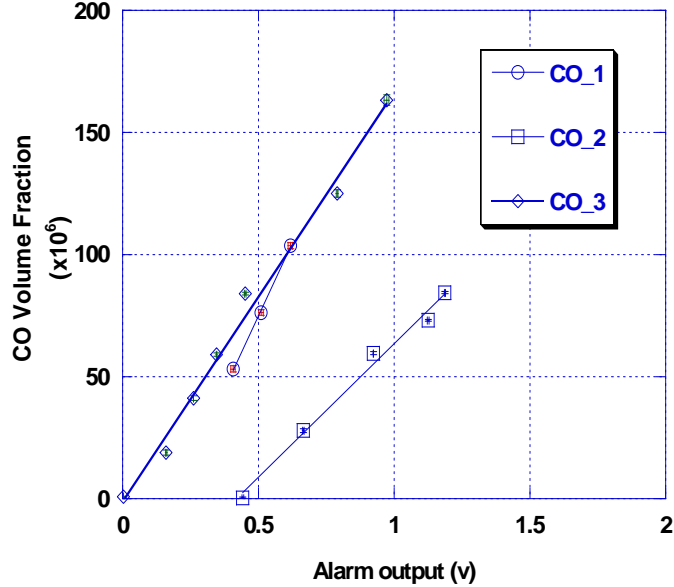


Figure 17. Calibration runs for CO alarms

2.6 Evaluation of Unmodified Alarm Response

Unmodified smoke alarms of the same models selected for modified alarms Ion-1, Ion-3 and Photo-1 were used in the test series at locations where thermal damage might potentially occur, and to supplement the analog output alarm results. Each of these alarms were powered with a previously unused 9 V alkaline battery and the alarm state was determined by monitoring the interconnect voltage signal. This signal changes from nominally 0 V to approximately 7 V to 9 V when the alarm threshold is met, with a 3 s delay in the response. No adjustment was made in the data for this delay.

In order to verify the manufacturer-specified alarm response, a number of alarms were tested after they had been used in fire tests. Cotton wick smoke, generated by the staged wick ignition device, was used to produce an increasing level of smoke in the FE/DE (the ignition protocol was different than the one used in the calibration of modified alarms.) After 30 s delay from the start of data logging, groups of wicks were ignited in series. The delay time between the application of power to the ignition coils was either 12 s or 30 s, with between one and four wicks ignited at each step. The FE/DE fan speed was set to 12 Hz which produced a mean axial velocity of 0.16 m/s at the center of the duct test section, and 50 mm (2 in) below the ceiling. Alarms pairs were placed in the FE/DE test section side by side and the interconnect voltage signal was recorded for each alarm. The nominal alarm sensitivities recorded on the alarms and the production range is given in table 2 along with the corresponding transmittance values over a 1.52 m (5.0 ft) path length.

Table 2. Listed unmodified alarm sensitivities.

Alarm Model	Sensitivity %/m (%/ft)	Sensitivity Range %/m (%/ft)	Transmittance	Transmittance Range (hi/low)
Ion-1	4.13 (1.26)	$\pm 1.2 (\pm 0.38)$	0.939	0.957/0.921
Ion-3	4.23 (1.29)	$\pm 1.7 (\pm 0.51)$	0.937	0.962/0.913
Photo-1	6.76 (2.06)	$\pm 4.3 (\pm 1.3)$	0.901	0.963/0.843

The following graphs show the upper laser transmittance and the alarm interconnect voltage for pairs of like-model alarms. The corresponding 1.52 m (5.0 ft) transmittance values equivalent to the model's listed sensitivity range are shown as dashed horizontal lines. At the test flow velocity, the smoke entry lag time should be short, thus detectors should alarm somewhere within the upper and lower transmittance boundaries.

Figures 18 – 27 show the results for 12 Photo-1 photoelectric type alarms. Typically, 8 wicks ignited in pairs of two every 12 seconds was sufficient to produce enough smoke to set off the alarms. Disposable alarms Disp-10 and Disp-46 appeared to be less sensitive than the majority of the photoelectric alarms. Disp-10 alarmed when a group of 16 wicks was used (figure 27). The light transmittance at alarm was typically at the middle sensitivity value. Thus, the unmodified alarms can be expected to provide alarms consistent with the manufacturer's specification. Similar and consistent alarm criteria will be chosen for the measurements from the modified alarms.

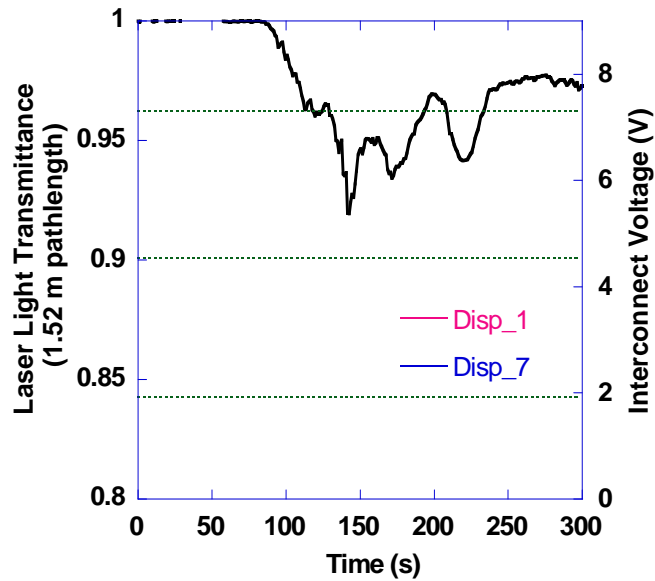


Figure 18. Photo-1, eight wicks – 12 s delay,
Disp 1 and Disp 7 alarms

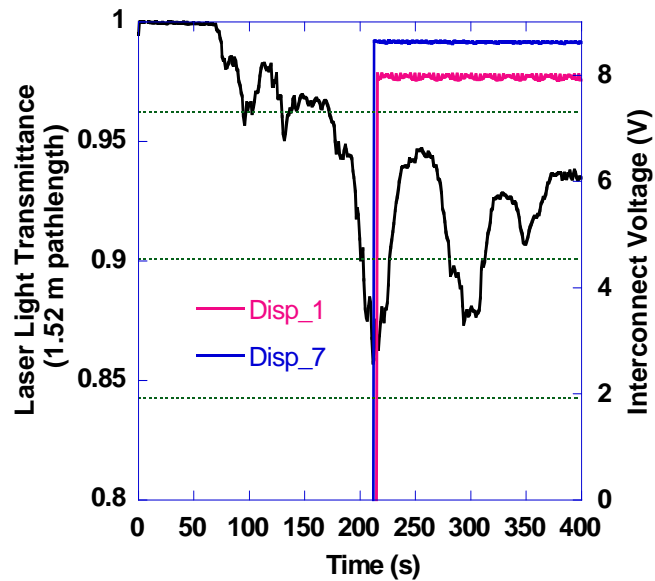


Figure 19. Photo-1, 16 wicks – 12 s delay,
Disp 1 and Disp 7 alarms

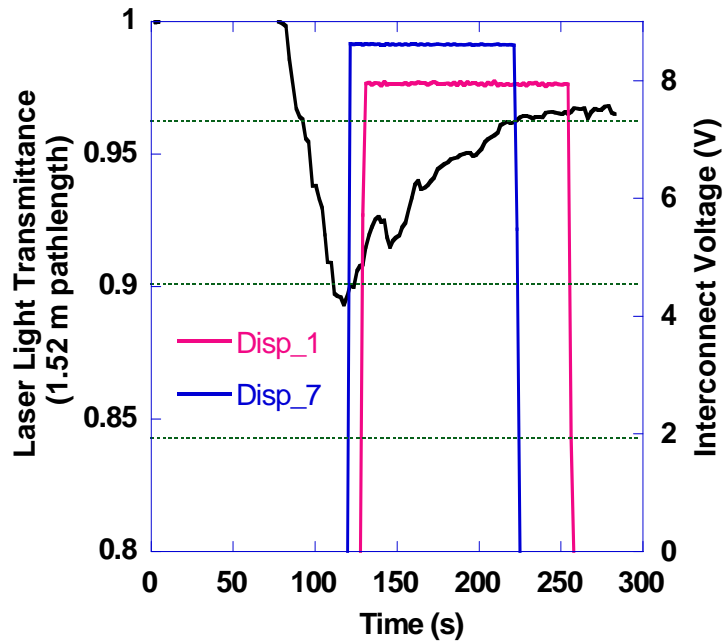


Figure 20. Photo-1, eight wicks – 12 s delay,
Disp 1 and Disp 7 alarms

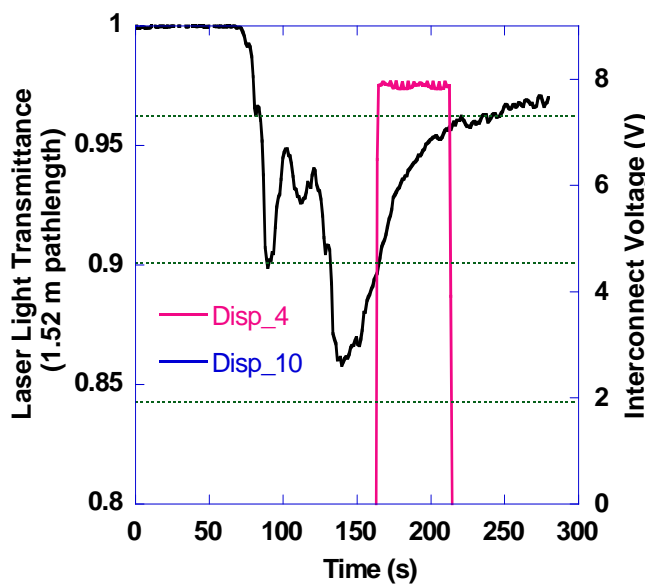


Figure 21. Photo-1, eight wicks – 30 s delay,
Disp 4 and Disp 10 alarms

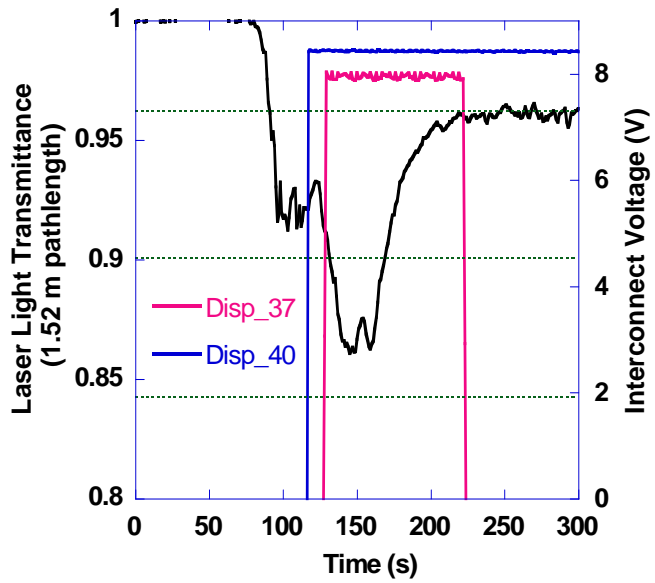


Figure 22. Photo-1, eight wicks – 12 s delay,
Disp 37 and Disp 40 alarms

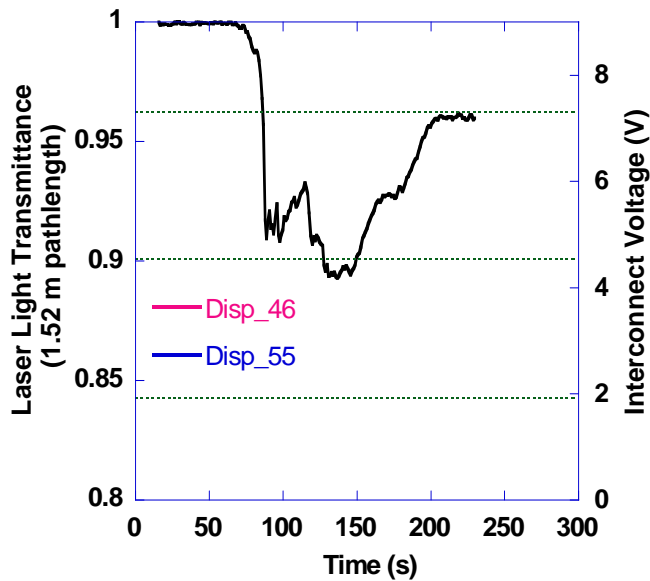


Figure 23. Photo-1, eight wicks, 12 s delay,
Disp 46 and Disp 55 alarms

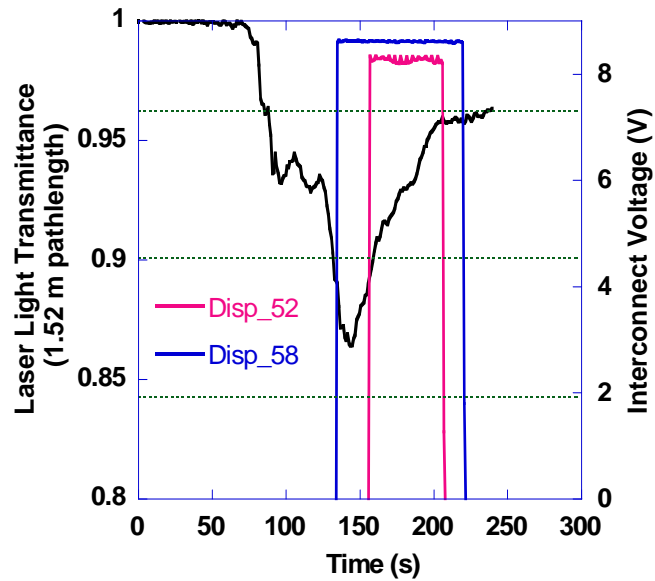


Figure 24. Photo-1, eight wicks – 12 s delay,
Disp 52 and Disp 58 alarms

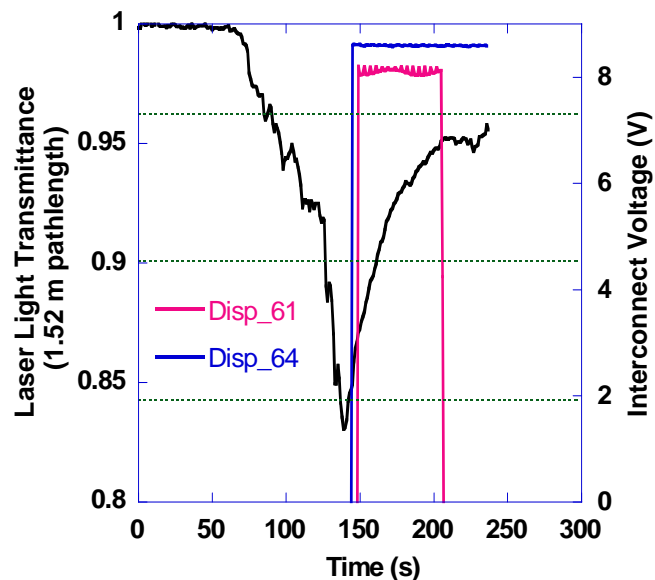


Figure 25. Photo-1, eight wicks – 12 s delay,
Disp 61 and Disp 64 alarms

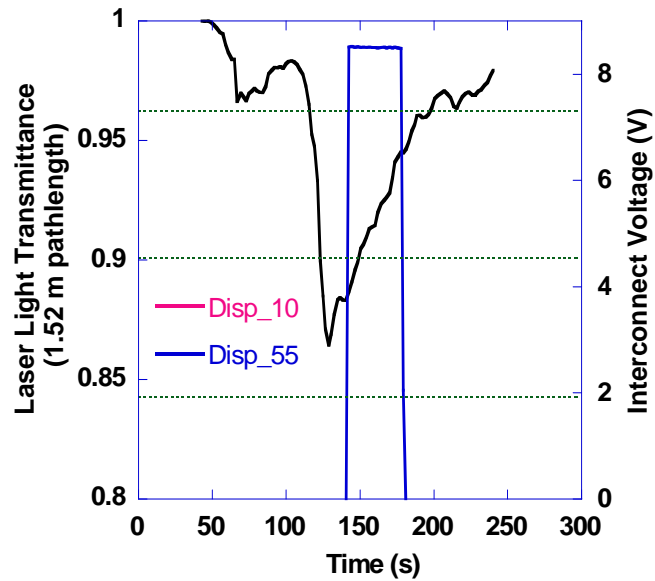


Figure 26. Photo-1, eight wicks – 12 s delay,
Disp 10 and Disp 55 alarms

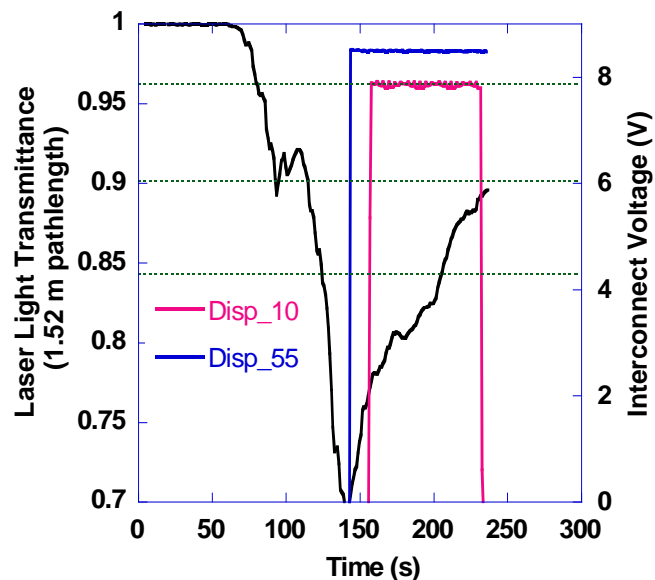


Figure 27. Photo-1, 16 wicks – 12 s delay,
Disp 10 and Disp 55 alarms

Figures 28 – 37 show the results for 12 Ion-1 ionization type alarms. Typically, 4-6 wicks ignited separately every 30 s was sufficient to produce alarms. The light transmittance at alarm was typically at the upper sensitivity value. On one occasion, the alarms were set off at transmittance levels above the upper sensitivity value.

Figures 38 – 47 show the results for 12 Ion-3 ionization type alarms. Typically, 3 wicks ignited separately every 30 s was sufficient to produce alarms. The light transmittance at alarm was typically above the upper sensitivity value for this alarm.

For the most part, these tests confirm that each model of unmodified alarm yielded consistent sensitivity results with cotton wick smoke generated in the FE/DE. The two ionization alarms with the same nominal sensitivity showed a demonstrable difference in the actual sensitivities for the alarms tested here. Moreover, the tendency for the ionization alarms to appear more sensitive than the nominal sensitivity listed on the alarms raises some questions related to the differences between smoke generation techniques, smoke properties, and measurement techniques of the UL smoke box and the FE/DE.

Recall that the steady smoke generated in the calibration tests falls within the allowed bounds of light transmittance versus MIC output up to a transmittance value of approximately 0.9 (figure 44). The MIC picoammeter was not functioning during the verification tests, so several cotton smolder tests were performed after it was repaired to assure consistent results with earlier tests (figure 8). These results, shown in figure 48, follow the lower sensitivity limit quite closely until a transmittance value of 0.94, then the FE/DE results deviate outside the UL limits for grey smoke. Additional tests were conducted to better quantify differences between the two ionization alarms relative to their response to the FE/DE smolder smoke. Separate tests using one, two, three, and four wicks were conducted. An Ion_1 and an Ion-3 alarm were placed in the test section, and the wicks were allowed to burn for several hundred seconds in order to achieve steady obscuration and MIC output values. The mean obscuration and MIC output along with the alarm state were obtained during the steady burning period. Table 3 shows the results for four tests.

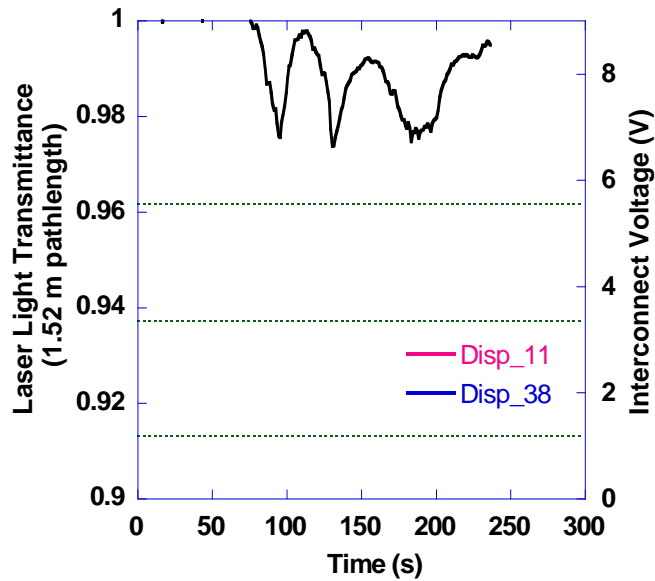


Figure 28. Ion-1, three wicks - 30 s delay,
Disp 11 and Disp 38 alarms

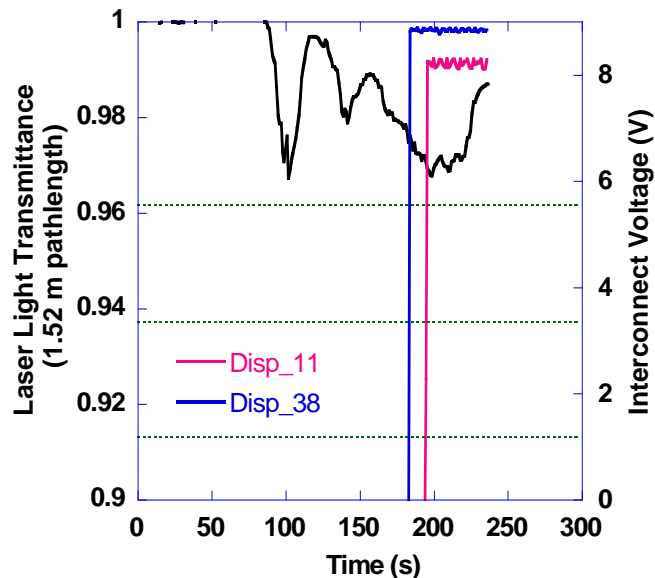


Figure 29. Ion-1, four wicks - 30 s delay,
Disp 11 and Disp 38 alarms

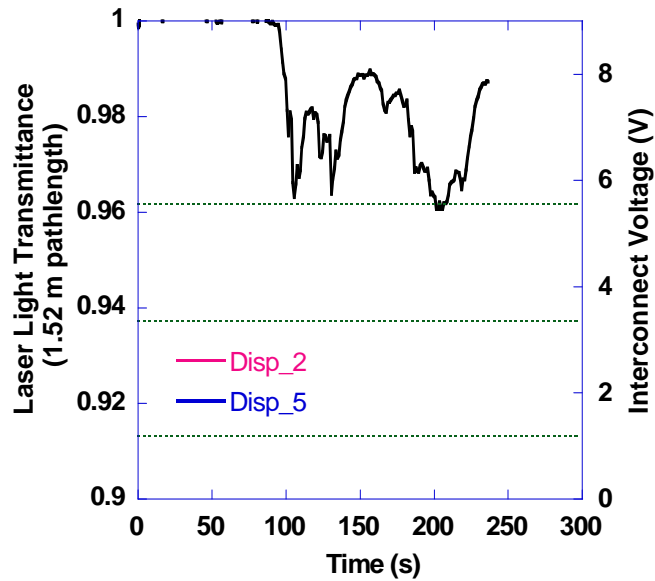


Figure 30. Ion-1, four wicks - 30 s delay,
Disp 2 and Disp 5 alarms

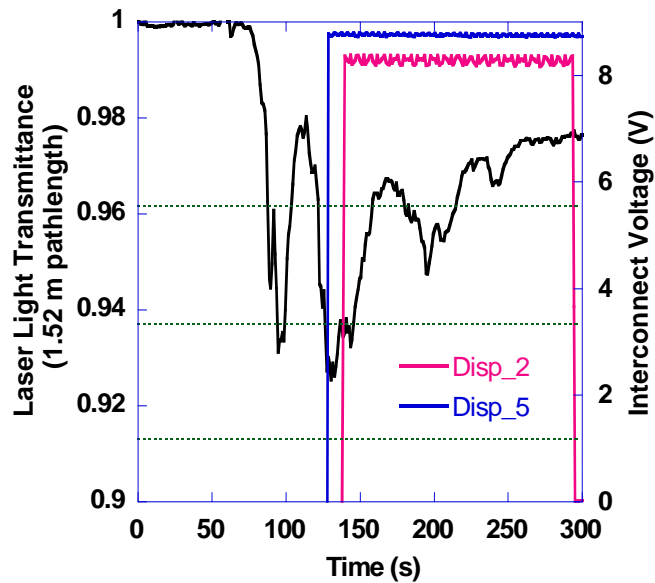


Figure 31. Ion-1, six wicks 12 s delay,
Disp 2 and Disp 5 alarms

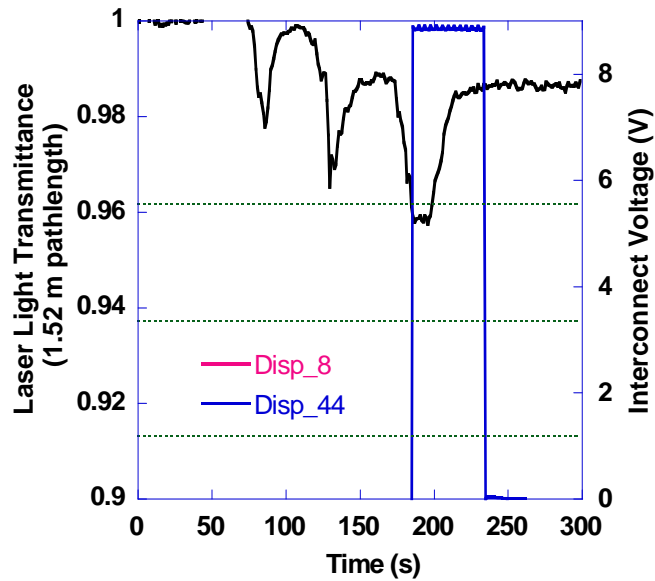


Figure 32. Ion-1, four wicks 30 s delay,
Disp 8 and Disp 44 alarms

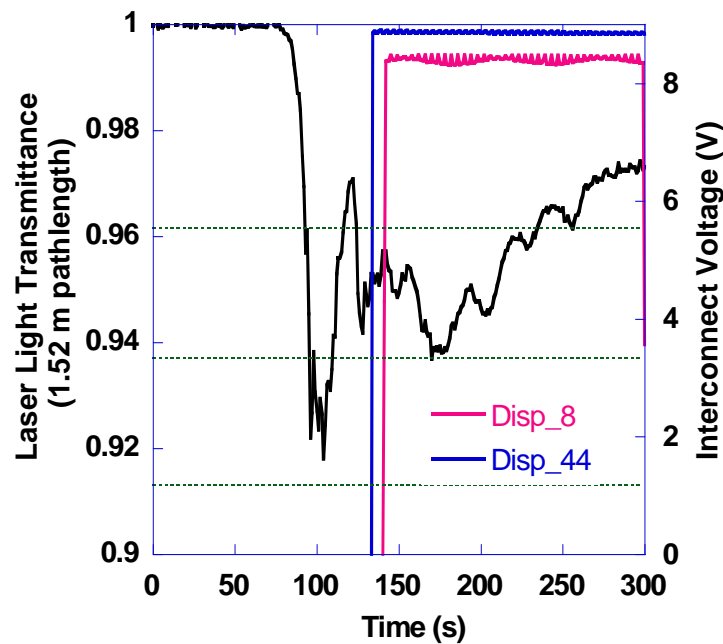


Figure 33. Ion-1, six wicks 12 s delay,
Disp 8 and Disp 44 alarms

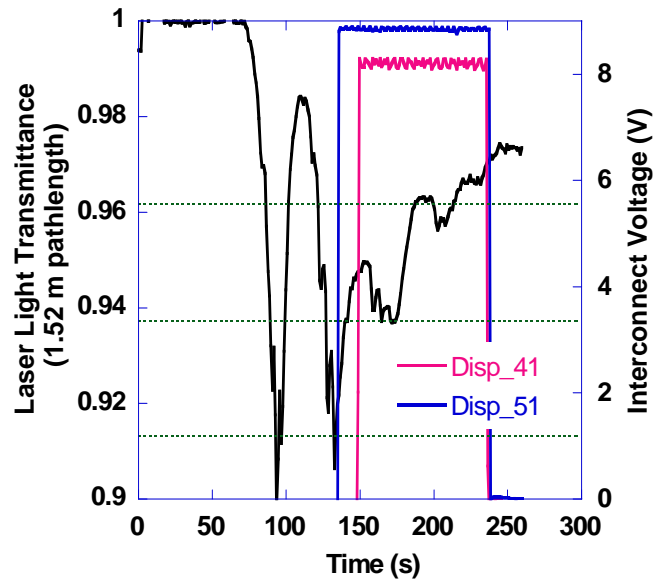


Figure 34. Ion-1, six wicks 12 s delay,
Disp 41 and Disp 51 alarms

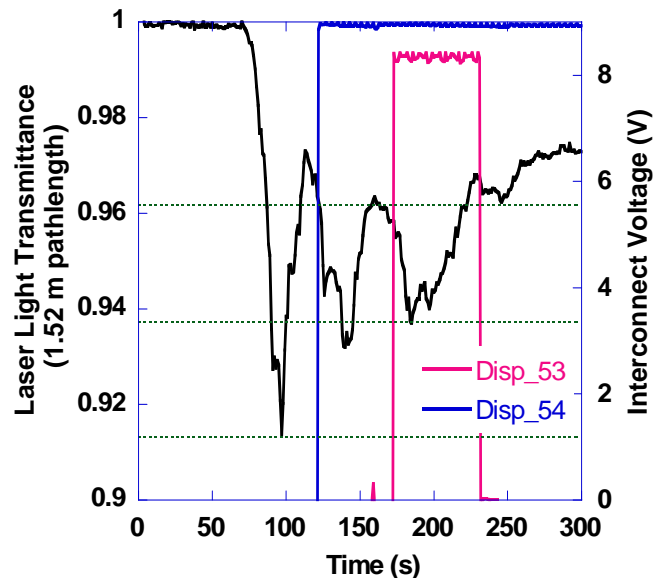


Figure 35. Ion-1, three wicks 12 s delay,
Disp 53 and Disp 44 alarms

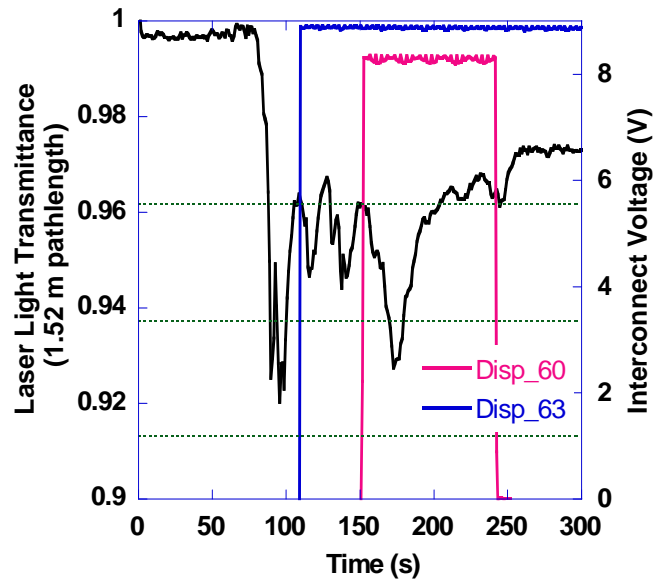


Figure 36. Ion-1, six wicks 12 s delay,
Disp 60 and Disp 63 alarms

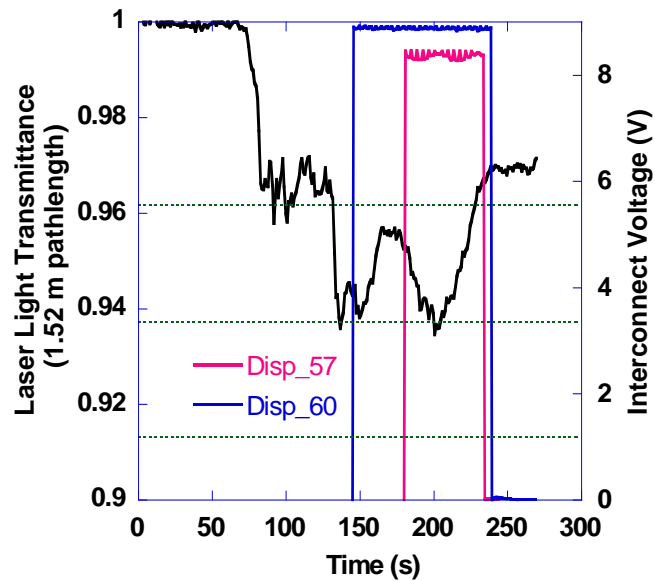


Figure 37. Ion-1, six wicks 12 s delay,
Disp 57 and Disp 60 alarms

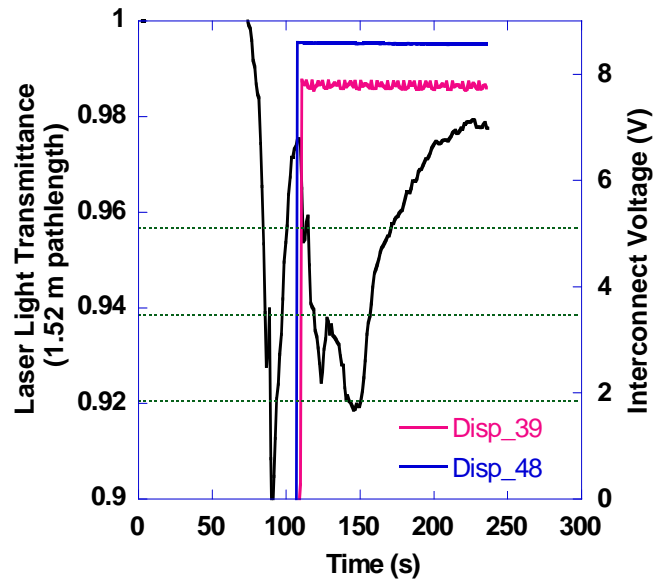


Figure 38. Ion-3, six wicks - 12 s delay,
Disp 39 and Disp 48 alarms

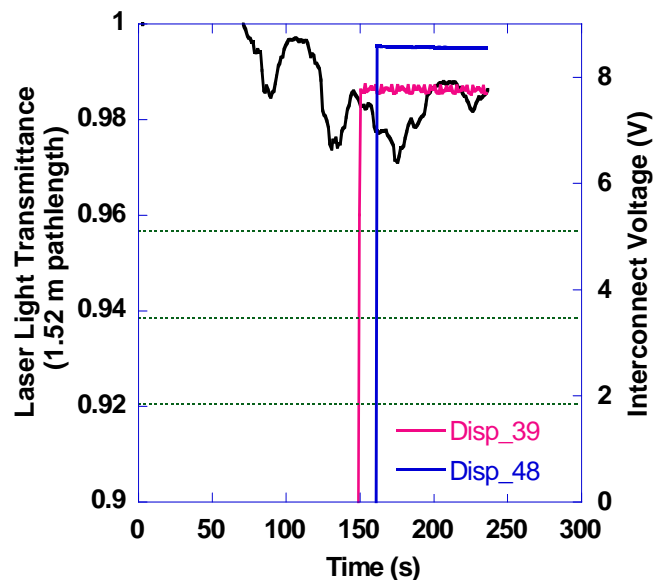


Figure 39. Ion-3, four wicks - 30 s delay,
Disp 39 and Disp 48 alarms

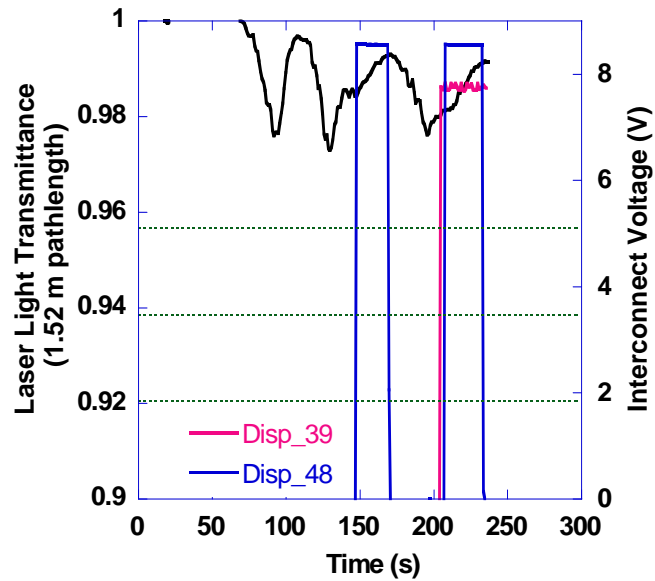


Figure 40. Ion-3, three wicks 30 s delay,
Disp 39 and Disp 48 alarms

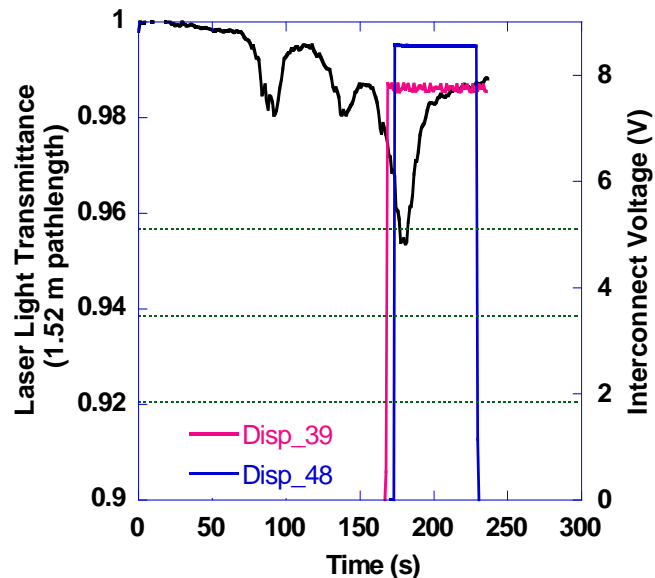


Figure 41. Ion-3, three wicks 30 s delay,
Disp 39 and Disp 48 alarms

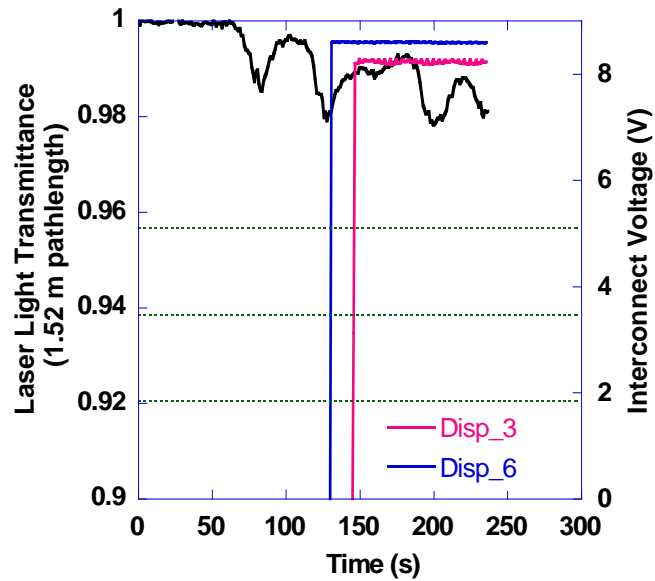


Figure 42. Ion-3, three wicks 30 s delay,
Disp 3 and Disp 6 alarms

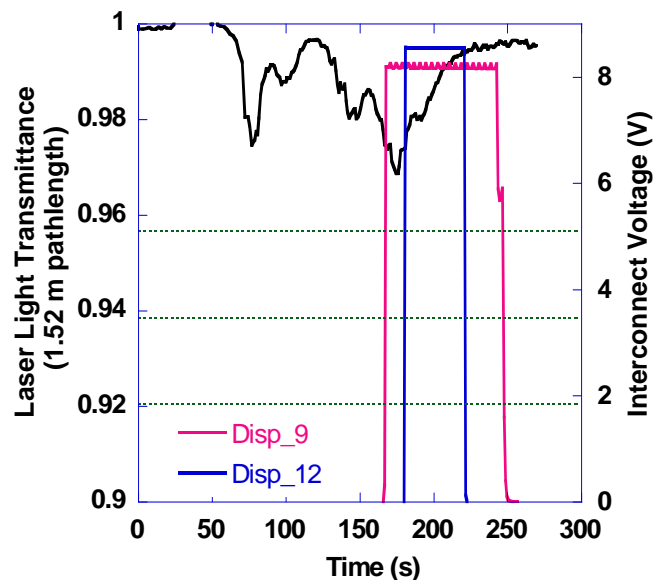


Figure 43. Ion-3, three wicks 30 s delay,
Disp 9 and Disp 12 alarms

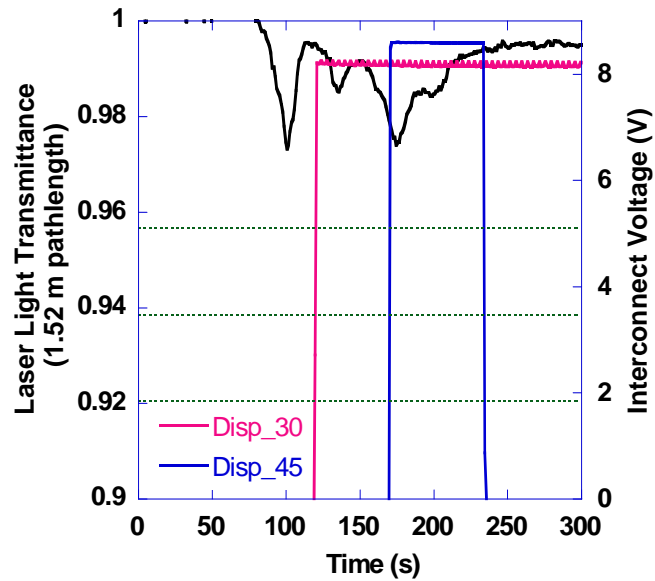


Figure 44. Ion-3, three wicks 30 s delay,
Disp 30 and Disp 45 alarms

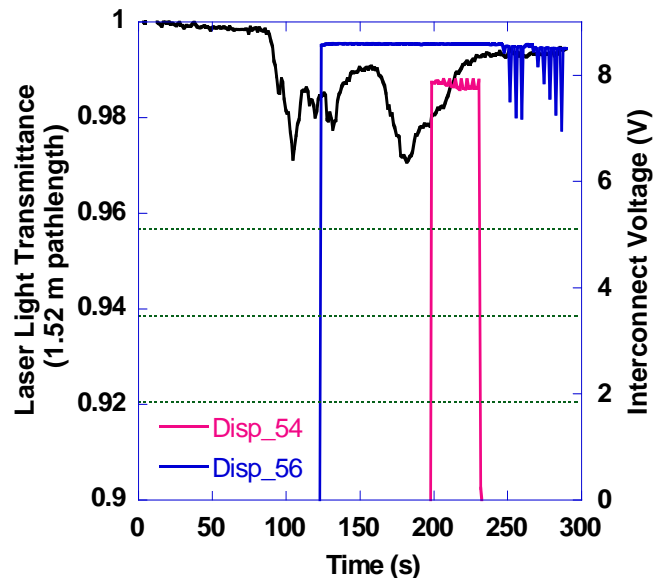


Figure 45. Ion-3, three wicks 30 s delay,
Disp 54 and Disp 56 alarms

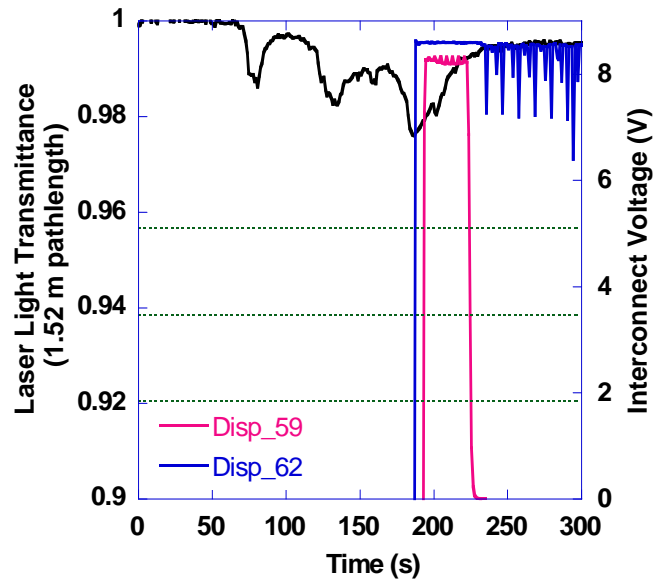


Figure 46. Ion-3, three wicks 30 s delay,
Disp 59 and Disp 62 alarms

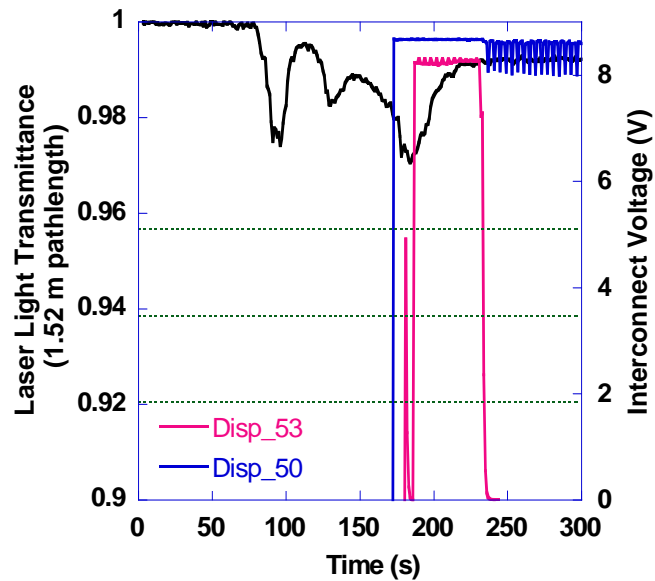


Figure 47. Ion-3, three wicks 30 s delay,
Disp 53 and Disp 50 alarms

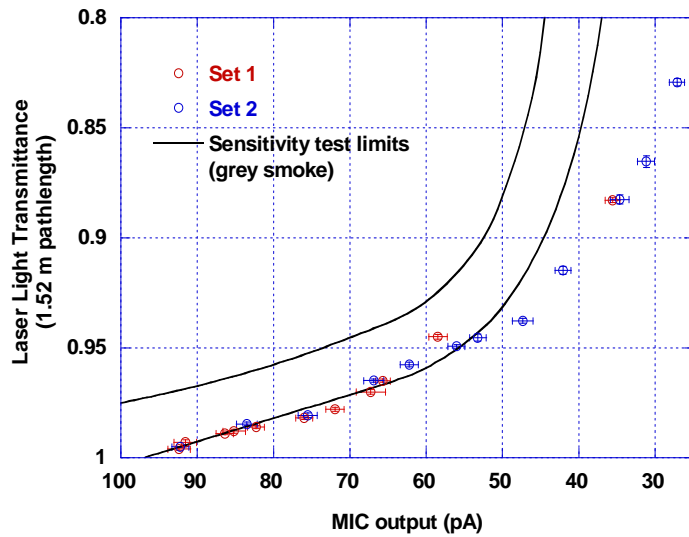


Figure 48. UL grey smoke (smolder smoke) sensitivity limits and FE/DE data

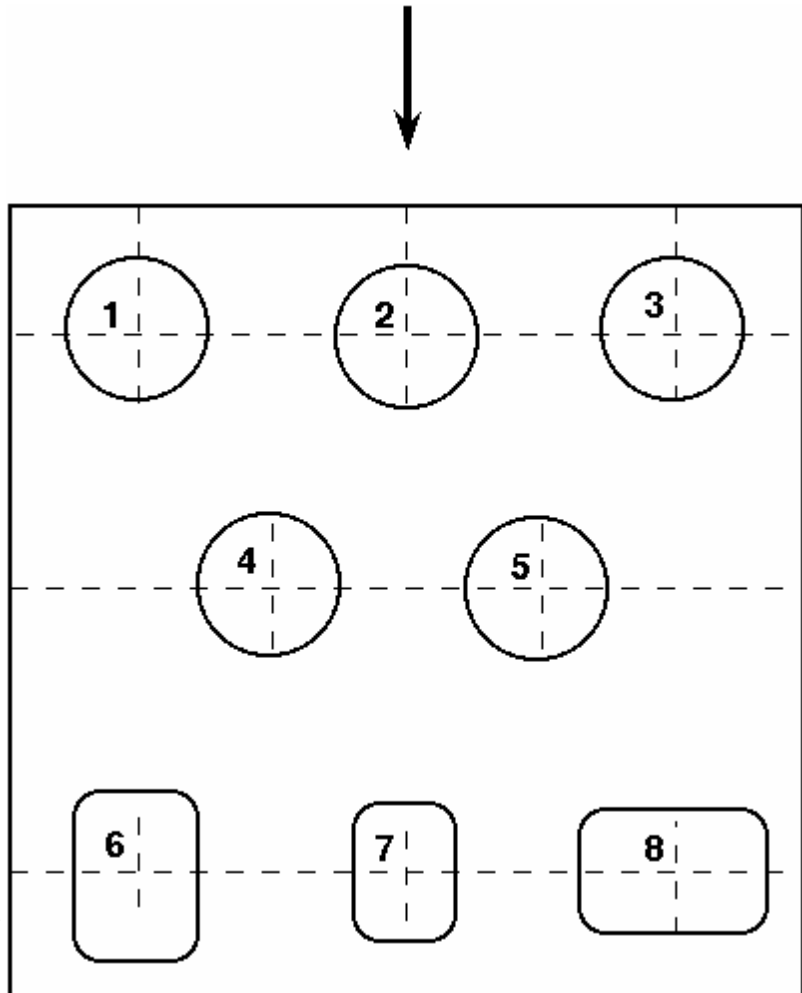
Table 3. MIC output and obscuration during tests of two ionization alarms

Number of wicks	Alarm state	Transmittance	MIC output	Obscuration (%/m / %/ft)
1	Ion-1 - off Ion-3 - off	0.985	85.2	1.0 / 0.31
2	Ion-1 - off Ion-3 - on	0.981	77.1	1.3 / 0.39
3	Ion-1 - off Ion-3 - on	0.965	68.3	2.4 / 0.72
4	Ion-1 - on Ion-3 - on	0.958	63.5	2.9 / 0.87

From the table above, an obscuration ranging from 1.3 %/m to 2.9 %/m (0.39 %/ft to 0.87 %/ft) was necessary for the devices to trip an alarm state. To insure the device would be expected to alarm (to insure both devices trip an alarm state would require an obscuration of 2.9 %/m or 0.87 %/ft), an approximate minimum value of $2.8 \%/\text{m} \pm 1.6 \%/\text{m}$ ($0.85 \%/\text{ft} \pm 0.5 \%/\text{ft}$) was used as representative of this range. This would correspond to MIC output values of 80.6 pA, 59.5 pA, and 50.9 pA for high, nominal and low sensitivity.

2.7 Effect of Sensor Board Location on Response

The test board layout was a compromise between placing multiple alarms at approximately the same physical location, while limiting the local flow effects the crowding of alarms will have and the biasing of sensor response due to position. The layout of the test board is shown in figure 49. Since the primary purpose of this study was the performance of smoke alarms, preference was given to the positioning of the smoke alarms and positions 1–5 were reserved for smoke alarms, while positions 6–8 were reserved for CO alarms. The arrow indicates the board orientation in the expected resultant flow during the fire tests. It is obvious from the layout that positions 4 and 5 may experience a flow blocking effect.



A series of tests were carried out in the FE/DE to quantify the

Figure 49. Test board layout

effects of the test board position of a smoke sensor on its response for 6 flow conditions. The test board was mounted on the ceiling of the FE/DE duct at the test section approximately 20 cm from the laser beam. Duplicate tests were performed on two different board configurations at 3 separate FE/DE fan speeds with and without a baffle placed upstream of the test section. The baffle is a 10 cm high by 20 cm long steel plate oriented across duct flow. Its function is to promote velocity fluctuations that are similar to those observed in room flows in section 6. Table 4 shows the mean axial velocity at a height 5 cm below the ceiling and standard deviation for each configuration. Figures 50 – 52 show the results for the three fan speeds with and without the baffle present.

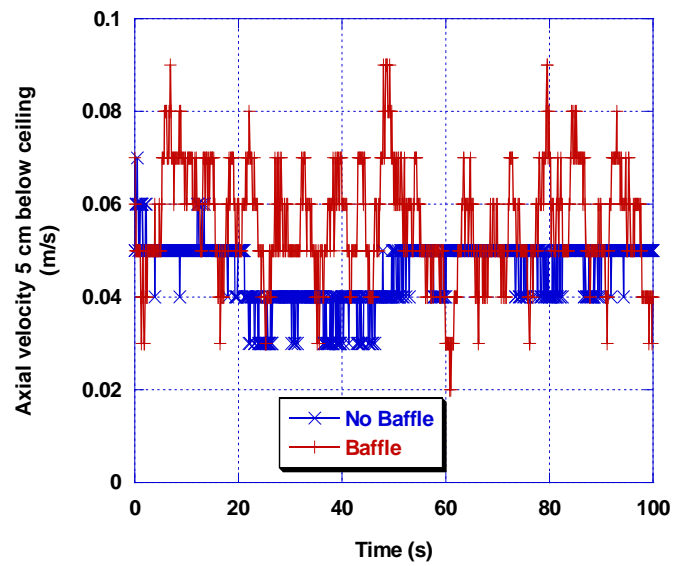


Figure 50. Axial velocity at a fan speed of 5 Hz

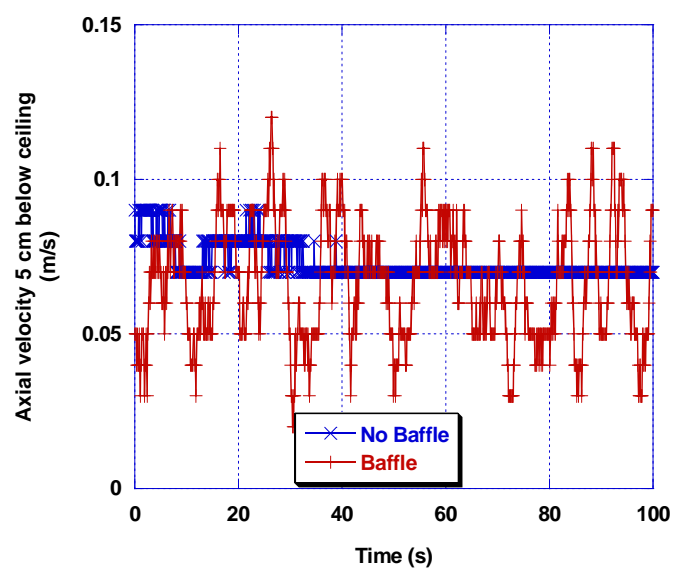


Figure 51. Axial velocity at a fan speed of 7 Hz

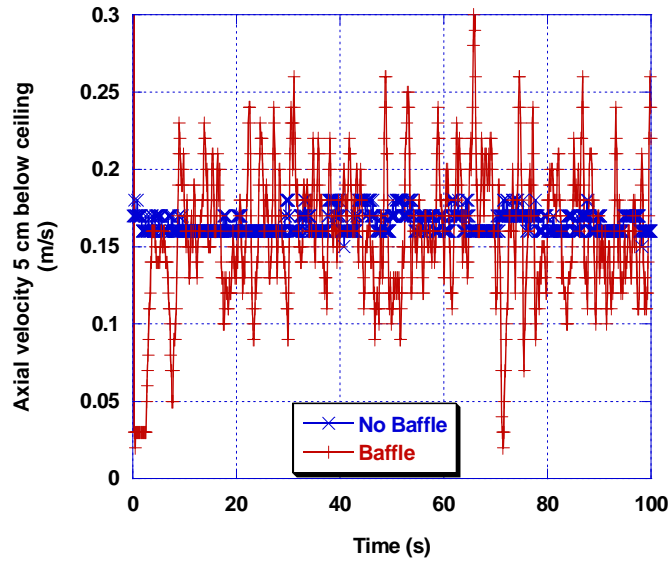


Figure 52. Axial velocity at a fan speed of 12 Hz

Table 4. Mean axial velocity 5 cm below ceiling

Fan speed		With baffle (m/s)	Without baffle (m/s)
5Hz	Velocity	0.057	0.047
	Standard deviation	0.01	0.004
7Hz	Velocity	0.073	0.073
	Standard deviation	0.021	0.005
12 Hz	Velocity	0.159	0.162
	Standard deviation	0.043	0.01

Alarm positions for board 1 are: position 1 - Ion-3- - -6, position 2 - Ion-1- - -1, position 3 - Photo-1- - -3, position 4 - (Ion-4- - -8 and Photo-3- - -8; these sensors are co-located in the same alarm housing), and position 5 empty. Alarm positions for board 2 are: position 1 is empty, position 2 - Ion-3- - -13, position 3 - (Ion-4- - -3 and Photo-3- - -3), position 4 - Ion-3- - -4, and position 5 - Photo-1- - -6. Thus, a Photo-1 type detector was in a front location on board 1 and a rear location on board 2, while Ion-4 and Photo-3 were in a rear location on board 1 and in a front location on board 2. Ion-1 was located in the front on board 1 and in a rear location on board 2; however, since location 1 is empty on board 2, the full effects of blockages are not expected. Ion-3 remained in a front location on each board. Smoke was generated with the same staged wick ignition device described earlier, using eight pairs of wicks with a 12 s ignition delay between pairs. Figures 53-76 show the results for each alarm.

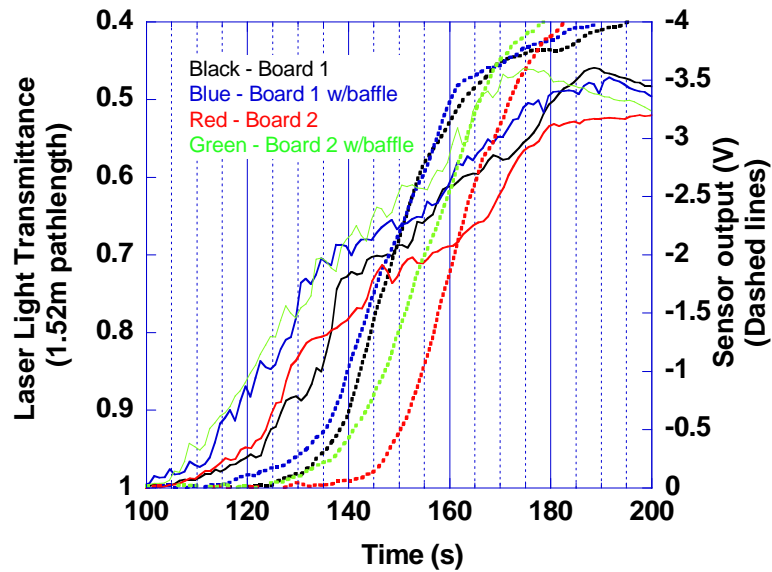


Figure 53. Ion-1 response, fan speed 5 Hz (see table 4)

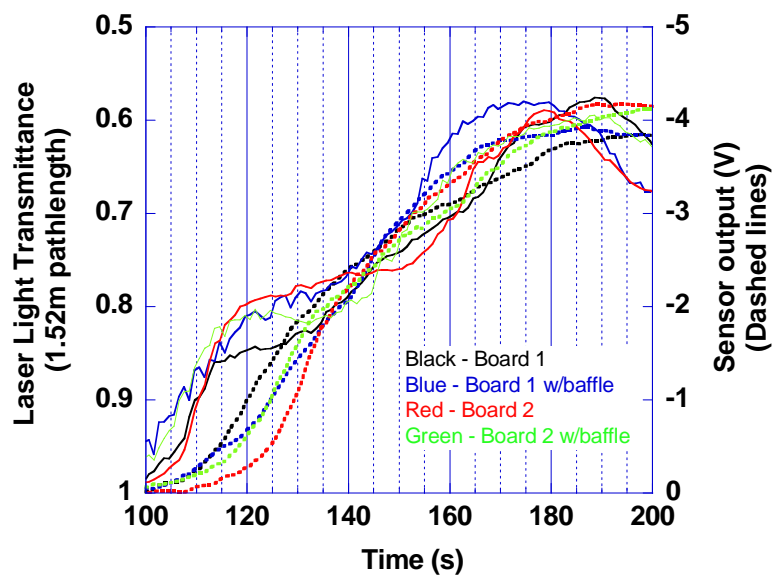


Figure 54. Ion-1 response, fan speed 7 Hz

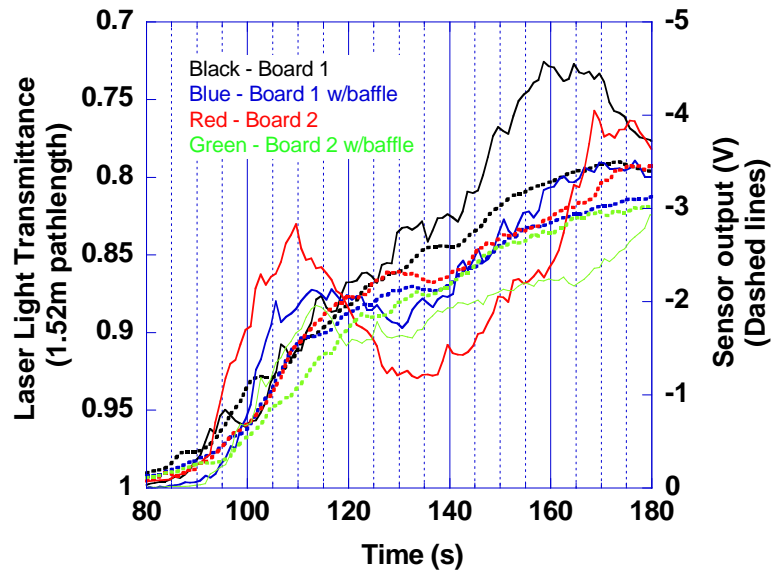


Figure 55. Ion-1 response, fan speed 12 Hz

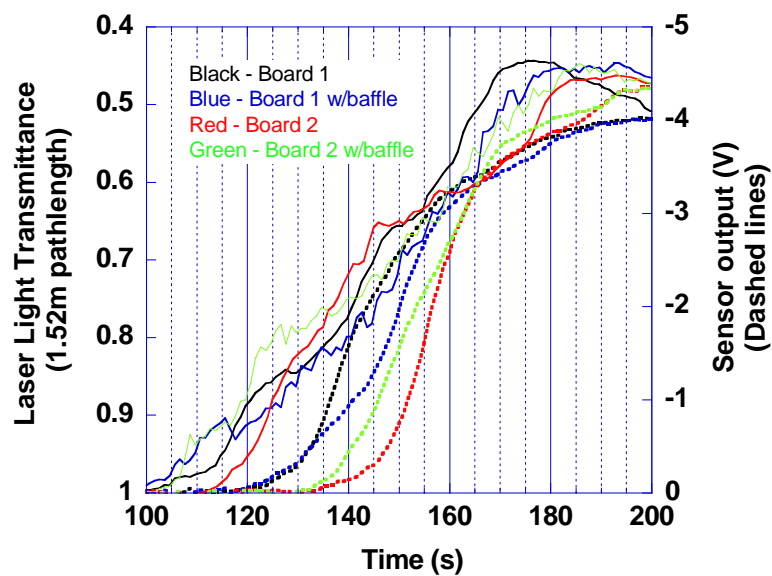


Figure 56. Ion-1 response, fan speed 5 Hz - repeat test

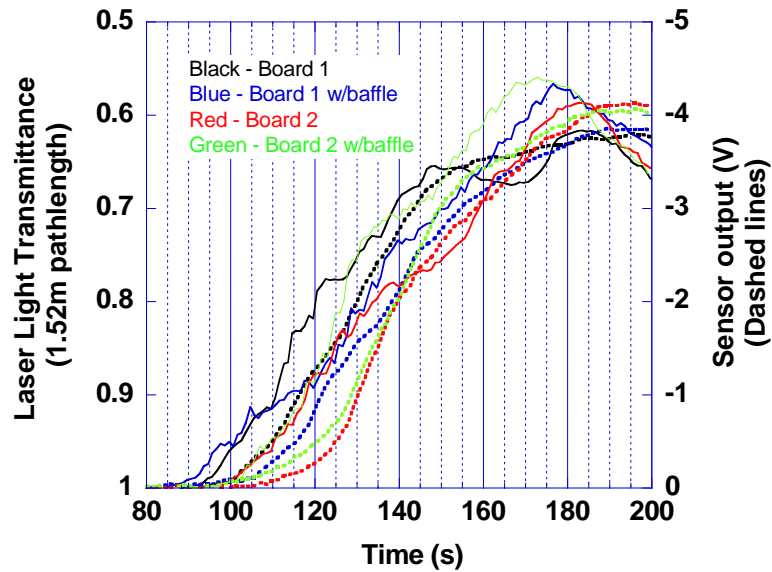


Figure 57. Ion-1 response, fan speed 7 Hz - repeat test

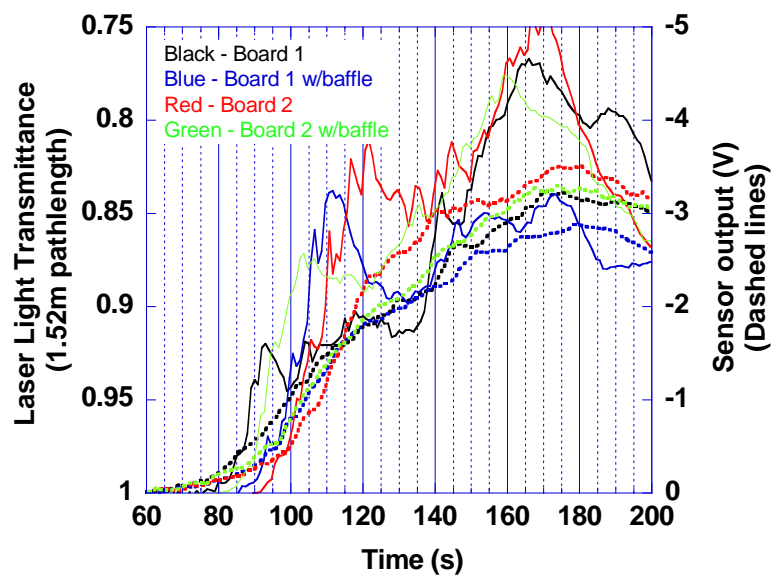


Figure 58. Ion-1 response, fan speed 12 Hz - repeat test

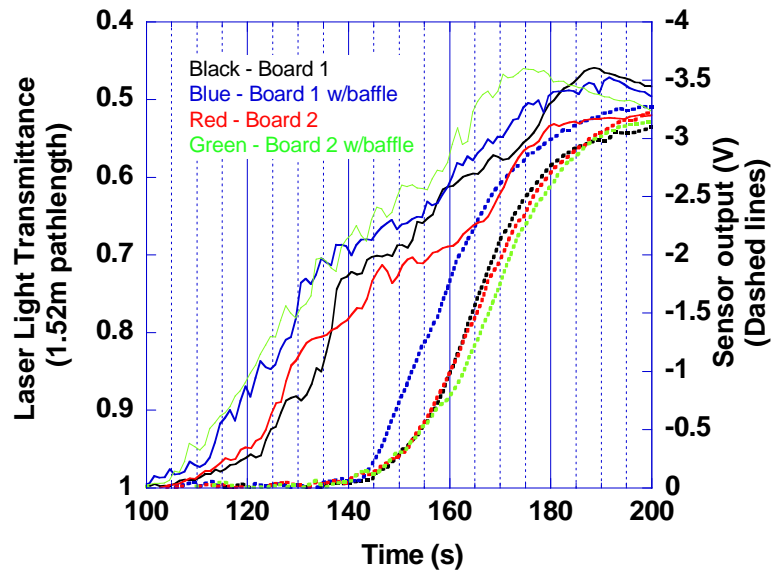


Figure 59. Ion-3 response, fan speed 5 Hz

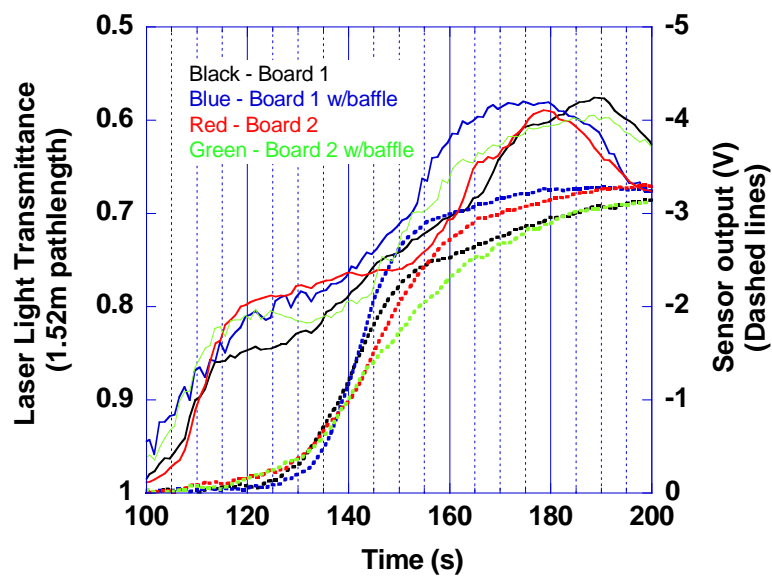


Figure 60. Ion-3 response, fan speed 7 Hz

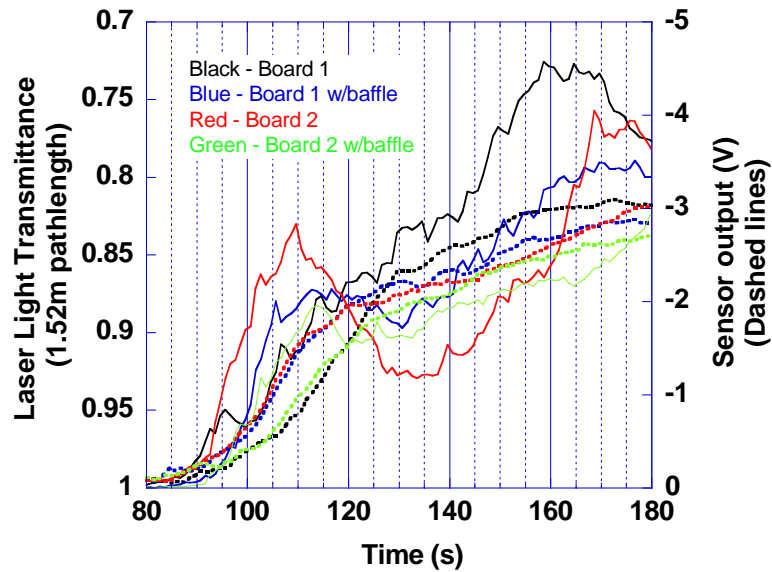


Figure 61. Ion-3 response, fan speed 12 Hz

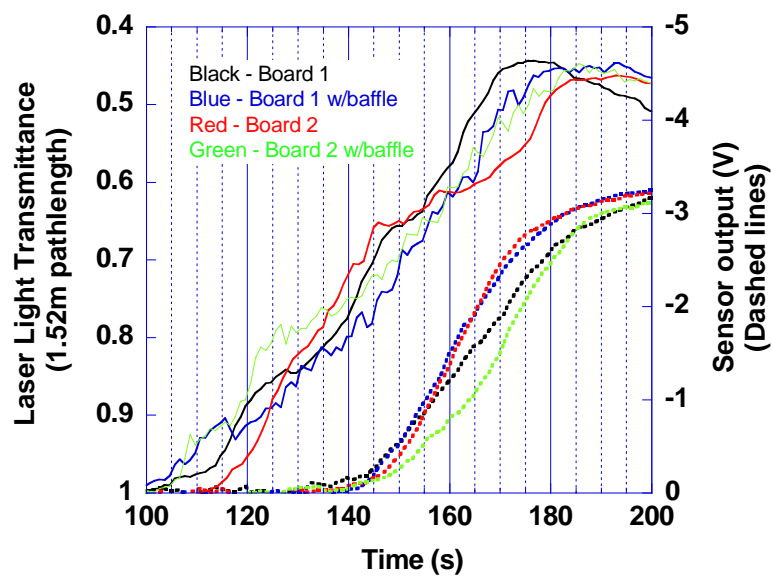


Figure 62. Ion-3 response, fan speed 5 Hz - repeat test

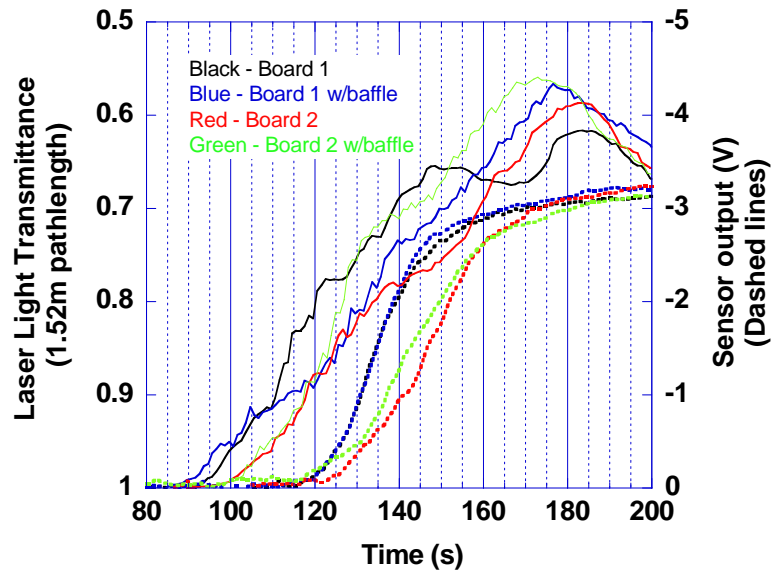


Figure 63. Ion-3 response, fan speed 7 Hz - repeat test

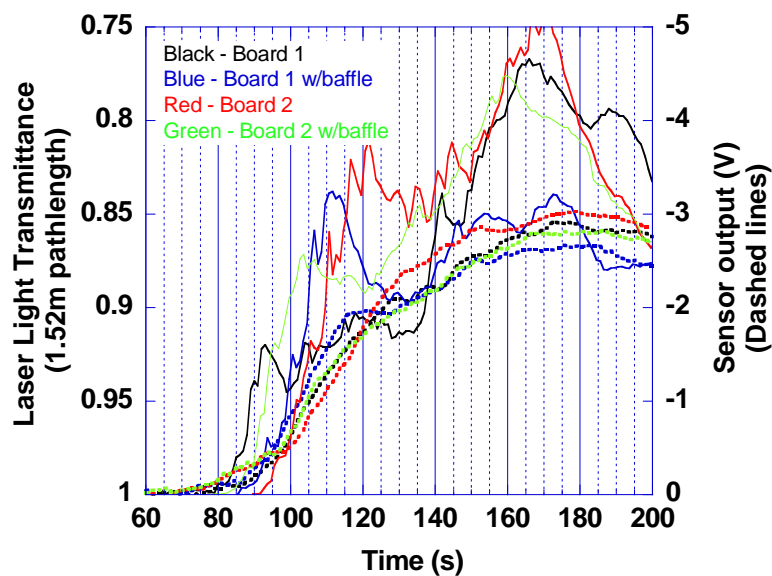


Figure 64. Ion-3 response, fan speed 12 Hz - repeat test

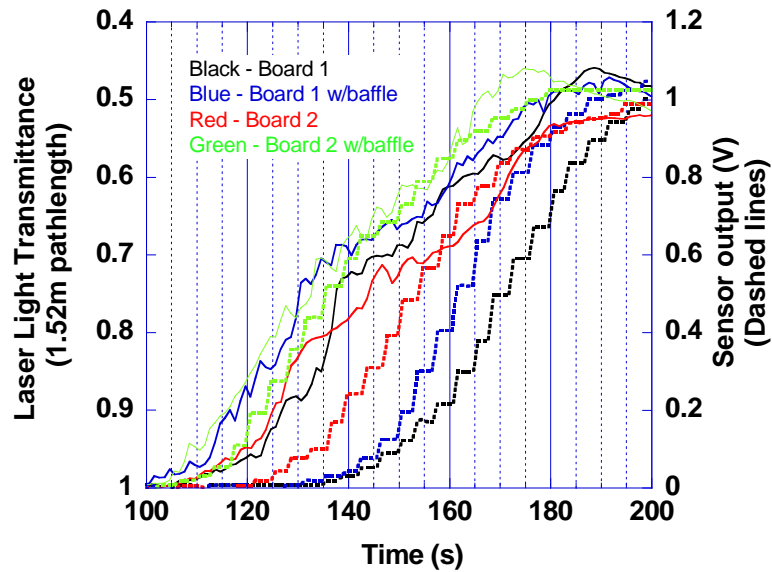


Figure 65. Ion-4 response, fan speed 5 Hz

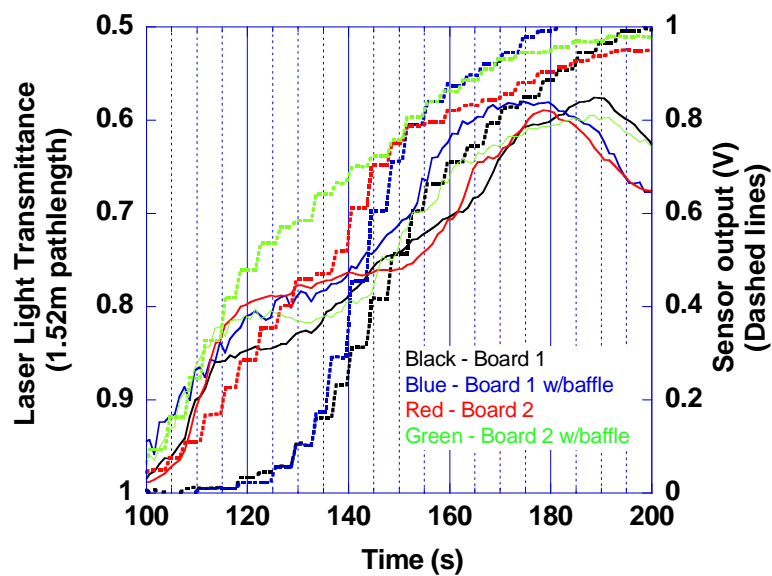


Figure 66. Ion-4 response, fan speed 7 Hz

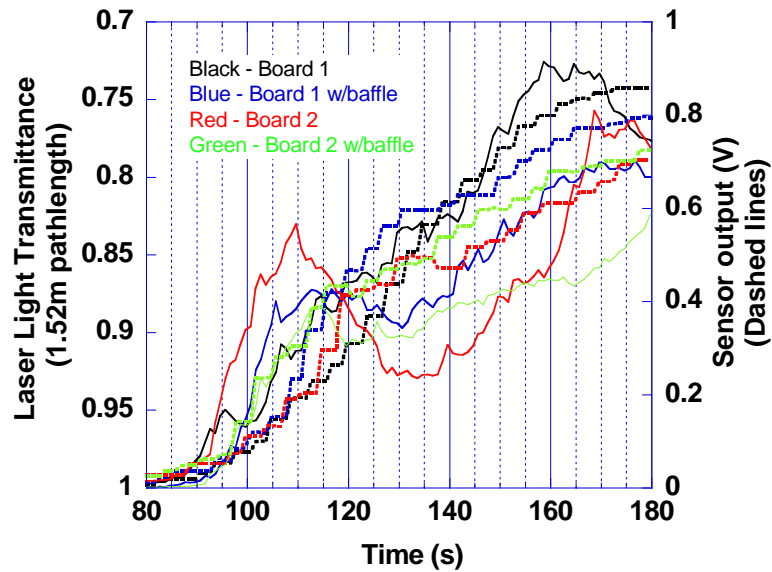


Figure 67. Ion-4 response, fan speed 12 Hz

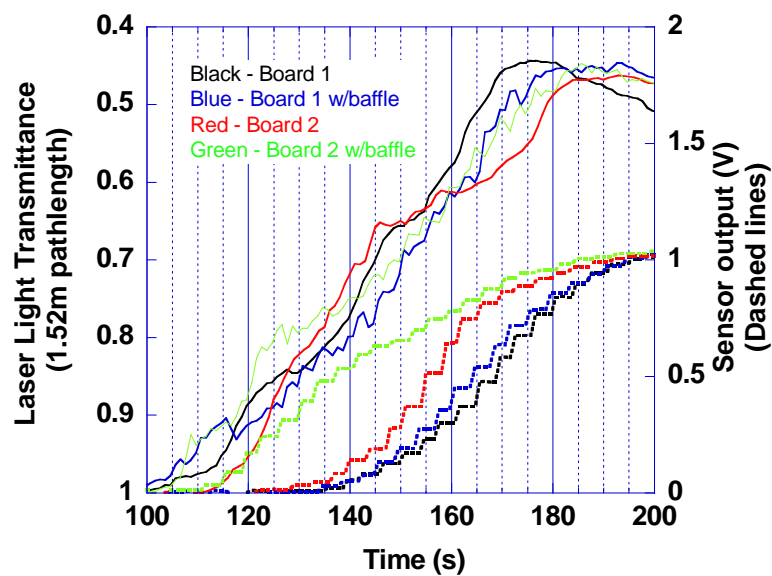


Figure 68. Ion-4 response, fan speed 5 Hz - repeat test

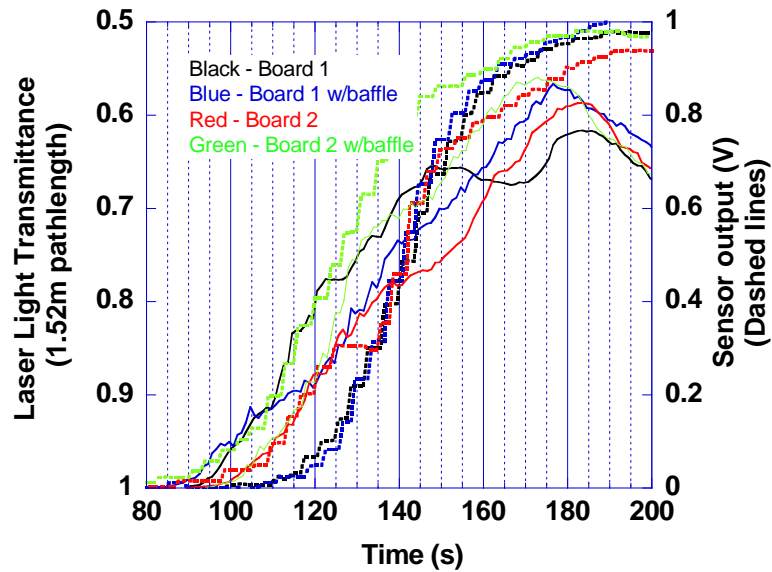


Figure 69. Ion-4 response, fan speed 7 Hz - repeat test

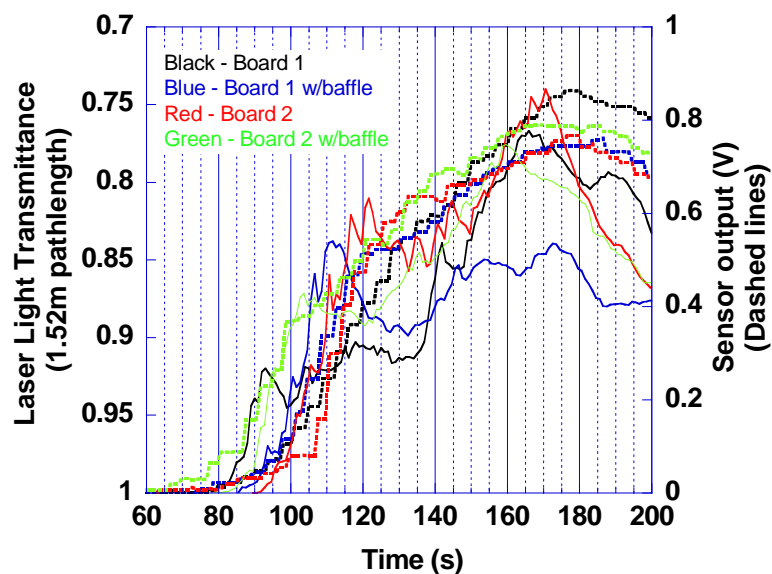


Figure 70. Ion-4 response, fan speed 12 Hz - repeat test

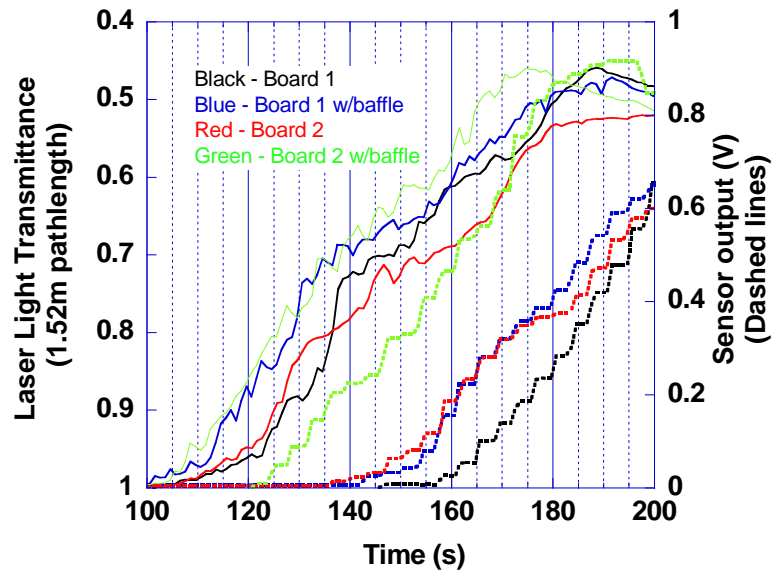


Figure 71. Photo-3 response, fan speed 5 Hz

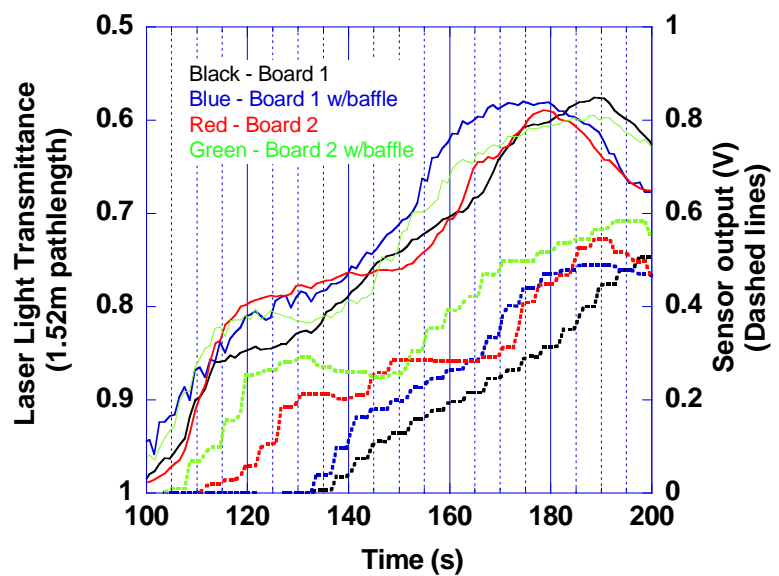


Figure 72. Photo-3 response, fan speed 7 Hz

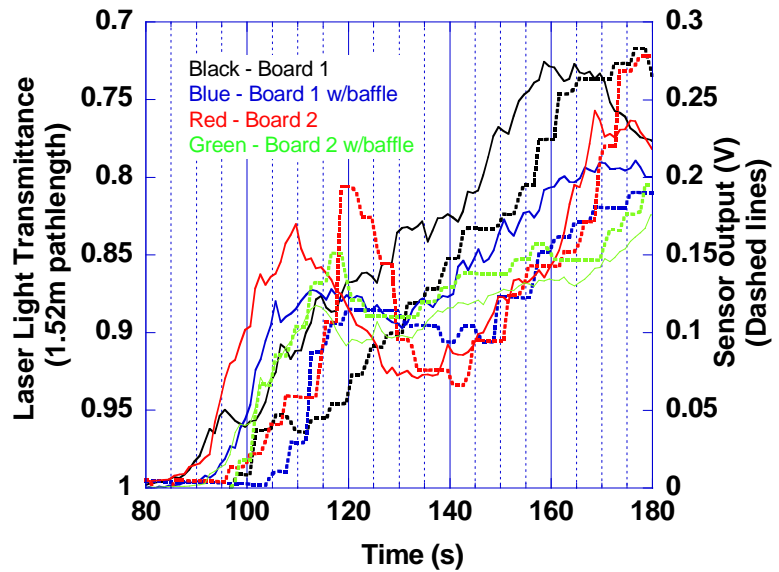


Figure 73. Photo-3 response, fan speed 12 Hz

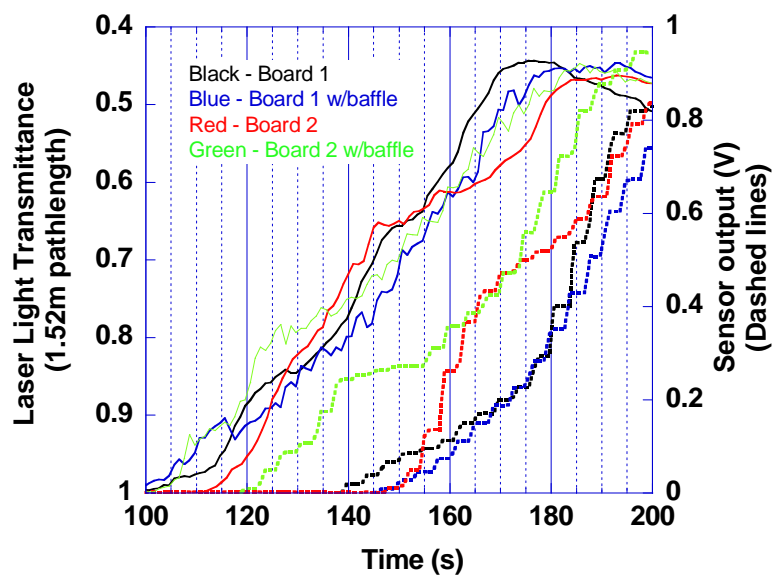


Figure 74. Photo-3 response, fan speed 5 Hz - repeat test

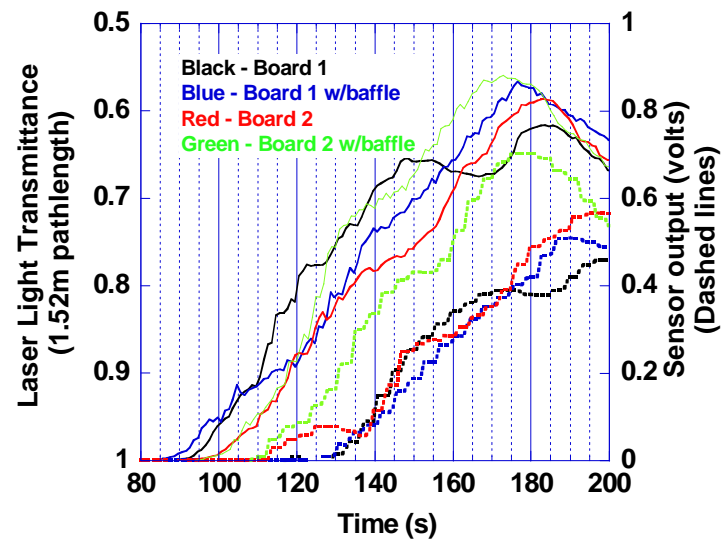


Figure 75. Photo-3 response, fan speed 7 Hz - repeat test

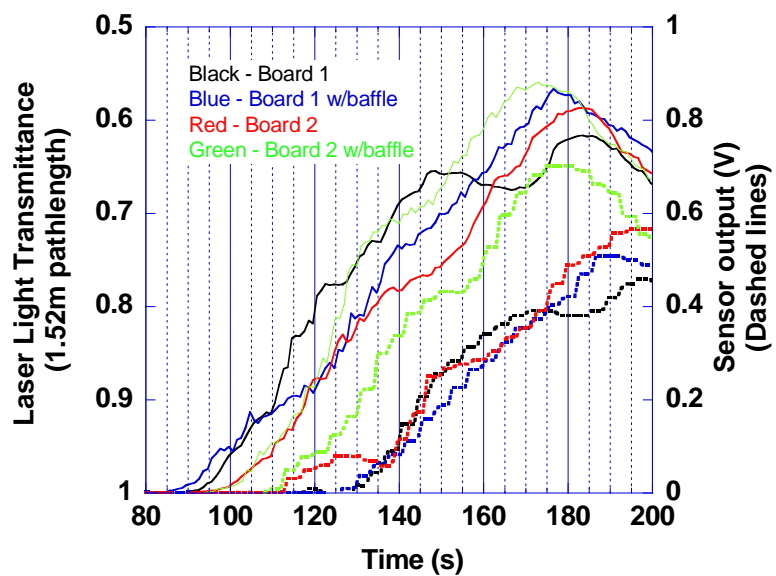


Figure 76. Photo-3 response, fan speed 7 Hz - repeat test

A photo-1 alarm malfunctioned and the results for that alarm type are not included. The results show at low flow (5 Hz) there is an additional response delay on the order of 10 s at alarm concentrations for alarms placed in positions 4 and 5 versus the front three positions due to the additional transport time and blockage effects. At 7 Hz, the effect is less pronounced, on the order of a 5 s delay. At 12 Hz there appears to be no effect. In general, the baffle lessens the effect of position on the alarm response at the low flows. It is concluded that at all but the low flows there is little or no appreciable bias affecting the alarm response and the board position. It is important to note that this simultaneous data were only available for the ionization alarms since only one photoelectric alarm was included in the data. The effects of background flows are discussed further in section 6 from testing of nuisance sources in the manufactured home.

2.8 Thresholds for Modified Alarms

Since the modified CO and smoke alarms do not produce an alarm signal, appropriate thresholds need to be specified to perform the calculations of time to alarm presented in the Appendix A. Selection of alarm thresholds was driven by the desire to consistently apply the same reasonable criterion for each sensor type. Moreover, high and low ranges were specified for photoelectric and ionization alarms characteristic of allowed production ranges. For CO alarms, high and low ranges were specified to indicate sensitivity of a fixed threshold.

Table 5 gives the alarm thresholds used in the fire test series analysis. The justification for the CO alarm threshold and range is based on levels that should be above potential house CO concentration

levels. The photoelectric alarm threshold and range are indicative of typical nominal values and falls within the observed alarm threshold for the unmodified photoelectric alarms tested in the FE/DE. The ionization alarm threshold and range are indicative of typical nominal values, however, the observed alarm threshold for one unmodified ionization alarm fell outside the range. It was decided to use the nominal threshold value of 4.3 %/m (1.3 %/ft) based on two observations. First, the cotton smoke source appears to meet the UL criterion for typical ionization alarm values, and second, it is a more conservative value than the apparent alarm thresholds for the unmodified ionization alarms. Furthermore, the average relative time difference between an alarm sensitivity settings of 4.3 %/m and 3.2 %/m (that is, 100 times the {time to alarm at 4.3%/m – time to alarm at 3.2 %/m} divided by the time to alarm at 4.3 %/m

Table 5. Threshold criteria for modified alarms

	Low	Mid	High
Ionization (%/m / %/ft)	2.6 / 0.8	4.3 / 1.3	5.9 / 1.8
Photoelectric (%/m / %/ft)	3.3 / 1.0	6.6 / 2.0	9.8 / 3.0
CO (volume fraction / ppm)	2.5×10^{-5} / 25	5.0×10^{-5} / 50	1.0×10^{-4} / 100

for all (modified) ionization alarms in all tests was computed to be 2.9 %, indicating that the time to reach alarm is not particularly sensitive to threshold settings near the chosen 4.3 %/m setting used for these fire tests.

3 Fire Source Test Scenarios and Geometries

In order to evaluate the performance of residential smoke alarms in-situ, a test series was designed to encompass multiple fire scenarios, residential geometries, and alarm technologies. This section describes the design of the test series.

3.1 Scenario Development

Of key importance to the representativeness of the study was the selection of the test scenarios. These include the room of fire origin, ignition source and first item ignited, and the ventilation conditions that affect the fire development and combustion chemistry. Here we began with an NFPA analysis of USFA's NFIRS data on fatal residential fires conducted for CPSC [18]. The statistics were categorized according to:

- fire location (living room, bedroom, kitchen, and other),
- fire type (smoldering, flaming, and fast flaming),
- first item ignited.

The data were divided into the most frequent fires, and fires resulting in the greatest number of deaths. Relatively hazardous fires may be fires that occur more frequently than others, or ones that result in a high number of deaths. Of particular interest are fires that occur relatively frequently, and when they do, they result in a disproportionately high death rate. Table 6 shows the top ten scenarios for frequency of occurrence and number of deaths. Flaming and smoldering upholstered furniture and mattresses account for the top four most deadly fire scenarios. Flaming cooking materials are involved more than five times more frequently than any other material. The scenarios chosen for testing included the top five ranked by number of deaths, and among the top ten ranked by frequency of occurrence:

- smoldering upholstered furniture in the living room,
- flaming upholstered furniture in the living room,
- smoldering mattress in the bedroom,
- flaming mattress in the bedroom, and
- cooking materials in the kitchen.

These chosen scenarios are consistent with typical scenarios included for the performance-based design option in NFPA 101 [19] and available guides for performance-based design [20].

Table 6. Top fire scenarios ranked by frequency of occurrence, 1992 – 1996

Location	Fire Type	First Item Ignited	Frequency
Ranked by Frequency of Occurrence			
Kitchen	Flaming	Cooking Materials	82 905
Bedroom	Flaming	Mattress	15 914
Kitchen	Flaming	Wire / Cable	7499
Bedroom	Smoldering	Mattress	6437
Kitchen	Fast Flaming	Cooking	5234
Bedroom	Flaming	Wire / Cable	4551
Kitchen	Flaming	Interior Wall Covering	4271
Living Room	Smoldering	Upholstered Furniture	4060
Living Room	Flaming	Upholstered Furniture	3715
Living Room	Flaming	Wire / Cable	3481
Ranked by Number of Deaths			
Living Room	Smoldering	Upholstered Furniture	372
Bedroom	Smoldering	Mattress	251
Bedroom	Flaming	Mattress	249
Living Room	Flaming	Upholstered Furniture	160
Kitchen	Flaming	Cooking Materials	142
Kitchen	Flaming	Clothing	79
Living Room	Flaming	Wire / Cable	61
Living Room	Flaming	Interior Wall Covering	52
Bedroom	Flaming	Clothing	51
Kitchen	Flaming	Structural Member / Framing	50

Source: 1992 – 1996 NFIRS Data [18]

3.2 Material Selection

3.2.1 Upholstered Furniture

Once the fire scenarios were determined, the materials were procured. The primary goal of each material was to provide a realistic residential fire signature. The burning behavior of individual items, however, can vary dramatically depending upon the specific materials, geometry, and construction used to fabricate the items. Therefore, two different pieces of upholstered living room furniture were selected in order to take advantage of different combustion characteristics of the fuels. Figures 77 and 78 show the upholstered chair selected for the smoldering experiments. The smoldering chair weighed 34 kg. Extended propagation (greater than one hour) of the smoldering front necessitates a large quantity of foam for the seat cushion. The seat cushion consisted of 79 % urethane foam and 21 % synthetic fiber. The cushioning in the rest of the chair consists of 68 % urethane foam, 29 % felted textile fibers of unknown kind, 2 % resin treated synthetic fiber, and 1 % olefin foam. The frame of the chair was constructed of wood.

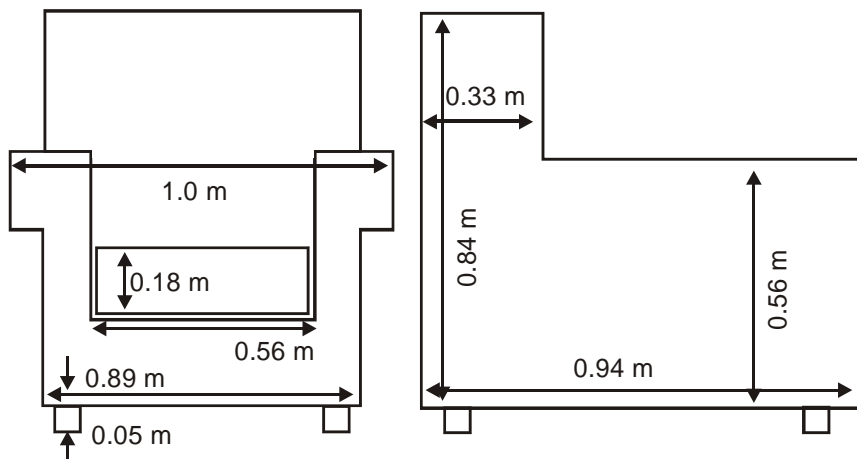


Figure 77. Measurements of upholstered chair used for smoldering experiments



Figure 78. Upholstered chair used for smoldering experiments

The flaming chair was chosen with a lower foam content than the smoldering chair to reduce the peak heat release rate of the chair. A high peak heat release rate may have resulted in unintentional damage to the test structures. Thus, the total quantity of foam in the flaming chair was less than the total quantity of foam in the smoldering chair. The quantity of wood in the framing was not a consideration because the fires were always extinguished prior to the framing becoming substantially involved. Figures 79 and 80 show the chair selected for the flaming living room experiments.

The flaming chair weighed 28 kg. The seat cushion consisted of 79 % polyurethane foam and 21 % polyester fiber. The remaining cushioning consisted of 28 % polyurethane foam and 72 % felted textile fiber of unknown composition. A separate back pillow consisted of 100 % polyester fiber. The frame was constructed of wood.

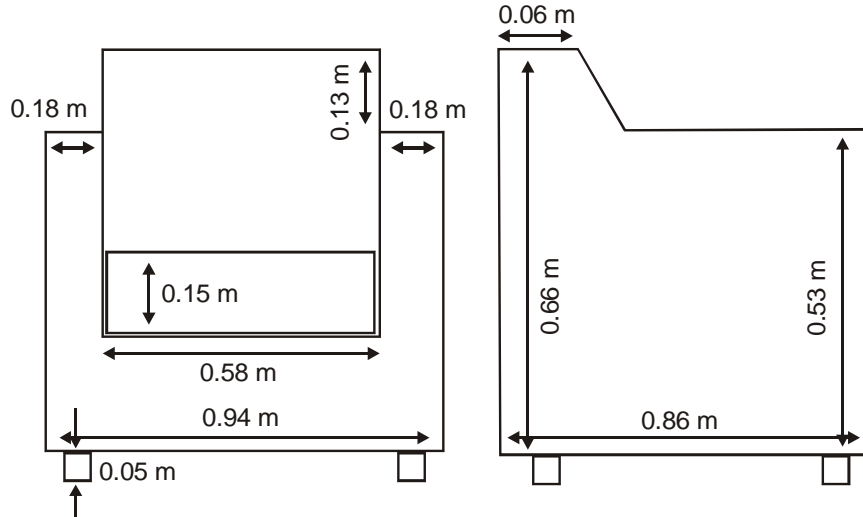


Figure 79. Measurements of upholstered chair used for flaming experiments

Both smoldering and flaming chairs were obtained from a furniture rental retailer in order to reproduce the flaming or smoldering characteristics of lived-in furniture.



Figure 80. Upholstered chair used for flaming experiments

3.2.2 Mattress

For the smoldering and flaming bedroom scenarios, a single mattress style was obtained. The twin size mattress had a “pillow-top” layer of foam. While the “pillow-top” mattresses are popular due to the extra cushioning it provides, the layers of foam also provide a route for the smoldering front to spread. The stuffing material consisted of 66 % resin treated shredded padding of unknown composition and 34 % polyurethane foam. The mattress rigidity was provided by a metal innerspring unit. Figure 81 shows a picture of the mattress. The mattress mass was 19 kg.



Figure 81. Mattress used for smoldering and flaming experiments

3.2.3 Cooking Materials

The most frequently occurring fire in the United States is the cooking materials fire. 500 mL of 100 % corn oil was heated on a gas range until the fuel ignited and was consumed in the fire. Corn oil was selected because it is commonly used and a repeatable fuel source.

	
Corn Oil	Corn Oil in Pan on Gas Range

Figure 82. Corn oil used for kitchen cooking materials fire experiments

3.3 Ignition Methodology

There were three primary ignition sources: flaming, smoldering, and cooking. The flaming ignition source required a moderate flame source which would quickly ignite the material. The smoldering source necessitated a slow, steady introduction of heat to the material in order to initiate a self-propagating smolder front. The cooking material ignition source was easier to define with a gas cooking range heating source. The size, timing, and location of each source were designed to give repeatable results, to the extent possible.

3.3.1 Flaming Ignition

One of the goals of the experiments was to quantify the performance of differing smoke detector technologies, which suggests that a slower fire growth rate will act to more clearly differentiate smoke detector alarm times. Thus, a relatively small ignition source, an electric match, was chosen. An electric match (see figure 83) is a cardboard match book with the cover flipped back, and with a small gauge nichrome wire loop run through the sulfur ends of the matches. The other end of the wire was attached to a switched power source. When the switch was closed, the wire heated quickly, igniting the matchbook within 2 s. Since the match book would burn out quickly, a folded piece of paper surrounding the match book assembly extended the flaming for approximately 20 s to ensure ignition of the surrounding material.



Figure 83. “Electric match” used for flaming ignitions

The geometric placement of the electric match assembly was selected in order to minimize the fire growth rate. Beyond the characteristics of the fuel, the flame spread rate is largely determined by the available surface area and the orientation of the surface. In a horizontal orientation, the area of material involved in the combustion process grows in a circular manner, away from the origin. Thus, eliminating any direction for the flames to propagate reduces the surface area available to the fire. Locating the origin at the edge of a horizontal surface reduces by half the available surface area. Flames travel more rapidly up vertical surfaces than across horizontal surfaces due to buoyant convection of the heated gases.

In order to reduce the fire growth rate, the origin was located away from large vertical surfaces (the arms and back of the chair and the sides of the mattress) since flames travel more rapidly

vertically than horizontally. The electric match was located near an edge or corner to minimize the available surface area. The location of the electric match was in the front of the chair between the cushion and the frame. This minimized the horizontal surface area and maximized the distance to the arms and back as shown in figure 84. A similar rationale was used to select the ignition point for the mattress, also shown in figure 84.

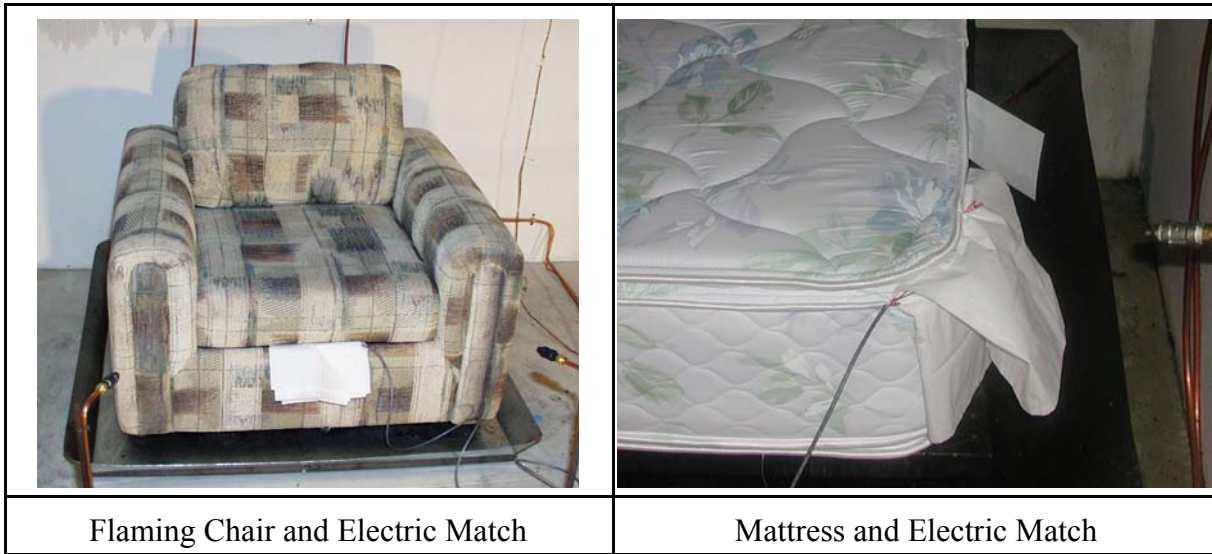


Figure 84. Location of “electric match” ignition source for flaming upholstered chair and mattress experiments

3.3.2 Smoldering Ignition

Sustained smoldering in the urethane foam was difficult to reliably reproduce. If the rate of heating was too high, the foam would either melt and move away from the smoldering region, or runaway reactions would transition the material to flaming combustion. If the rate of heating was too low, the heat input would not sustain the pyrolysis of the material and the smoldering front would extinguish. 30 min to 120 min of smoldering could be achieved in these experiments, if sufficient urethane foam was available, using the techniques described here.

Figure 85 shows the smoldering rod fabricated for these tests. The rod material was ceramic through which nichrome wire was enclosed. The total length of wire was about 0.76 m (30 in) A loop was formed by the wire at the end of the rod. The diameter of the loop was approximately 0.13 m (5 in). The wires were connected to a variac to control the voltage (and thus the current applied) to the loop.

Smoldering was initiated with a low current that was slowly increased as necessary to insure sufficient heat to sustain extended smoldering of the polyurethane foam. Typical heat output was approximately 0.2 kW. A thermocouple, attached to the top surface of the seat cushion or mattress above the wire loop was monitored during the test to insure continued smoldering. The test was terminated once flaming occurred.



Figure 85. Rod used for smoldering ignitions
approximately 0.2 kW. A thermocouple, attached to the top surface of the seat cushion or mattress above the wire loop was monitored during the test to insure continued smoldering. The test was terminated once flaming occurred.

3.3.3 Cooking Ignition

The cooking oil fire scenario produced both extended pyrolyzing and extended flaming combustion. The 500 mL of corn oil was poured into a 0.3 m (12 in) diameter aluminum saute pan. A propane burner provided approximately 1.5 kW to the underside of the pan, typical of cooking applications. The corn oil pyrolyzed for a period of time, after which a transition to flaming occurred, consuming the remainder of the corn oil. Figure 86 shows the heating ignition source.



3.4 Test Geometry

3.4.1 Manufactured Home

The manufactured home geometry represented an array of residential layouts. The arrangement of the manufactured home was sufficiently generic as to represent an apartment, condominium, or small ranch house, in addition to a manufactured home. The primary partitioning of the 85 m² (910 ft²) home consisted of three bedrooms, one full bathroom, one kitchen/dining area, one living room, and two hallways. Each bedroom also

Figure 86. Heating ignition source with cooking oil

contained a small closet. Figure 87 shows the general layout of the manufactured home. For testing, the doors to the bedroom 3 and the bathroom were always closed. Conditions in the middle bedroom were monitored during the tests to assess the tenability of the environment behind the closed door. In the bathroom, a partially open window (0.06 m^2) minimized the pressure differential to the outside during tests. Additionally, both doors leading outside the manufactured home were closed during testing. The ceiling of the manufactured home was peaked on the long axis, reaching a height of 2.4 m (8 ft). The outside walls of the manufactured home were approximately 2.1 m (7 ft) in height. The slope of the ceiling was approximately 8.4° . Smoke detector arrays were mounted parallel to the ceiling.

3.4.2 Two-story Home

The two-story home in Kinston, N.C. was a brick-clad 3 bedroom home, 139 m^2 (1490 ft^2) in size. The first floor consisted of a foyer, den, family room, kitchen, dining room, bathroom, and stairwell to the upstairs. The home did not have a basement. The 2 car garage was accessible from the first floor den. The second floor consisted of a stairwell to the downstairs, hallway, 2 bathrooms, and two smaller bedrooms and one master bedroom. Figures 88 and 89 show the layout of the two-story home.

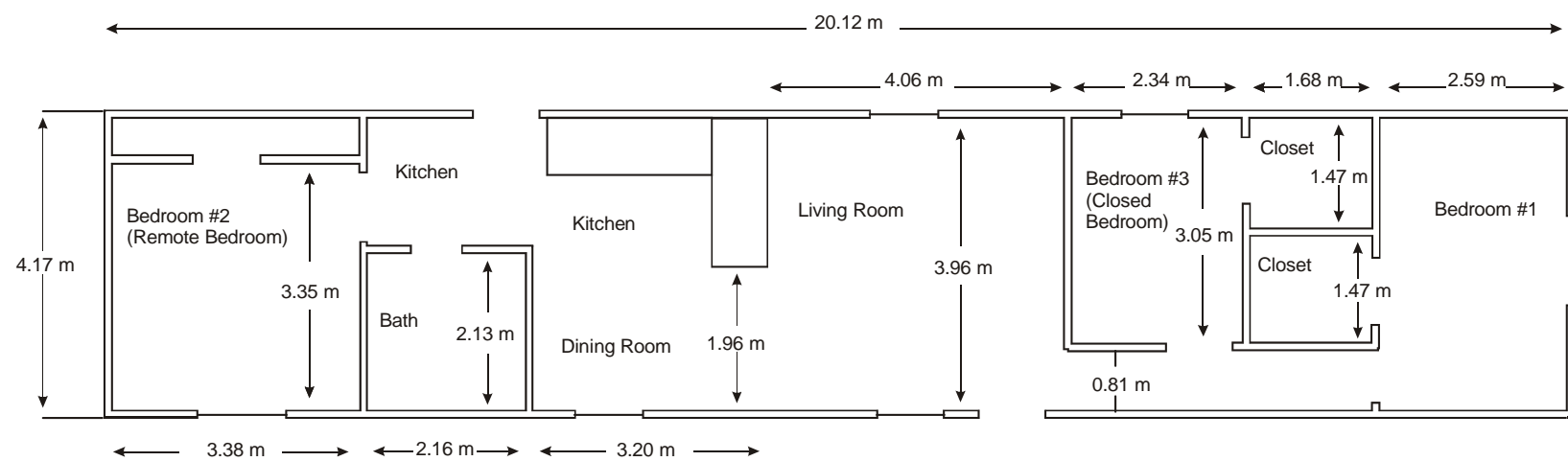


Figure 87. Layout of manufactured home used for test of smoke alarm performance

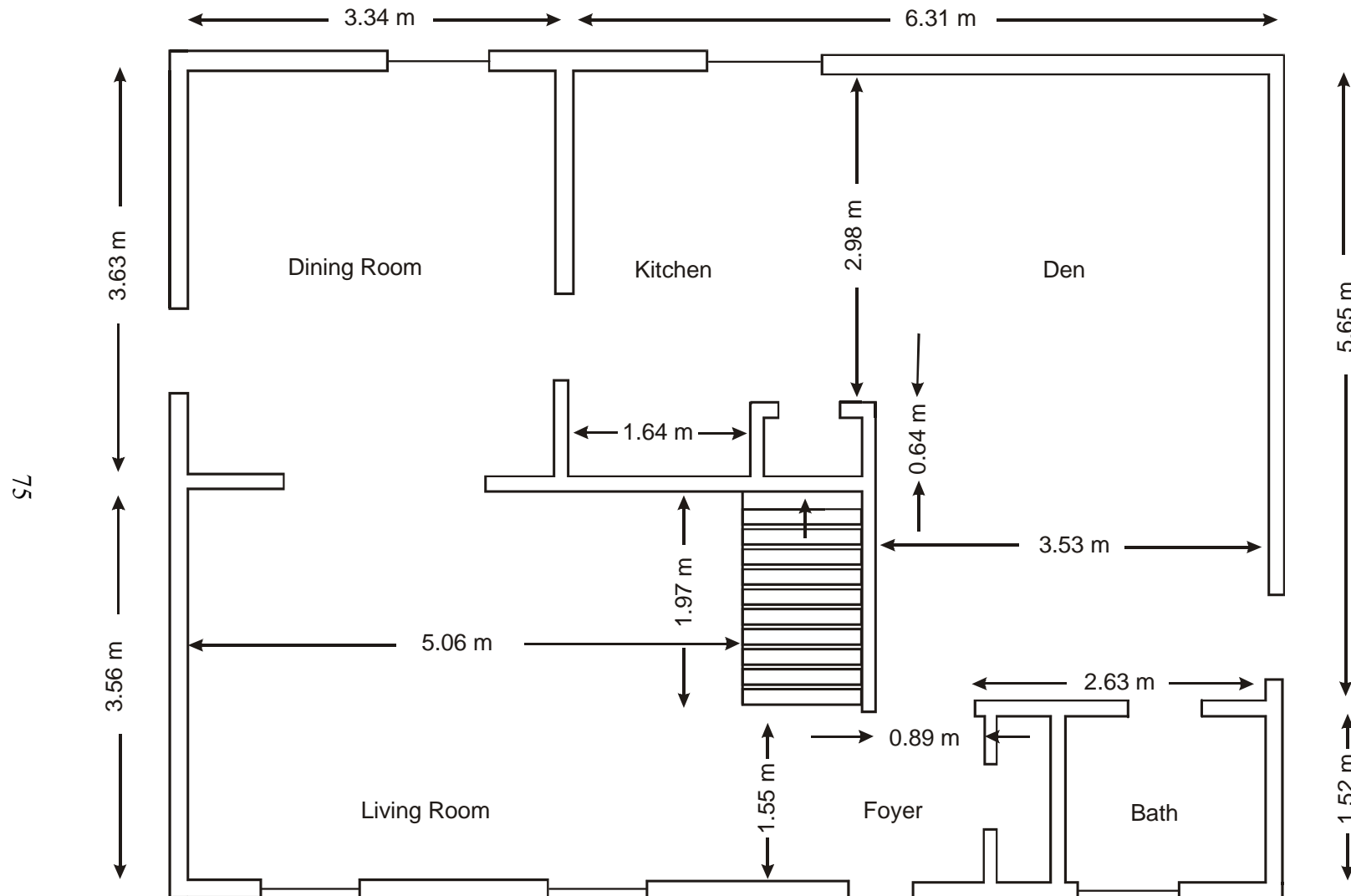


Figure 88. Layout of first floor of two-story home used for tests of smoke alarm performance

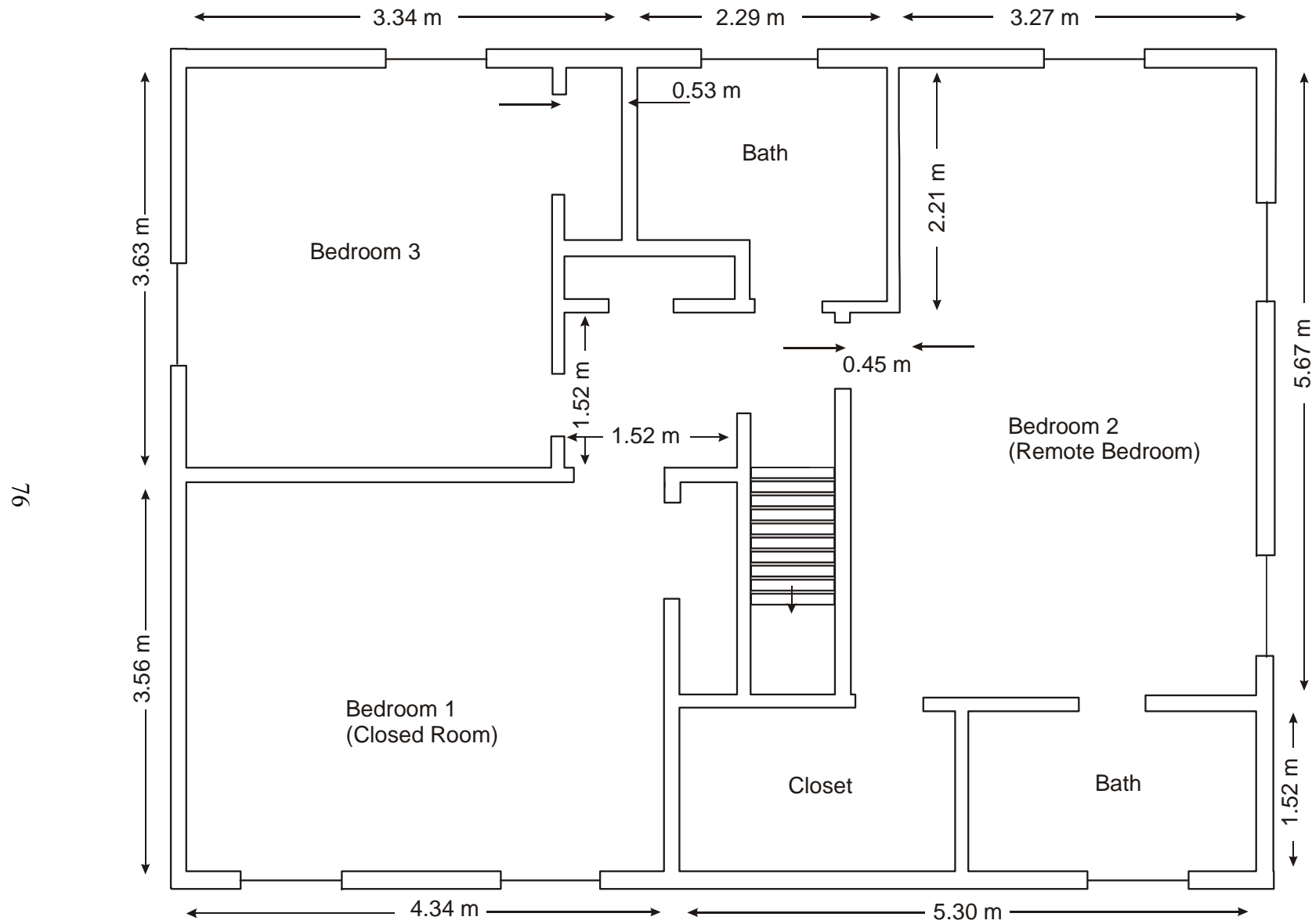


Figure 89. Layout of second floor of two-story home used for tests of smoke alarm performance

4 Fire Source Testing Instrumentation

Fire produces heat, smoke, and toxic gases, all of which can threaten human life. In these experiments environmental parameters that have an impact on human response were measured. Parameters included temperature rise, toxic gas production, and smoke obscuration. Aspects of these that can be measured directly include the gas temperature, mass loss of the burning item, species concentrations, including CO, CO₂, O₂, and other gases. The instrumentation and methods used to measure each of these quantities are discussed below. Readers interested in a general overview of large-scale fire testing data collection and analyses are referred to Peacock and Babrauskas [21].

4.1 Temperature

Temperature measurements were accomplished using small diameter, bare-bead type K thermocouples. Thermocouple trees that consist of thermocouples spaced evenly from floor to ceiling provide a measure of vertical temperature stratification (an example is shown in figure 90). Bare-bead trees were arranged in the room of origin, in at least one remote bedroom, and along the egress path to provide vertical temperature distributions as a function of time. The bare-bead thermocouples were constructed from 0.25 mm diameter wire. Table 7, below, summarizes the location of

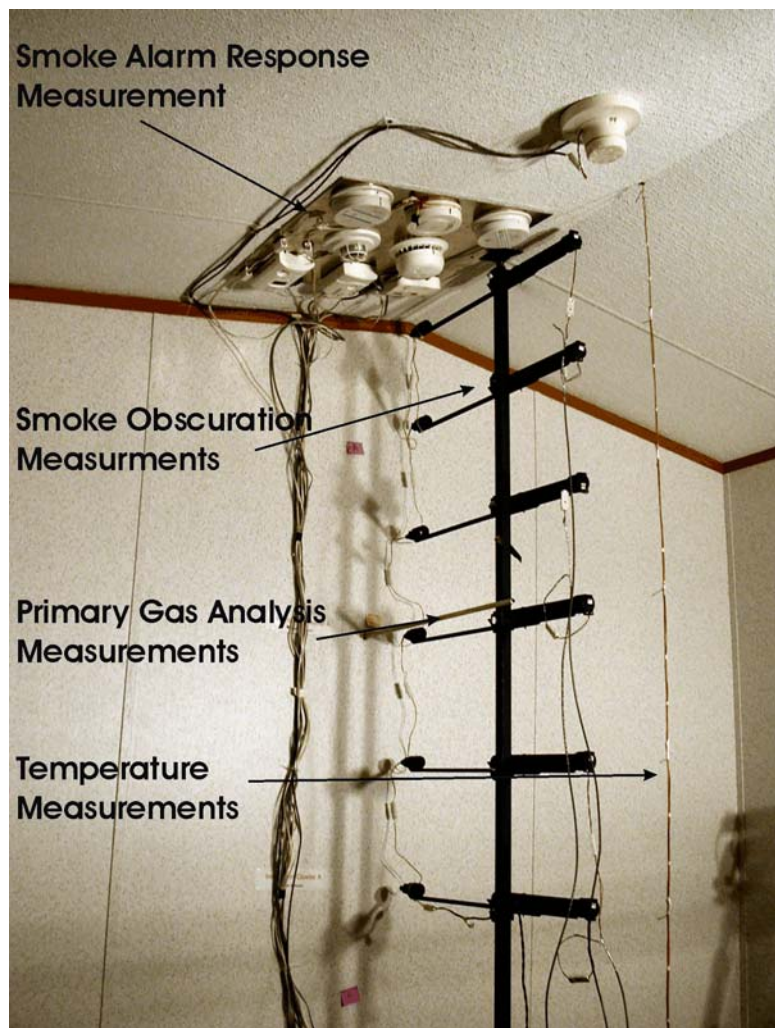


Figure 90. Sample instrumentation showing relative locations of temperature, primary gas analysis, smoke obscuration, and smoke alarm response measurements

temperature measurement in the different test structures. Figures 91 to 93 show the instrumentation in the manufactured home and two-story home, respectively.

For a series of well-controlled gas burner tests [22], the standard uncertainty for peak gas temperature was found to be $\pm 16^\circ\text{C}$. These are expressed as the standard deviation of the peak values for 12 replicate tests. While random error in the current experiments is expected to be comparable to these values, additional uncertainty due to variation in the ignition and fire growth of the fire sources from this test series can be expected. Replicate tests were conducted for this report to better quantify uncertainty.

Table 7. Locations for temperature measurement in tests of smoke alarm response

Structure	Location	Vertical Positions (mm from ceiling)
Manufactured Home	Bedroom 2 (remote bedroom)	20, 300, 610, 900, 1220, 1520, 1820
	Bedroom 1 (room of fire origin for mattress tests)	20, 300, 610, 900, 1220, 1520, 1820
	Hallway 1 (outside bedroom 2)	20, 300, 610, 900, 1220, 1520, 1820
	Hallway 2 (outside bedrooms 1 and 3)	20, 300, 610, 900, 1220, 1520, 1820
	Living area (room of fire origin for upholstered chair and cooking oil tests)	20, 300, 610, 900, 1220, 1520, 1820
	Hallway 2 (near living room)	20, 300, 610, 900, 1220, 1520, 1820
	Bedroom 3 (closed bedroom)	1520
Two-Story House	Bedroom 2 (remote bedroom)	20, 300, 610, 900, 1220
	Second floor hallway	20, 300, 610, 900, 1220
	Bedroom 3 (room of fire origin for mattress tests)	20, 300, 610, 900, 1220
	First floor foyer	20, 300, 610, 900, 1220
	First floor den	20, 300, 610, 900, 1220
	Living room (room of fire origin for upholstered chair tests)	20, 300, 610, 900, 1220
	Kitchen (room of fire origin for cooling oil tests)	20, 300, 610, 900, 1220

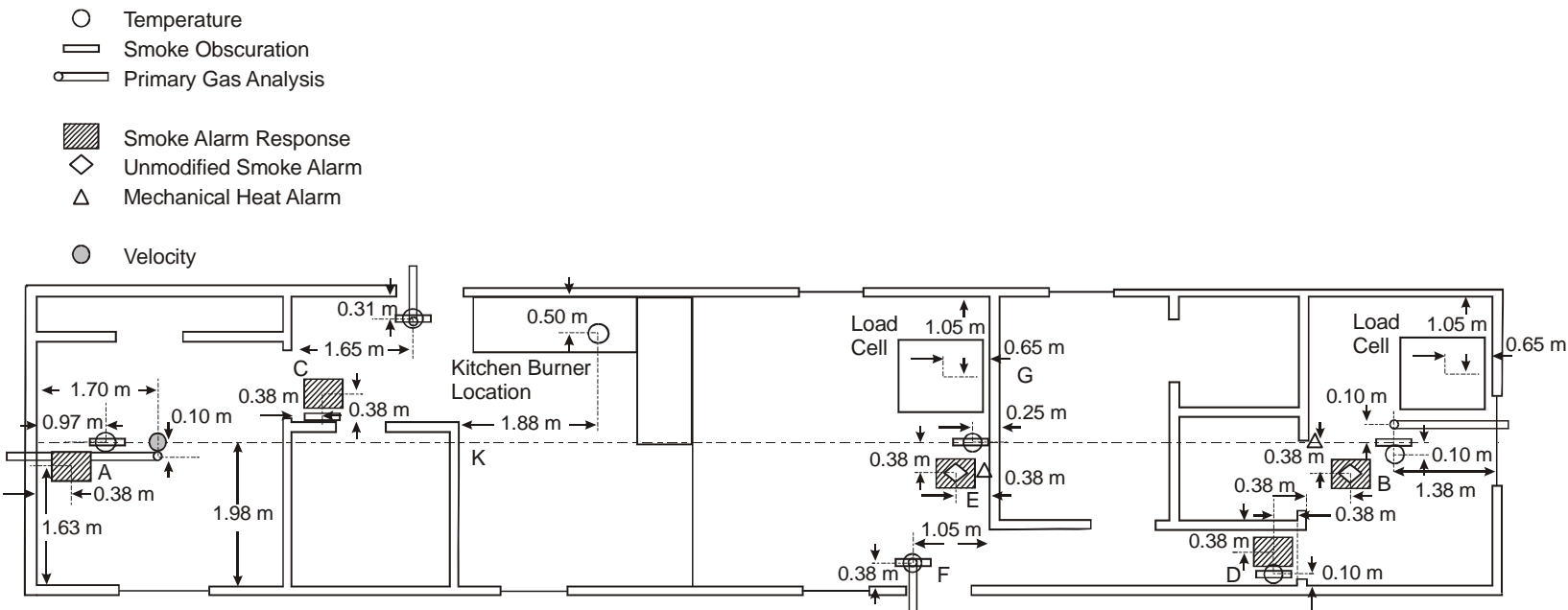


Figure 91. Instrumentation in manufactured home during tests of smoke alarm performance

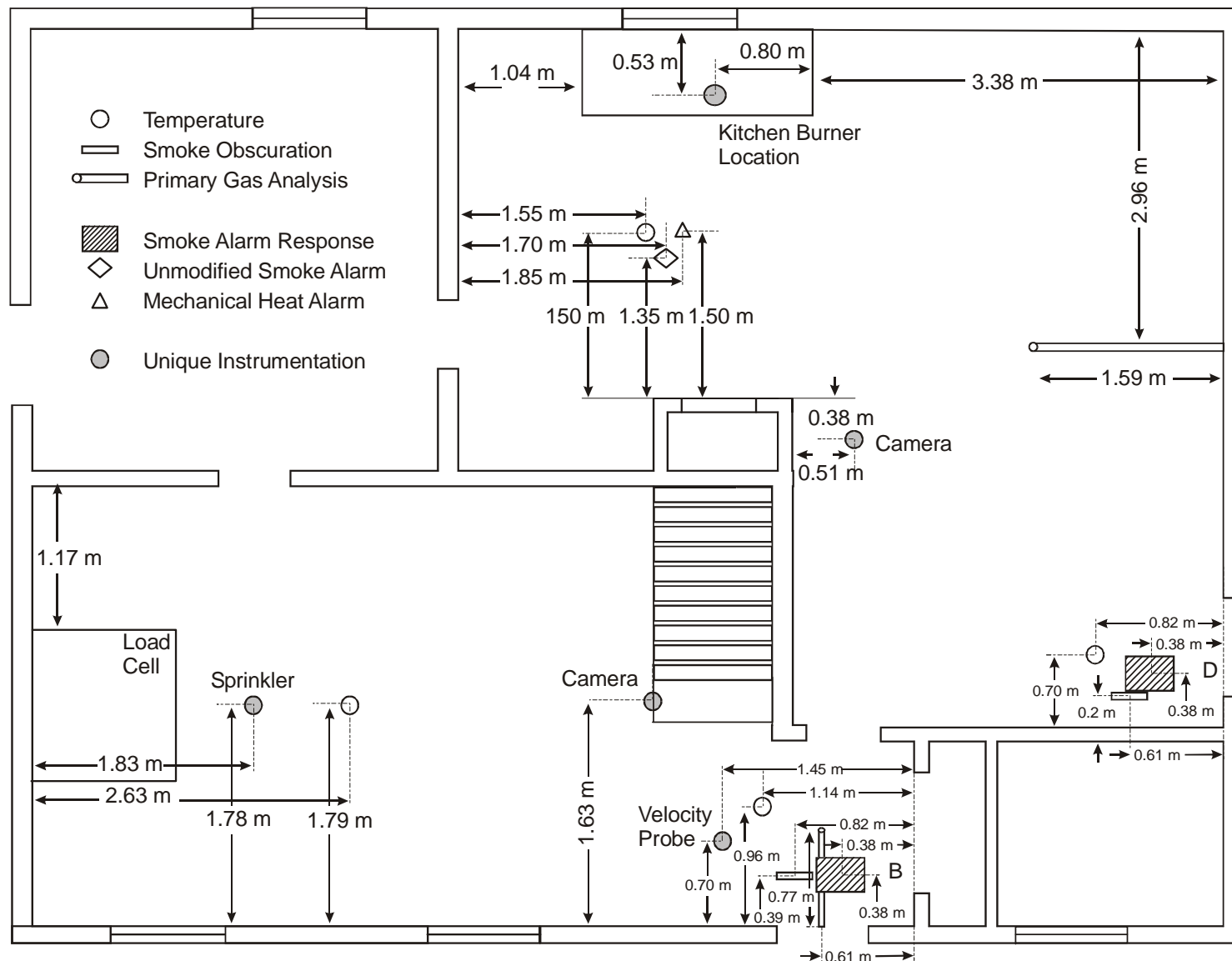


Figure 92. Instrumentation in first floor of two-story home during tests of smoke alarm performance

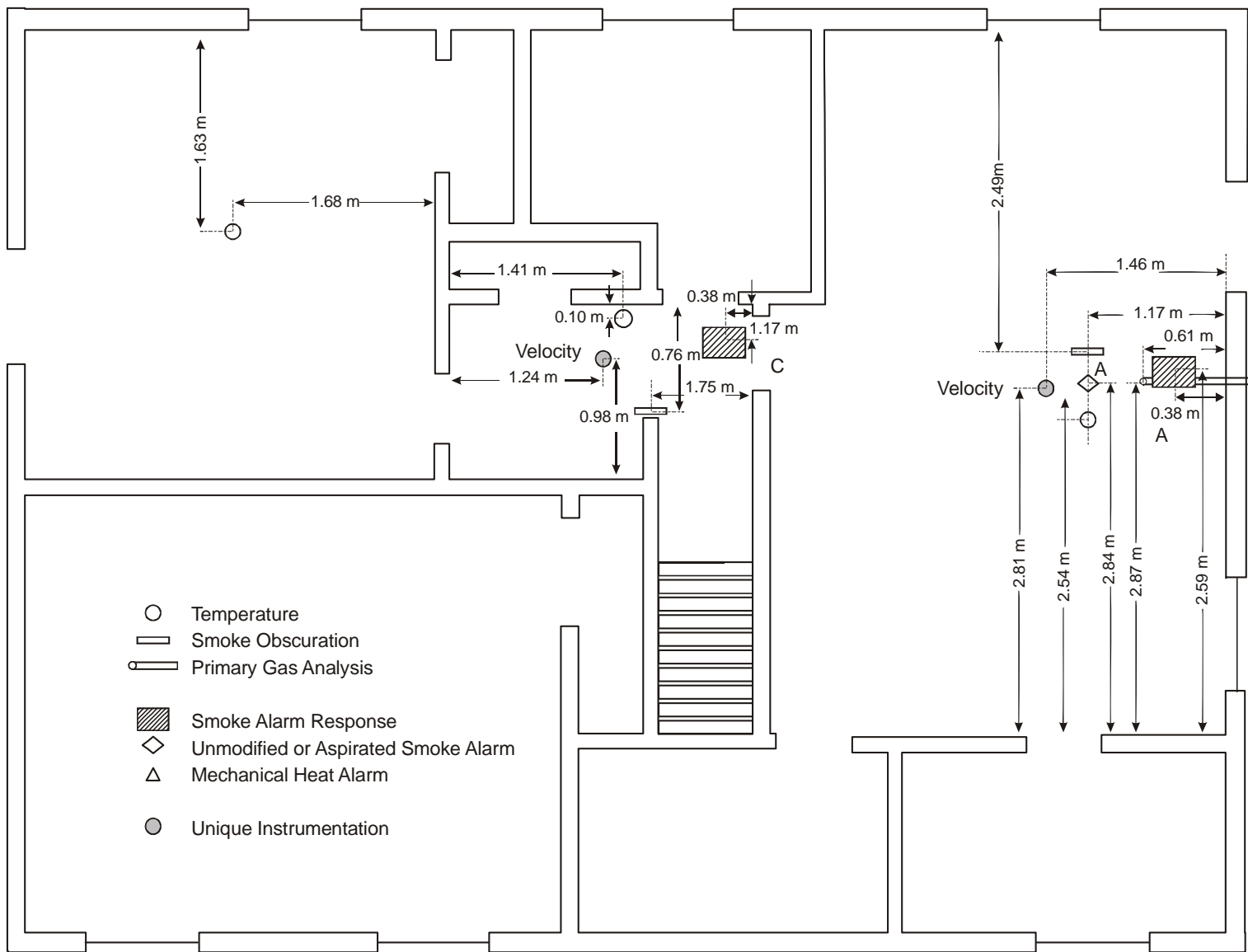


Figure 93. Instrumentation in second floor of two-story home during tests of smoke alarm performance

4.2 Sample Mass

Mass loss from the object of fire origin was recorded using a floor-mounted load cell apparatus. Figure 94 shows the apparatus for one of the flaming ignition tests. As the object of fire origin is consumed by the fire, the mass decreases. The mass was measured over time, yielding the instantaneous measure of specimen mass, as well as the total mass consumed by the fire. The mass loss rate is simply the rate of change of the measured mass loss. It is determined from the slope of a straight line fit through seven adjacent points to minimize noise in the instantaneous measurements. Mass loss rate is directly correlated with the generation of combustion products (toxic species, smoke, etc.), as well as heat release rate.

Standard uncertainty for the mass loss measurements is expressed as a percentage of the full-scale resolution of the load cells. For the load cell used for these tests, this is approximately ± 2 g. While random error in the current experiments is expected to be comparable to these values, additional uncertainty due to variation in the ignition and fire growth of the fire sources from this test series can be expected. Replicate tests were conducted for this report to better quantify uncertainty.



Figure 94. Example of mass loss measurement showing upholstered chair on load cell prior to one of the flaming ignition tests and load cell apparatus mounted beneath manufactured home

4.3 Primary Gases – CO, CO₂, and O₂

Measurement of CO, CO₂, and O₂ concentrations, along with temperature and smoke obscuration, provide an assessment of the tenability of a fire environment and allow determination of available egress time (discussed in section 5.4). CO and CO₂ measurements were performed with nondispersive infrared (NDIR) analysis. NDIR works on the principle that a gas species will absorb infrared light at a known wavelength. These instruments are carefully designed to avoid absorption bands that are near those of strong interfering bands such as those of water. O₂ measurements were made using paramagnetic analyzers. In these tests, primary gas concentration measurements were made in the room of fire origin, in at least one remote bedroom and at two points along the egress path. An example of the measurement point at one of the locations is shown in figure 90. For all experiments and locations, the NDIR gas analysis sampling point was located at an elevation of 1.5 m (5 ft) from floor level. Table 8, below, summarizes the location of gas analysis in the two test geometries.

Table 8. Locations for primary gas measurement in tests of smoke alarm response

Structure	Location	Vertical Positions (mm from ceiling)
Manufactured Home	Bedroom 2 (remote bedroom)	900
	Bedroom 1 (only for mattress tests)	900
	Hallway 1 (outside bedroom 2)	900
	Living area (only for upholstered chair and cooking oil tests)	900
	Hallway 2 (near living room)	900
Two-Story House	Bedroom 2 (remote bedroom)	900
	First floor foyer	900

Upstream of the analyzers, the gas stream was filtered to remove particulates and also passed through ice water and dry ice traps to remove water from the samples. Each analyzer was calibrated with a known concentration of gas prior to each test to insure correct operation and provide appropriate small corrections to manufacturer-supplied calibration curves. Typically, this correction was less than 1 % of the measured value. Additionally, delay times to account for line delays in the instrumentation for each measurement location was determined by introducing a gas pulse at the measurement point and noting the time required for the analyzer to respond.

With different line lengths, vacuum pumps, and filters in each analyzer system, these delays can be expected to be different for each analyzer. With multiple replicates, this delay ranged from $9\text{ s} \pm 1\text{ s}$ to $34\text{ s} \pm 3\text{ s}$. Test data were shifted to account for these delay times.

For a series of well-controlled gas burner tests [22], the standard uncertainty for oxygen concentration, carbon dioxide concentration, and carbon monoxide concentration was found to be $\pm 0.6\%$ volume fraction, $\pm 0.4\%$ volume fraction, and $\pm 0.06\%$ volume fraction, respectively. These are expressed as the standard deviation of the peak values for 12 replicate tests. While random error in the current experiments is expected to be comparable to these values, additional uncertainty due to variation in the ignition and fire growth of the fire sources from this test series can be expected. Replicate tests were conducted for this report to better quantify uncertainty.

4.4 FTIR Gas Analysis

In the manufactured home tests, the secondary gas measurement was performed by representatives from National Research Council of Canada using FTIR (Fourier Transform Infrared) techniques. FTIR gas analysis provides measures of additional gases which may effect tenability, such as HCN, HCl, NO, or NO_2 , in addition to providing a second measure of CO and CO_2 . Data on secondary gases are included as Appendix B.



(a)



(b)

4.5 Optical Density

Optical density was measured using laser-based light extinction measurement trees. A laser beam's signal strength is measured over time. As smoke passes through the laser beam, the smoke absorbs and reflects a fraction of the light, reducing the light level at an in-line receiver. Figure 95 shows the two designs of smoke obscuration instruments used in the tests. The light source was a low-cost laser pointer consisting of Class II laser diode with a stated wavelength range of 630 nm to 680 nm and a maximum power output of less than a 1

Figure 95. Optical density instrument designs

mW, coupled to a plastic lens. The laser was powered by a regulated power supply set at a constant voltage of 4.50 V. The light receiver was a silicon photovoltaic cell (i.e., solar cell) where the open-circuit voltage was monitored by an analog voltage input channel of the data acquisition system. The “clean air” voltage was typically between 0.15 V and 0.3 V depending on the smoke meter, and its alignment before a test. Prior to each test, the smoke meters were powered up, allowed to reach a steady state, and calibrated with neutral density filters covering a range in optical densities. Neutral density filters typically have an uncertainty of 2 % of the stated value. The data were fitted to calibration curves, which were then used to compute the optical densities from the voltages gathered during the subsequent test. The relative uncertainty of the field-calibrated smoke meters was typically 10 % of the reading.

Optical density was measured near smoke alarms, in the room of origin, in at least one remote bedroom, and along the egress path. Smoke obscuration coupled with irritant effects may impair the ability of occupants to egress in fires [23]. Figure 90 shows an example set of smoke obscuration instruments in one of the bedrooms of the manufactured home. Measurements of smoke obscuration from floor to ceiling were made in the room of fire origin, at least one remote bedroom, and at locations along the egress path. Table 9, below, summarizes the location of optical density measurements in the two test geometries.

As testing progressed, the design of the optical density instruments evolved. Three different designs were used in the three test series. In test 1-15, the design shown in figure 95a was used. Although the simplest design, the output of the in-line receiver changed at high temperature. Since the primary focus of these tests was early detection, the design provided reasonable results for all but the hottest measurement locations. For tests 20-41, the design was modified to include high temperature insulation around both the laser and receiver ends of the instrument (figure 95b). In addition, for tests 30-41, more insulation was added along with a glass window on the receiver end to clearly define the path length.

Table 9. Locations for primary optical density measurements in tests of smoke alarm response

Structure	Location	Vertical Positions (mm from ceiling)
Manufactured Home	Bedroom 2 (remote bedroom)	20, 900
	Bedroom 1 (room of fire origin for mattress tests)	20, 900
	Hallway 1 (outside bedroom 2)	20, 900
	Hallway 2 (outside bedrooms 1 and 3)	20, 900
	Living area (room of fire origin for upholstered chair and cooking oil tests)	20, 900
	Hallway 2 (near living room)	20, 900
	Bedroom 3 (closed bedroom)	1020
Two-Story House	Bedroom 2 (remote bedroom)	20, 900
	Second floor hallway	20, 900
	First floor foyer	20, 900
	First floor den	20, 900

The main function of the field test smoke meters was to provide obscuration data for assessing tenability limits. An optical density of 0.25 m^{-1} (1.5 m from the floor) was used in the analysis as the tenability criterion for smoke obscuration. It is important to note that heat transfer from hot gases transported to the smoke meters causes their voltage output to drift, giving a false indication of smoke and a larger apparent optical density than what would be due to the smoke in the optical path. The time after a significant amount of heat transfer occurred represents a period of smoke meter operation where the smoke obscuration results would not be reliable.

Smoldering fire tests typically did not produce significantly elevated temperatures, thus the uncertainty in a smoke meter obscuration measurement during smoldering phases is essentially the ambient temperature calibration uncertainty. Laboratory tests on un-insulated and insulated smoke meters indicated that a temperature change approximately $20 \text{ }^{\circ}\text{C}$ to $40 \text{ }^{\circ}\text{C}$ over 100 s to 200 s, would start to affect the reliability of the computed smoke obscuration by the end of the heating period (the insulated meters performed better.) Therefore, caution must be used when analyzing these smoke meter results anytime the ambient temperature has changed. During the flaming phase of these tests, the optical density tenability limits were reached prior to significant smoke meter heating.

4.6 Smoke Properties

In addition to optical density, other smoke properties were measured in selected tests in one or more locations. Figure 96 shows the instrumentation in the two-story home. The aerosol mass concentration was recorded with a tapered-element oscillating microbalance (TEOM model 1100, Rupprecht and Pastashnick Co., Inc) designed for diesel soot monitoring. This is a widely used instrument for continuous recording of mass concentration. It consists of a filter attached to a tube oscillating in an inverted pendulum fashion. Particle-laden flow is drawn through the filter and down the tube. Aerosol particles that deposit on the filter change the frequency of oscillation, which is sensed and converted into a change in mass. The flow rate is fixed at 3.00 L/min, hence the aerosol mass concentration can be computed. The air entering the instrument is heated to approximately 45 °C. The range of the instrument was between 0.2 mg/m³ to about 500 mg/m³ with an absolute uncertainty if 0.1 mg/m³. An attempt was made to sample from two different locations during some of the manufactured home tests by switching between the sampling locations every 30 s with a two-way valve. The TEOM had problems recovering after flow switching, and this technique was abandoned.



Figure 96. Smoke properties measurement showing collection lines (foreground) and smoke velocity measurement (background)

The number concentration was recorded with a condensation particle counter (model 3022A, Thermo-systems Inc.) This instrument counts all particles in the range of 10 nm to over 3 µm by growing them to a single size via condensation of alcohol vapor and then counting them individually via single-particle light scattering, or by calibrated photometry. The instrument can record up to 1×10^7 particles/cm³. This upper range was extended to 8×10^8 particles/cm³ by employing a 80:1 diluter. The stated relative uncertainty is 10 % of reading up to 5×10^5 particles/cm³. As with the TEOM, an attempt was made to sample from two different locations in the two-story home tests. By switching the flow between two locations every 60 s it was possible to record the number concentration at 60 s intervals every 120 s for each location.

Finally, a size distribution measurement of the smoke was made using a cascade impactor. A micro-orifice, uniform-deposit impactor (MOUDI) was used. It is a 12-stage impactor that measures the sized distribution from 18 μm down to 0.03 μm . The MOUDI requires 28.3 SLM flow. It provides a time-averaged size distribution over its collection time period. Aerosols over a narrow aerodynamic size are collected on pre-weighed filters by impaction at each stage. After the last stage, a final filter collects all particles that were not impacted. The standard uncertainty of mass collected on any single stage is 0.01 mg. Typically, a sum of over 2 mg of material was collected on all stages. The mass fraction of aerosol on each stage is computed and was used to estimate the mass median aerodynamic particle diameter and the width of the size distribution.

Ionization chambers were constructed to emulate the response of a measuring ionization chamber (MIC) to provide an estimate of the first moment of the size distribution. The design of these chambers is described in Section 6. In addition to the ionization chambers, individual modified residential ionization alarms were located at the sampling position for the chambers. Figure 97 shows the response of a modified alarm exposed to cotton smolder smoke generated in the FE/DE as compared to the Y value computed from a MIC located inside the FE/DE. The modified alarm was located inside a plenum and drew air from the FE/DE duct at the test section location. This comparison was used to compute Y values from the voltage data from all four modified alarms. In order to compute a Y value from the voltage, the voltage signal must be transformed into a variable that ranges from 0 to 1 over a smoke concentration of 0 to infinity (where the MIC goes from 100 pA to 0 pA, and the normalized change in current goes from 0 to 1). The data in figure 97 were fitted via non-linear least squares regression to the following equation:

$$Y = X(2 - X)/(1 - X) \text{ where}$$

the voltage was transformed into X ,
the normalized current change,
by $X = (V_{\max} - V_0)/(V - V_0)$;
 V_0 is the initial clean air voltage and
 V_{\max} is a maximum value obtained
via the regression.

The regression curve is shown in figure 97. A best-fit value for V_{\max} was 3.139 V with a standard error of 0.013 V. A correlation coefficient of 0.9975 indicates a good fit with the equation. Above values of $Y = 2.3$, the equation was extrapolated. Propagating the

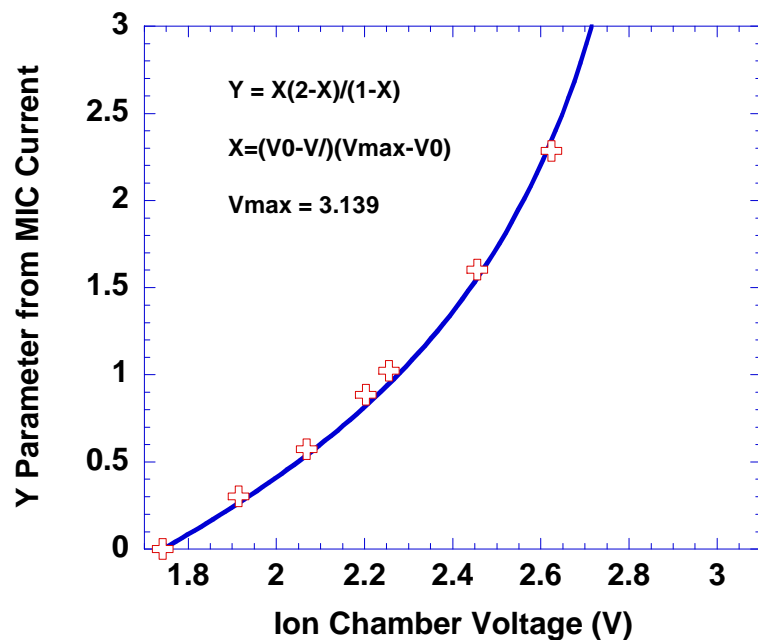


Figure 97. Calibration of residential ionization chamber

uncertainty in X when computing Y yields a combined standard uncertainty in computed Y of 0.022.

All sample lines were 9.5 mm (3/8 in) OD copper tubing. The main sampling location in the manufactured home tests was 25 mm below the ceiling in the remote bedroom, 1.60 m from the window and 1.65 m from the wall opposing the door. Air was flowed through the ionization chamber, and a fraction of the flow leaving the chamber was sent to the TEOM. Additionally, a sampling location was located 25 mm below the ceiling in the hallway 1.70 m from the back bedroom door, and 0.50 m from the exterior wall. The air sample from this location went to an ionization chamber.

The main sampling location in the two-story home was 25 mm below the ceiling in the upstairs remote bedroom 1.57 m from the back wall and 1.60 m from the garage side wall. The secondary sampling location was 25 mm below the ceiling in the den 2.44 m from the back wall and 1.60 m from the garage sidewall.

4.7 Smoke and CO Alarm Response

Figure 98 shows one of the alarm arrays. Alarm response was measured by direct recording of the voltage signal from ionization smoke alarms, photoelectric smoke alarms, and CO alarms arranged for analog output, instead of the more common alarm threshold. By recording analog output, the performance of the alarms at any desired threshold setting as well as the potential use of algorithms that reduce nuisance alarms can be evaluated. The analog signal was compared to unmodified alarms purchased in local, retail outlets, in the laboratory to verify that the modifications did not affect the alarm performance (see section 2.8 for details). Alarms were located in typical, code-required locations, as well as in the room of origin, in order to determine the effectiveness of alternative siting rules. In the room of fire origin, three unmodified alarms were used to avoid destruction



Figure 98. Measurement station showing several alarms arranged for testing

of the limited supply of analog-modified alarms (figure 99). For these alarms, the interconnect signal was monitored to determine the time of alarm. Table 10 summarizes the alarm locations for the two test structures.

Table 10. Alarm and sprinkler locations in tests of smoke and CO alarm response

Structure	Location
Manufactured Home	Smoke and CO Alarms – Bedroom 2 (remote bedroom)
	Smoke and CO Alarms and Tell-tale Sprinkler – Bedroom 1 (room of fire origin for mattress tests)
	Smoke and CO Alarms – Hallway 1 (outside bedroom 2)
	Smoke and CO Alarms – Hallway 2 (outside bedrooms 1 and 3)
	Smoke and CO Alarms and Tell-tale Sprinkler – Living area (room of fire origin for upholstered chair and cooking oil tests)
	Smoke and CO Alarms – Hallway 2 (near living room)
Two-Story House	Smoke and CO Alarms – Bedroom 2 (remote bedroom)
	Smoke and CO Alarms – Second floor hallway
	Smoke and CO Alarms – First floor foyer
	Tell-tale Sprinkler – Living Room
	Smoke and CO Alarms – First floor den

4.8 Sprinkler Response

Residential sprinklers have made significant market penetration in multi-family housing. Many current codes include independent requirements for smoke alarms and sprinklers. This is not necessarily the most effective arrangement but limited data exist that demonstrate the relative performance of the combination. Sprinkler response was measured using an air pressurized (so called telltale) sprinkler. A small quantity of water at the sprinkler head provides an appropriate thermal sink. Upon activation, the pressure in the sprinkler line drops to ambient and the activation time is recorded as the time of this pressure drop. For the test installation, pipe lengths were sufficiently short so that measurement delay from sprinkler activation to noted response was less than 2 s. Typical residential sprinklers (listed for installation in a sloped ceiling with up

to a 26.6 ° pitch for the manufactured home) were installed in the room of fire origin in accordance with the requirements of NFPA 13D, Standard for the Installation of Sprinkler Systems in One- and Two-Family Dwellings and Manufactured Homes. The sprinklers had a listed activation temperature of 68 °C (155 °F) with a K-factor of 5.5 and were appropriate for spacing up to 6 m (20 ft). Table 10 summarizes the alarm locations for the two test structures.



Figure 99. Measurement station showing unmodified smoke alarms arranged for testing

4.9 Mechanical Heat Alarm Response

Mechanical heat alarms were located in the room of origin in accordance with the requirements of NFPA 72, the National Fire Alarm Code. The heat alarms were listed for 57 °C (135 °F) activation at a spacing up to 21 m (70 ft). Heat alarm response can be compared to the performance of other smoke and heat alarms. Activation was recorded by the acoustic signal emitted by the device.

5 Fire Source Test Results and Calculations

In this section, experimental test results are presented which characterize the environment in typical residential fire scenarios. Data presented include the time varying concentrations of CO, CO₂, and O₂, gas velocities, smoke obscuration, and temperature at multiple locations in the structure. Additional measurement of smoke particle size and concentration are discussed later in the report.

5.1 Tests Conducted

Real-scale tests of current smoke, heat, and carbon monoxide alarms in actual homes with appropriate contents as fuels provide a base of data to evaluate the performance of modern residential alarm technologies. Fire scenarios (including ignition source, first item ignited, and room of fire origin) were selected based upon a statistical analysis of available fire loss data. Selected fires include a mattress fire in a bedroom, upholstered chair fire in a living area, and a cooking oil fire in a kitchen. In most tests, a single item fire was used. In one test, additional items in the room of fire origin were allowed to ignite to more fully characterize fire growth in the structure. Table 11 summarizes the 27 tests conducted in the manufactured home. Similarly, table 12 shows the 9 tests conducted in the two-story home. Multiple replicates of most scenarios were included to quantify repeatability and measurement uncertainty in the experiments.

Inclusion of all of the test data would overwhelm this report, with several thousand readings per instrument, 150 instruments per test, and 36 tests. All of the data from the tests conducted are available in two companion reports, one for the tests conducted in the manufactured home [24], and one for the tests conducted in the two-story home [25]. For each of the tests, these two reports include a summary of the test conditions and ignition source. Graphs of all test data along with spreadsheets of the data are included.

For this report, detailed presentation and analysis will be included for one of the tests. For this test, all of the measured data characterizing the environment (temperature, gas concentrations, smoke obscuration, and specimen mass loss) will be presented. For one of the alarm locations, data from all of the alarms (multiple photoelectric, ionization, aspirated photoelectric, and heat alarms) will be presented. Details of calculations to determine individual alarm times and to estimate time to untenable conditions will be discussed.

For the remainder of the tests, the results of identical analyses will be summarized.

Table 11. Test conditions for tests conducted in a manufactured home

Test	Ignition	Fuel Package	Fire Location	Comments
SDC01	Smoldering	Chair	Living Area	
SDC02	Flaming	Chair	Living Area	
SDC03	Smoldering	Mattress	Bedroom	Ignition failure
SDC04	Smoldering	Mattress	Bedroom	
SDC05	Flaming	Mattress	Bedroom	
SDC06	Smoldering	Mattress	Bedroom	
SDC07	Flaming	Mattress	Bedroom	
SDC08	Smoldering	Mattress	Bedroom	
SDC09	Flaming	Mattress	Bedroom	Bedroom door closed
SDC10	Flaming	Chair	Living Area	
SDC11	Smoldering	Chair	Living Area	
SDC12	Heating	Cooking Oil	Kitchen Area	
SDC13	Heating	Cooking Oil	Kitchen Area	
SDC14	Smoldering	Mattress	Bedroom	Bedroom door closed
SDC15	Flaming	Chair	Living Area	
SDC30	Smoldering	Chair	Living Area	Ignition failure
SDC31	Smoldering	Chair	Living Area	
SDC32	Flaming	Chair	Living Area	Ignition failure
SDC33	Flaming	Chair	Living Area	
SDC34	Smoldering	Chair	Living Area	
SDC35	Flaming	Chair	Living Area	
SDC36	Flaming	Mattress	Bedroom	Bedroom door closed
SDC37	Smoldering	Mattress	Bedroom	
SDC38	Flaming	Mattress	Bedroom	
SDC39	Flaming	Mattress	Bedroom	
SDC40	Smoldering	Mattress	Bedroom	
SDC41	Heating	Cooking Oil	Kitchen Area	

Table 12. Test Conditions for tests conducted in a two-story home

Test	Ignition	Fuel Package	Fire Location	Comments
SDC20	Flaming	Mattress	Bedroom	Bedroom door closed
SDC21	Smoldering	Mattress	Bedroom	Alarms not reached
SDC22	Flaming	Mattress	Bedroom	Ignition failure
SDC23	Smoldering	Chair	Living Room	
SDC24	Heating	Cooking Oil	Kitchen	
SDC25	Flaming	Chair	Living Room	
SDC26	Flaming	Chair	Living Room	
SDC27	Smoldering	Chair	Living Room	Air-conditioning upstairs
SDC28	Flaming	Fully furnished room	Living Room	

5.2 Test Data

As an example of the analysis details, test SDC05 was chosen. This test was a flaming mattress test in a bedroom of the manufactured home. It was chosen as a single representative test, but does include all of the relevant test data. In addition for this test, all of the alarm types responded to the fire. Figures 100 through 121 present the data from test SDC05.

Mass loss of the burning mattress is shown in figure 100. Mass loss grows from shortly after ignition to a peak of approximately 150 g at the end of the test. Like all of the tests in the project, this test was terminated once untenable conditions had been reached in the path of egress from the home. A manually-operated water spray from copper tubing directed at the burning chair (see figure 94) at the end of the test quickly suppressed the fire resulting in a sharp drop in mass loss at the end of the test as the water collected in the pan supporting the mattress. The initiation of this manual suppression is noted in the figure as “Initiation of Suppression.”

Figures 101 to 107 show measured profiles of gas temperature from ceiling to floor in several locations throughout the home. In the ignition location (in a bedroom at one end of the manufactured home, noted as “Main Bedroom” for this report), temperatures reached 120 °C near the ceiling (20 mm from the ceiling) and 98 °C near face level (900 mm below ceiling or 1.5 m from the floor) at the end of the test. Further from the fire, peak temperatures were naturally lower, ranging from 87 °C just outside the main bedroom down to 42 °C in the bedroom farthest from the fire. In the closed bedroom, temperatures remain near ambient.

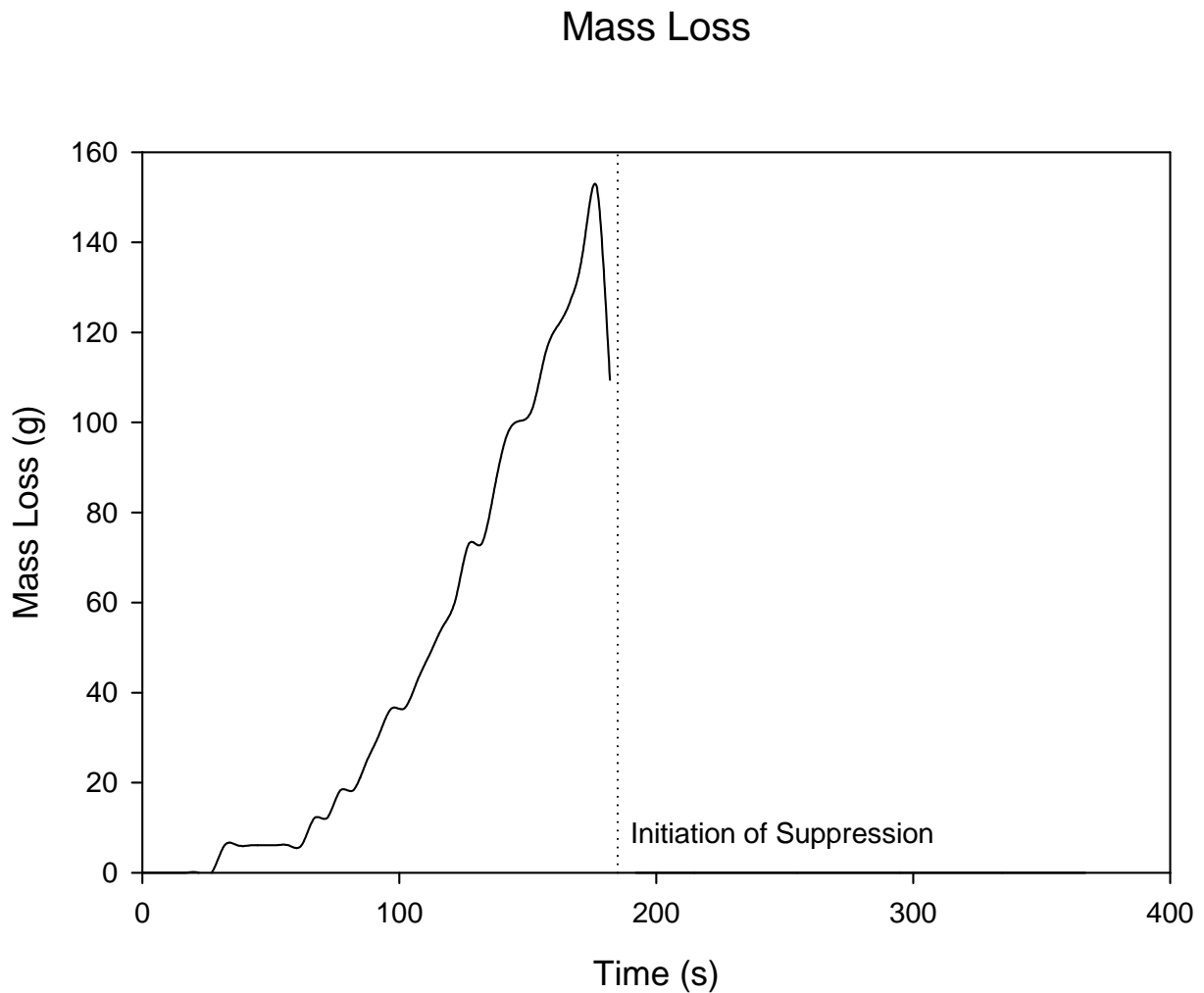


Figure 100. Mass loss of burning mattress during flaming ignition test of a mattress, test SDC05
(Note that the mass loss is averaged to minimize noise in the data. Thus, peak mass loss and initiation of suppression do not exactly coincide)

Remote Bedroom

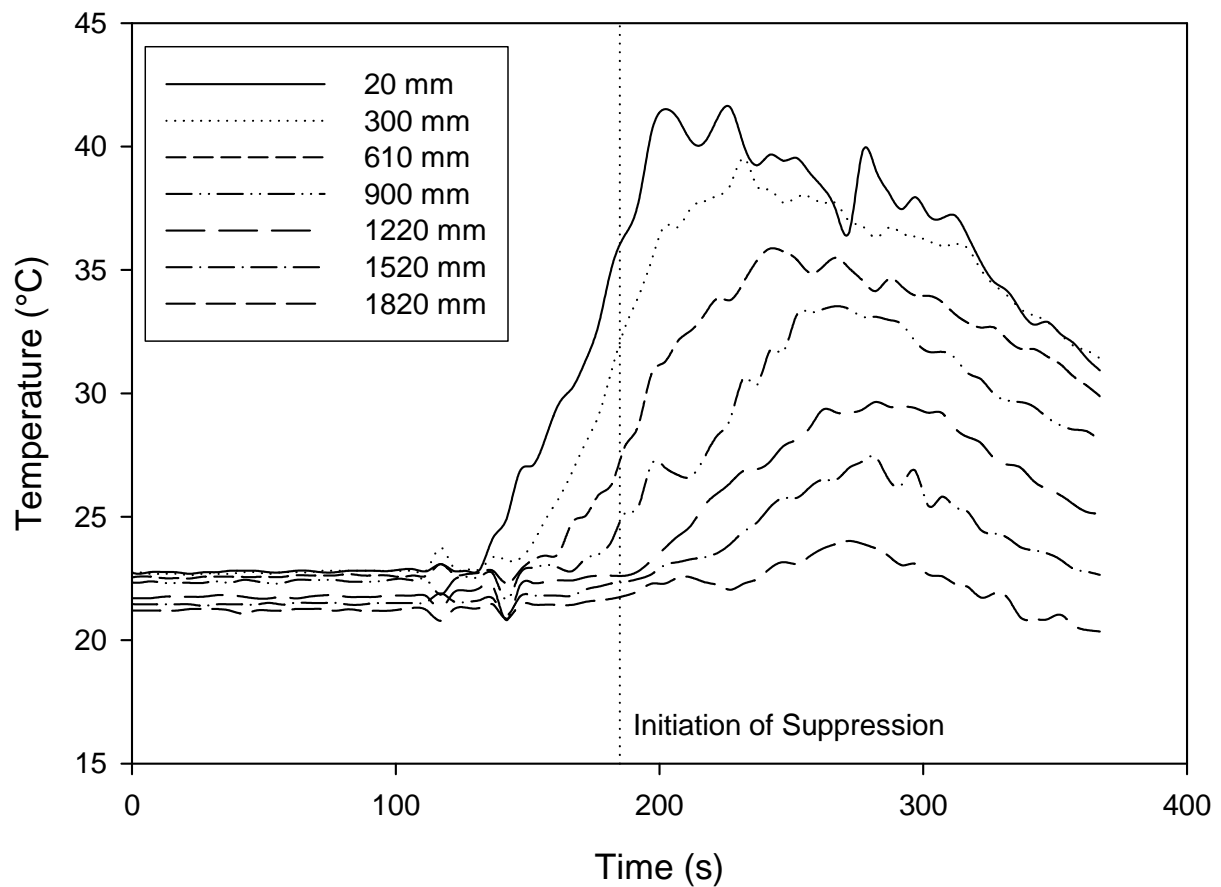


Figure 101. Gas temperatures from ceiling to floor in remote bedroom during a flaming ignition test of a mattress, test SDC05

Main Bedroom

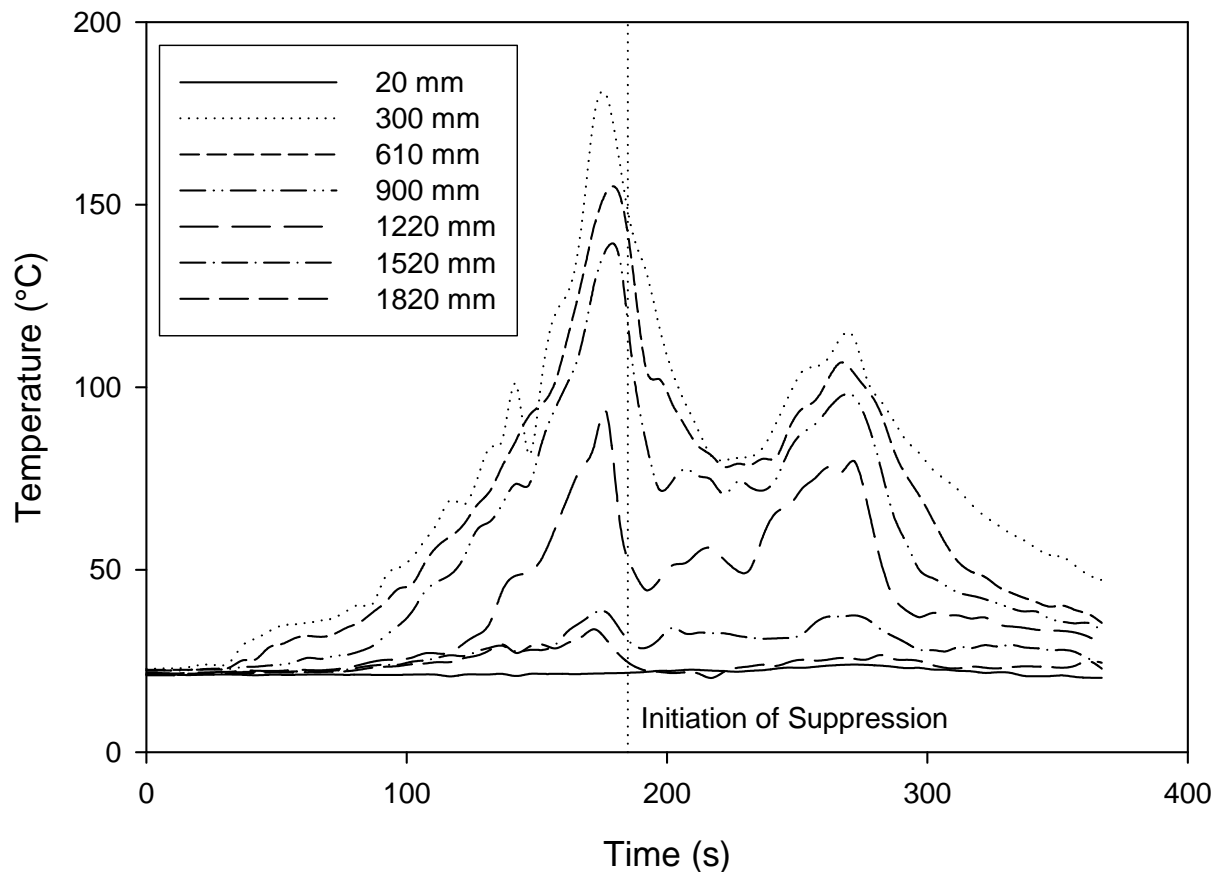


Figure 102. Gas temperatures from ceiling to floor in main bedroom (ignition location) during a flaming ignition test of a mattress, test SDC05

Hallway Outside Remote Bedroom

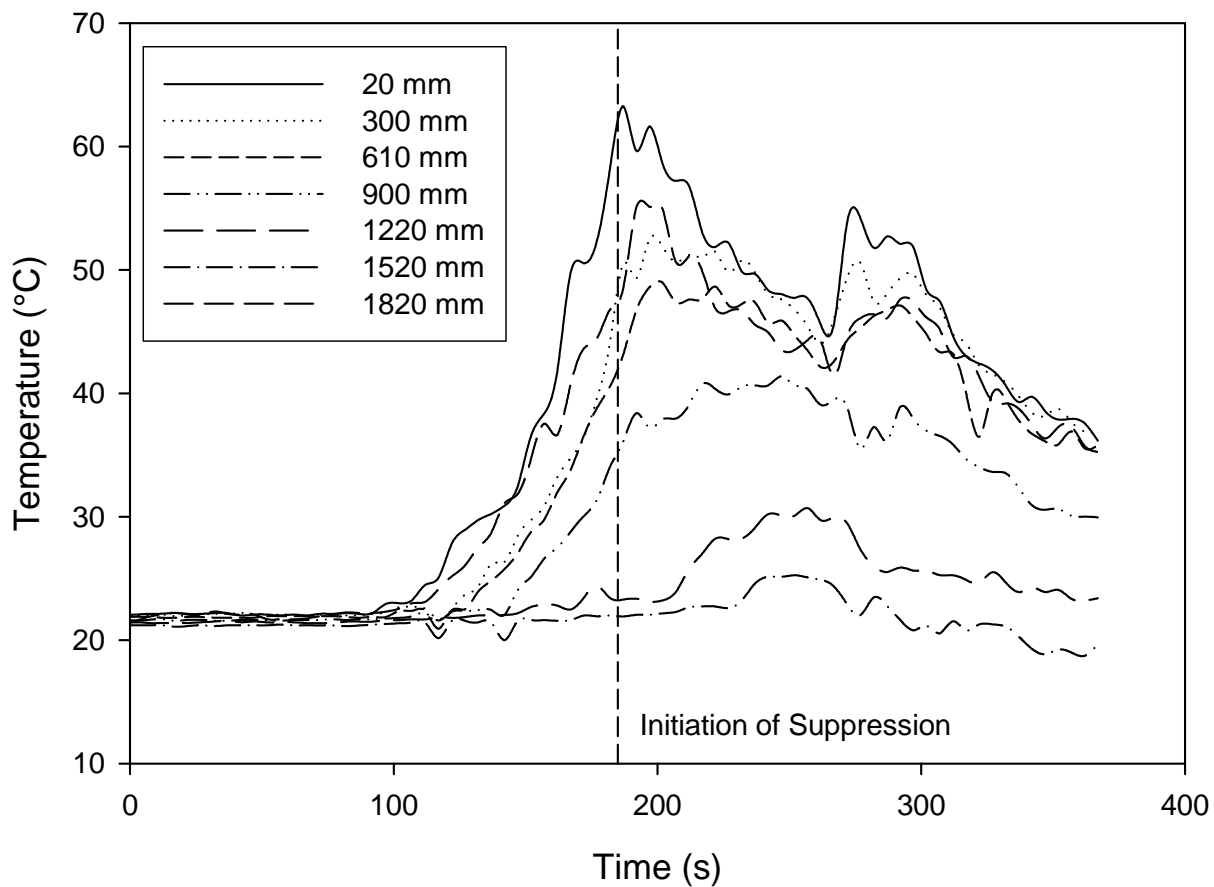


Figure 103. Gas temperatures from ceiling to floor in hallway outside remote bedroom in a flaming ignition test of a mattress, test SDC05

Hallway Outside Main Bedroom

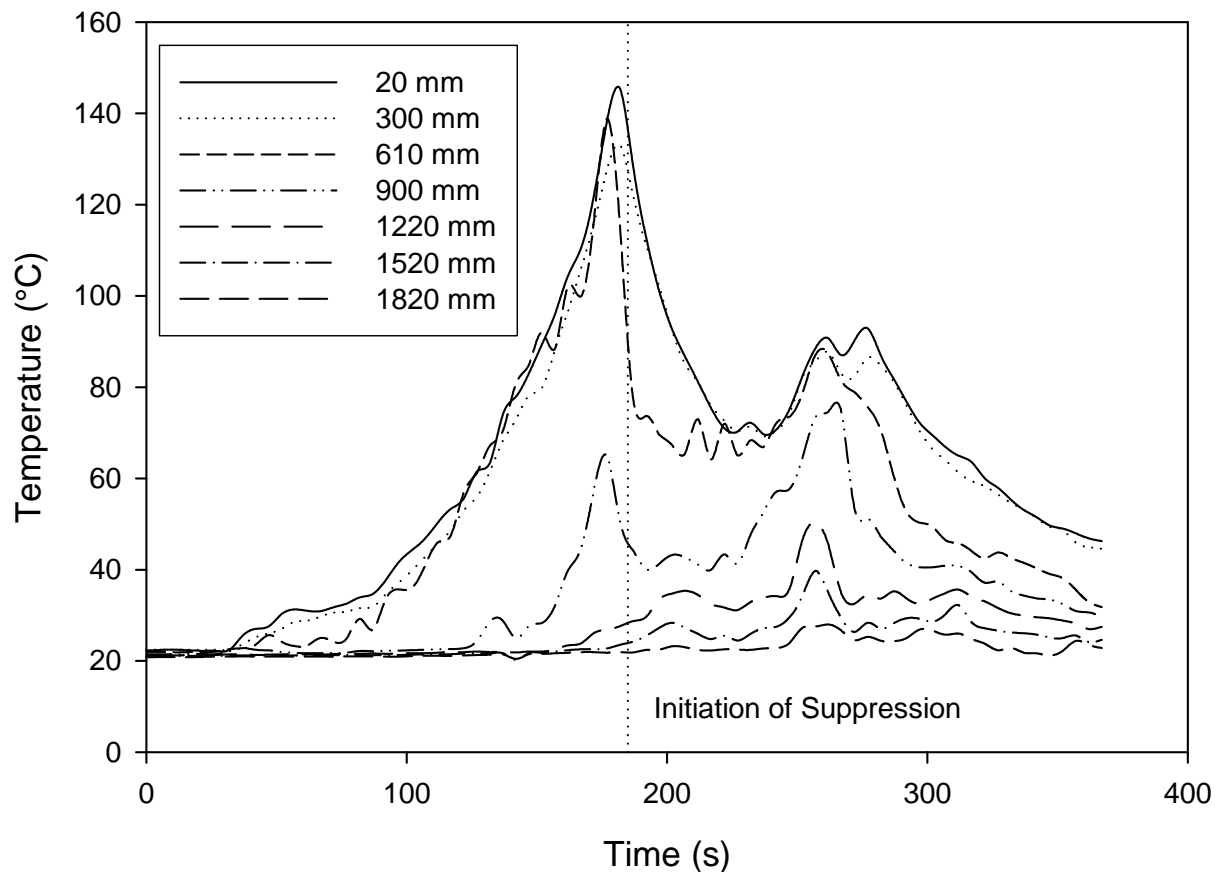


Figure 104. Gas temperatures from ceiling to floor in hallway outside main bedroom in a flaming ignition test of a mattress, test SDC05

Living Room

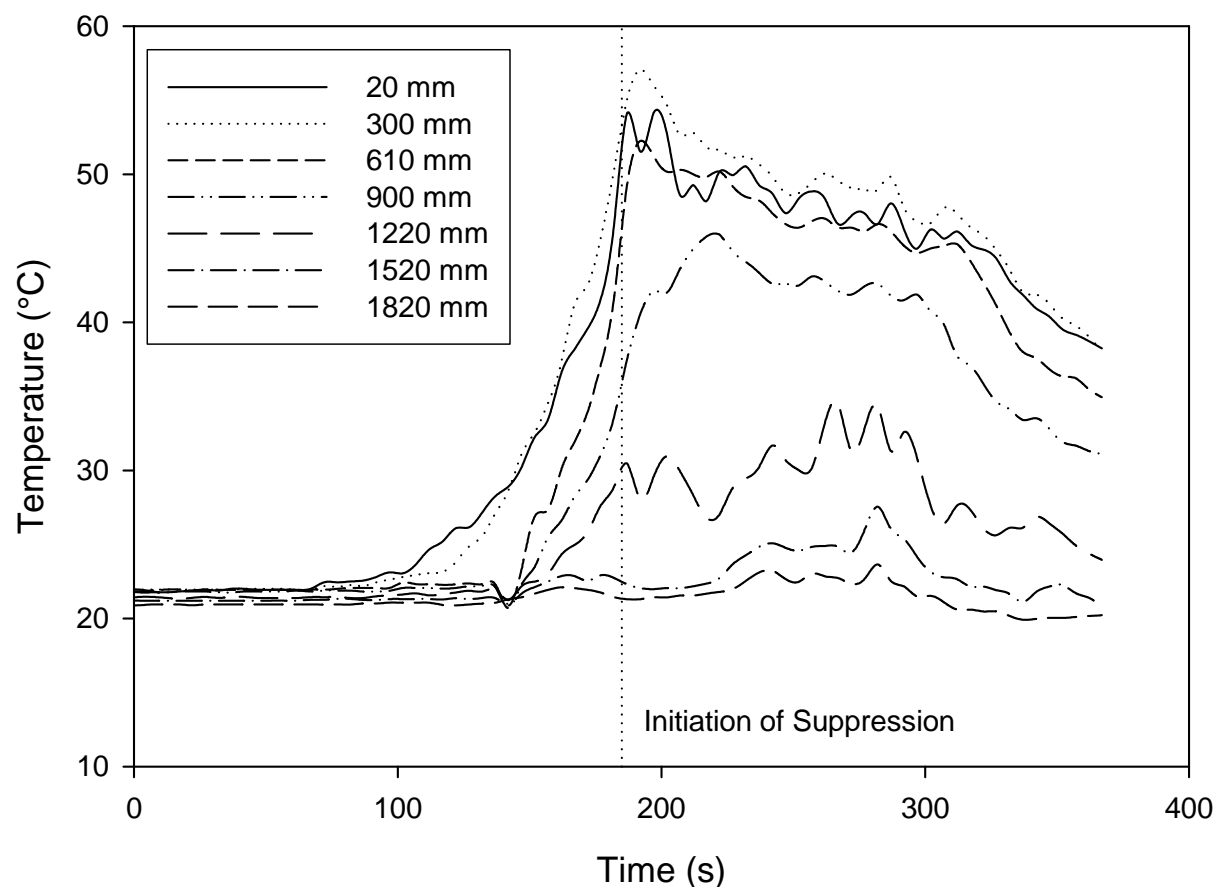


Figure 105. Gas temperatures from ceiling to floor in living area during a flaming ignition test of a mattress, test SDC05

Front Door Hallway

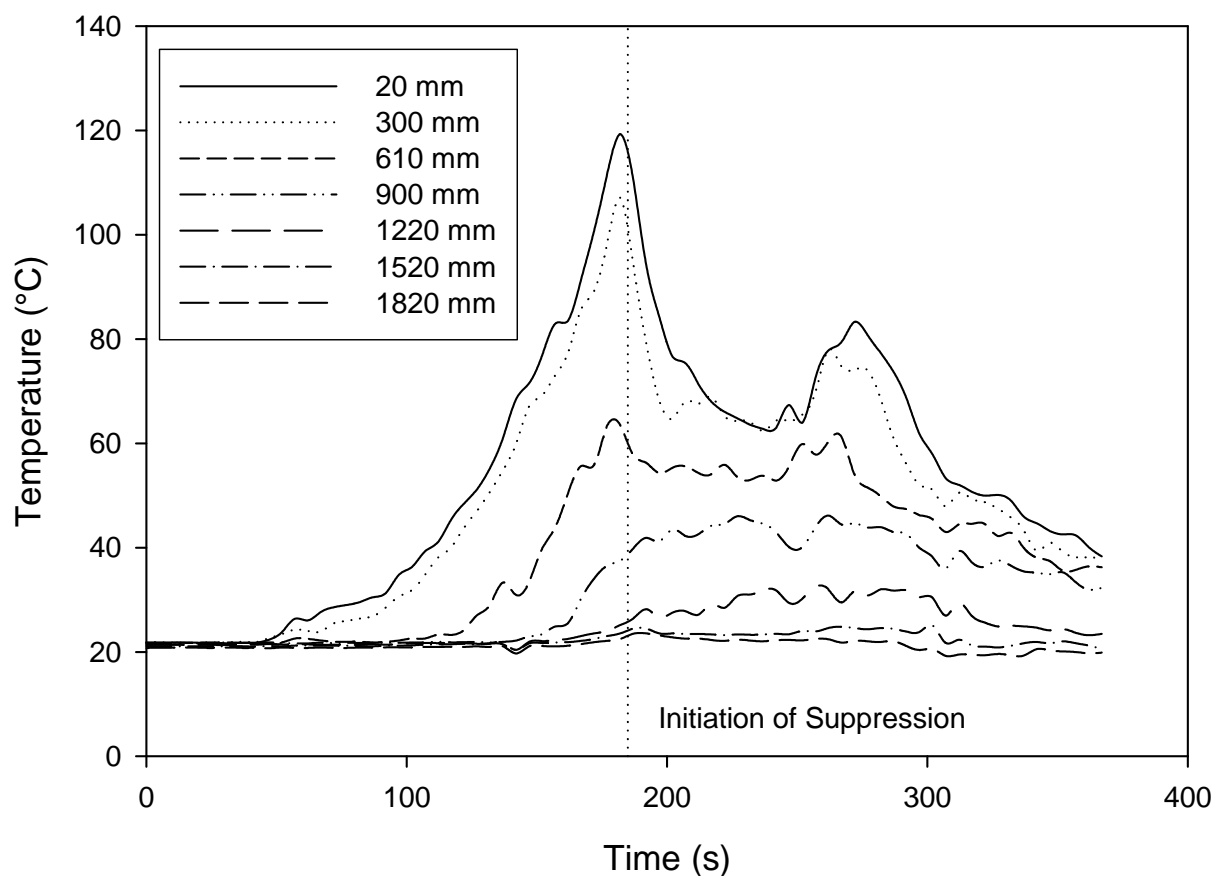


Figure 106. Gas temperatures from ceiling to floor in front door hallway during a flaming ignition test of a mattress, test SDC05

Closed Bedroom

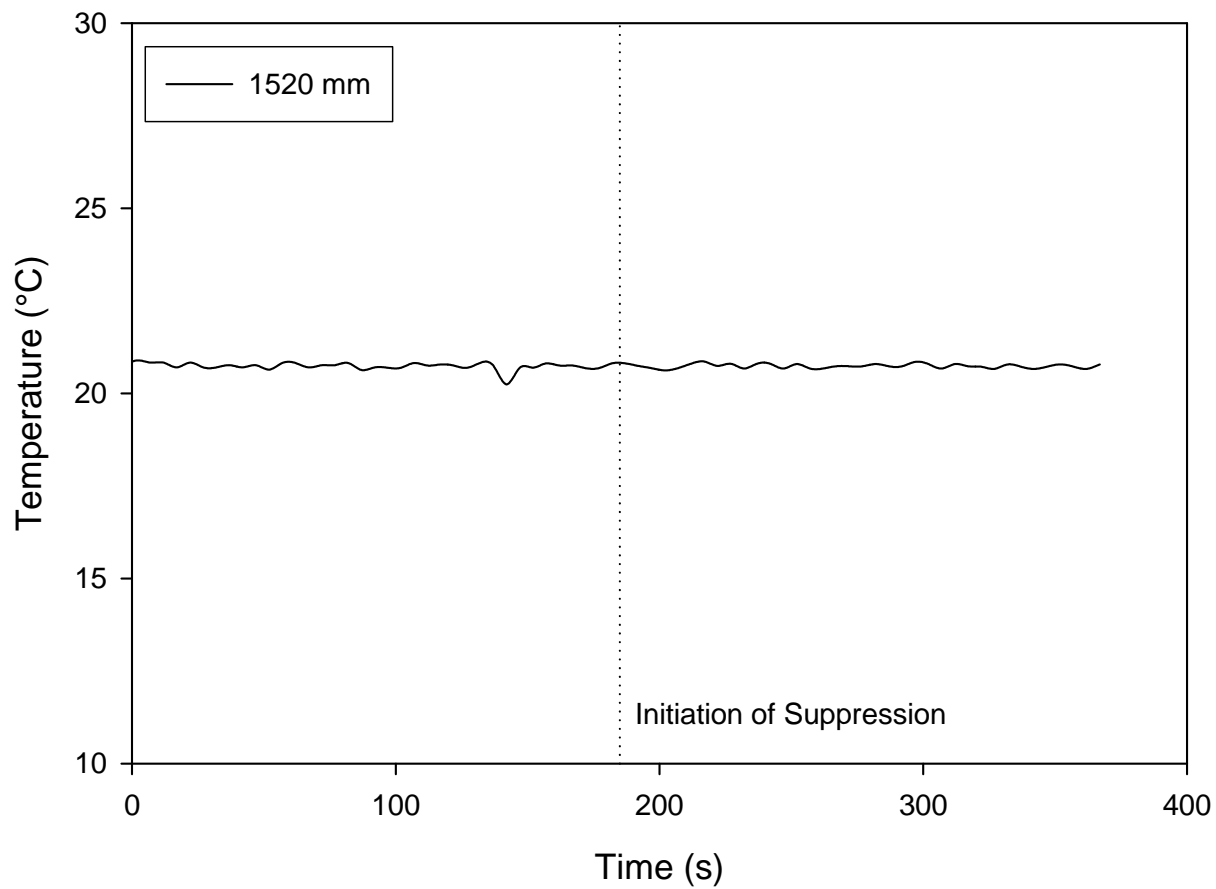


Figure 107. Gas temperature in closed bedroom during a flaming ignition test of a mattress,
test SDC05

Figures 108 through 114 show smoke obscuration near the ceiling (20 mm below the ceiling) and near face height (900 mm from ceiling or 1.5 m from floor) at several locations throughout the home. Like the gas temperatures, peak values are highest near the fire (an optical density of nearly 5.0 m^{-1} near the ceiling in the main bedroom) and peak values less than 2.0 m^{-1} further removed from the fire. In the main bedroom, the smoke meter near the ceiling shows an initial peak beginning about 50 s not evident in other locations. Examination of the video for this test shows little reason for this initial peak so it may indicate a malfunction in the instrument.

Values at the 1.5 m level are naturally lower, typically below 1.0 m^{-1} . In the closed bedroom, an increase in obscuration is noticeable, but still near ambient levels throughout the test.

Figure 115 shows carbon monoxide concentration 900 mm below ceiling level (1.5 m from the floor) at several locations throughout the home. Peak values range from a high of 0.099 % volume fraction near the fire down to 0.043 % volume fraction remote from the fire – both shortly after initiation of suppression. Just prior to suppression, these values are 0.049 % volume fraction and 0.017 % volume fraction, respectively. Similarly, values from carbon dioxide (figure 116) range from 2.3 % volume fraction near the fire down to 0.74 % volume fraction remote from the fire overall and 2.0 % volume fraction down to 0.25 % volume fraction prior to suppression. Oxygen concentration (figure 117) lowers quickly in the main bedroom fire room to a low of about 19 % volume fraction. By the end of the test, concentrations at all measurement points are similar at just under 20 % volume fraction.

A total of 43 fire alarms were monitored in each test. Figures 118 to 121 show the measured output for the alarms at one measurement location (just outside the main bedroom). Many of the smoke alarms (figure 118) respond within about 40 s after ignition. In this test, all but one of the alarms responded to the fire. One alarm, Ion-4 (see figure 10 for details of the alarm identification codes), showed little response by the end of the test. The carbon monoxide alarms (figure 119) begin to respond within about 50 s, with significant output after 100 s. One of the alarms, CO-1, was inadvertently disconnected during this test. The heat alarm at 127 s (figure 120) and tell-tale sprinkler at 147 s (figure 121) respond within 20 s of one another. One of the photoelectric alarms shows little response until late in the test.

5.3 Calculation of Alarm Times

For each of the analog alarms, voltage readings were converted to engineering units typical for the alarm – obscuration for smoke alarms (from table 1) and concentration for carbon monoxide alarms (from a linear calibration with reference gases). Calibrations of each individual alarm was determined in the FE/DE (see section 2) and are shown in table 13. Typical alarm points for each type of alarm were used to determine a time of alarm for each alarm at each measurement location:

Remote Bedroom

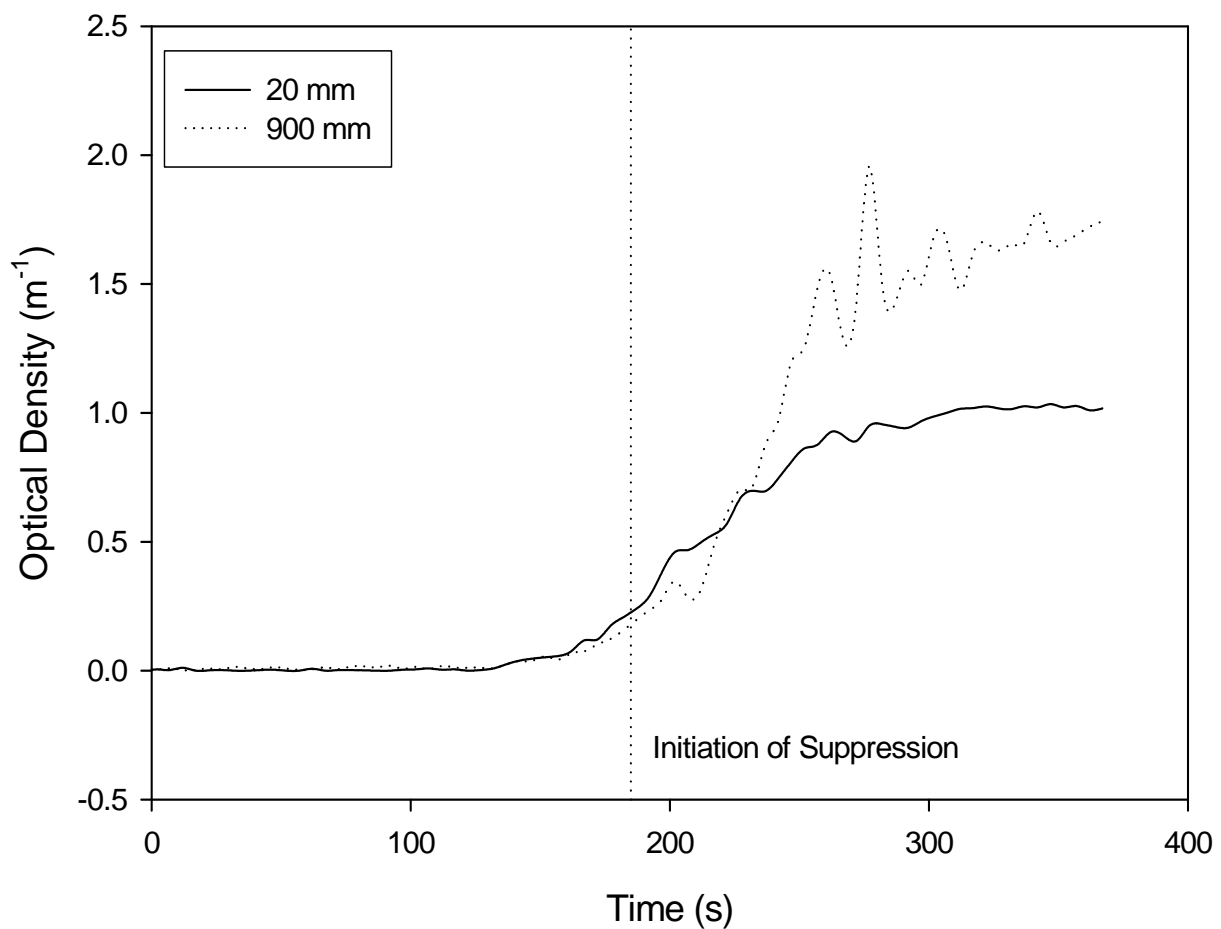


Figure 108. Smoke obscuration at 20 mm and 900 mm below ceiling in remote bedroom during flaming ignition test of a mattress, test SDC05

Main Bedroom

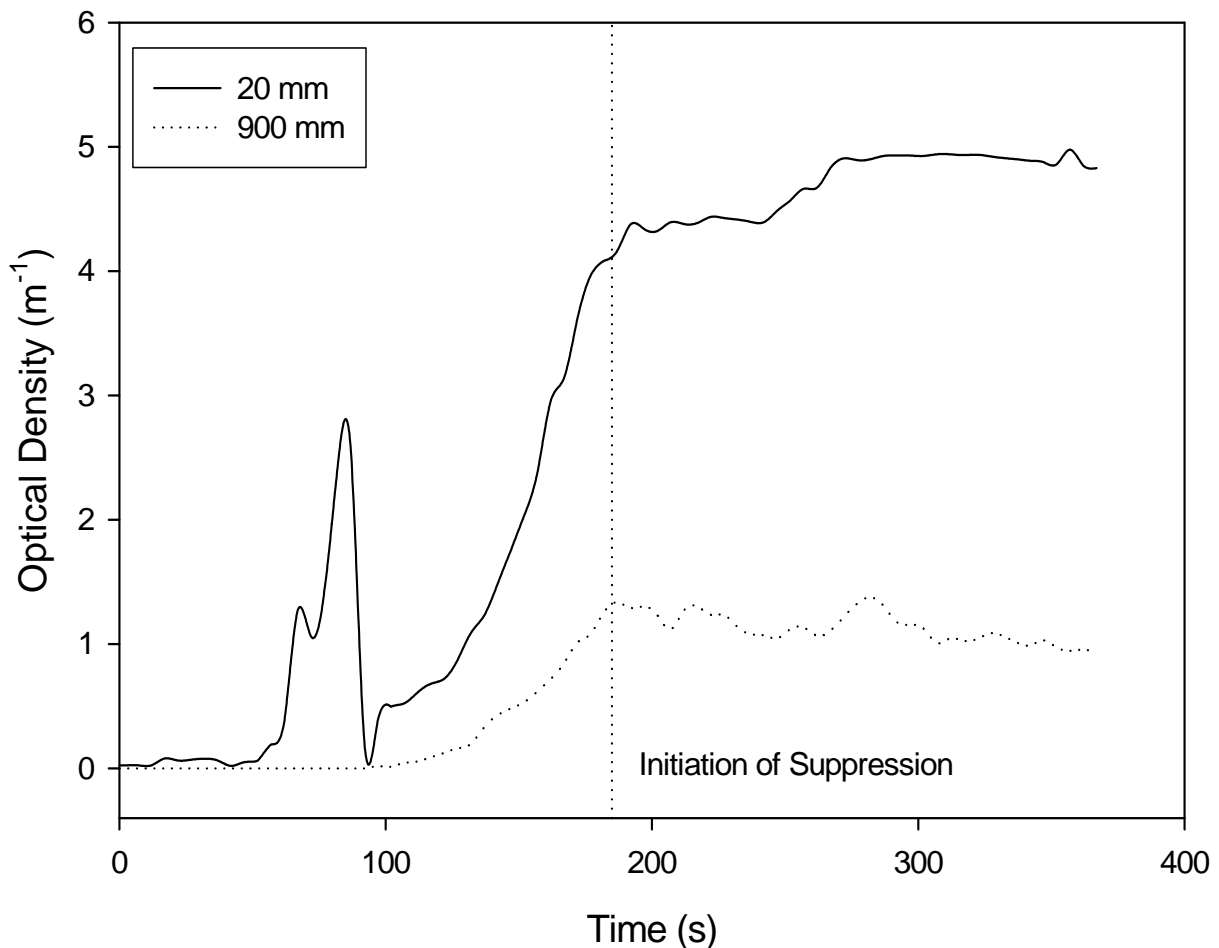


Figure 109. Smoke obscuration at 20 mm and 900 mm below ceiling in main bedroom (ignition location) during flaming ignition test of a mattress, test SDC05

Hallway Outside Remote Bedroom

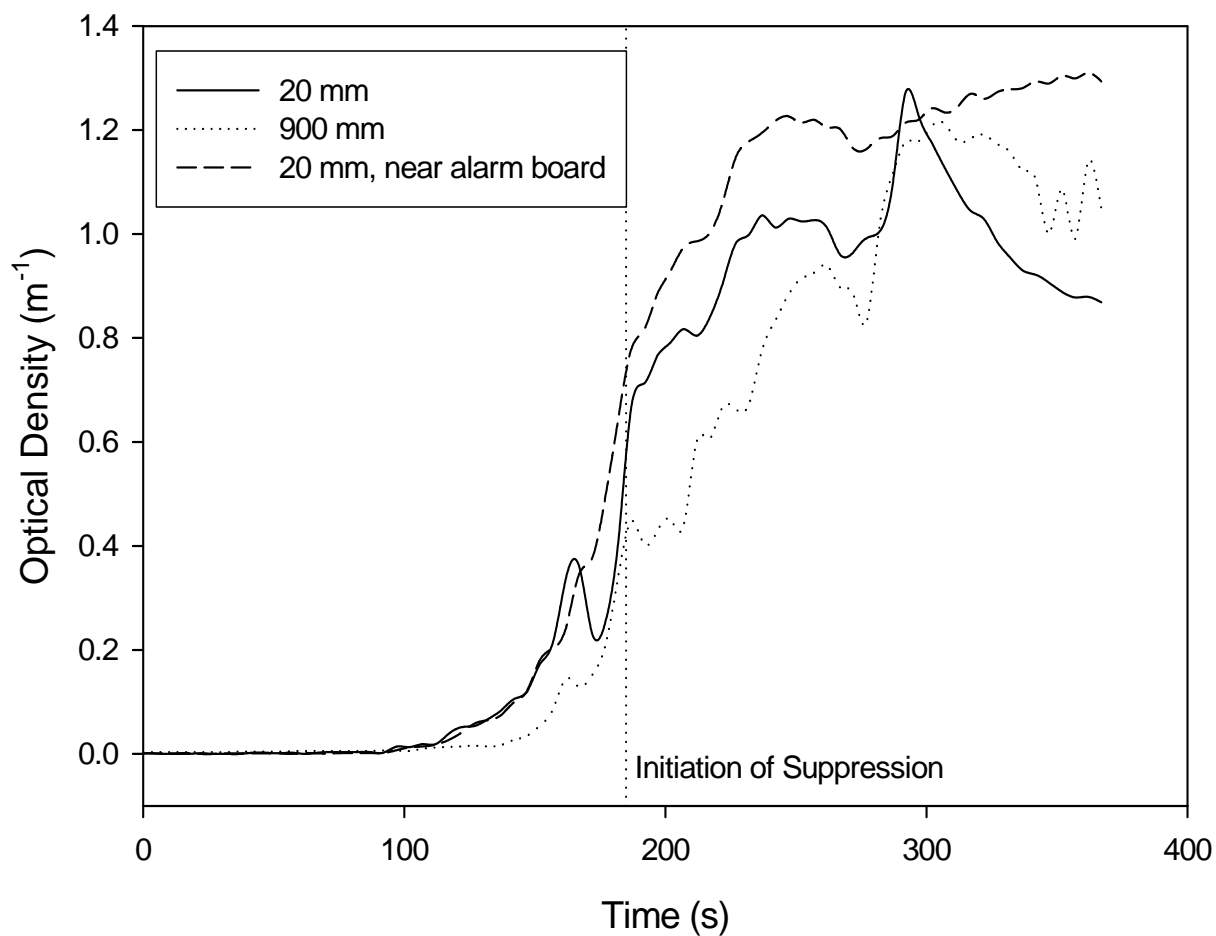


Figure 110. Smoke obscuration at 20 mm and 900 mm below ceiling in hallway outside remote bedroom during flaming ignition test of a mattress, test SDC05

Hallway Outside Main Bedroom

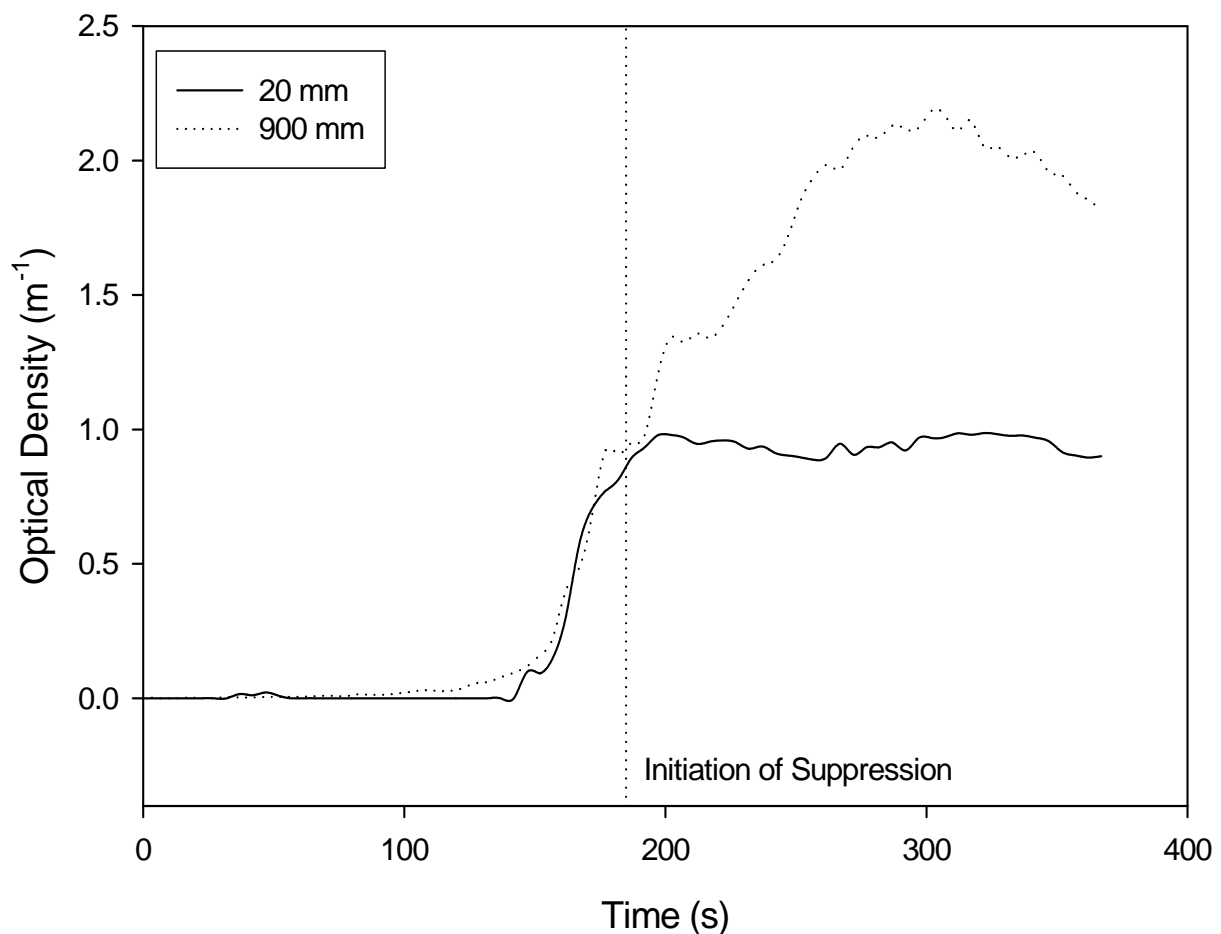


Figure 111. Smoke obscuration at 20 mm and 900 mm below ceiling in hallway outside main bedroom during flaming ignition test of a mattress, test SDC05

Living Room

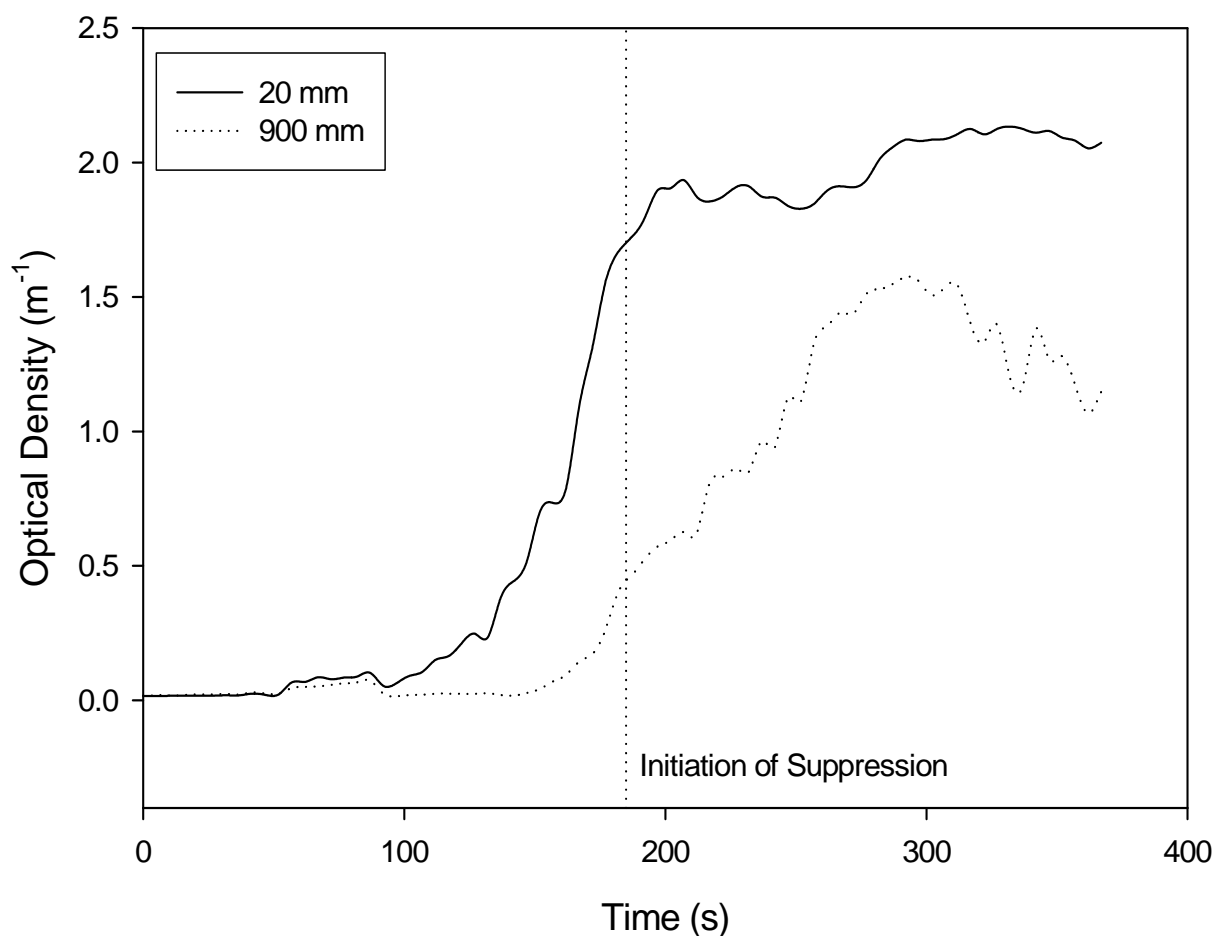


Figure 112. Smoke obscuration at 20 mm and 900 mm below ceiling in living area during flaming ignition test of a mattress, test SDC05

Front Door Hallway

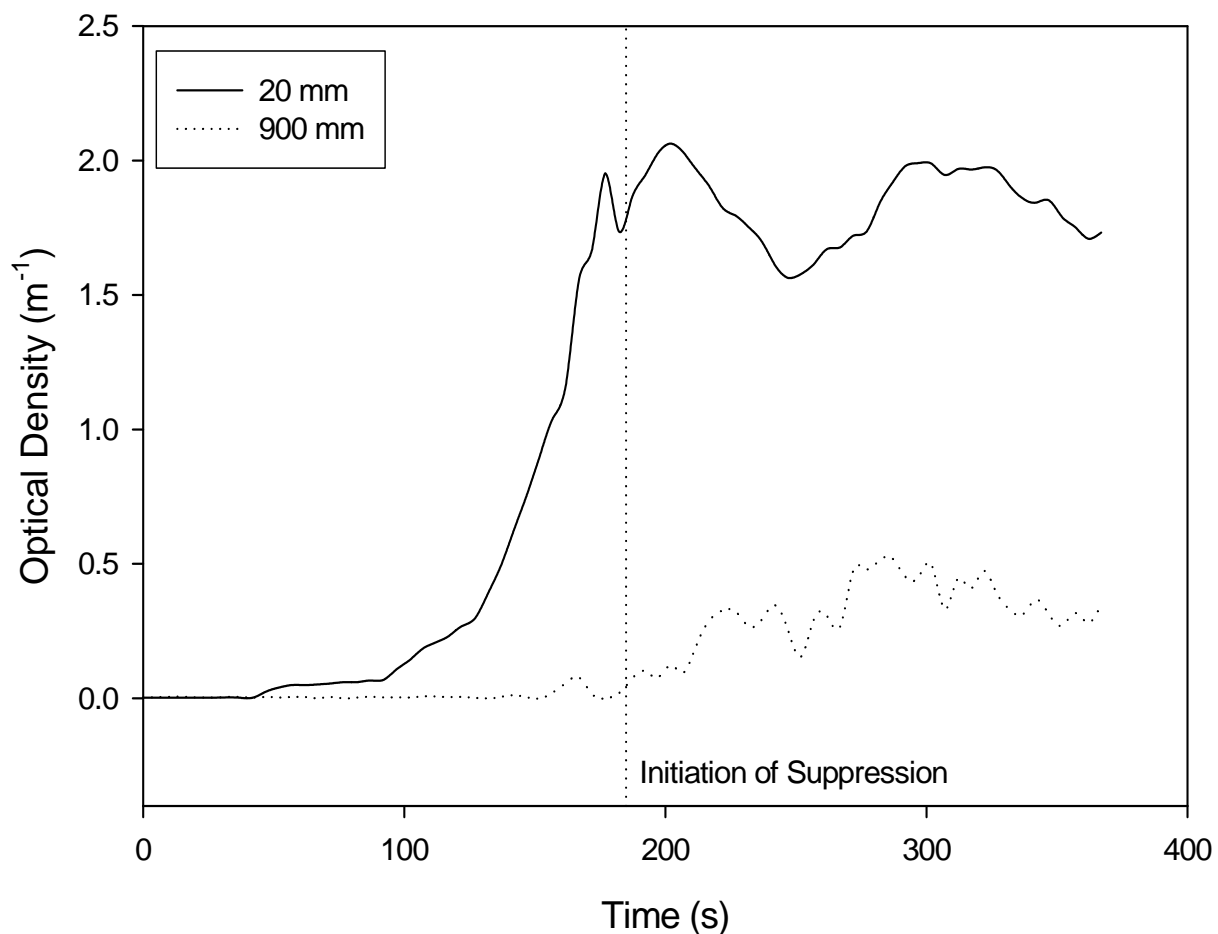


Figure 113. Smoke obscuration at 20 mm and 900 mm below ceiling in front door hallway during flaming ignition test of a mattress, test SDC05

Closed Bedroom

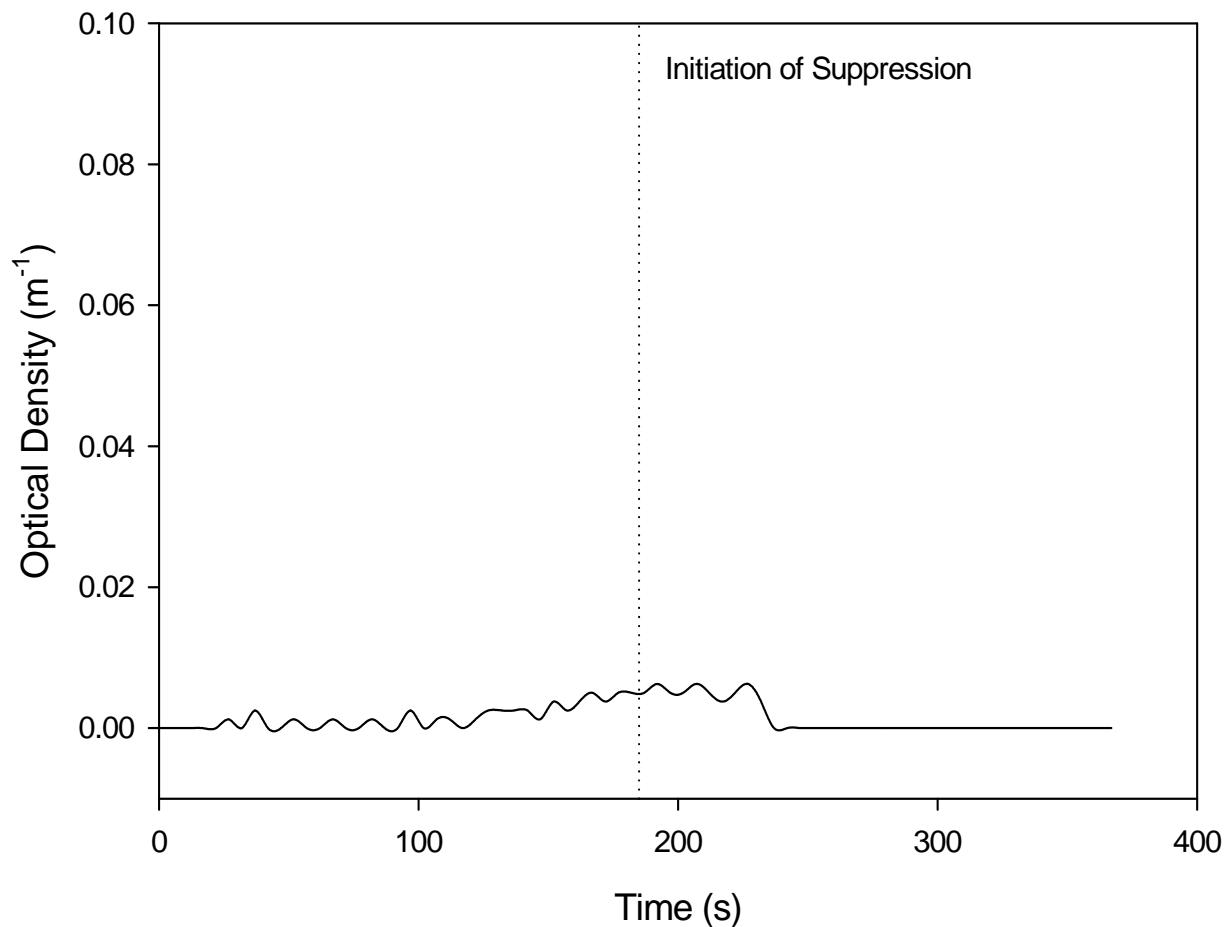


Figure 114. Smoke obscuration at 1520 mm below ceiling in closed bedroom during flaming ignition test of a mattress, test SDC05

Carbon Monoxide

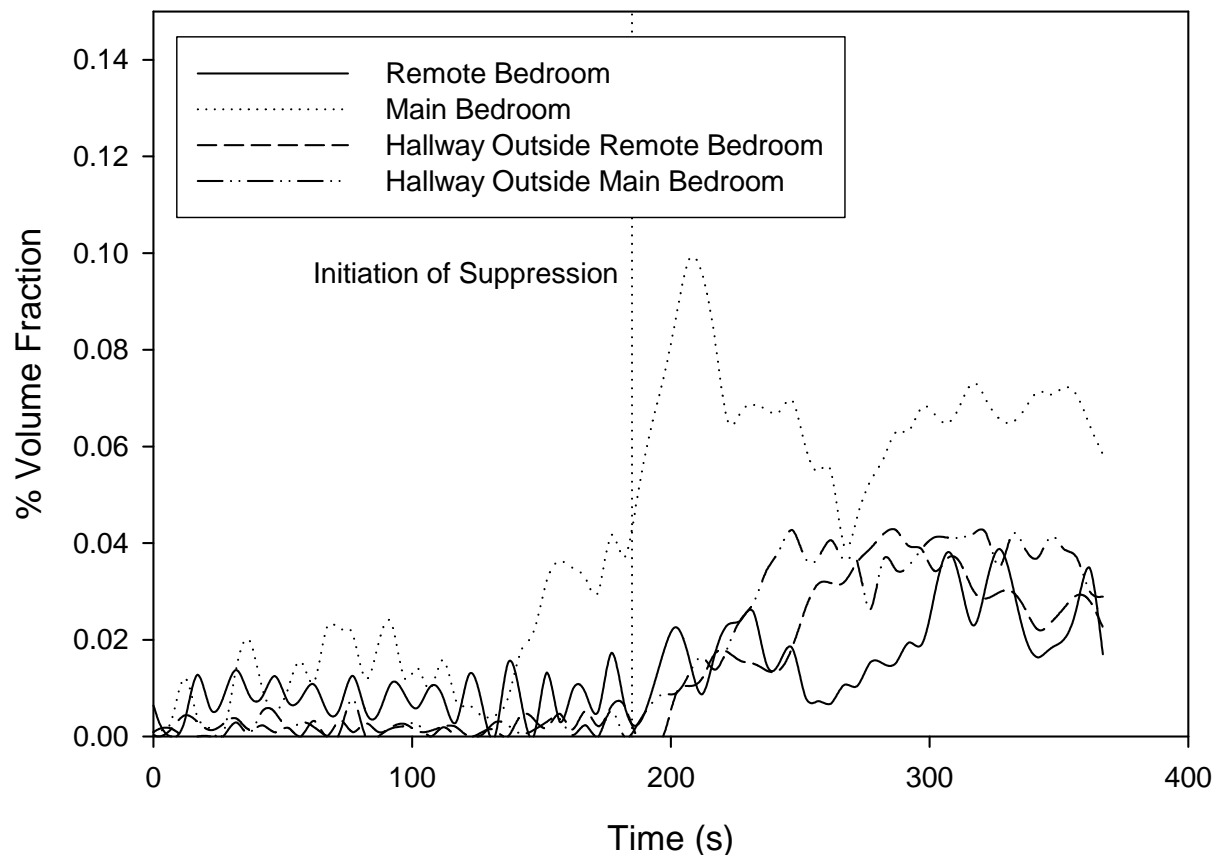


Figure 115. Carbon monoxide concentration 900 mm below ceiling at four locations during a flaming ignition test of a mattress, test SDC05

Carbon Dioxide

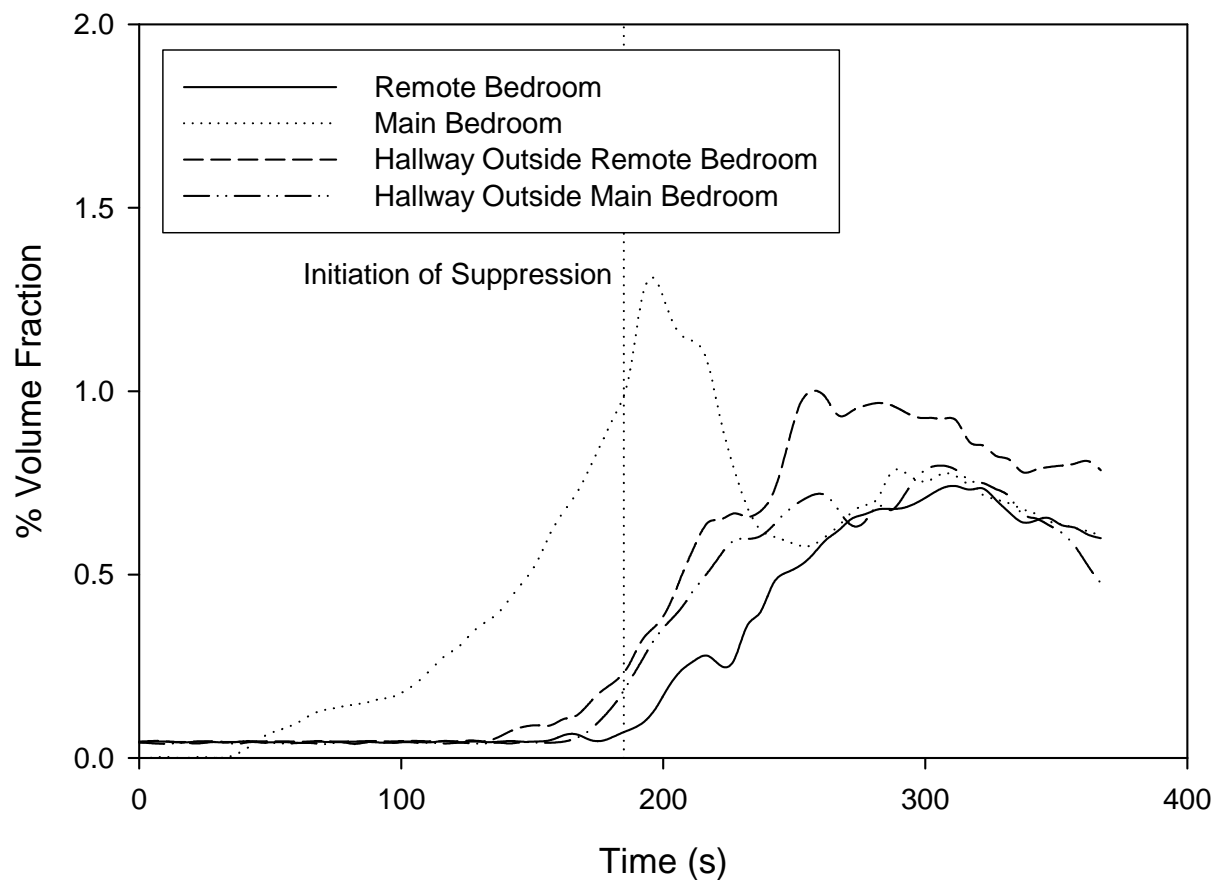


Figure 116. Carbon dioxide concentration 900 mm below ceiling at four locations during a flaming ignition test of a mattress, test SDC05

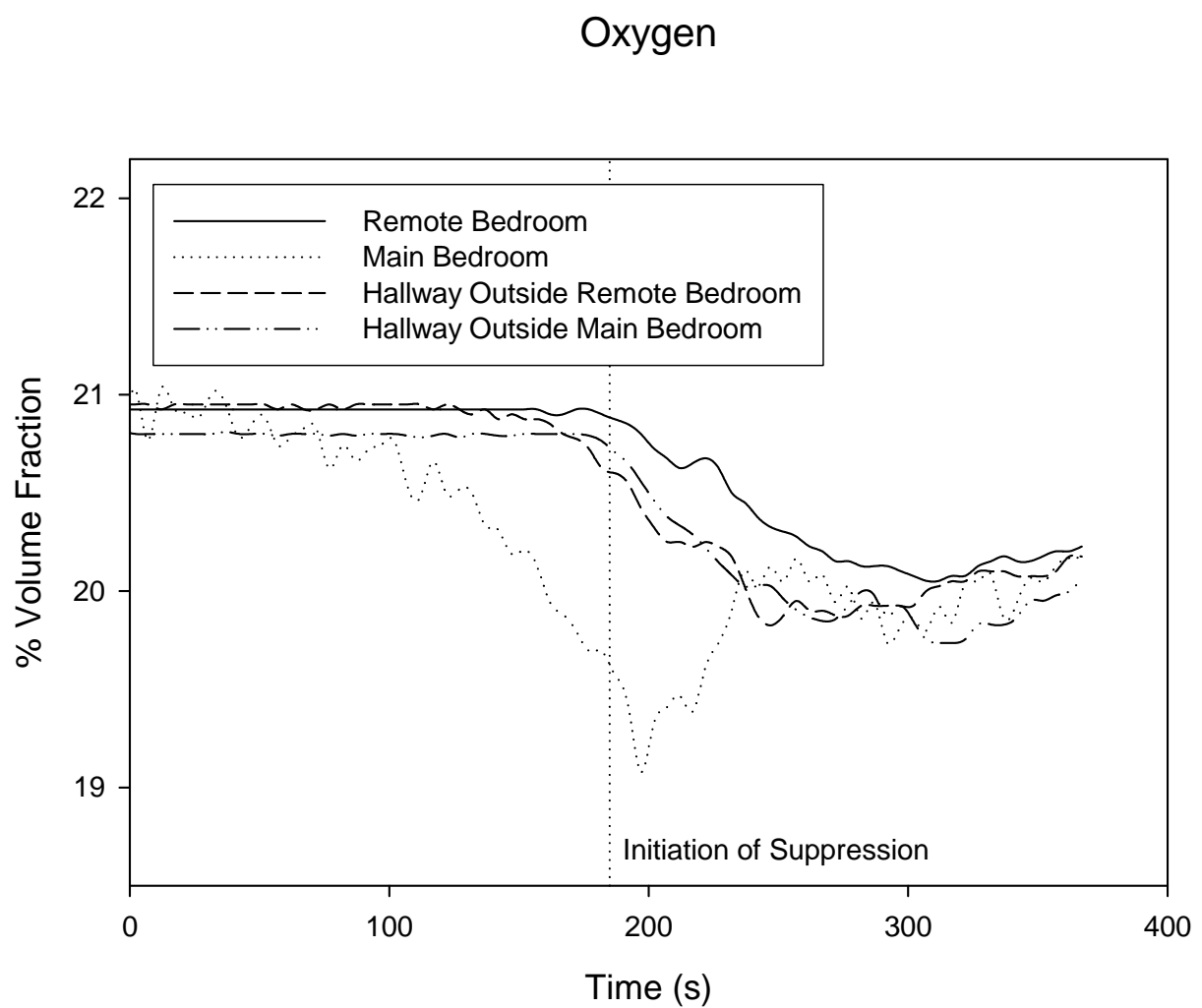


Figure 117. Oxygen concentration 900 mm below ceiling at four locations during a flaming ignition test of a mattress, test SDC05

Smoke Alarm Output

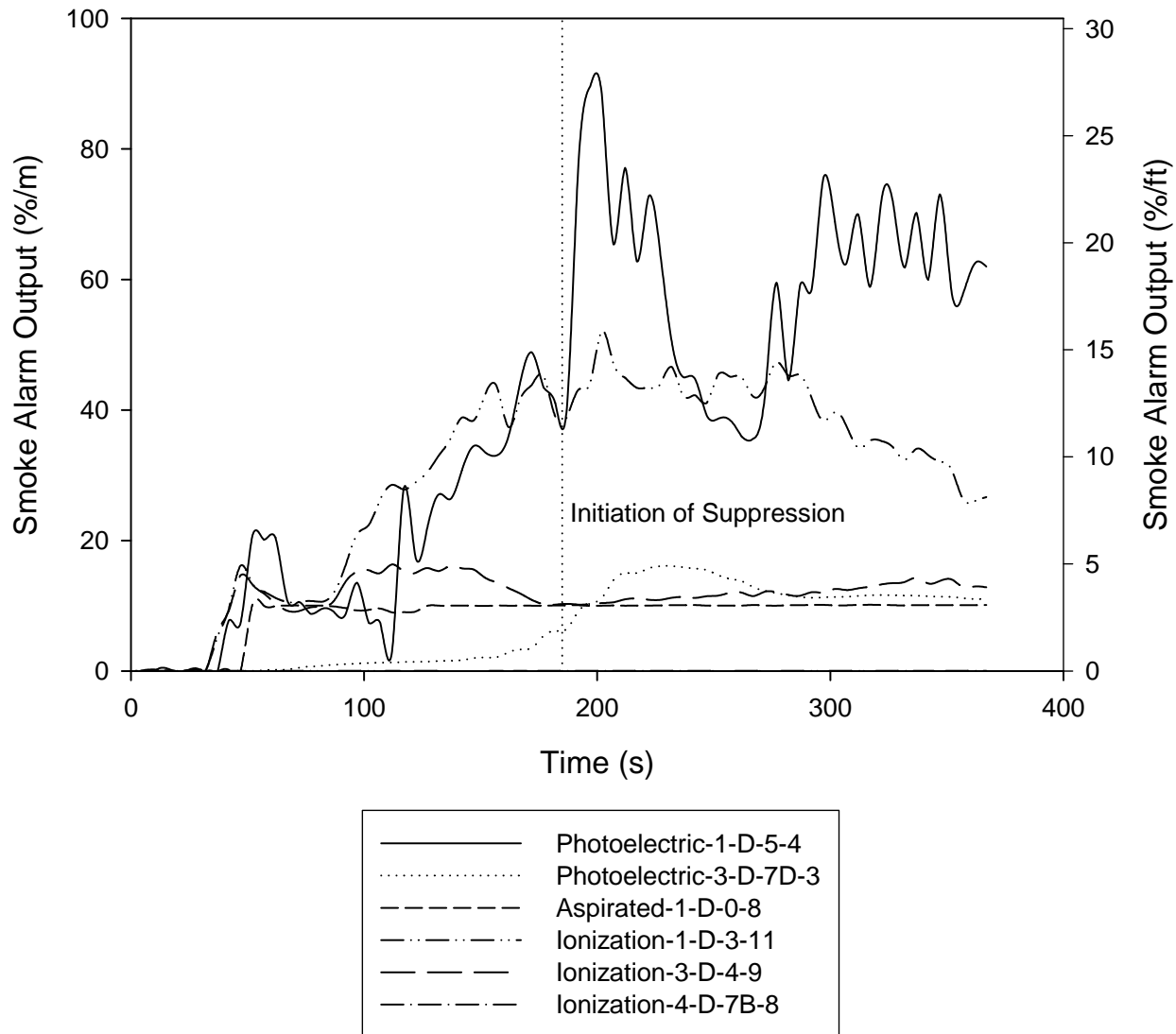


Figure 118. Measured output for several analog-modified smoke alarms in hallway outside main bedroom during a flaming ignition test of a mattress, test SDC05

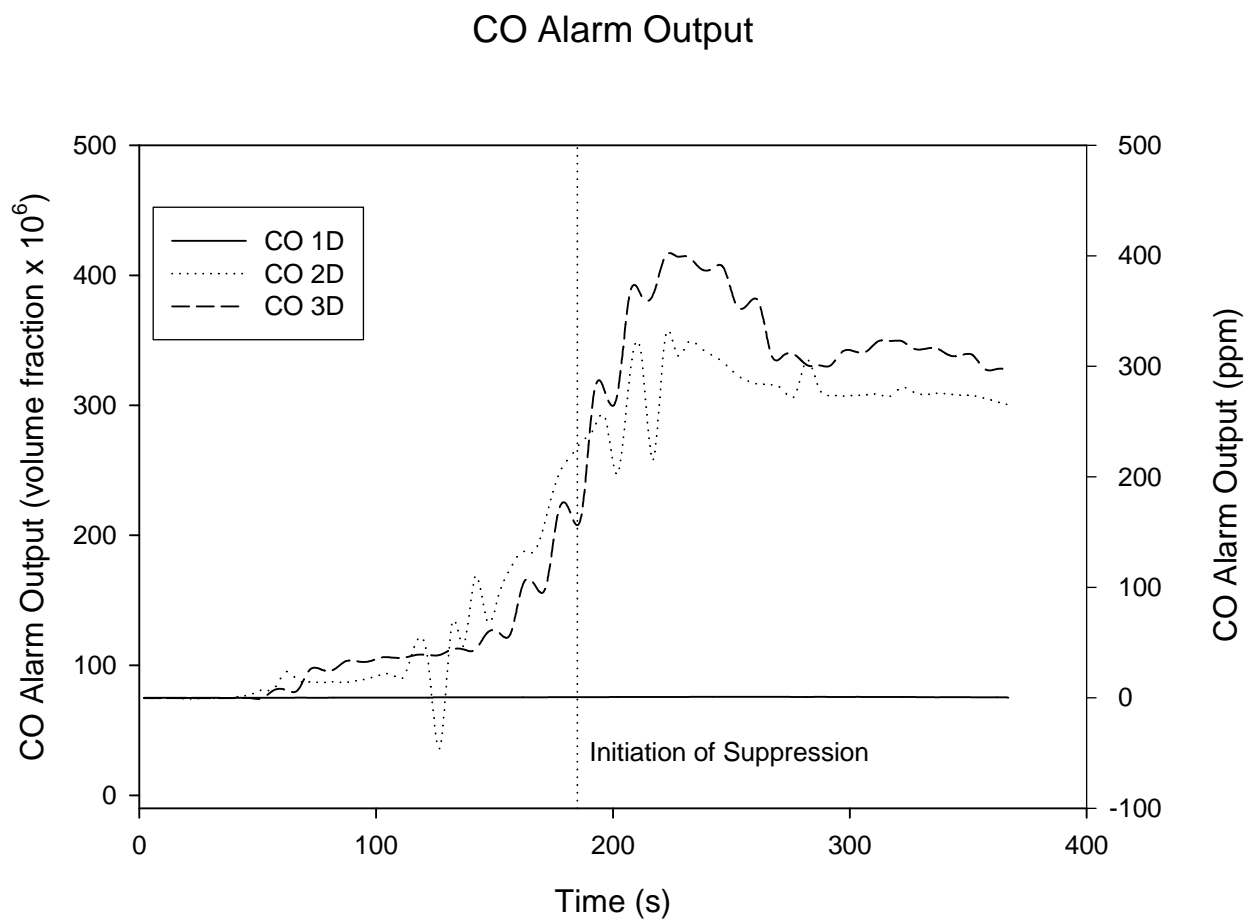


Figure 119. Measured output for several analog-modified carbon monoxide alarms in hallway outside main bedroom during a flaming ignition test of a mattress, test SDC05

Heat Alarm

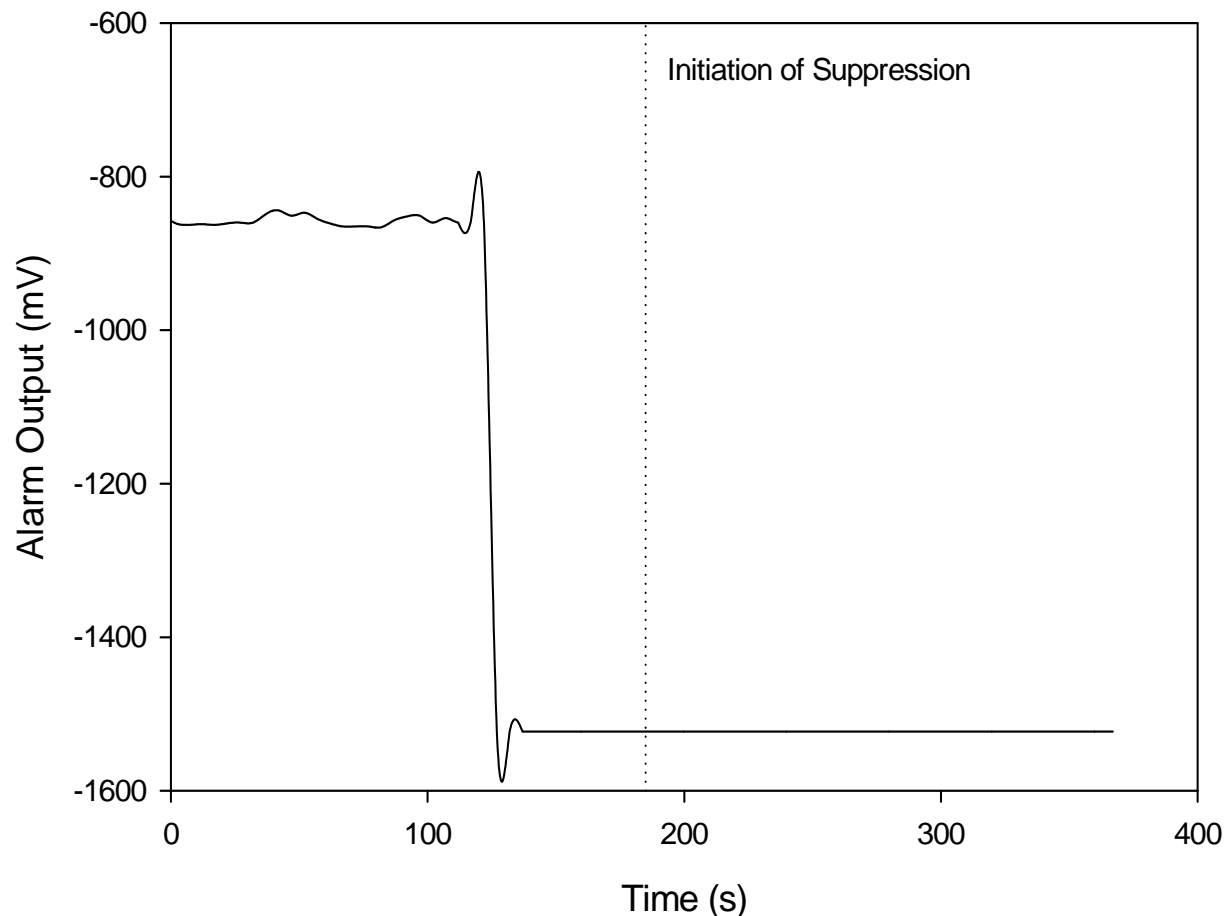


Figure 120. Measured output for a heat alarm in hallway outside main bedroom during a flaming ignition test of a mattress, test SDC05

Sprinkler Response

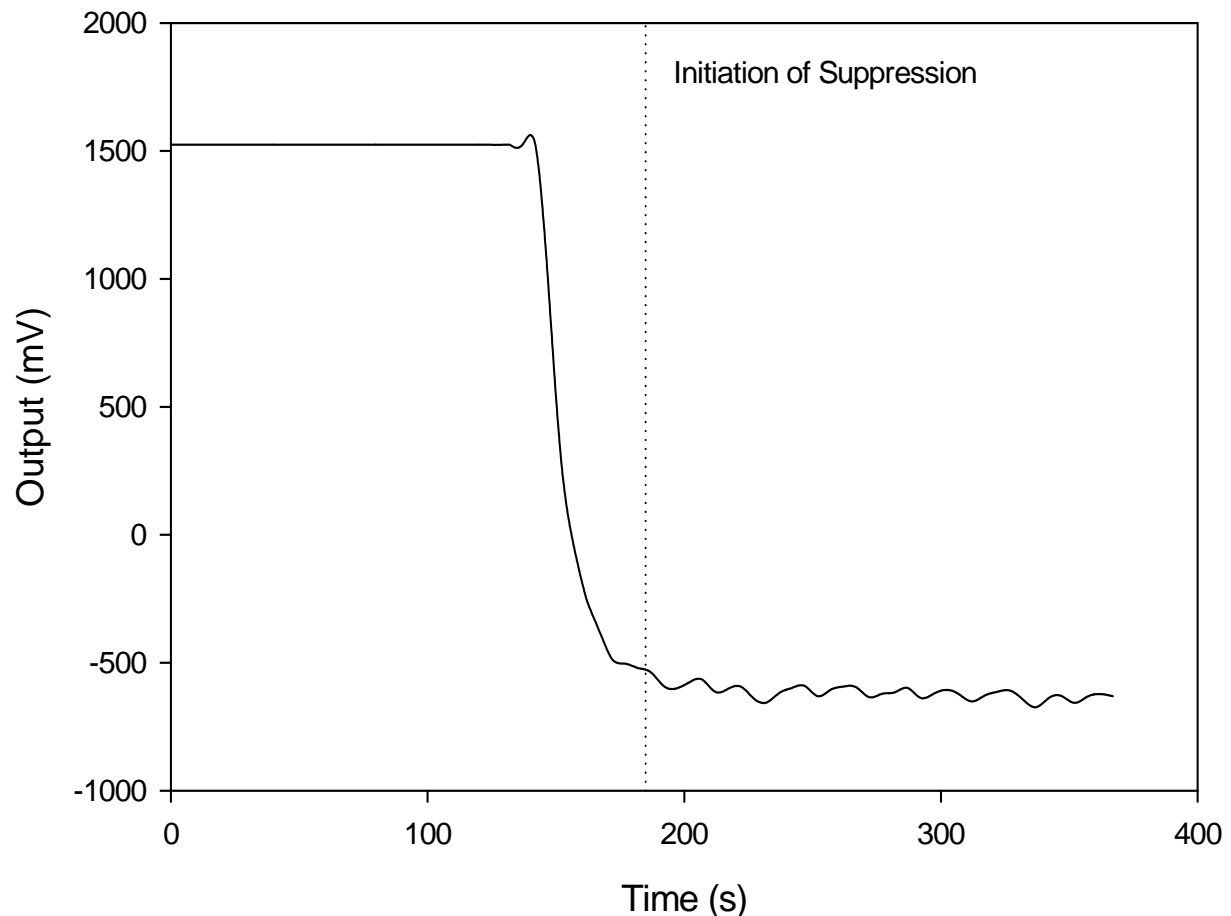


Figure 121. Measured output for a tell-tale residential sprinkler in hallway outside main bedroom during a flaming ignition test of a mattress, test SDC05

- carbon monoxide alarms – 50×10^{-6} volume fraction (50 ppm)
- ionization alarms – 4.3 %/m (1.3 %/ft)
- photoelectric alarms – 6.6 %/m (2 %/ft)

Section 2.8 discusses determination of these alarm points. For some alarms, a single alarm time was obvious from the output (for example, see figure 120). For the one location in the hallway outside the main bedroom, alarm times are shown in table 13. For this location, all alarms reached typical alarm points in times ranging from a first alarm at 37 s to one shortly after initiation of manual suppression at 192 s. For many alarms, the choice of alarm point had little effect on the resulting alarm times.

Table 13. Alarm Times for Several Smoke Alarms in Hallway Outside Main Bedroom During Flaming Ignition Test of a Mattress, Test SDC05

ID	Calibrations (from table 1)		Alarm Times (s)		
	m_0	m_1	low	mid	high
Smoke Alarm	ION-1-D-3-7	0	2.09	37	37
Smoke Alarm	ION-3-D-4-13	0	1.14	37	37
Smoke Alarm	PHOTO-1-D-5-4	-1.96	6.88	42	42
Smoke Alarm	ASPIRATED-1-D-0-8	-1.27	1.84	52	52
CO Alarm	CO-1-D-1-5	-43.6	233.3	n.a. ^b	n.a.
CO Alarm	CO-2-D-2-2	-45.1	93.0	142	142
CO Alarm	CO-3-D-3-5	-3.44	165.5	87	147
					177

a – Alarms Ion-4 and Photo-3 are components of a dual mode alarm, but were not functioning for this test

b – n.a. = no activation indicated

5.4 Calculation of Time to Untenable Conditions

5.4.1 Tenability Limits

The time available for occupant egress is simply the amount of time from the first indication of a fire (in this case, the alarm time) to the time at which conditions become untenable. This topic has been the subject of current work by an international committee of experts working as ISO Technical Committee (TC) 92, subcommittee (SC) 3. This group has published a technical standard, ISO TS 13571, that recommends limits of human tolerance to fire products [26].

These limits are also consistent with the recommendations in the SFPE Handbook of Fire Protection Engineering. Additional discussion of ISO TS 13571 is included in section 7.2

Heat exposure: The current version of ISO TS 13571 includes equations for calculating incapacitation from skin exposure to radiant heating, from exposure to convected heat resulting from elevated gas temperatures, from exposure to the incapacitating effects of asphyxiant gases, and from exposure to irritant gases.

For these tests, heat exposure is determined as an effect of only elevated gas temperatures. At early times of fire development typical of the tests included in this project, the effects of radiant heating would be negligible. Thus, the Fractional Effective Dose (FED) for heat exposure is given from ISO TS 13571 as:

$$FED_{HEAT} = \sum_{t_1}^{t_2} \frac{T^{3.4}}{5 \times 10^7} \Delta t \quad (5)$$

where T is in °C and Δt is in min.

Exposure to toxic gases: The FED equation for the incapacitating effects of asphyxiant gases, derived from the current version of ISO TS 13571 is:

$$FED_{GASES} = \sum_{t_1}^{t_2} \frac{CO}{35000} \Delta t + \sum_{t_1}^{t_2} \frac{e^{(HCN/43)}}{220} \Delta t \quad (6)$$

where CO and HCN are in volume fraction $\times 10^6$ (ppm) and Δt is in min. CO and HCN are the average values over the time increment Δt . The person “receives” incremental doses of smoke until an incapacitating value of FED is reached.

To determine a time to incapacitation, an FED value of 0.3, indicating incapacitation of the susceptible population was used [26]. This limit was used for both heat and gas tenability. While this is a conservative limit, it is reasonably consistent with the 1975 study. Section 7.6 compares tenability limits in the two studies.

ISO TS 13571 also includes an equation for incapacitation from irritant gases. The primary gas analysis available for this report included only CO, CO₂, and O₂; data on irritant gases were not available.

Smoke obscuration: For smoke obscuration, an optical density of 0.25 m⁻¹ was used as a tenability criterion, a value typically used by the smoke alarm industry. For all calculations, temperature, smoke obscuration, and gas concentration values 900 mm below the ceiling (1.5 m from the floor) were used. This height was intended to be representative of the mouth and nose height for a typical adult during egress from the home.

5.4.2 Tenability Times

Chapter 8 of the National Fire Alarm Code [27] entitled Fire Warning Equipment for Dwelling Units states that the primary function of a dwelling fire warning system is to, "... provide a reliable means to notify the occupants of a dwelling unit of the presence of a threatening fire and the need to escape to a place of safety before such escape might be impeded by untenable conditions in the normal path of egress." The chapter further explains that, "Fire warning systems for dwelling units are capable of protecting about half of the occupants in potentially fatal fires. Victims are often intimate with the fire, ..., such that they cannot escape even when warned early enough that escape should be possible." This is consistent with the earlier research of McGuire and Ruscoe [2]. When escape is not practical, other strategies such as protection-in-place, assisted escape or rescue may be necessary.

Similarly, the Life Safety Code [28] states in 4-1.1, "The goal of this code is to provide an environment for the occupants that is reasonably safe from fire and similar emergencies by the following means: (1) Protection of occupants not intimate with the initial fire development. (2) Improvement of the survivability of occupants intimate with the initial fire development."

The limitations applicable to the protection of people intimate with the fire are common and recognize the associated difficulties and costs of such protection. Based on this position in the Codes, the performance criteria applied to the fire alarms in this study were based on the egress time provided between alarm and the time that selected tenability criteria were exceeded at any point in the primary egress path in the home but not including the instruments located at the fire source. These instruments were used to quantify conditions produced by the fire but were not counted towards escape as they represent the conditions to which a person intimate with the fire would experience.

Table 14 shows calculated tenability values for test SDC05. The time to untenable conditions and value for each calculated tenability calculation is shown. To judge available safe egress time, the minimum time to untenable conditions for measurement locations outside the room of fire origin was used. For this test, only the smoke obscuration reached untenable conditions in times ranging from 137 s to 217 s.

In the room of fire origin, the main bedroom, the convected heat criteria was close to untenable with an FED value of 0.273 – near the tenability criterion of $FED = 0.3$. Results of tenability calculations for all of the tests is included as Appendix A.

Table 14. Calculated tenability for a flaming ignition test of a mattress, test SDC05

Measurement Location	Time from Ignition to Untenable Conditions (s)	Final Tenability Value at End of Test
ISO Gas FED = 0.3		
Remote Bedroom (A)	n.r. ^a	0.012
Burn Room Bedroom (BEK)		0.07
Hallway Outside Remote Bedroom (C)		0.021
Front Door Hallway (F)		0.028
ISO Convected Heat = 0.3		
Master Bedroom (A)		0.009
Burn Room Bedroom (BEK)		0.273
Hallway Outside Remote Bedroom (C)		0.016
Hallway Outside Main Bedroom (D)		0.013
Living Area (E)		0.02
Front Door Hallway (F)		0.022
Closed Bedroom (G)		0.004
Smoke Obscuration = 0.25 m⁻¹		
Remote Bedroom (A)	197*	0.276
Burn Room Bedroom (BEK)	137	0.329
Hallway Outside Remote Bedroom (C)	182	0.341
Hallway Outside Main Bedroom (D)	162	0.403
Living Area (E)	177	0.26
Front Door Hallway (F)	217 ^b	0.291
Closed Bedroom (G)		0.006

a – tenability limit not reached by end of test

b – occurs after initiation of suppression

5.5 Assessment of Overall Alarm Performance

With 43 separate alarms throughout the structure in each test, an assessment of overall performance of the alarms requires some grouping of the alarms. For existing homes (and all homes, prior to 1993) smoke alarms are required outside the sleeping rooms and on each additional story of the home. For this report, this arrangement will be referred to as “every level” and represents the minimum arrangement allowed by code. In 1993 the National Fire

Alarm Code was revised to require smoke alarms in every bedroom for new construction in addition to the every level locations. We will refer to this arrangement as “every level + bedrooms.” Finally, the greatest escape times would be guaranteed only if smoke alarms were required in every room – an arrangement that has never been required in any code. Such an “every room” result represents the maximum required performance that can be contrasted against “every level” as the minimum required performance as a function of number and location. Alarm times for heat alarms and residential sprinklers are based on the activation of devices in the room of fire origin.

Table 15 shows the overall smoke alarm performance for test SDC05 using typical alarm points as defined in section 5.3. For each alarm type, the time of first alarm activation is noted as a “First Alarm” time. The average of all alarms in a category is noted as “Average.” The time to the last alarm activation is noted as “Last Alarm.” Finally, the total number of alarms in a group which activated is shown. Table 16 shows activation times for several other technologies that may be used in conjunction with smoke alarms. Individual calculations for all of the alarms in all of the tests is included as Appendix A. A summary of these results is included in the discussion section, below.

Table 15. Activation times for several smoke alarms during a flaming ignition test of a mattress, test SDC05

		First Alarm (s)	Average (s)	Last Alarm (s)	Activated	Total Alarms
Every Level	Photoelectric	42	85	127	2 of 2	10
	Ionization	37	77	117	4 of 4	
	Aspirated	52	85	117	2 of 2	
	Dual	107	135	162	2 of 2	
Every Level + Bedrooms	Photoelectric	42	95	167	4 of 4	19
	Ionization	32	83	147	8 of 8	
	Aspirated	52	112	167	3 of 3	
	Dual	107	147	172	4 of 4	
Every Room	Photoelectric	42	99	167	5 of 5	25
	Ionization	32	80	147	10 of 10	
	Aspirated	52	106	167	4 of 4	
	Dual	107	160	192	6 of 6	

Note – Dual alarm Ion4/Pho3D was not functioning during this test

Table 16. Activation times for several alternative technologies during a flaming ignition test of a mattress, test SDC05

		First Alarm (s)	Average (s)	Last Alarm (s)	Activated
Every Level	CO	132	174	197	5 of 6
Every Level + Bedrooms	CO	132	189	237	8 of 9
Every Room	CO	132	182	237	10 of 12
	Heat	140	140	140	1 of 1
	Tell-tale Sprinkler	147	147	147	1 of 1

5.6 Aerosol Concentration and Size Measurements

The amount of smoke, its particle size distribution, and light scattering properties in the case of photoelectric sensors affect the response of smoke alarms. Mulholland and Lui studied the response of ionization and photoelectric alarms to nearly mono-disperse (single size) di-octyl phthalate aerosols over a size range from 0.05 μm to 1.1 mm [29]. Theory and experimental results have established the relationship between the response of an ionization-type alarm and the product of the aerosol number concentration and the count mean diameter [16, 30]. (The count mean diameter is defined as the sum over all sizes of the number of particles of a given size times the particle diameter divided by the total number of particles.) For light scattering photoelectric alarms, the size relationship is more complex for the range of particle sizes found in smoke. In addition, the light scattering properties of the material that forms the particles is important.

Surrogate measures of smoke concentration via light extinction techniques, such as the laser beam smoke extinction meters used in this study, may provide approximate measures of smoke mass concentration by application of Bouguer's Law if an appropriate specific extinction coefficient is known for the smoke causing the extinction. In the case of soot generated from flaming fires, an estimated mean value of 8.7 m^2/g with an expanded uncertainty (95 % confidence interval) of 1.1 m^2/g computed from a wide range of experiments has been reported [31]. In the case of non-soot smolder smokes, the specific extinction coefficient lies typically between 3 m^2/g to 5 m^2/g .

The concentration and size distribution of smoke aerosols were measured during several selected tests conducted in the first manufactured home series and the two-story home series.

Measurements of the aerosol number and mass concentration were recorded at fixed locations for selected tests. In addition, the continuous voltage output from modified residential ionization smoke alarms (some installed in plenums through which room air was drawn in and others located at the sampling location) were recorded. Response of these alarms was related to the response of a MIC reference chamber to establish an effective chamber constant for the modified alarms. The combination of these measures allows for an estimation of two mean particle sizes (the count mean diameter and the diameter of average mass) and potentially the width of the size distribution as a function of time. In a select number of fire tests, cascade impactor samples were collected and analyzed to estimate the mass median aerodynamic diameter and the geometric standard deviation for those samples.

5.6.1 Mass and Number Concentration

The number concentration, ion chamber, and mass concentration results for 15 tests are presented below. In addition to these results, estimates of the count mean diameter and diameter of average mass were computed at selected time periods.

SDC01 was a smoldering chair test in the manufactured home. Figure 122a shows the mass and number concentrations measured in the remote bedroom. Except for a slight increase at 1400 s, the number concentration declined until 5200 s when it started to climb rapidly. Mass concentration started to climb at 5400 s and peaked around 7200 s when suppression action was taken.

Figure 122b shows the ionization chamber results in terms of the dimensionless “Y” parameter. The two flow-through ionization chambers were Ion 1 and Ion 2. Ion 3 and Ion 4 were located next to the sampling locations at the ceiling. Ion 1 and Ion 3 were measuring the hallway location, and Ion 2 and Ion 4 were measuring the remote bedroom location. This was the arrangement for the tests conducted in the manufactured home. For the most part, the flow-through and room ionization chambers sampling the same location responded similarly, with no significant response time difference. The difference between the two sampling locations reflects smoke transport time and differences in smoke concentration and size distribution.

In this particular test, there appears to be a discrepancy since the remote bedroom responded sooner and achieved a higher level than the hallway location. A possible explanation for this observation is that the back bedroom window was left open, and the bay doors to the test facility were also open during this test. Flow into the test building imposed a pressure gradient in the manufactured home that restricted flow down the hallway. Repeat tests where the window was closed and the building doors shut did not show this effect.

SDC02 was a flaming chair test in the manufactured home. Figure 123a shows the number and mass concentrations for this test. Both started rising around 100 s. Figure 123b shows the ionization chamber results. The hallway chambers responded within 20 s of ignition, while the remote bedroom chambers responded 70 s after ignition. The difference between the response of the remote bedroom chambers and the mass and number concentration is attributed to differences in aerosol transport time to the instruments.

SDC06 was a smoldering mattress test in the manufactured home. Figure 124 shows the number concentration and the ionization chamber results. The mass concentration was not recorded during this test. The number concentration declined until about 6000 s when it shot up after the mattress flamed. The initial decrease in number concentration appears to be related to decrease in the ambient number concentration during the long period the house was closed up. Ionization chambers started to increase slightly around 2800 s then climbed rapidly between 5700 s and 5900 s.

SDC07 was a flaming mattress test in the manufactured home. Figure 125 shows the number concentration and the ionization chamber results. Again, mass concentration was not recorded during this test. The hallway chambers increased rapidly around 50 s while the remote bedroom chambers increased nearly as rapidly, but delayed until about 130 s. The number concentration started to increase very rapidly at 150 s.

SDC08 was a smoldering mattress test in the manufactured home. Figure 126a shows the number and mass concentrations for this test. Number concentration was flat and no mass concentration was recorded until about 3750 s, 70 s after the mattress started to flame, when both increased rapidly. Figure 126b shows the ionization chamber results. The chambers located in the hallway and target room started rising as early as 500 s. The hallway ionization chambers increased rapidly around 3680 s, while the target room chambers did the same around 3730 s.

SDC10 was a flaming chair test in the manufactured home. Figure 127a shows the number and mass concentrations for this test. The number concentration started rising about 130 s after ignition with the mass concentration following 10 s later. Figure 127b shows the ionization chamber results. The hallway chambers started to increase sharply at 55 s, while the remote bedroom chambers started to rise between 110 s and 120 s.

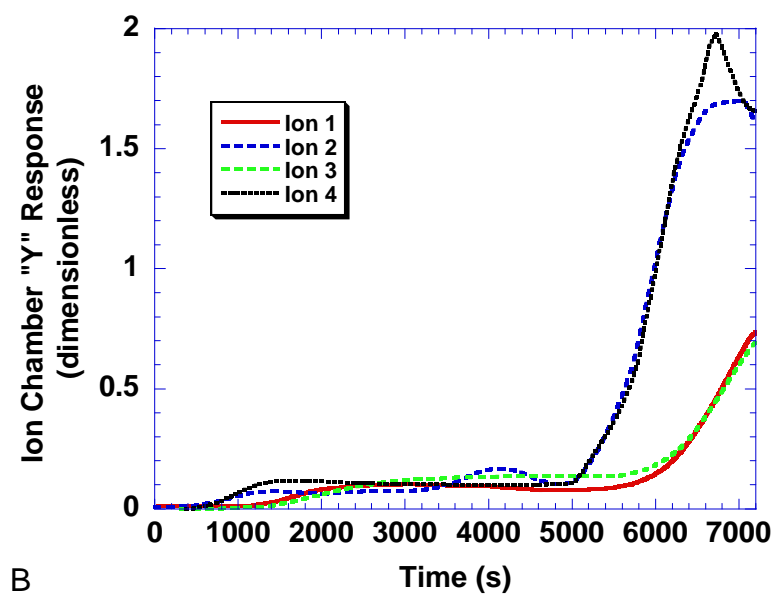
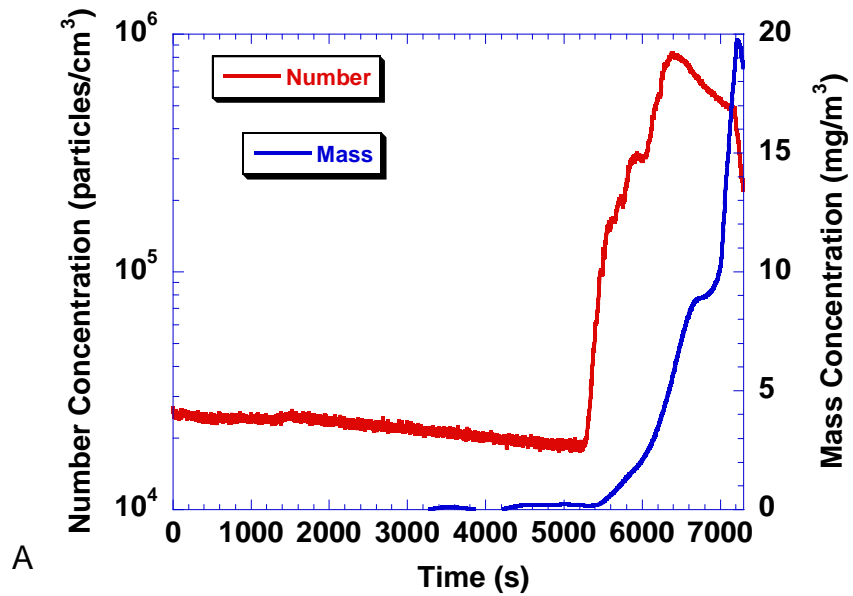


Figure 122. Smoke properties for smoldering chair scenario SDC01

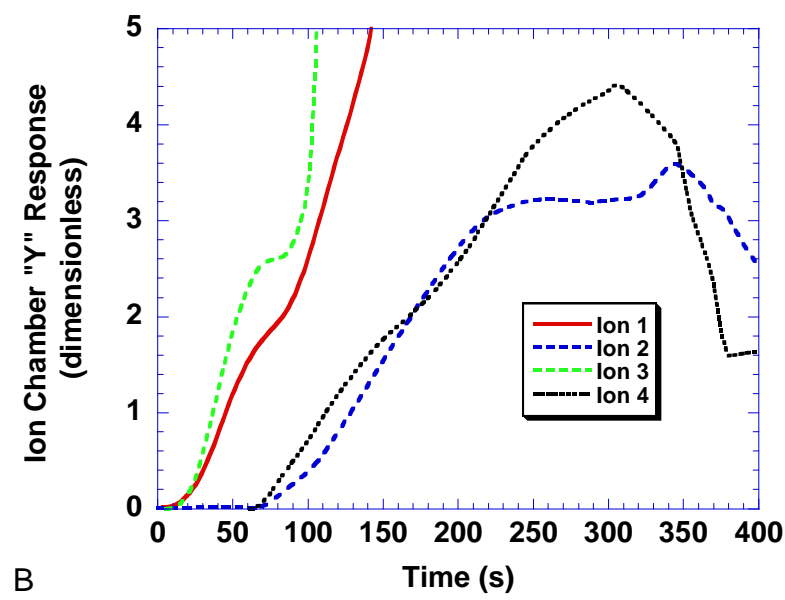
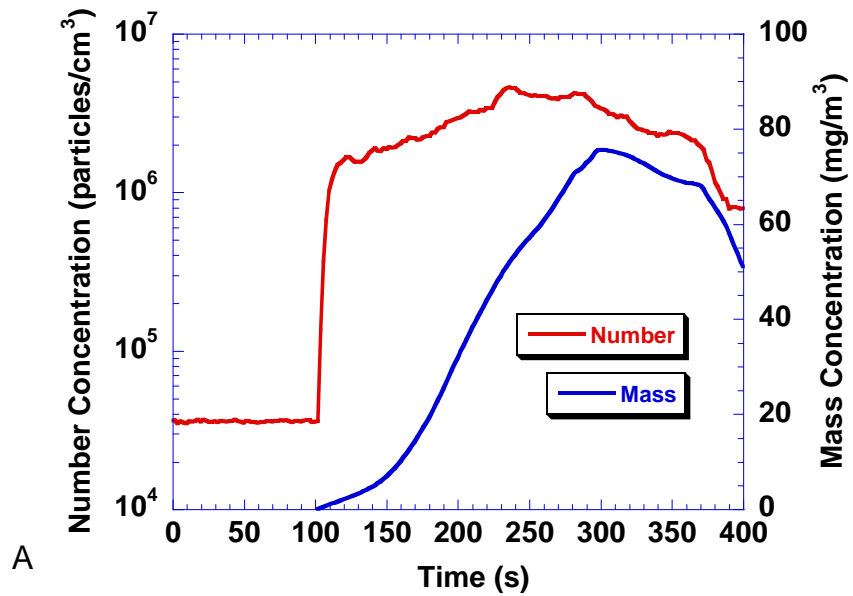


Figure 123. Smoke properties for flaming chair scenario SDC02

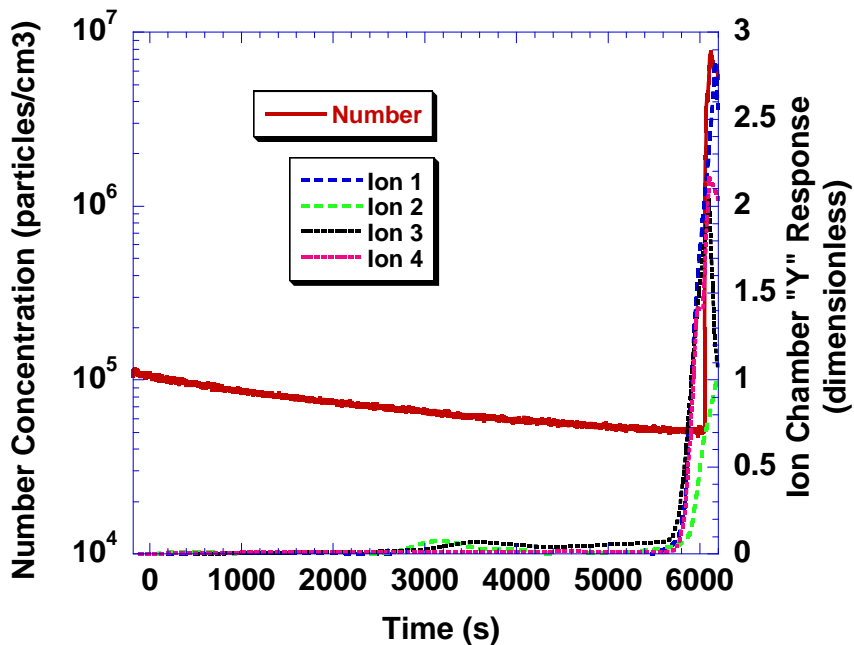


Figure 124. Smoke properties for smoldering mattress scenario
SDC06

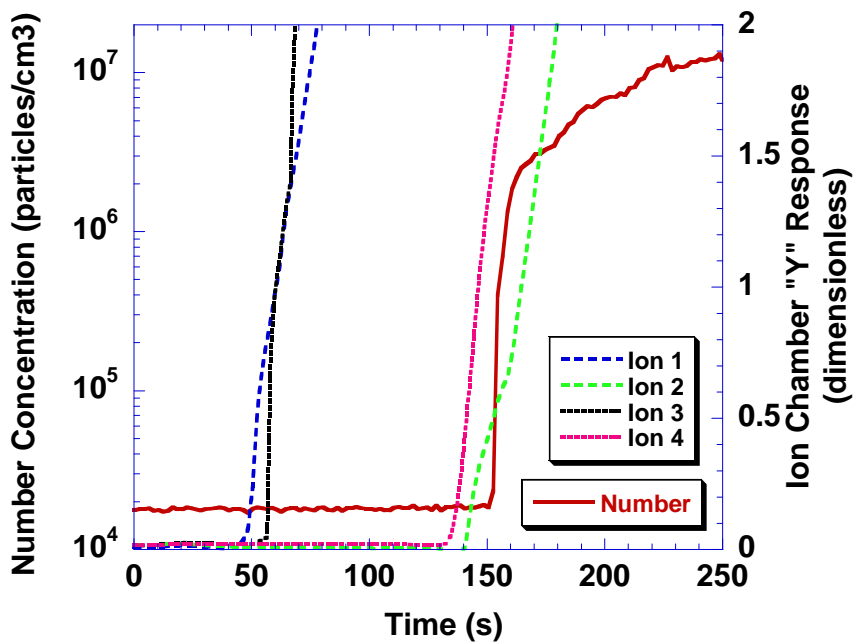


Figure 125. Smoke properties for flaming mattress
scenario SDC07

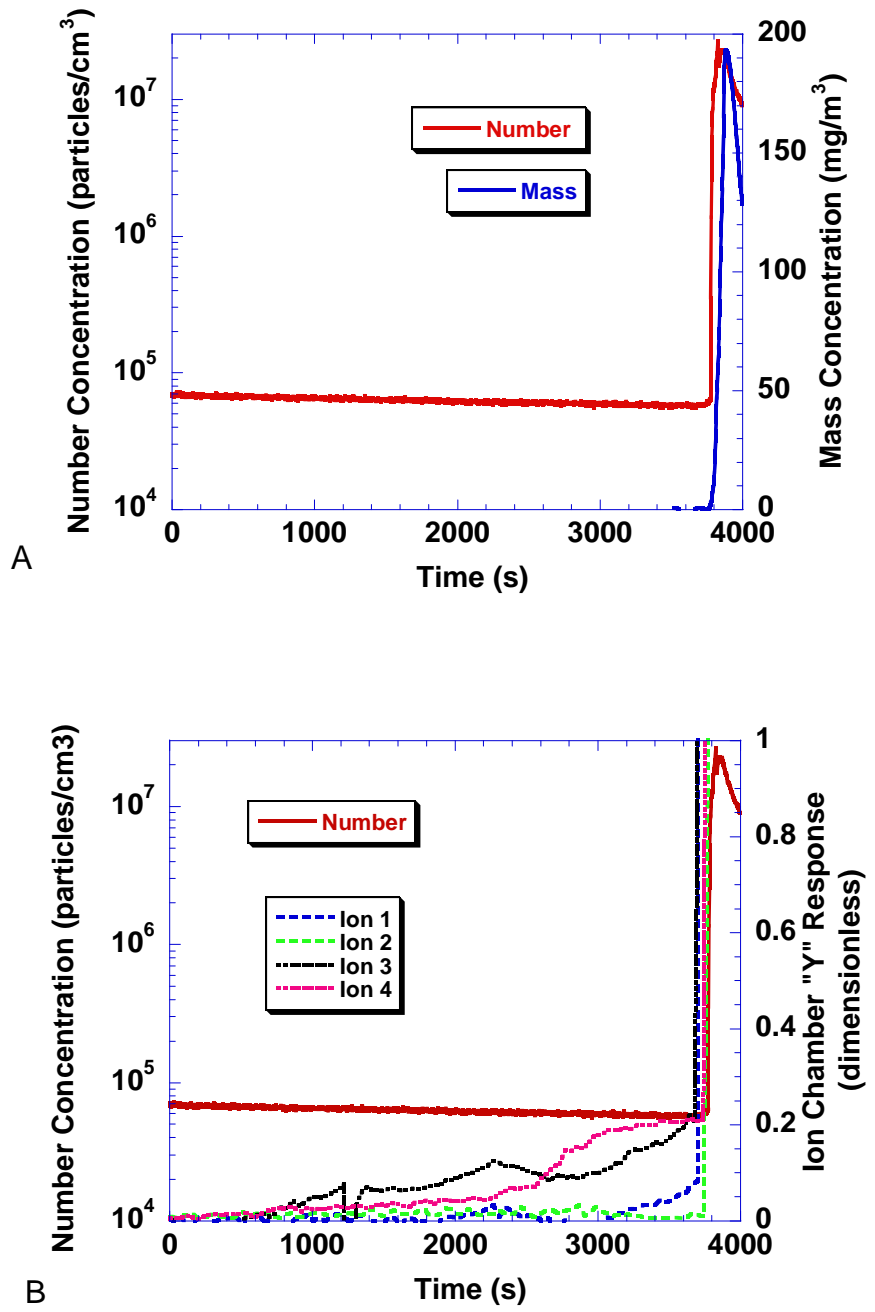


Figure 126. Smoke properties for smoldering mattress scenario SDC08

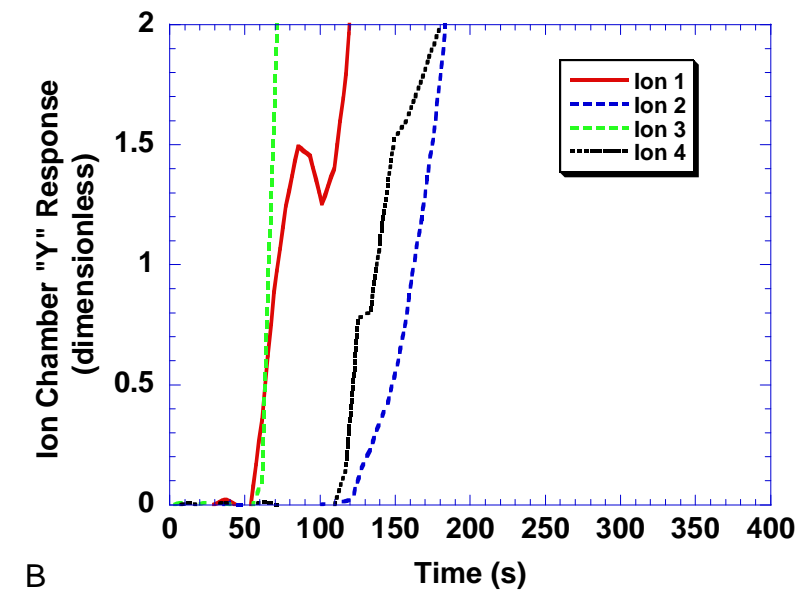
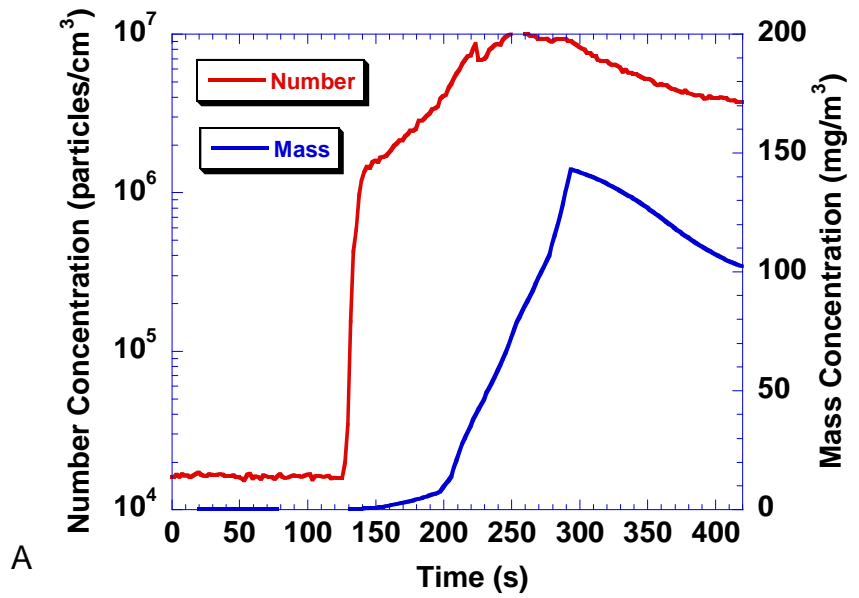


Figure 127. Smoke properties for flaming chair scenario SDC10

SDC11 was a smoldering chair test in the manufactured home. Figure 128a shows the number and mass concentrations for this test. Only after transition to flaming at about 4200 s do both number and mass concentrations start to rise. Figure 128b shows the ionization chamber results. The two chambers located inside the manufactured home started rising around 1000 s, while the two flow-through chambers remained at nominally zero until after transition to flaming when all chambers increased rapidly. The environmental conditions that caused the room chambers to increase early in the test evidently were not transported to the flow-through chambers. It could be condensation or volatile particulates.

SDC12 was a cooking oil fire in the manufactured home. Figure 129 shows the number concentration and ionization chamber results. The number concentration started to increase at about 200 s due to the small particles produced by the gas burner. The number concentration increases at a moderate rate until transition to flaming at about 1400 s. The hallway ionization chambers started to increase almost immediately after ignition of the burner, while the remote bedroom chambers did not start increasing until about 500 s. All ionization chambers reached relatively high levels before ignition of the cooking oil.

SDC13 was a repeat of the cooking oil fire in the manufactured home. Figure 130 shows the number concentration and ionization chamber results. The results are similar to SDC12.

SDC14 was a smoldering mattress fire with the burn bedroom door closed in the manufactured home. Figure 131 shows the number concentration and ionization chamber results. Around 3400 s the mattress transitioned to flaming, and smoke was forced out the door cracks, which caused the hallway chambers to increase rapidly. The smoke drifted back to the remote bedroom and caused the bedroom ionization chambers to rise along with the number concentration. Around 4000 s the burn bedroom door was opened, the mattress burst into flames again, and consequentially, much more smoke was transported to the remote bedroom. Soon after, the exterior doors were opened and the fire extinguished.

SDC23 was a smoldering chair test in the two-story home. Figure 132a shows the number and mass concentrations recorded in the den. The mass concentration started to increase at 1000 s while the number concentration started to increase at 2000 s. Around 4600 s the number and mass concentration started to increase rapidly. Figures 132b and 132c show the number concentration and flow-through ionization chamber results for the den and remote bedroom locations respectively. The den ionization chamber started to rise at 600 s and reached a peak at 2000 s. After 3800 s the data from the den ionization chamber was invalid. The remote bedroom ionization chamber started to rise at 1400 s, while the number concentration started to increase at 1600 s, leveled off to a plateau, then increased rapidly again at 4200 s. The ionization chamber increased rapidly at 4600 s.

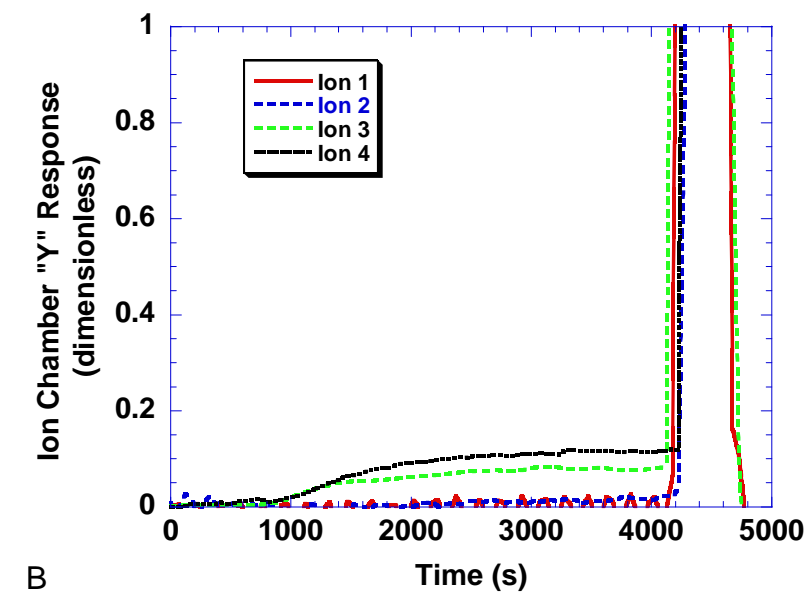
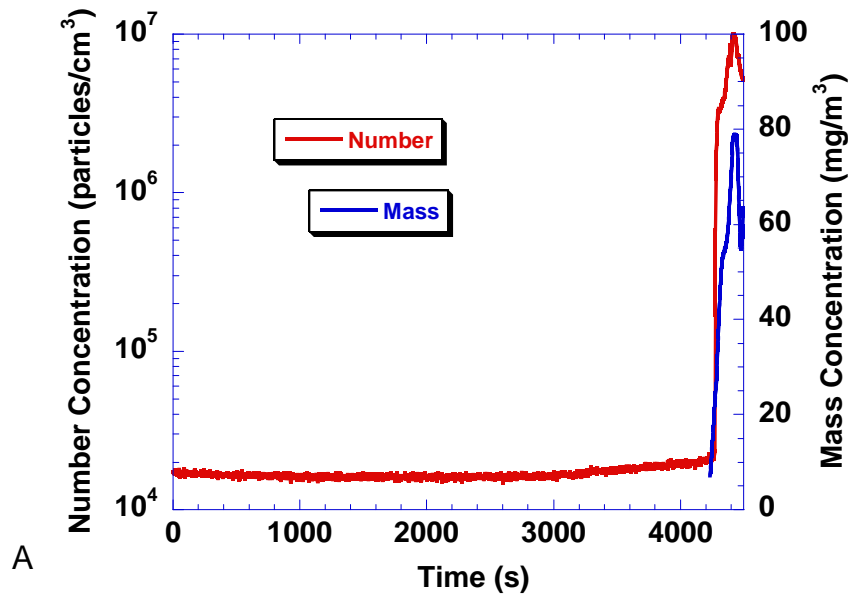


Figure 128. Smoke properties for smoldering chair scenario SDC11

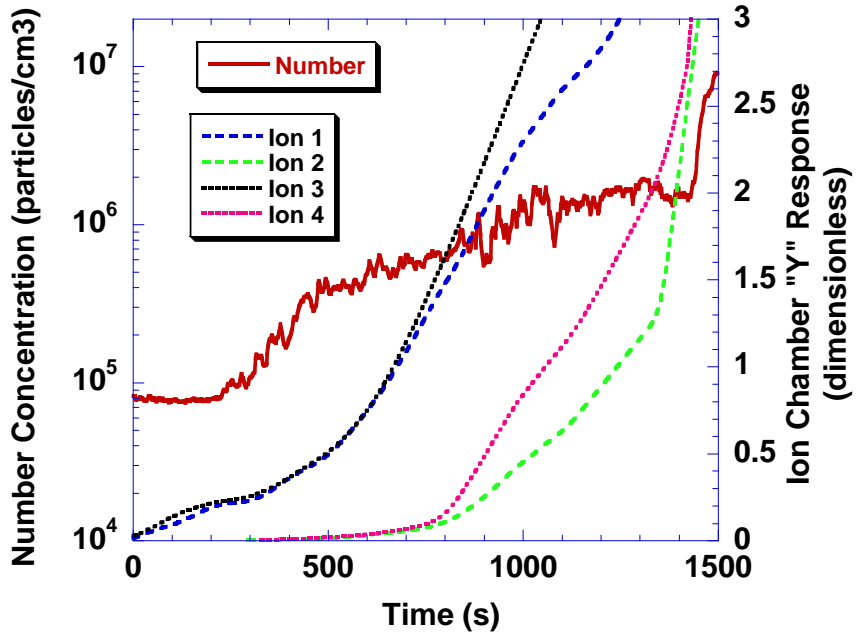


Figure 129. Smoke properties for cooking oil fire scenario SDC12

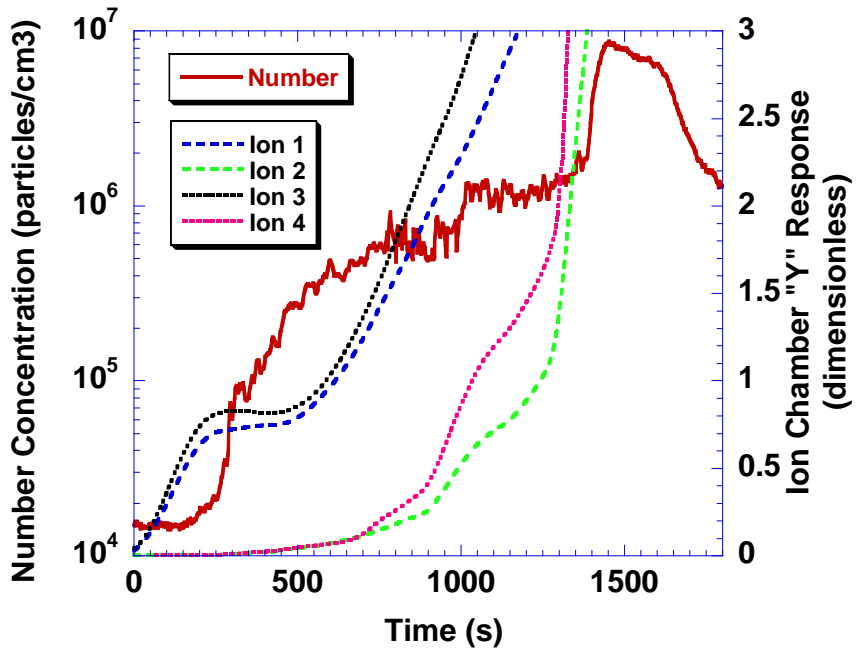


Figure 130. Smoke properties for cooking oil fire scenario SDC13

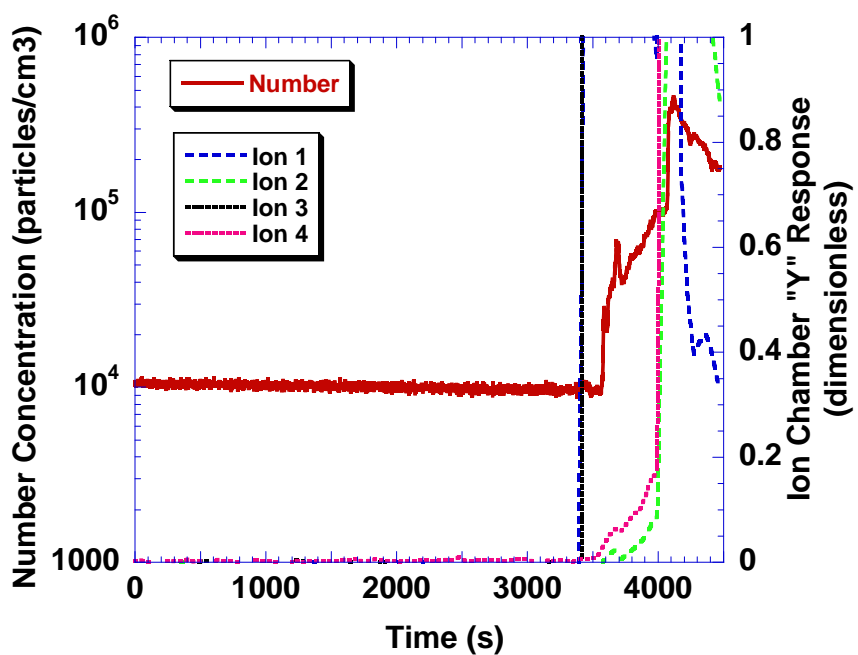


Figure 131. Smoke properties for smoldering mattress with burn room door closed SDC14

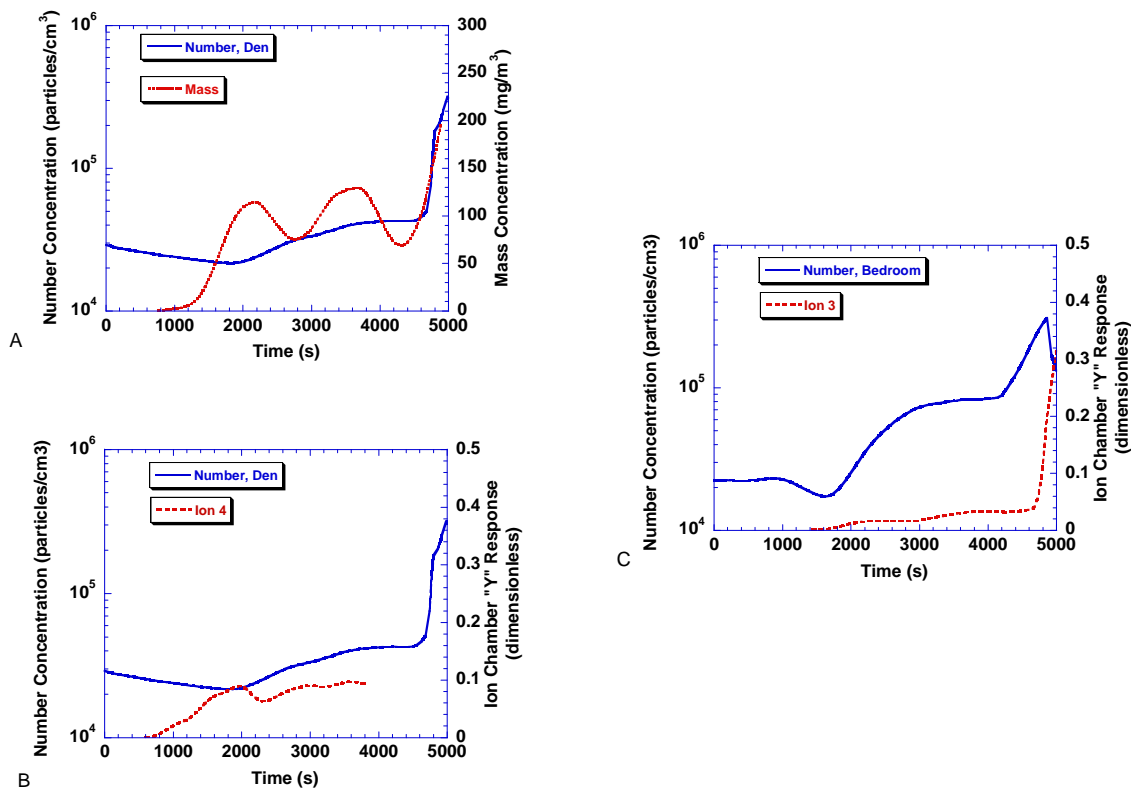


Figure 132. Smoke properties for smoldering chair scenario SDC23

SDC24 was a cooking oil fire in the two-story home. Figure 133a shows the number and mass concentrations recorded in the den. The number concentration started to increase almost immediately following ignition of the gas burner. The mass concentration started to increase at 600 s, and rose at an ever-increasing rate until the instrument upper range was reached at 1750 s. Figure 133b shows the number concentration and ionization chamber results for the den. From 200 s to 1400 s the ion chamber signal increased steadily. From 1400 s to the peak at 1700 s the signal increased at a steeper rate. Figure 133c shows the number concentration and ionization chamber results for the remote bedroom. The number concentration increased steadily up to 1700 s when both it and the ionization chamber signal rose rapidly.

SDC25 was a flaming chair test in the two-story home. Figure 134 shows the mass concentration and ionization chamber results. The condensation particle counter was inoperable for this test and subsequent tests below. The den and remote bedroom ionization chamber signals started to increase rapidly around 110 s and 125 s respectively. The mass concentration in the den started to rise at 125 s and peaked around 275 s.

SDC26 was a repeat of the flaming chair test above. Figure 135 shows the mass concentration and ionization chamber results. The results were similar to SDC25, but it appears that the early fire growth period was longer.

SDC27 was a smoldering chair test with an operating window-mounted air conditioning unit located in the remote bedroom. Figure 136 shows the mass concentration and ionization chamber results. Interestingly, the remote bedroom ionization chamber started to increase before the den ionization chamber, and reached a higher level. The mass concentration increased steadily from 1000 s to 3500 s.

5.6.2 Particle Size Analysis

5.6.2.1 Cascade Impactor Tests

The size distribution results for each MOUDI cascade impactor run are presented below. It is customary to fit impactor data to a log-normal size distribution and report the mass median aerodynamic diameter (equivalent spherical particle with unit density) and geometric standard deviation.

Here, two techniques were used to fit the data: graphically on a log-probability chart, and by non-linear regression curve fitting of the data. On log-probability paper, a log-normal distribution is described by a straight line. Data points are fitted to a straight line that is weighted toward fitting the points around the 50 % probability. The geometric standard deviation was estimated by taking the ratio of the diameter at 50 % to the diameter at 16.1 %. Results for the MOUDI tests are presented in table 17. The sampling time was identified along

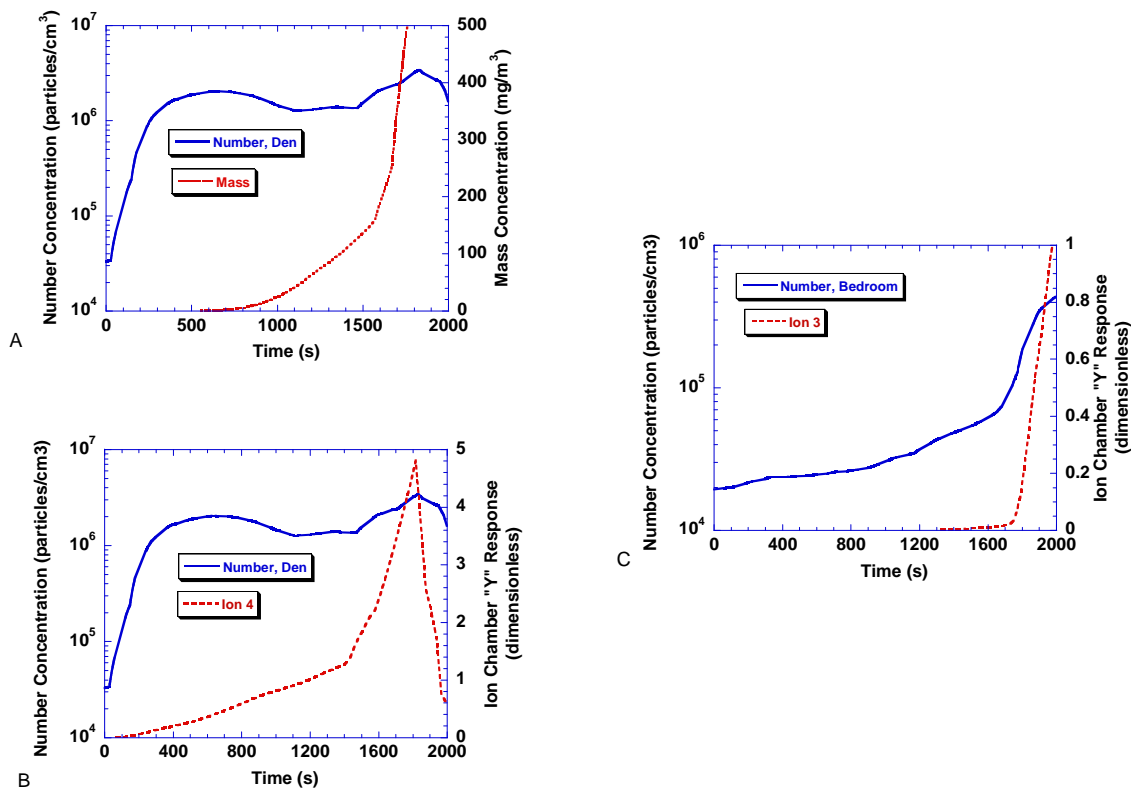


Figure 133. Smoke properties for cooking oil fire scenario SDC24

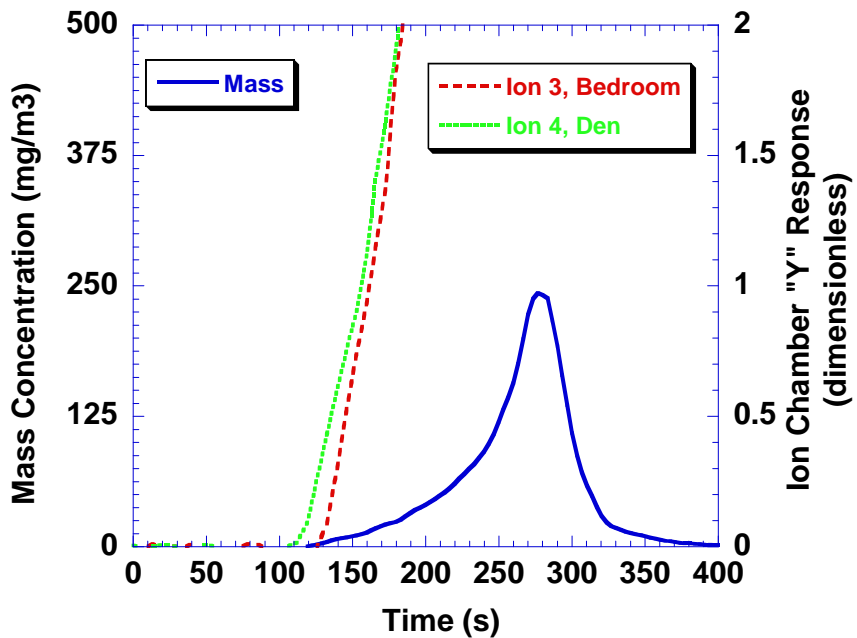


Figure 134. Smoke properties for flaming chair scenario SDC25

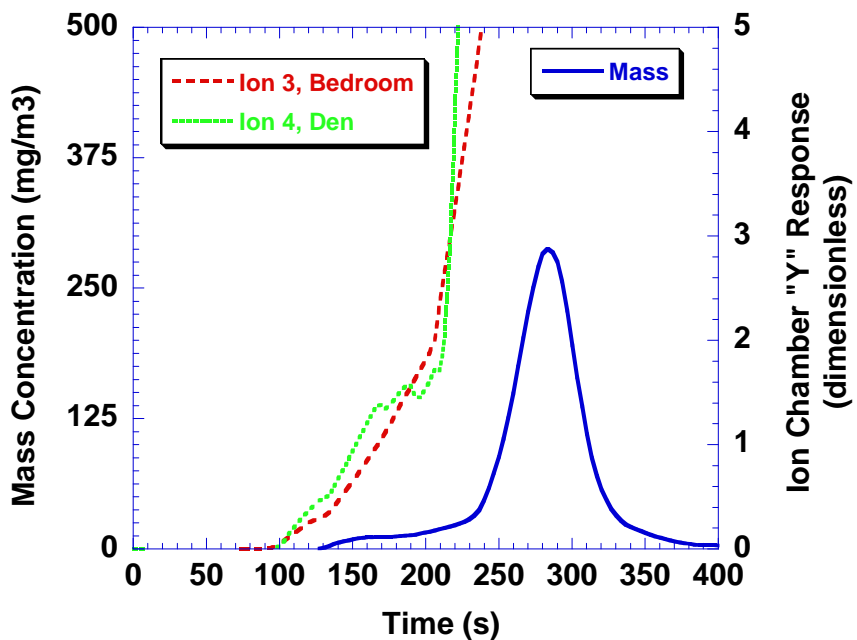


Figure 135. Smoke properties for flaming chair scenario SDC26

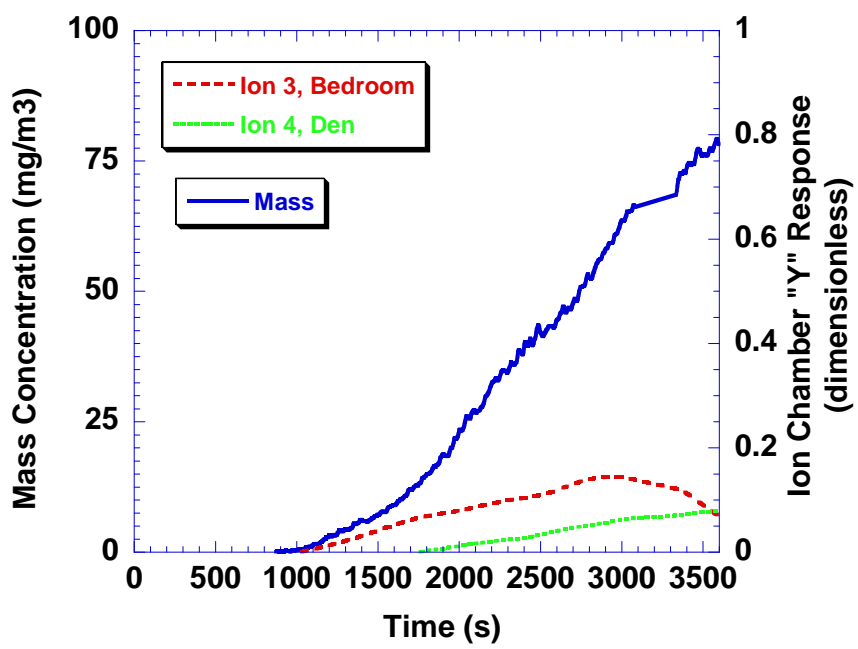


Figure 136. Smoke properties for smoldering chair scenario
with air conditioning SDC27

Table 17. Cascade impactor results

Test	Sampling start / duration (s)	L-P fit MMAD (μm)	L-P fit σ_g	L-S fit MMAD (μm)	L-S fit σ_g	Mean Mass concentration, U_C (mg/m^3)
SDC02 Flaming Chair	360 / 60	0.32	4.0	--	--	78.3 1.7
SDC10 Flaming Chair	200 / 60	0.33	4.1	--	--	87.1 1.7
SDC12 Cooking Oil	980 / 240	1.0	2.5	1.09	2.59	41.3 0.4
SDC13 Cooking Oil	830 / 270	1.0	2.7	0.93	2.86	16.8 0.4
SDC23 Smoldering Chair	3520 / 600	2.3	1.7	2.68	1.78	11.5 0.2
SDC27 Smoldering Chair	1850 / 300	2.2	1.7	2.46	1.67	15.0 0.4

L-P fit – log probability fit

MMAD – mass median aerodynamic diameter

σ_g – geometric standard deviation

L-S – least squares

U_C – combined standard uncertainty

with the average mass concentration obtained from the sum of masses on all stages and the backup filter.

Figures 137 and 138 show the results for SDC02 and SDC10, repeats of the flaming chair scenario. The collection times were nominally the same and near the end of the test. The mass median aerodynamic diameters of 0.32 μm and 0.33 μm were within 5 % and the geometric standard deviations were nominally the same. The data from these two runs were not fitted by non-linear regression due to poor fitting of the very broad data. The aerodynamic size distribution of soot agglomerates yields very broad distribution. Cleary [32] reported mass median diameters of soot from an acetylene diffusion flame ranging from 0.3 μm to over 8 μm depending on the fuel flow. The open agglomerate structure of soot produces a drag force greater than an equivalent spherical volume and consequently, an agglomerate cross-sectional diameter is much greater than its aerodynamic diameter.

Figure 139 shows the results for SDC12 and SDC13, repeats of the cooking oil fire scenario in the manufactured home. Sample collection was conducted prior to ignition of the hot oil. The aerosol was made up of condensed pyrolyzate from the hot oil. The mass median diameters obtained from the log-probability fit for the two tests were the same (1.0 μm), while the non-linear regression fits were within 17 % of each other with a mean value of 1.01 μm . The various geometric standard deviations ranged from 2.59 to 3.0.

Figure 140 shows the results for SDC23 and SDC27, the smoldering chair tests in the two-story home. SDC27 differed from SDC23 by the placement and operation of a window air conditioning unit in the remote bedroom. The two samples were collected at different time periods from the beginning of the tests. The mass median aerodynamic diameters estimated by the log-probability fits were within 5 % of each other for the repeated tests, while the non-linear regression fits were within 9 % of each other. The mass median aerodynamic diameters computed by the non-linear regression were higher than those estimated by the log-probability fits by 16 % and 12 % for SDC23 and SDC 27 respectively.

5.6.2.2 Particle size from moment analysis

Estimates of the count mean diameter and diameter of average mass were computed from the number concentration, flow-through ionization chamber results and mass concentration data for selected time periods of several tests. The ratio of the ionization chamber “Y” to the number concentration is proportional to the count mean diameter, while the cubed root of the quotient the mass concentration to the number concentration is proportional to the diameter of average mass. Details of this analysis are available [33]. The material density factors into the calculation and when unknown, it was assumed to be 1 g/cm³. The results are presented in the tables below where each table was dedicated to a particular scenario.

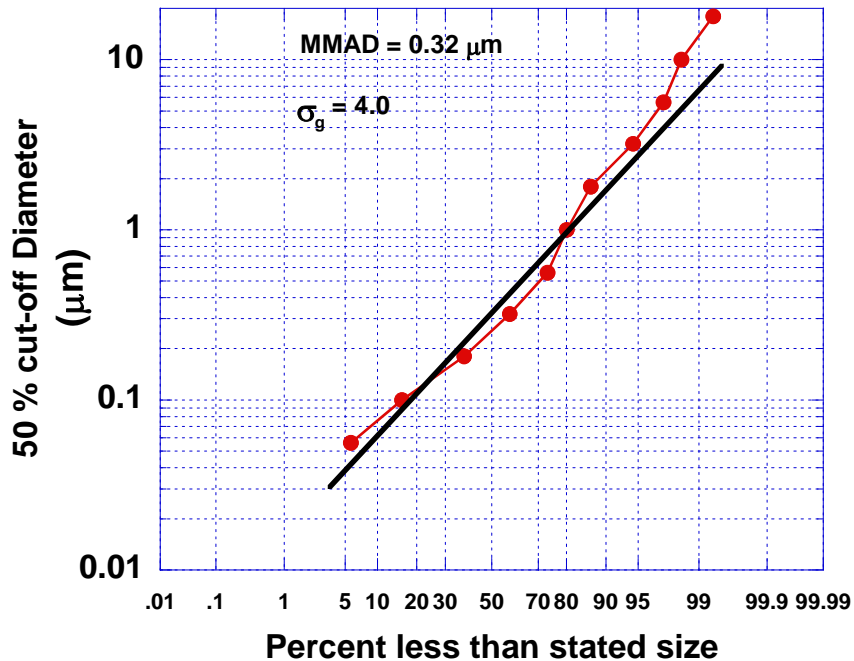


Figure 137. Cascade impactor results for flaming chair scenario SDC02

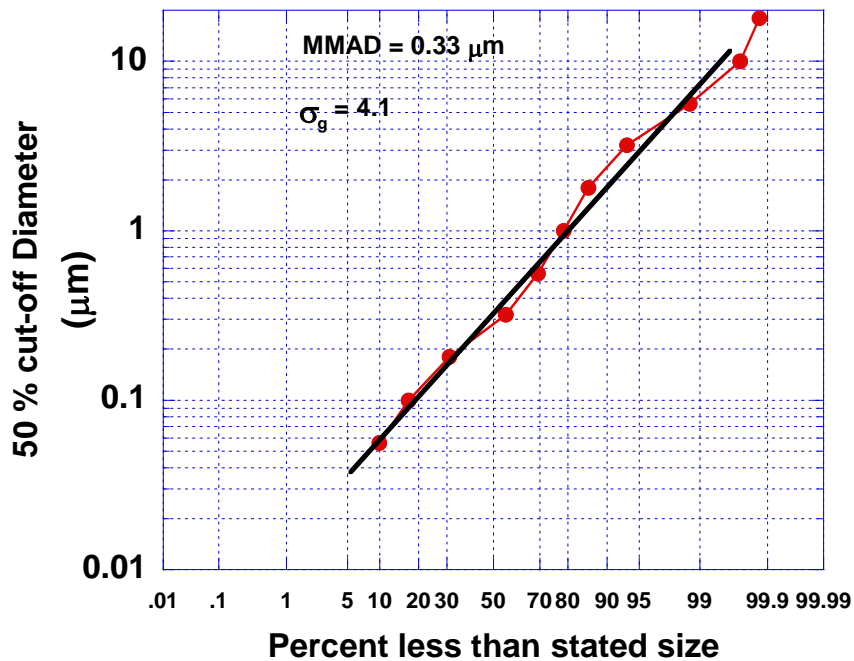


Figure 138. Cascade impactor results for flaming chair scenario SDC10

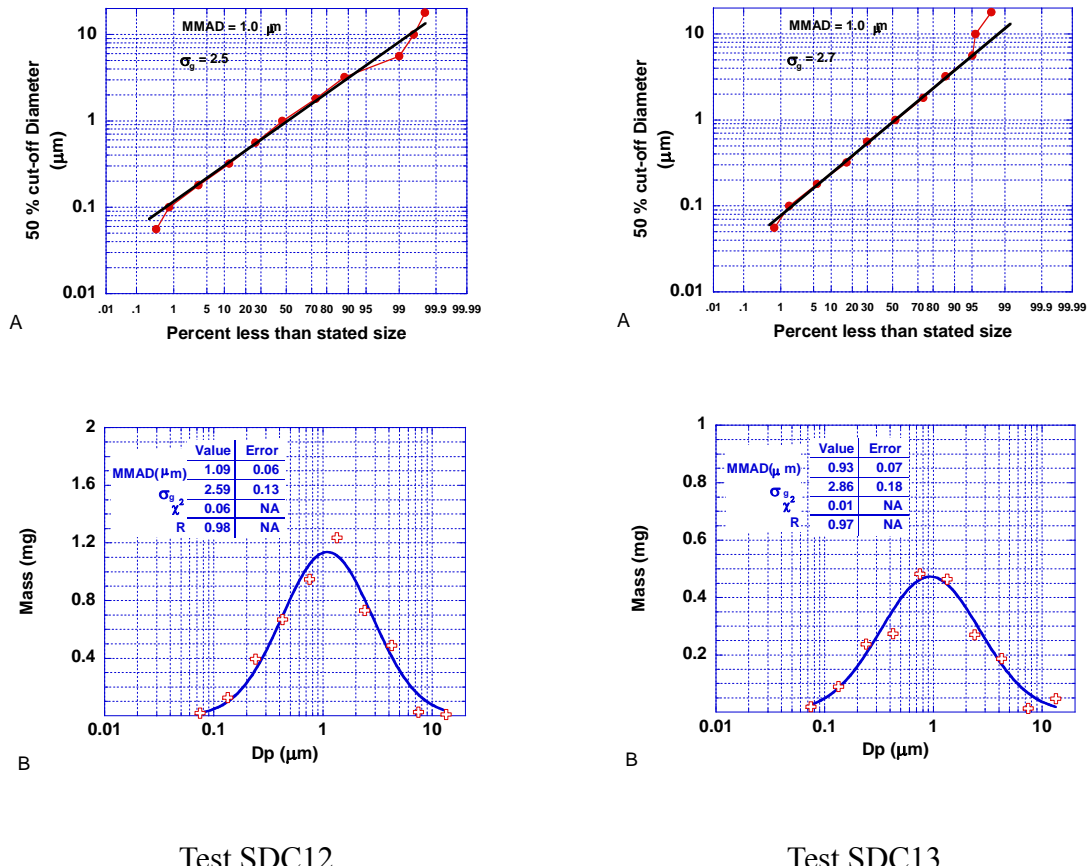
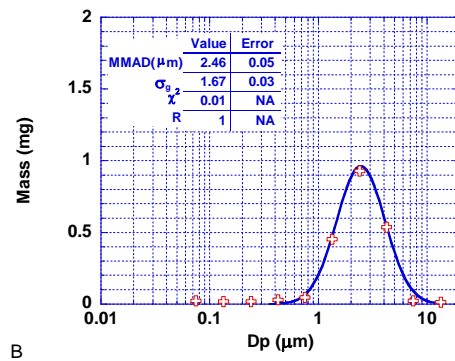
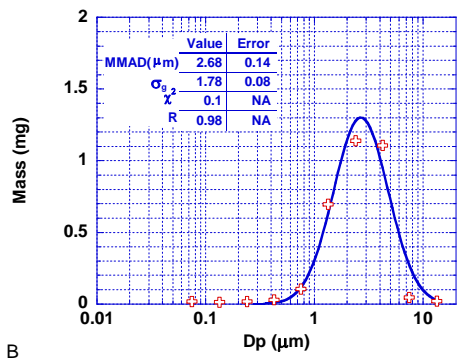
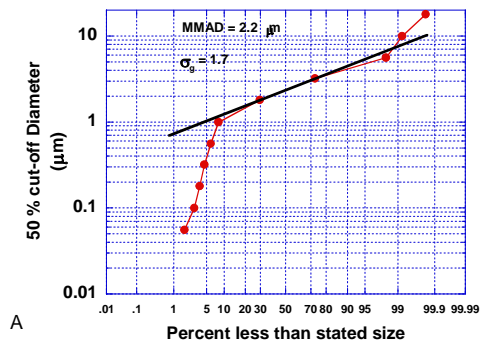
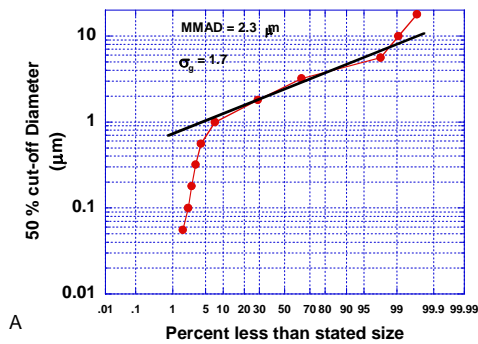


Figure 139. Cascade impactor results for cooking oil fire scenarios SDC12 and SDC13



Test SDC23

Test SDC27

Figure 140. Cascade impactor results for smoldering chair fire scenarios SDC23 and SDC27

Table 18 presents the results for the smoldering chair scenario. Estimates were made for three tests during the smoldering period. For a fixed location, the observed trend was that both the count mean diameter (CMD) and diameter of average mass (Dam) increased as time increased. The exception to that trend was the estimate at 3000 s for SDC01, where the smoldering rate had leveled off for a long period. The diameter of average mass estimates from SDC01 were inconsistent with the count mean diameters. The most likely cause was a sampling bias where the room mass concentration was underestimated. Recall that during the manufactured home tests, the aerosol passed through the ionization chamber first, then it flowed to the TEOM. It was likely that a significant fraction of large particles were lost inside the ionization chamber and did not add to the mass concentration. The MOUDI size distribution measurement in the remote bedroom during SDC23 compares favorably with the den mean sizes estimated at 3000 s.

Table 18. Estimated particle size from smoldering chair scenario

Test	Time (s)	Number Conc. (cm ⁻³)	"Y" Ion Chamber	Mass Conc. (mg/m ³)	CMD, Uc (μm)	Dam,Uc (μm)
SDC01	3000	21900	0.072	-	1.0, 0.2	-
	6400	8.02x10 ⁵	1.55	5.35	0.64, 0.13	0.23
	7000	5.21x10 ⁵	1.55	10.5	0.93, 0.19	0.34
SDC23 (den) (bedroom)	3000	35600	0.096	85.3	0.82, 0.16	1.7, 0.2
	3520	64600	.017	-	0.08, 0.02	-
SDC24 (den)	850	1.83e ⁶	.658	9.46	0.11, 0.02	0.21, 0.02
	1110	99000	0.913	44.7	0.22, 0.04	0.41, 0.04
	1400	25600	1.27	123.5	0.39, 0.08	0.62, 0.06

Table 19 presents the results for a flaming chair scenario and a smoldering mattress fire after it transitioned to flaming. The count mean diameter was computed using a chamber constant for flaming soot of 0.025 cm² [262]. Again, the mass concentrations for the manufactured home test (SDC02) were suspected to be low. Table 20 presents the results for the cooking oil scenario. After an initial increase in particle size, the count mean diameter remained relatively constant prior to ignition of the oil.

The concentration and size distribution measurements provide a more fundamental characterization of the smoke levels compared to the light extinction measurements. The data gathered here provide detailed information that may be used to help interpret the smoke alarm responses observed in these tests, and to specify the smoke production rate and size characteristics for modeling exercises.

Table 19. Estimated particle size from flaming sources

Test	Time (s)	Number Conc. (cm ⁻³)	“Y” Ion Chamber	Mass Conc. (mg/m ³)	CMD, U _c (μm)	D _a m, U _c (μm)
SDC02	275	3.98x10 ⁶	3.18	68.1	0.32, 0.06	0.26
	360	1.13x10 ⁶	2.77	53.5	0.98, 0.19	0.3
SDC06 (flaming)	6150	6.51x10 ⁶	2.88	-	0.18, 0.04	-

Table 20. Estimated particle size from cooking oil fire scenario

Test	Time (s)	Number Conc. (cm ⁻³)	“Y” Ion Chamber	Mass Conc. (mg/m ³)	CMD, U _c (μm)	D _a m, U _c (μm)
SDC12	1325	1.80x10 ⁶	1.25	-	0.21, 0.04	-
	1550	7.62x10 ⁶	4.44	-	0.18, 0.04	-
SDC13	850	6.16x10 ⁵	0.23	-	0.11, 0.02	-
	1250	1.26x10 ⁶	1.01	-	0.24, 0.05	-
	1550	7.03x10 ⁶	5.51	-	0.24, 0.05	-

5.7 Measurement Uncertainty

Replicate tests were performed for the manufactured home tests to assess the uncertainty in alarm times and time to untenable conditions based on measurements of temperature, smoke obscuration, and toxic gas concentrations. Table 21 shows standard uncertainties expressed as a relative error (in this case calculated as the ratio of the standard uncertainty for replicate tests and the average value for the replicate tests).

Table 21. Variability for tenability time and alarm time during tests of residential smoke alarms (expressed as the ratio of standard uncertainty for replicate tests and the average value for these tests)

Tenability Time (%)	Alarm Time			
	Ionization Alarm (%)	Photoelectric Alarm (%)	Aspirated Alarm (%)	CO Alarm (%)
Flaming	10	24	28	32
Smoldering	32	30	51	39
Cooking Oil	6	64	7	34

6 Residential Smoke Alarm Nuisance Source Testing

Smoke alarms are susceptible to alarming when exposed to non-fire aerosols. In residential settings, this typically involves cooking activities or transient, high humidity conditions (i.e., “shower steam”). The Smoke Detector Operability Survey: Report on Finding [6] conducted by the U.S. Consumer Products Safety Commission reported that about one half of the 1012 respondents indicated they experienced nuisance alarms, with 80 % of those attributed to cooking activities, and an additional 6 % citing steam from bathrooms. Dust, and tobacco smoke are also mentioned sources. The Survey also reported that of the alarms with missing or disconnected batteries, or disconnected AC power, more than one third of respondents indicated that power was removed due to nuisance alarms. The Smoke Detector Operability Survey: Engineering Laboratory Analysis found that there was a correlation between the occurrence of nuisance alarms and the sensitivity of the alarm, location of the alarm relative to the nuisance source, and the condition (cleanliness) of the alarm [34]. A field study of nuisance alarms in the Native American community reported that of 80 households with one or more ionization alarms 63 reported nuisance alarms [3]. The activities associated with these alarms and the percentage of detectors implicated in said nuisance alarms were: cooking (77 %), steam from bathroom (18 %), cigarettes (6 %), and fireplace/wood stove (4 %), other, unknown and chirping (low battery alert) (12 %). The types of cooking activities identified with nuisance alarms included: frying, baking, boiling, and toaster/toaster oven. This study concluded that the type of sensor technology, and the location of an alarm play an important role in the frequency of nuisance alarms in residential settings.

The benefits of an alarm that is relatively insensitive to common nuisance sources while maintaining a high sensitivity to a wide range of fire scenarios are self-evident. In the last decade, a significant research effort has been expended to achieve more robust fire detection with a focus on new sensors (including gas sensing), signal processing techniques, and advanced algorithm development [35], [36], [37], [38]. The practical implementation of any new technologies on a broad basis depends on the participation of several key entities including: research organizations, standards bodies, testing organizations, and the commercial sector. The demonstration of improved fire detection, both enhanced sensitivity to fire and insensitivity to nuisance sources, through detector performance testing is a necessary objective. While standard fire tests are designed to quantify a given alarm’s ability to detect fire conditions (e.g., UL 268 [39], and EN-54 [40] fire sensitivity tests), there are no consensus standards to test its ability to reject nuisance alarms.

The objective of this research task was to develop a basis for standard residential nuisance source testing. The approach taken is to define a set of nuisance scenarios, replicate the events that cause nuisance alarms, and quantify the important variables that cause nuisance alarms. Translating the results to a set of nuisance source conditions reproducible in a suitable test-bed (i.e., a test room or the fire emulator/detector evaluator) would allow for more comprehensive detector performance testing. Preliminary tests were performed in the FE/DE with this in mind. Programming realistic and reproducible fire and nuisance conditions in the FE/DE is an ongoing research project at NIST.

6.1 Nuisance Scenario Tests

Nuisance scenario tests were performed in the manufactured home used for other tests in this study. The selections were based on what are commonly thought to be causes of residential nuisance alarms, and scenarios were designed to mimic normal activities (i.e. no intentional food burning, with the exception of toasted bread). No consideration was given to the probability of occurrence for any given scenario; the objective was to gather data on a number of scenarios. The bulk of the scenarios were related to cooking activities including: frying, deep-frying, baking, broiling, boiling, and toasting. In addition, cigarette smoking and candle burning were included. Neither a “shower steam” scenario, nor dust exposure test were performed in the manufactured home. Both have been investigated in the FE/DE in prior studies. Three smoldering fire scenarios (smoldering polyurethane foam, beech wood blocks and cotton wick) were examined for comparative purposes.

A schematic of the manufactured home is shown in figure 141. The dark shaded areas were closed off. During most tests, all external doors and windows were closed. Most scenarios were repeated with and without a floor fan blowing air from the master bedroom into the kitchen/living room area.

6.2 Instrumentation

Aerosol concentrations, temperature, humidity, flow velocity and analog output from photoelectric, ionization and carbon monoxide sensors were gathered. Most tests were videotaped. Figure 141 shows the approximate ceiling location of all the measurement positions. Details of the measurement are given below. Note, carbon monoxide data were not presented in the graphs, but are included in the data files, which in addition include all analog sensor outputs. The complete data set is available in electronic form [41].

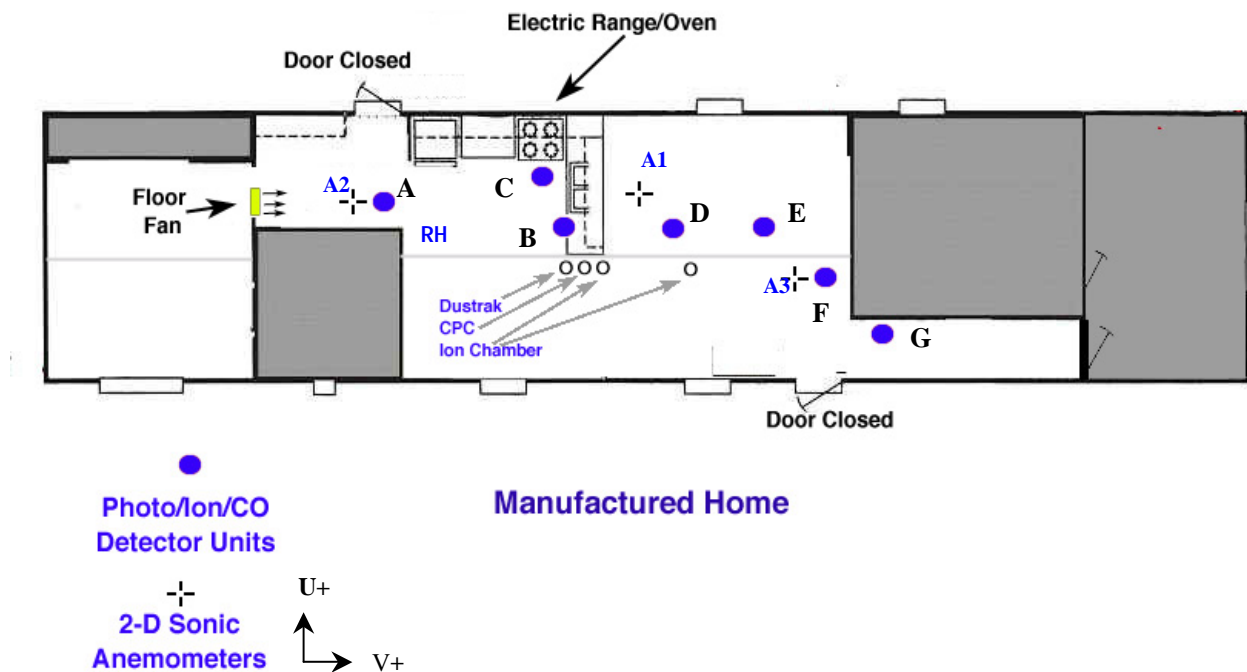


Figure 141. Schematic of the manufactured home for nuisance testing

6.2.1 Aerosol Instruments

Two portable aerosol instruments were used to gather aerosol number and mass concentrations during the tests. Number concentration was recorded with a TSI model 3007 portable condensation particle counter (CPC). This instrument is capable of counting particles greater than 10 nm in diameter up to concentrations of 5×10^5 particles/cm³ with an uncertainty of 10 % of the reading. The upper concentration range of the instrument is insufficient for many fire and nuisance conditions so the air sample was diluted with a fixed amount of clean air prior to entering the CPC. The air sample was drawn through a 1.5 m long, 6 mm ID PVC tube (Tygon brand, which is recognized to have low electrostatic particle loss characteristics.) to a laminar flow element that was attached to one branch of a "Y" tube fitting. The other branch of the fitting was attached to a HEPA filter, while the main branch was attached to the inlet of the CPC. The CPC internal pump draws air from the sampling tube and clean (particle-free) air through the filter into the unit. With this arrangement, approximately a 20 to 1 dilution of the air sample is achieved. The dilution ratio for each test was obtained by computing the ratio of undiluted to diluted background room aerosol. The uncertainty in the dilution ratio is estimated to be 2%. A TSI model 8520 "Dustrak" portable aerosol mass monitor was used to gather the aerosol mass concentration. This device is a light scattering photometer that analyzes the light scattered at an angle of 90° from particles flowing through the device. Its default calibration is set to the respirable fraction of standard ISO 12103-1 A1 test dust. It has a range from

0.001 mg/m³ to 150 mg/m³. The effective particle size measurement range is 0.1 µm up to 10 µm. The device can be calibrated for any aerosol with scattering properties different from the test dust provided the true mass concentration is determined. Here, the default calibration was used, so any given mass concentration measurement reported is relative and related measure to an equivalent mass of test dust. Since the device is not calibrated to each of the aerosols produced in the nuisance tests, the uncertainty in the measurement is not determined.

However, the results are proportional to the mass concentration and correspond directly to the scattering signal strength of photoelectric detectors with an equivalent amount of aerosol in its sensing region. Both the CPC and Dustrak log data to internal memory along with a time stamp every second. Data were downloaded after each test.

Two flow-through ionization chamber devices were constructed from commercially available ionization alarms. Figure 142 is a schematic diagram of this device. To make the modification, the horn from the alarm circuit board was removed, and the voltage from the IC circuit pin that follows the chamber current was monitored. 17 cm³/s of room air was drawn through each device and each circuit was powered by 9.00 V from a regulated power supply. These devices function effectively as measuring ionization chambers (MIC), and their voltage output can be correlated to a MIC chamber current. Figure 143 shows the voltage output from the ion chamber devices and the MIC current for cotton smolder smoke generated in the FE/DE. The ion chamber device was located outside the FE/DE test section and the air sample was drawn into the devices by 1.5 m long, 10 mm ID copper tubing. The ion chamber voltage

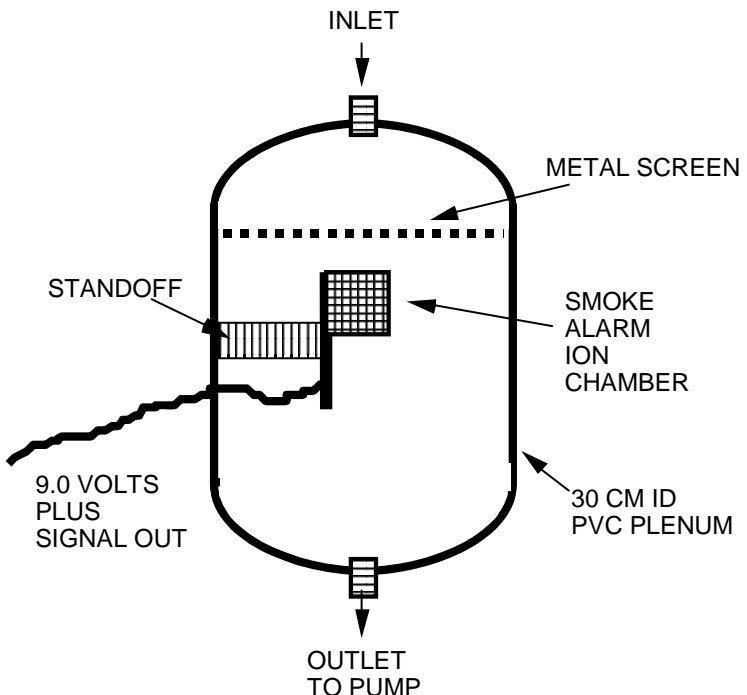


Figure 142. Ion chamber schematic

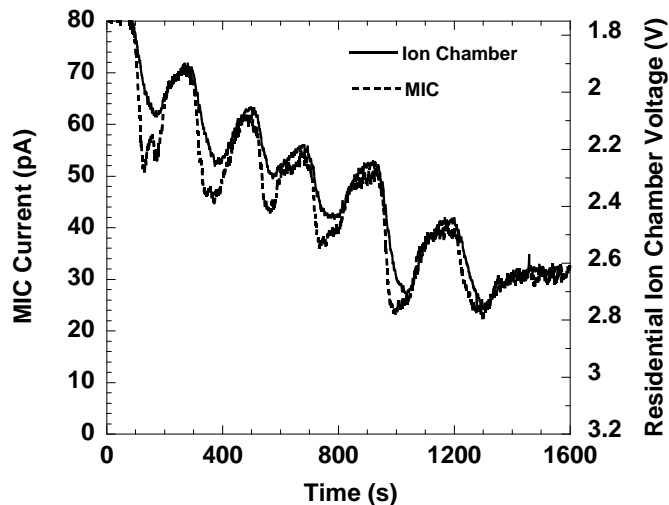


Figure 143. Response of the ion chamber and MIC to cotton smolder smoke

lags the MIC current due to the time difference between the aerosol transport through the tubing and chamber filling, but the steady voltage value is proportional to the MIC current. The reported ion chamber values in the nuisance tests below differ by a constant value due to differing amplifier gains.

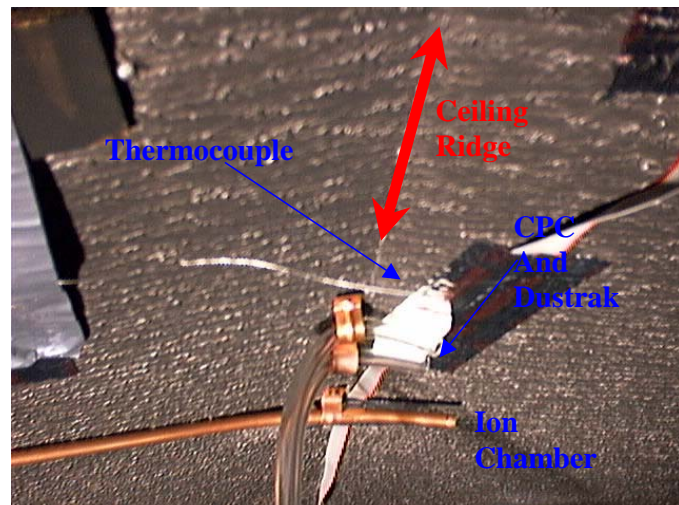
In the nuisance tests, the copper tubes used to transport the air sample to the devices were 2.5 m long. Chamber #1 was located in the living room area, while chamber #2 was located in the kitchen area next to the other aerosol sampling points (figure 140).

6.2.2 Temperature and Humidity

A type-K 0.5 mm stainless steel sheathed thermocouple monitored the ceiling air temperature. It was placed at the aerosol sampling location, 3 cm below the ceiling.

Figure 144 is a picture showing the thermocouple placement along with the CPC, Dustrak, and ion chamber 2 sampling lines.

An Oakton 35612 series thermohygrometer probe was used to monitor the relative humidity throughout the experiments. The probe was positioned 2.0 m off the floor at the position indicated by “RH” in figure 141. The stated measurement uncertainty for this device is 2.5 % of the reading.



6.2.3 Flow Velocity

Three CATI sonic anemometers (Applied

Figure 144. Thermocouple and sampling line placement

Technologies Inc.) were used to record the two-component air velocities perpendicular to the sloped ceiling at a depth of 5 cm. Their locations are shown in figure 141 and identified as anemometer A1, A2, and A3. The component velocity orientation is also shown.

These devices use piezoelectric crystals to form ultrasonic transducers that can send and receive ultrasonic pulses. The forward and backward travel time of these pulses are used to compute the component velocity between two opposing transducers. The anemometers record the mean velocity over a 15 cm sonic path length (which equals the distance separating opposing transducers) at a frequency of up to 10 Hz. The measurement resolution is 1 cm/s with a stated uncertainty of 1 cm/s.

6.2.4 Analog Output Photoelectric, Ionization and Sensors

Seven commercially available dual photo/ion smoke alarms were modified at NIST to provide continuous analog output (figure 145). The modifications made to the alarms included removing the horn, modifying the circuit board to suppress the alarm mode, and speeding up the IR light source to a flash rate of approximately every 2 s. The photodetector was disconnected from the circuit board and monitored by a peak detection circuit. The photodetector signal was amplified with an op-amp circuit then sent over a multi-conductor ribbon cable to a single board computer (SBC) dedicated to each modified alarm. The signal was amplified by an instrument amplifier then, sent to the peak detector. The peak detector was reset every 2 s by a 1 ms digital signal pulse to the gate of a MOSFET attached across the peak circuit's holding capacitor. The voltage stored by the peak detector was sampled by the analog input circuit of the SBC every 2 s, just prior to the reset. The SBC processed this data with a 3-point median filter to suppress spurious signals. The voltage follower IC pin output that follows the chamber current was sampled to obtain the ionization signal. An electro-chemical CO cell removed from a commercially available CO alarm was fitted in the dual smoke alarm housing at the horn's previous location. The voltage drop across a resistor placed across the cells terminals was sampled. Both the Ion and CO voltages were sent to instrument amplifiers prior to being sampled by the analog input of the SBC. A 10 k Ω thermistor was located in the dual smoke alarm just sticking out of the detector housing at the LED light pipe hole.

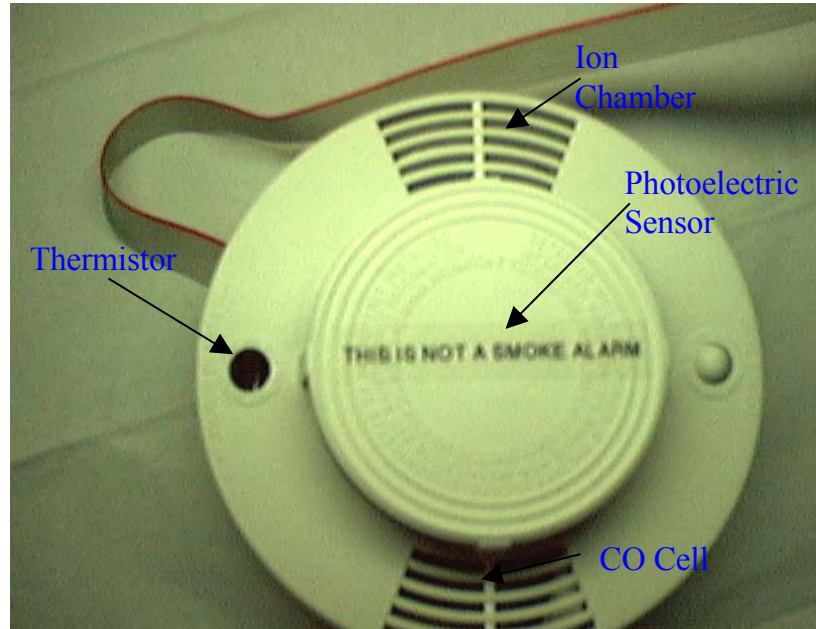


Figure 145. Photo, Ion, CO and thermistor unit

The SBC logged the photo, ion, and CO sensor voltages every two seconds to non-volatile flash ram. The data were downloaded after each test. The voltages were expressed as 8 bit characters to minimize data storage. Each detector was calibrated in the FE/DE with the cotton wick smoke, and the sensor values are presented in engineering units of extinction (m^{-1}) and mole fraction of CO. The locations of the sensor packages are indicated on figure 141 and represented in the results by the letters A - G.

On several occasions, the SBC data were monitored via a data stream sent over a serial port to a laptop. This was observed to corrupt some of the sensor data saved to the flash ram, consequently, some data columns were left blank in the test data files. One photo sensor monitoring circuit did not function properly and was omitted from the test data files (Unit E).

6.3 Results

Selected results for each of the tests performed are shown in the figures below. Data from all of the tests are available [41]. The time to reach photoelectric and ionization alarm points was determined from ion and photoelectric sensor calibration test data, and estimated alarm sensitivities appropriate for the FE/DE cotton wick smoke. Estimated high, medium and low sensitivities for both photoelectric and ionization alarms are given in Table 22. These values cover the range expected for residential smoke alarms for each sensor type.

Table 22. Alarm sensitivity for photoelectric and ionization sensors

Sensor	High sensitivity Extinction m ⁻¹ , (%/ft Obsc.)	Medium sensitivity Extinction m ⁻¹ , (%/ft Obsc.)	Low sensitivity Extinction m ⁻¹ , (%/ft Obsc.)
Photoelectric	0.05, 1.5	0.083, 2.5	0.117, 3.5
Ionization	0.016, 0.5	0.033, 1.0	0.050, 1.5

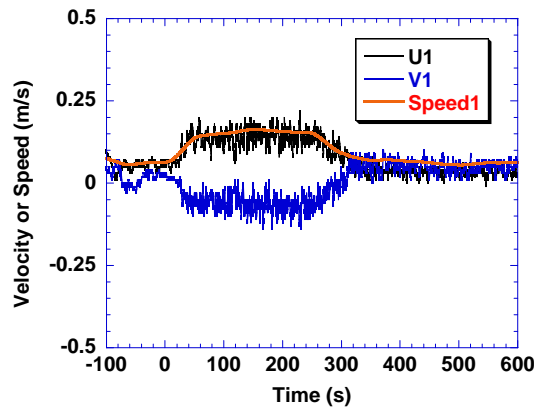
6.3.1 Toasting Scenarios

Either two slices of white bread or frozen bagel halves were placed in a two-slice toaster, located on the counter to the left of the range. The toaster's automatic pop-up mechanism was disabled by holding the lever in the *on* position with a wrap of wire attached to the bottom of the toaster. Power was applied by plugging in an extension cord attached to the toaster. The cord extended out of the manufactured home through an access hole. At time=0 the power was applied to the toaster. The toaster was left on for up to 300 s. This was sufficient to char ("burn") toast but not the frozen bagels. No flames were produced in these tests. This scenario is unique compared to all of the following nuisance scenarios in that it transitions from nuisance to an impending hazard as the bread chars since it could produce flames.

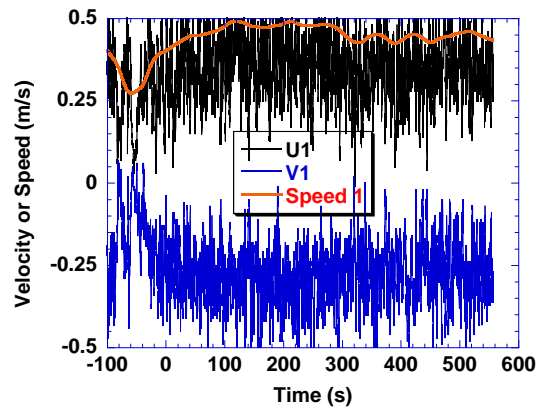
Three tests (two with bread, one with a frozen bagel) were conducted with no forced room air-flow, while an additional three tests were conducted with the floor fan operating. Similar background conditions, (i.e., fan or no fan) ostensibly produced the same flow conditions at the

measurement locations. In the repeated toasting bread test with no forced flow, the remote bedroom window was left open, which did affect the airflow slightly. Figure 146 shows the velocity components and speed. The reported speed is a time-smoothed representation computed from the component velocities. With no forced flow, background flow velocities were initially between 0 m/s and 0.1 m/s. After the toaster is turned on, the plume from hot gases is evident with computed speeds up to 0.2 m/s. When the toaster power was removed, the flow at location A1 returned to its low background value; the return to background values was less pronounced at locations A2 and A3. With the floor fan turned on, speeds between 0.15 m/s and 0.6 m/s were recorded. The effects of the toaster heat plume were not clearly evident in these velocity measurements.

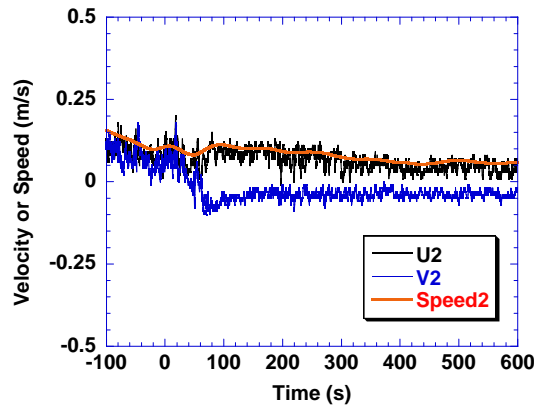
The results for each test are shown in a series of four graphs for each case. Figure 147A shows the computed time to reach various alarm thresholds for toasted bread with no forced flow. Every threshold for all photoelectric and Ion sensors was reached in this test. Note that at alarm location E is displayed in gray since no photoelectric alarm times are indicated; there was no functioning photoelectric alarm at this position. This notation is used in the figures that follow to indicate when no alarms were placed at a given position. In all cases the ion sensors reached the alarm thresholds before the photoelectric sensors. Generally, the closer the sensor was to the source the sooner the alarm threshold was reached. Figure 147B shows the temperature and relative humidity. There was approximately a 4 °C rise in temperature and a 7 % drop in relative humidity during the test. Figure 147C shows the mass concentration and the number concentration readings. The earlier increase in the number concentration and the later increase in the mass concentration correspond to the earlier ionization alarm times followed later by photoelectric alarm times. The Dustrak surpassed its maximum range of 300 mg/m³ from about 240 s to 300 s.



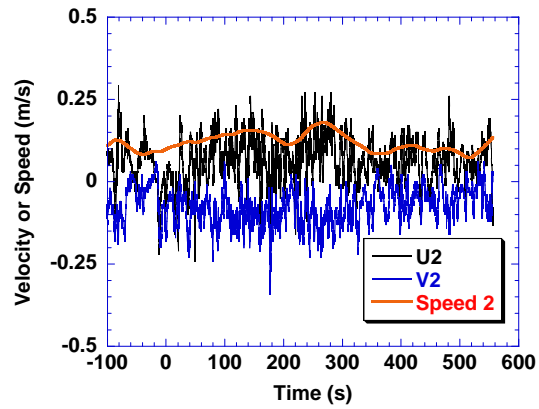
A (Bread, no forced airflow)



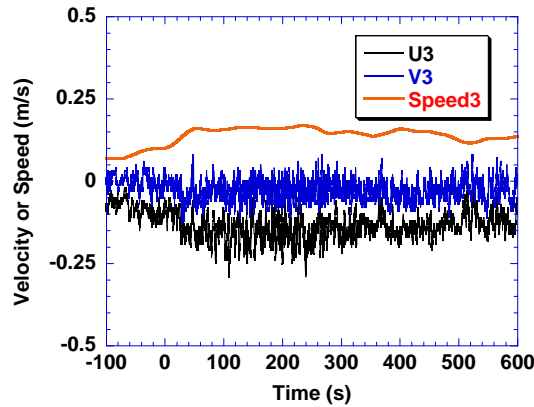
B (Bread, forced airflow)



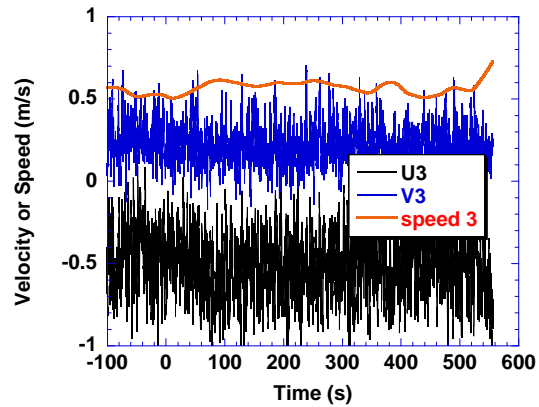
C (Bread, replicate, no forced airflow)



D (Bread, replicate, forced airflow)



E (Bagel, no forced airflow)



F (Bagel, forced airflow)

Figure 146. Velocity and speed components for toasting bread nuisance source with and without forced ventilation

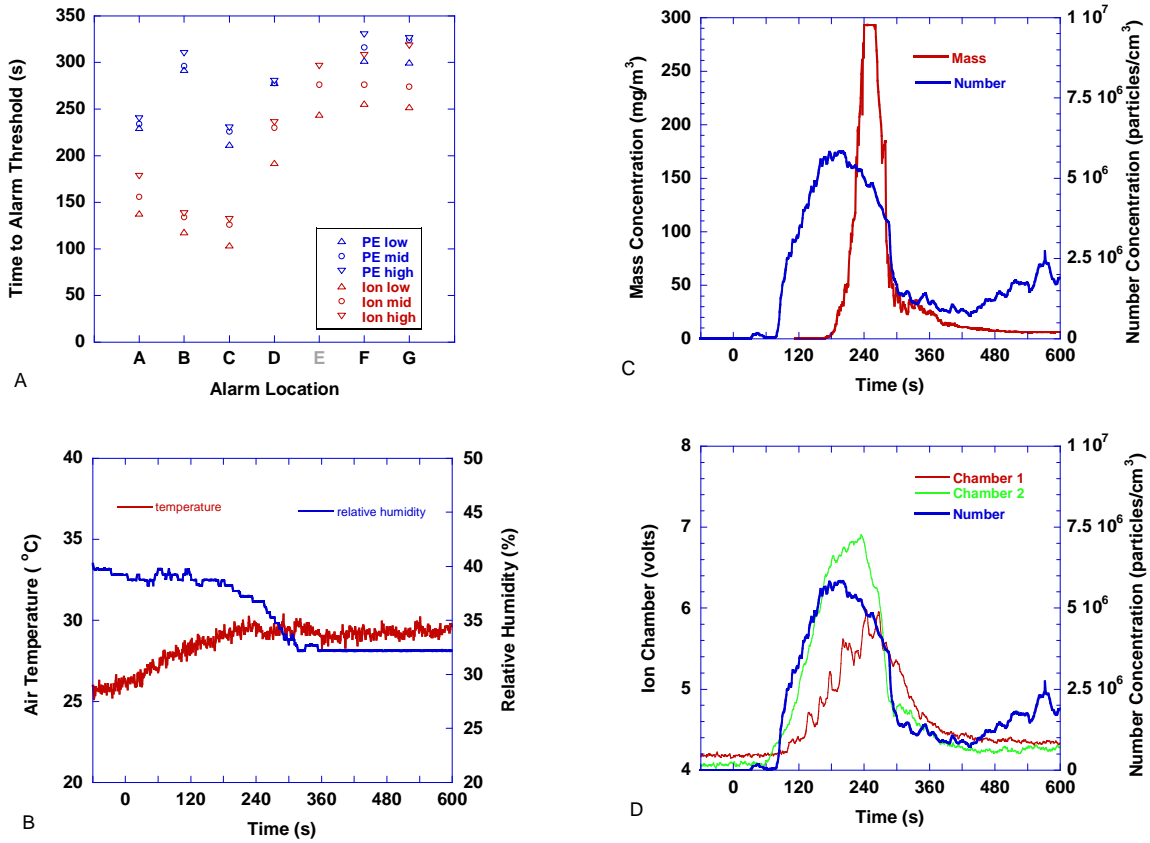


Figure 147. Toasting bread scenario - toaster on at $t=0$, off at 240 s. No forced flow

Figure 147D shows the number concentration and the voltage from the flow-through ion chambers. First, note that ion chamber 2 responds first and achieves a higher peak voltage due to the fact that it was located closer to the source. Second, note that the voltage signal from ion chamber 2 followed the number concentration curve which again is expected since they were at the same sampling location. The ion chamber voltage is related to the first moment of the particle size distribution, while the number concentration is essentially the zeroth moment of the size distribution. The ratio of these moments is equal to the count median diameter of the aerosol size distribution. Likewise, the ratio of the mass concentration (3rd moment) to the number concentration is proportional to another particle diameter, the diameter of average mass. These characteristic particle sizes were computed from these moments for several smoke and nuisance source aerosols generated in the FE/DE [33]. These calculations were possible because the MIC was used to get the first moment since previous research had established its proportionality constant, and a direct mass measurement was taken to obtain the 3rd moment.

One can still observe trends in these particle size statistics by examining the number concentration, ion chamber output and the Dustrak mass concentration. In figure 147D, it is observed that the number concentration and the ion chamber begin to rise at about 60 s and the rate of rise for each is constant up to 150 s. This implies that the count median diameter is constant while the number concentration increases. After 150 s the number concentration starts to level off then drop, while the ion chamber voltage continues to increase until it reaches a peak at 240 s. This implies that the count median diameter starts to increase from 150 s to 240 s. After 240 s the ion chamber voltage and the number concentration drop rapidly until reaching minimums at 420 s. The ion chamber voltage remains relatively flat while the number concentration starts to rise suggesting a decrease in the count median diameter from that point on.

In figure 147C, it is observed that the number concentration has reached its peak at 180 s before any significant amount of mass concentration was recorded. In fact, the mass concentration just begins to rise at 180 s. The rapid increase in mass concentration along with the decreasing number concentration implies a significant increase in the diameter of average mass as the Dustrak reaches its peak. The steep drop in the mass concentration also implies a significant decrease in the diameter of average mass since the number concentration is decreasing at a much lower rate. At 420 s the mass concentration continued to fall while the number concentration started to rise implying continuing decrease in the diameter of average mass.

Figure 148 shows the results for a repeated test where the remote bedroom window was left open. The times to reach alarm thresholds are similar to the initial toasted bread test. Again, the trends were increasing ambient air temperature and decreasing relative humidity. The mass concentration, number concentration and ion chamber voltages show more fluctuation due to the open window disturbing the room flows, but they achieved maximum values similar to the previous test. Note that the number concentration started out higher than normal room air background (1×10^6 particles/cm 3) because this test was run before the previous test aerosol concentration was cleared from the manufactured home.

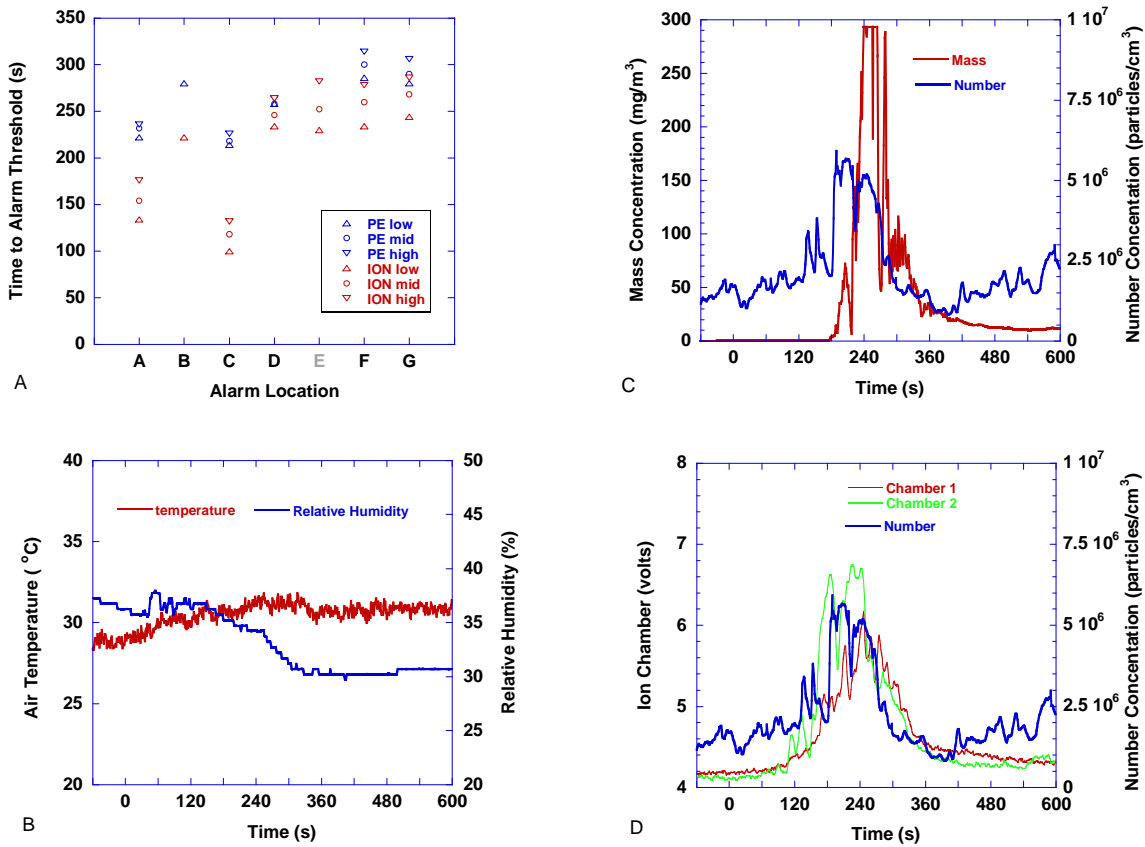


Figure 148. Toasting bread scenario – toaster on at $t=0$, off at 255 s.
No forced flow, remote bedroom window open

Figures 149 and 150 show the time to alarm results for the toasted bread cases with the floor fan on. Fewer alarm thresholds were reached compared to the cases without the fan flow, which was due primarily to the dilution effects of the forced flow. Consequently, the number and mass concentration and ion chamber voltage peaks were lower than the tests without the fan turned on. Another difference between the cases without and with the fan flow was the decay of the number concentration, mass concentration, and ion chamber voltage after the toaster was turned off, where after an initial drop, there was a more even linear decay in each of these values. The fan flow is promoting mixing throughout the entire volume of the open rooms. There was an observed difference between the two tests.

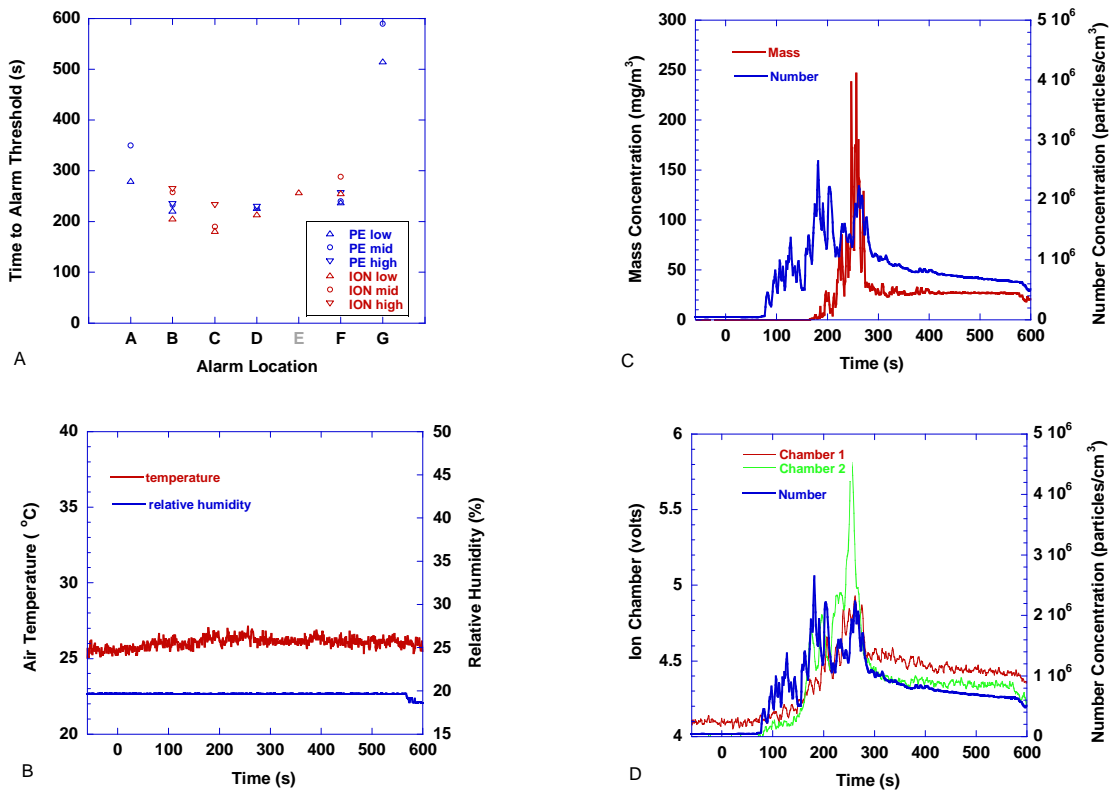


Figure 149. Toasting bread scenario - toaster on at t=0, off at 255 s. Room fan turned on

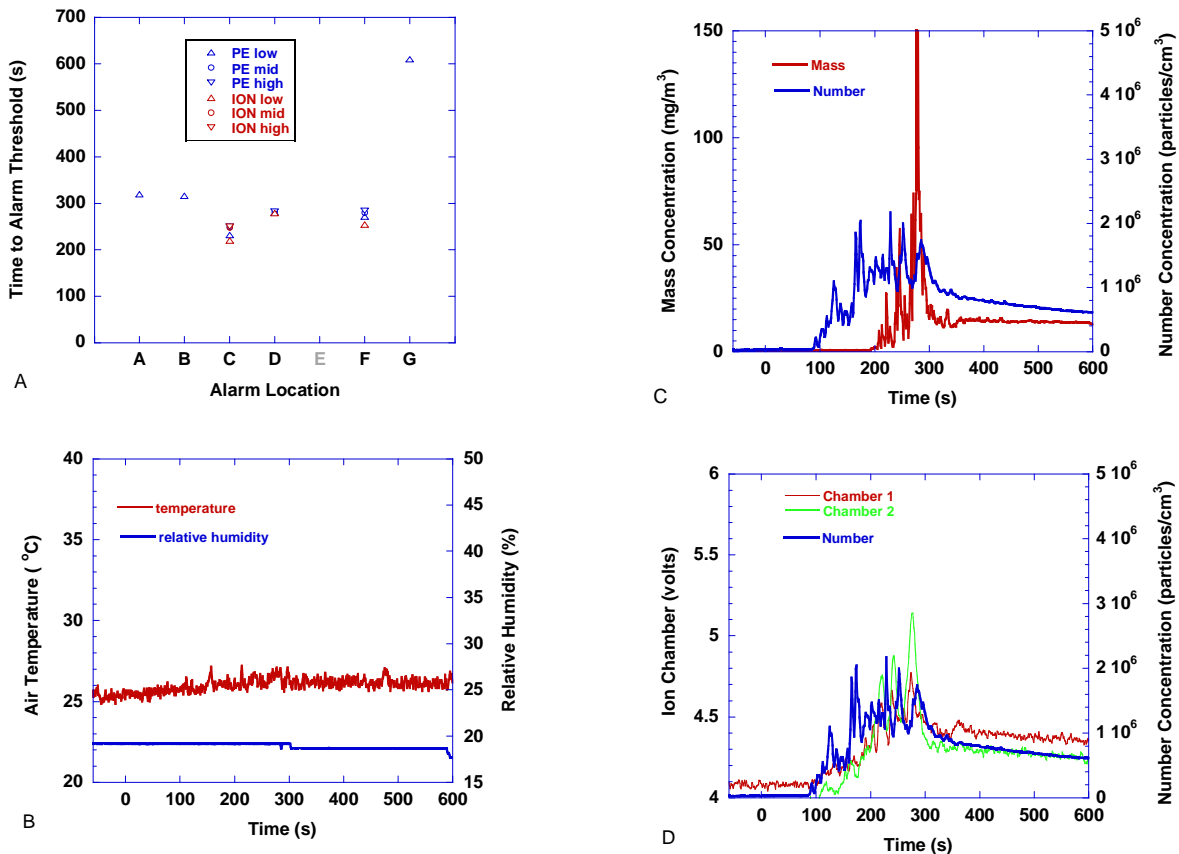


Figure 150. Toasting bread scenario - toaster on at $t=0$, off at 270 s. Room fan turned on

Figures 151 and 152 show the time to alarm results for the toasting frozen bagel tests. In these tests, only ionization alarm thresholds were achieved. The fan off, no forced flow test reached more threshold levels. The frozen bagels were toasted to a medium brown color and did not char significantly, thus the heavy gray smoke observed with the charring of bread was not present. The temperature and relative humidity show the same trend as the toasting bread scenarios. The peak number concentrations for these tests compare with the respective fan, no fan toasting bread scenarios, however, peak mass concentrations were an order of magnitude lower.

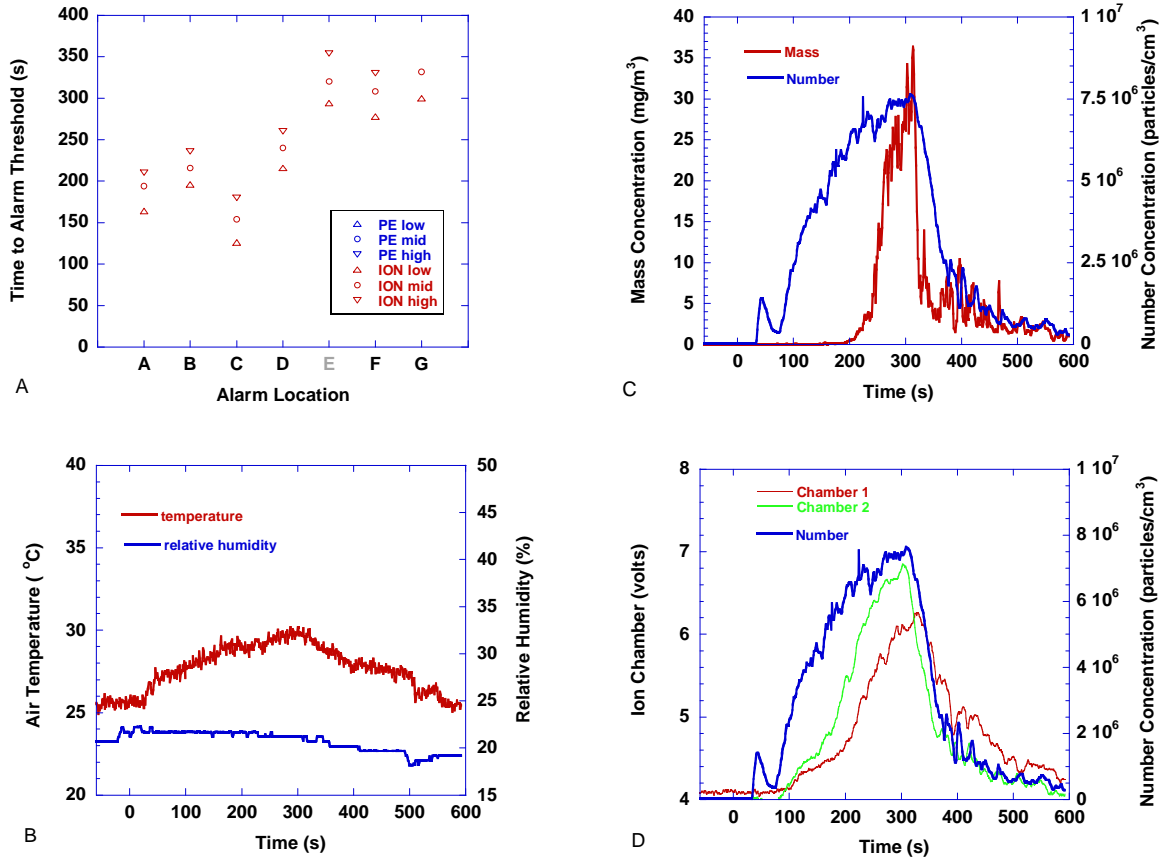


Figure 151. Toasting frozen bagel scenario – toaster on at $t=0$, off at 300 s. Room fan turned off

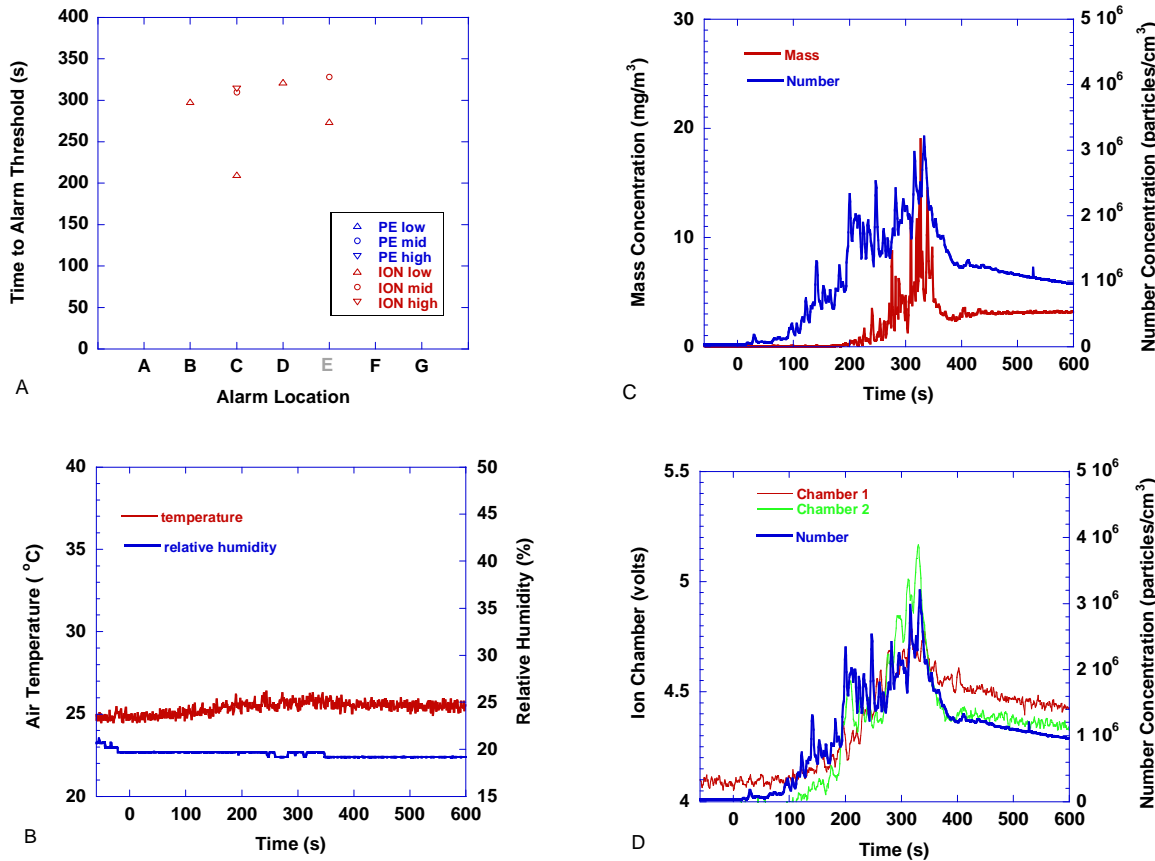


Figure 152. Toasting frozen bagel scenario – toaster on at $t=0$, off at 300 s. Room fan turned on

Several generalizations describe the toasting scenarios:

- For the most part, a high concentration of small particles produced in the early stages of toasting contributed to the ion alarm events.
- With no forced flow, the particles were carried to the ceiling and were transported far from the source at sufficient concentration to cause ionization alarms.
- Forced flow diluted the aerosol concentration such that only ionization alarms closest to the source were susceptible to reaching their threshold.

- Photoelectric alarm thresholds were met only after items started to char and produce visible smoke, i.e., the photoelectric alarms lag the ionization alarms due to the type of smoke aerosol produced.
- Forced flow reduced the number of photoelectric alarm thresholds met. However, at several locations, photoelectric alarm thresholds were met where ionization alarm thresholds were not.

6.3.2 Frying Bacon

Strips of bacon were fried in either a 300 mm (10 in) diameter cast-iron frying pan or 280 mm (9 in) aluminum non-stick frying pan heated by both a single-unit LPG hot plate (maximum output 4 kW) or the electric range (large burner, nominally 1.5 kW maximum output). With the electric range, the aluminum non-stick pan was pre-heated on the high setting, then turned down to medium high after the bacon was added. Cooking time was between 5 min to 6 min. With the LPG hot plate, LP gas was piped to the burner from a bottle located outside the manufactured home. After the burner was lit, the cast iron pan was pre-heated for 1 min, then, the bacon was added. Cooking time was 10 min. In all cases, approximately 230 g of bacon was cooked for a time sufficient to crisp the bacon, but not char it.

Figures 153 and 154 show results for bacon cooked in the cast iron pan with no forced air flow. (Note, there was no companion forced air flow test for this scenario.) Figures 153A and 154A show similar trends in that ionization alarm thresholds were reached first, followed by photoelectric alarm thresholds. For any fixed location, delays between ionization and photoelectric alarm ranged between several hundred seconds to 10's of seconds. The temperature rise was about 7 °C during these tests. From figure 154B, the ignition of the hotplate was apparent from a temperature spike at time = 0. The relative humidity initially increased, then decreased suggesting moisture driven off early the cooking process (as evidenced by condensed water vapor above the frying pan) was the primary cause (moisture from the combustion process also affects the relative humidity).

The number concentration rose to peak values of approximately 6×10^6 particles/cm³ at the end of the cooking time, while the mass concentration peaked at about 50 mg/m³ at the end of each test. The ion chamber voltages rose steadily from about 180 s to the end of the cooking time (660 s). There was no evident rise in the number concentration from the LP gas combustion alone.

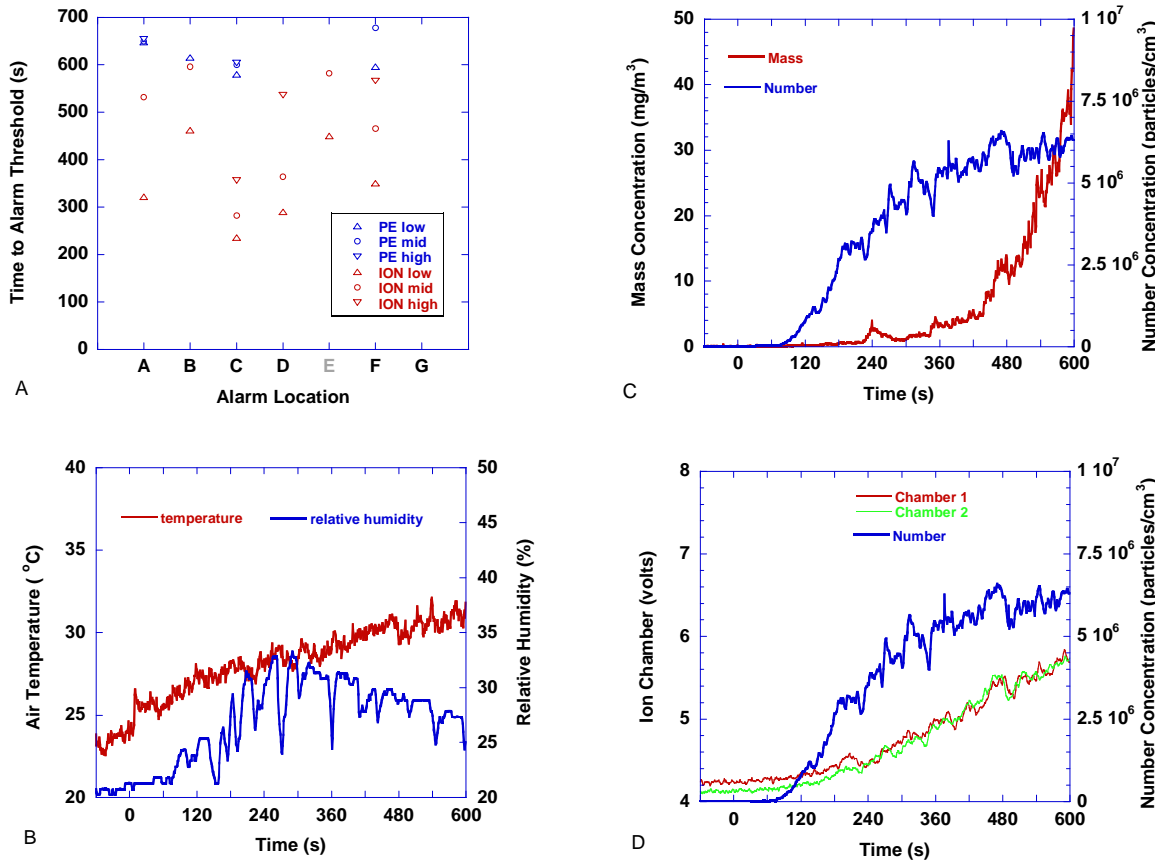


Figure 153. Frying bacon scenario - cast-iron pan, LPG hot plate, no forced flow, burner lit at $t=0$, bacon in pan at 60 s

Figure 155 shows the results for bacon cooked in the aluminum non-stick frying pan heated by the electric range with no forced air flow. Figure 155A shows the time to reach alarm thresholds. Usually, ionization thresholds were reached before photoelectric thresholds with the exception of the lower threshold at position G. Fewer thresholds were reached in this test compared to the cast iron frying tests above, even though the bacon was cooked to the same nominal doneness. The temperature rise was about 3 °C over the test time, and again the relative humidity increased to a peak, then decreased below the initial value by the end of the test.

There were two peaks in the number concentration attributed to the method of cooking (i.e. turning the bacon and moving it and pressing it with a spatula), on the order of 4×10^6 particles/cm³. The mass concentration also experienced two peaks, the early one about 20 mg/m³ and the latter one about 80 mg/m³. The ion chamber voltages follow the number concentration

trend and both experience two peak values. The magnitude of the second peak is greater than the first suggesting the mean particle size is larger, which is confirmed by the mass concentration peaks.

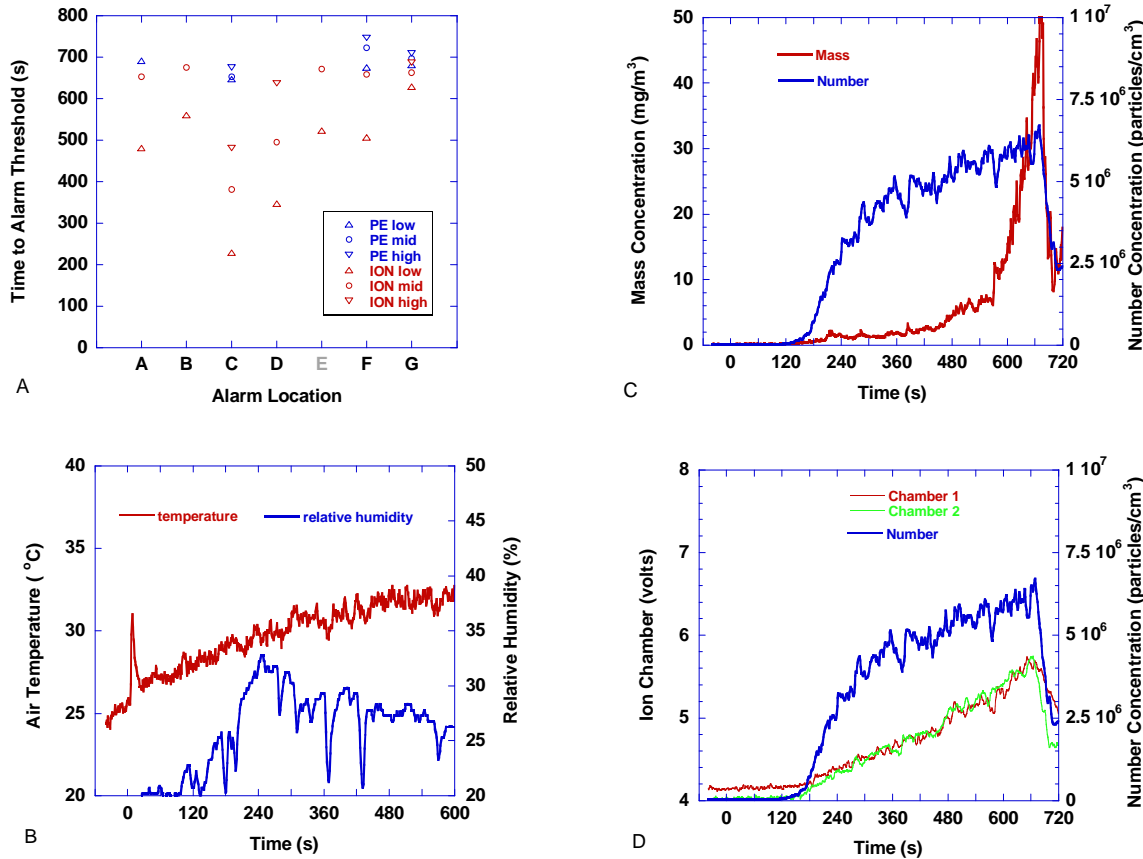


Figure 154. Frying bacon scenario - cast-iron pan, LPG hot plate, no forced flow, burner lit at $t=0$, bacon in pan at 60 s

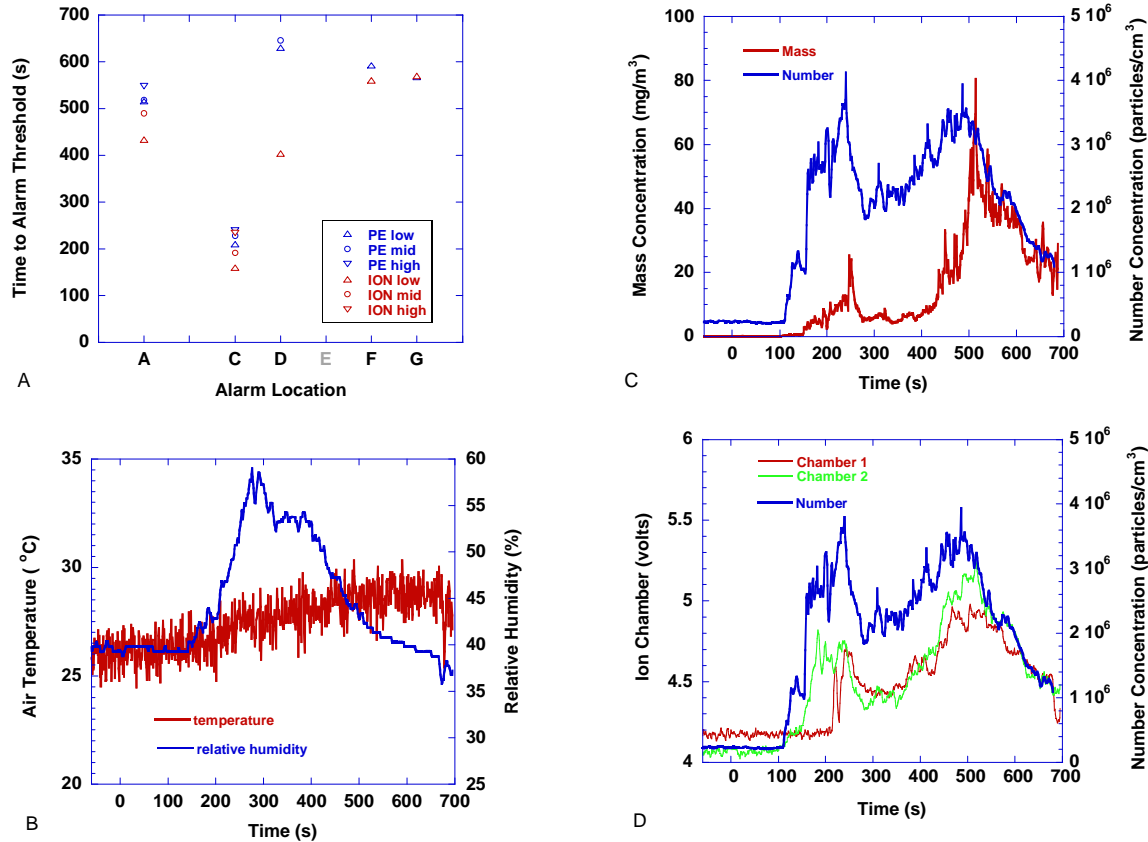


Figure 155. Frying bacon scenario - aluminum pan, electric range, no forced flow, bacon in pan at 120 s

Figure 156 shows the results for bacon cooked in the aluminum non-stick frying pan heated by the electric range with forced air flow. During this test, only photoelectric alarm thresholds were met, and then at three locations. A slight decrease in relative humidity was observed, as was a slight increase in temperature. The number concentration peaked at about 1×10^6 particles/cm 3 , while the mass concentration experienced a sharp peak to a value of 25 mg/m 3 . The ion chamber voltages follow the number concentration increase, but only reach values about 0.2 V above clean air background value.

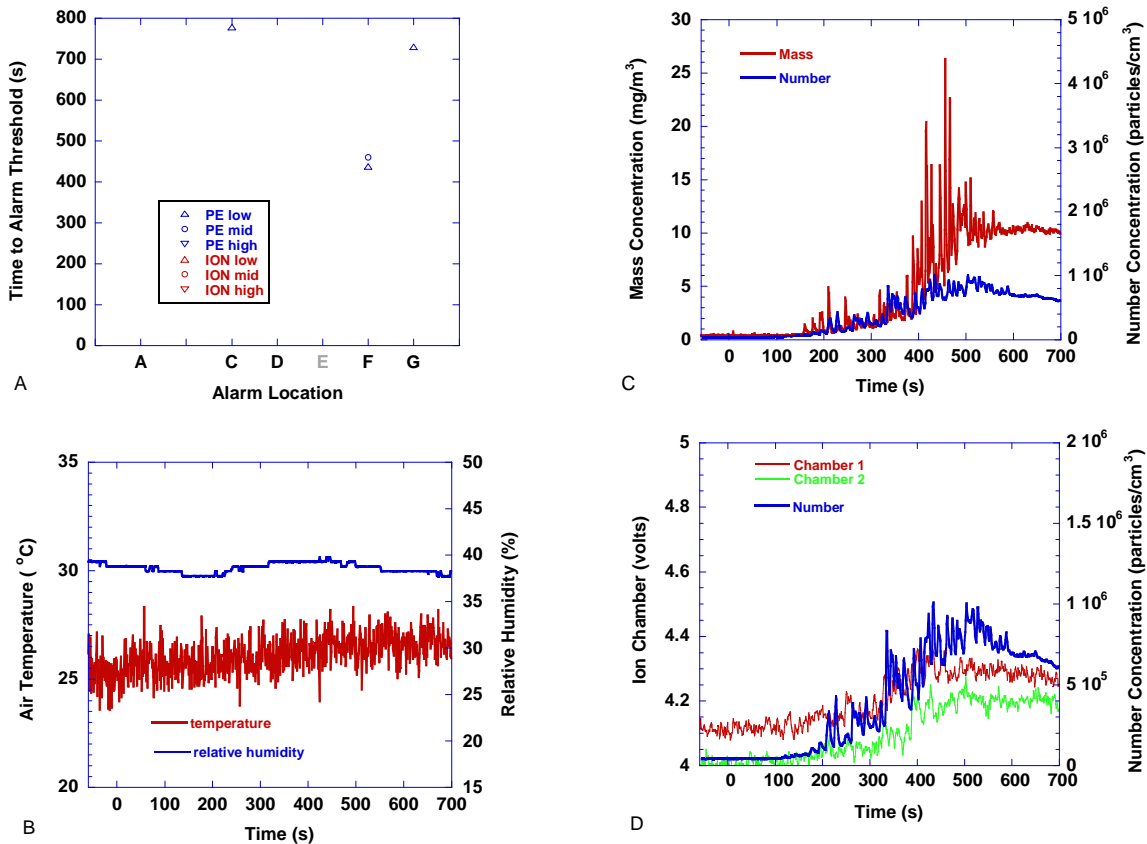


Figure 156. Frying bacon scenario - aluminum pan, electric range, floor fan on, bacon in pan at 120 s

Several generalizations describe the frying bacon scenarios:

- With no forced air flow, ionization alarm thresholds were met before photoelectric alarm thresholds at most locations.

- The combination of the type of pan and heat source affects the number of alarm thresholds met. The rendered byproducts from the bacon tended to stick to the cast iron pan and burn, producing more visible smoke during cooking.
- With forced airflow, all ionization alarms were suppressed, while three locations reached photoelectric alarm thresholds. The alarm closest to the source actually reached the lowest threshold after two alarms located farther from the source.

6.3.3 Frying Butter and Margarine

One tablespoon of butter or margarine was placed in either the aluminum or cast iron pan set on the large element burner. Power was set to high and the pan was left for 5 min to 6 min, then power was turned off and the pan was removed from the burner and set aside.

Figures 157 and 158 show results for repeated tests of butter heated in the aluminum pan with no force air flow. Both photoelectric and ionization alarm thresholds were met at most locations. Usually the ionization thresholds were reached first. In both tests, the temperature rose about 4 °C, while the relative humidity dropped from 20 % to 15 %. The mass concentration peaked at about 360 s at values of 150 mg/m³ and 300 mg/m³. Number concentration maximums were on the order of 5×10^6 particle/cm³. Ion chamber 2 voltage followed the number concentration curve, tracking peaks and valleys though advanced in time which is assumed to be due to a sample transport time difference. Ion Chamber 1 voltage on average is lower than chamber 2 voltage due to the fact that it is further from the source.

Figure 159 shows the results for butter heated in a cast iron pan with no forced air flow. Photoelectric alarms thresholds were met at all locations with working sensors (location E does not have a photoelectric sensor, and location C did not have a working sensor for this test) before ionization alarm thresholds were met. Temperature rise was about 6 °C, and a slight decrease in relative humidity was observed. Mass concentration peaked at over 300 mg/m³, while the number concentration peaked at about 4×10^6 particle/cm³. The ion chamber voltages follow the number concentration with chamber 2 peaking higher and slightly sooner than chamber 1.

Figure 160 shows the results for butter heated in a cast iron pan with forced air flow. All locations with photoelectric sensors reached alarm thresholds, while only 2 locations reached ionization thresholds, and usually after the photoelectric thresholds were met. Temperature rise was about 2 °C and the relative humidity dropped a few percent during the test, then rebounded at the end. No CPC data was taken during this test. Mass concentration peaked above 35 mg/m³, while the ion chamber voltages rose between 0.3 V and 0.4 V.

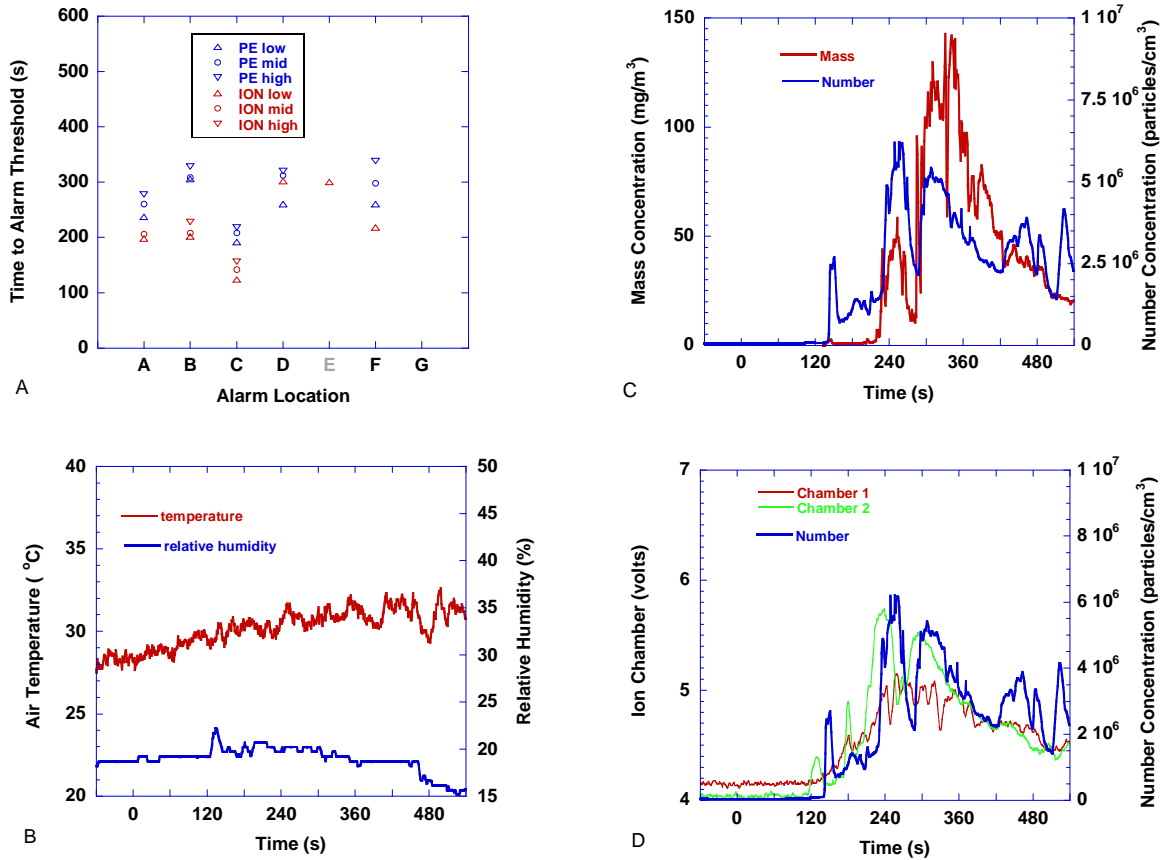


Figure 157. Frying butter scenario - aluminum pan, electric range, floor fan off, butter in pan at t=0

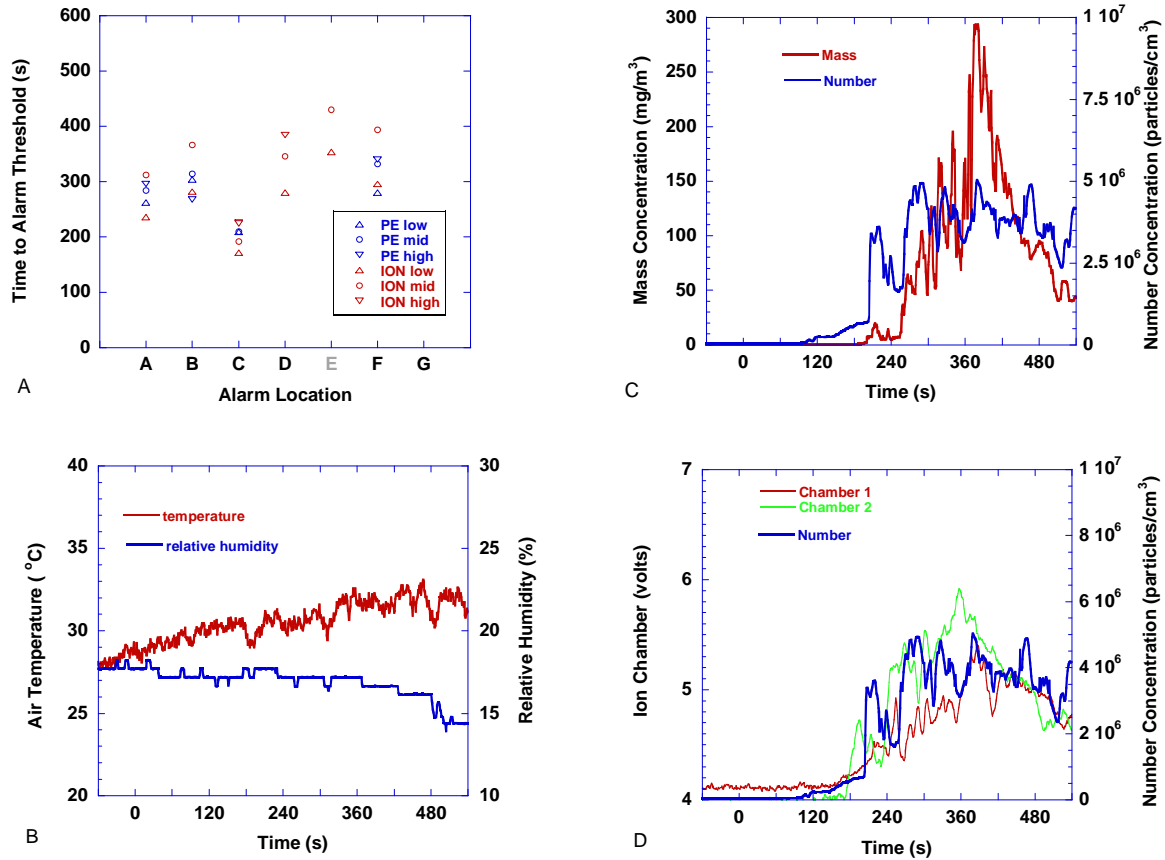


Figure 158. . Frying butter scenario - aluminum pan, electric range, floor fan off, butter in pan at $t=0$

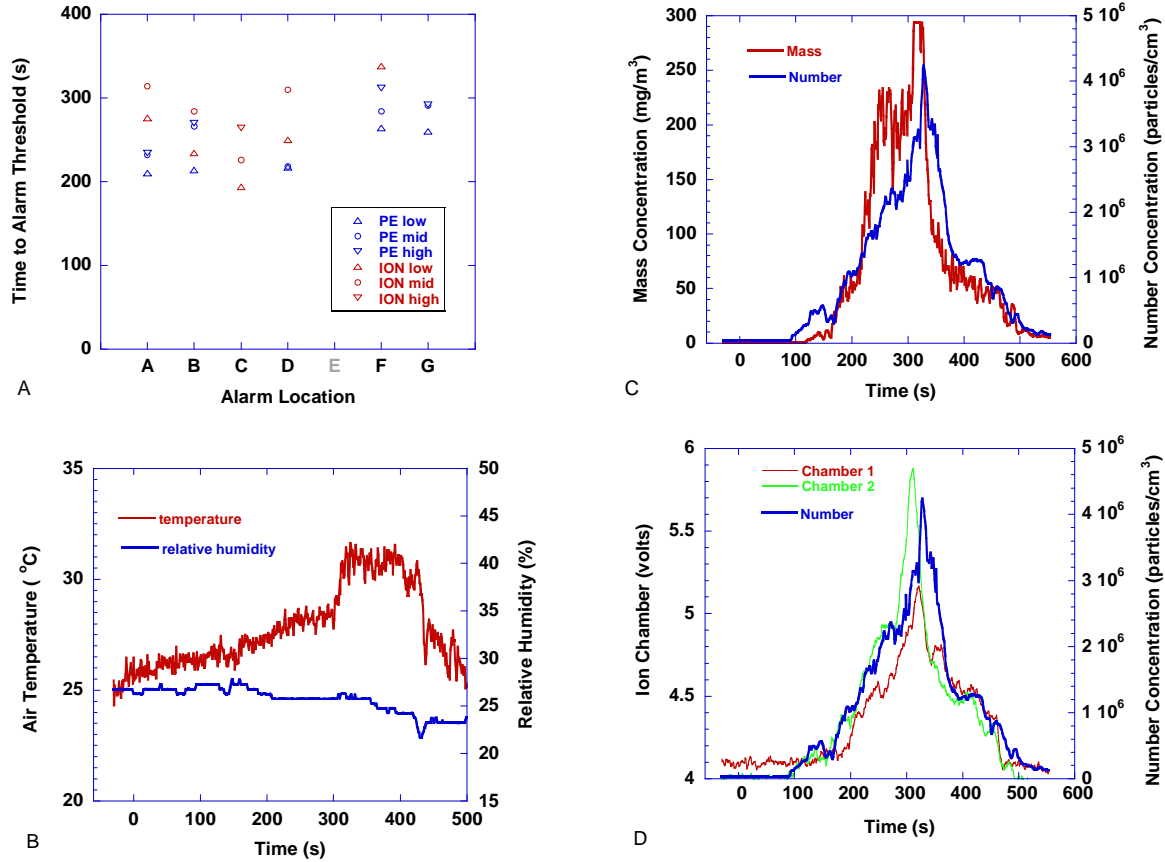


Figure 159. Frying butter scenario - cast iron pan, electric range, floor fan off, butter in pan at t=0

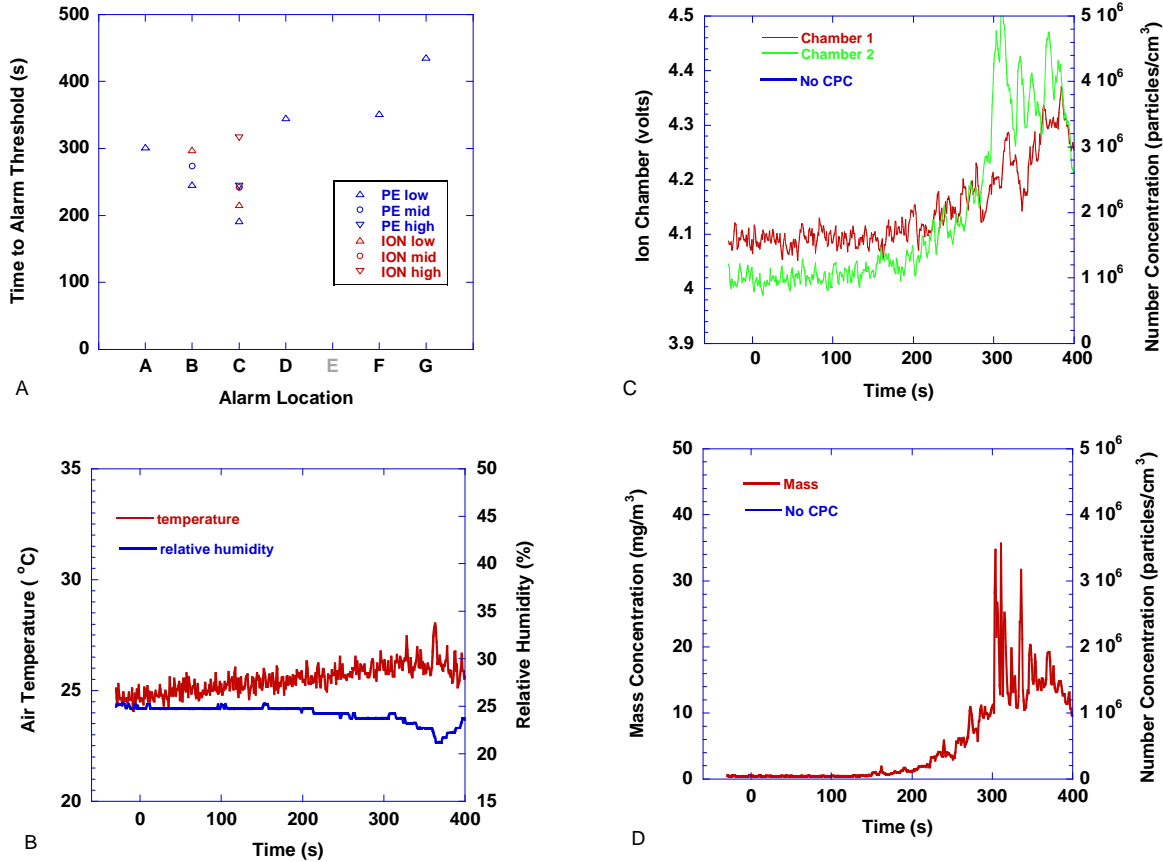


Figure 160. Frying butter scenario - cast iron pan, electric range, floor fan on, butter in pan at t=0

Figure 161 shows the results for margarine heated in a cast iron pan with no forced air flow. Photoelectric alarm thresholds were met at all six locations that had photoelectric sensors, while ionization threshold was met only at the location closest to the source. There was little change in temperature or relative humidity during the test. The mass concentration experienced a sharp peak of 100 mg/m^3 310 s into the test. Four of the six alarm locations had already reached photoelectric alarm thresholds before that peak mass concentration was recorded. Number concentration peaked at a value of approximately $2.8 \times 10^6 \text{ particles/cm}^3$. Ion chamber voltages rose between 0.5 V and 0.6 V for chambers 1 and 2 respectively.

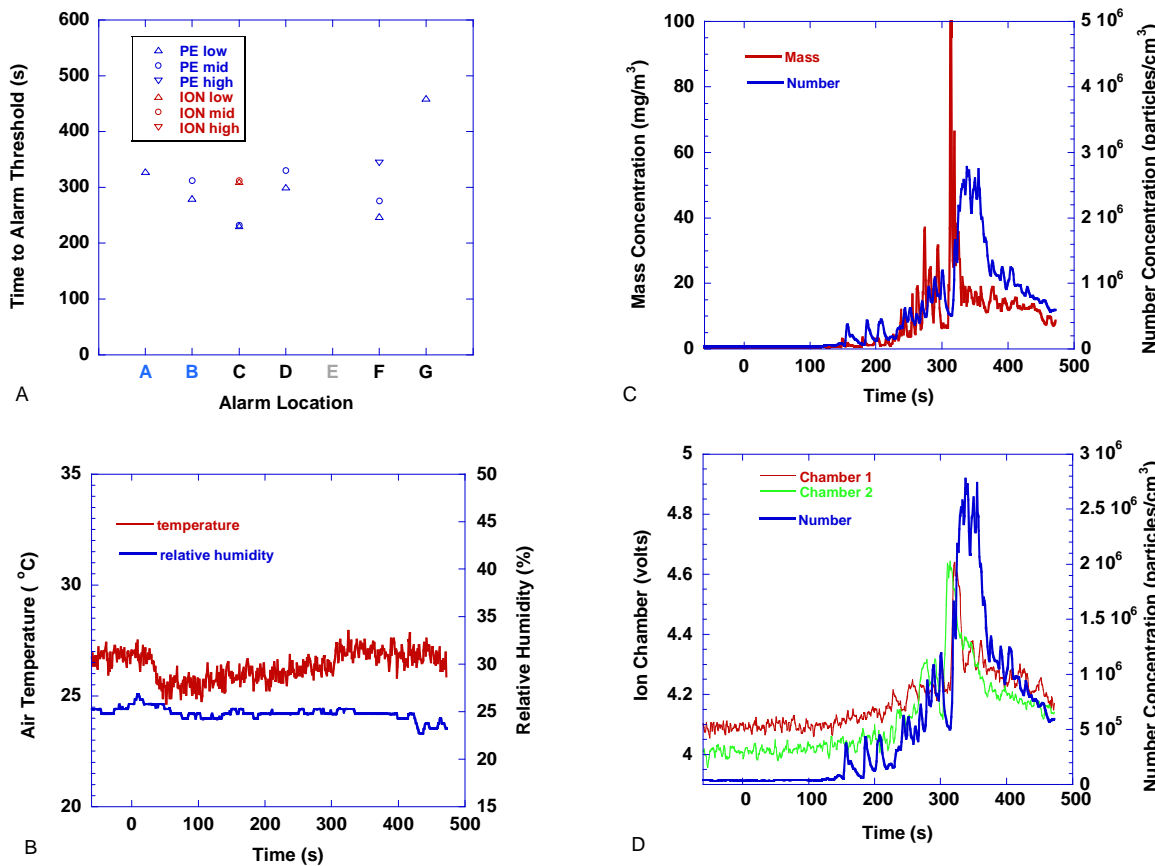


Figure 161. Frying margarine scenario - cast iron pan, electric range, floor fan off, margarine in pan at $t=0$

The following generalizations describe butter or margarine heated in pans.

- Heating butter in the aluminum non-stick pan caused ionization alarm thresholds to be achieved first, while heating butter or margarine in the cast iron pan caused photoelectric alarm thresholds to be achieved first.
- Forced air flow reduced the number of locations that reached ionization alarm thresholds, but not the number of photoelectric alarm thresholds.
- Butter in the cast iron pan with no forced flow produced more alarm threshold conditions slightly earlier than margarine tested under the same conditions.

6.3.4 Frying Hamburgers

Three 110 g (quarter pound) frozen hamburgers (28 % fat content) were cooked in the aluminum pan on the large electric burner. First, the pan was placed on the large electric burner and the power was set to high. After a preheat time (between 130 s to 160 s) the power was lowered to a medium-high setting. The hamburgers were placed in the heated pan. The hamburgers were flipped after approximately 4 min and cooked for an additional 5 min. The stove was turned off and the hamburgers were removed from the pan.

Figure 162 shows the results for test conditions with no forced flow. At about 250 s, a threshold was met by the photoelectric sensor closest to the source. The rest of the locations reached alarm thresholds between 400 s and 600 s. Some locations record photoelectric alarm thresholds first, while others record ionization alarm thresholds first. Temperature rose about 3 °C during the test while the relative humidity rose about 5 %. After initial peaks in the mass and number concentration, the mass concentration peaked at about 100 mg/m³, while the number concentration peaked at 4×10^6 particles/cm³. Ion chamber voltage rise was 1.4 V and 1.1 V for chambers 2 and 1 respectively.

Figure 163 shows the results for test conditions with force air flow and the living room window open. All locations with a photoelectric sensor reach alarm thresholds for that sensor. Only two locations recorded ionization alarm thresholds. The temperature rise was about 2 °C during the test, while the relative humidity rose about 3 %. Mass concentration peaked at about 30 mg/m³, while the number concentration peaked at 2×10^6 particles/cm³. The peak ion chamber voltage change was 0.4 V and 0.6 V for chamber 1 and 2 respectively.

Figure 164 shows the results for test conditions with forced air flow and the normal conditions of all exterior doors and windows closed. Five out of six locations reach photoelectric alarm thresholds, while none reach ionization alarm thresholds. The closer to the source the sooner the photoelectric thresholds were reached. Temperature rose about 2 °C, while the relative humidity

rose about 2 %. The mass concentration showed several short duration spikes, with the highest peak about 30 mg/m^3 . The number concentration peaked at about $1.6 \times 10^6 \text{ particles/cm}^3$. Peak ion chamber voltage change was about 0.5 V for each chamber.

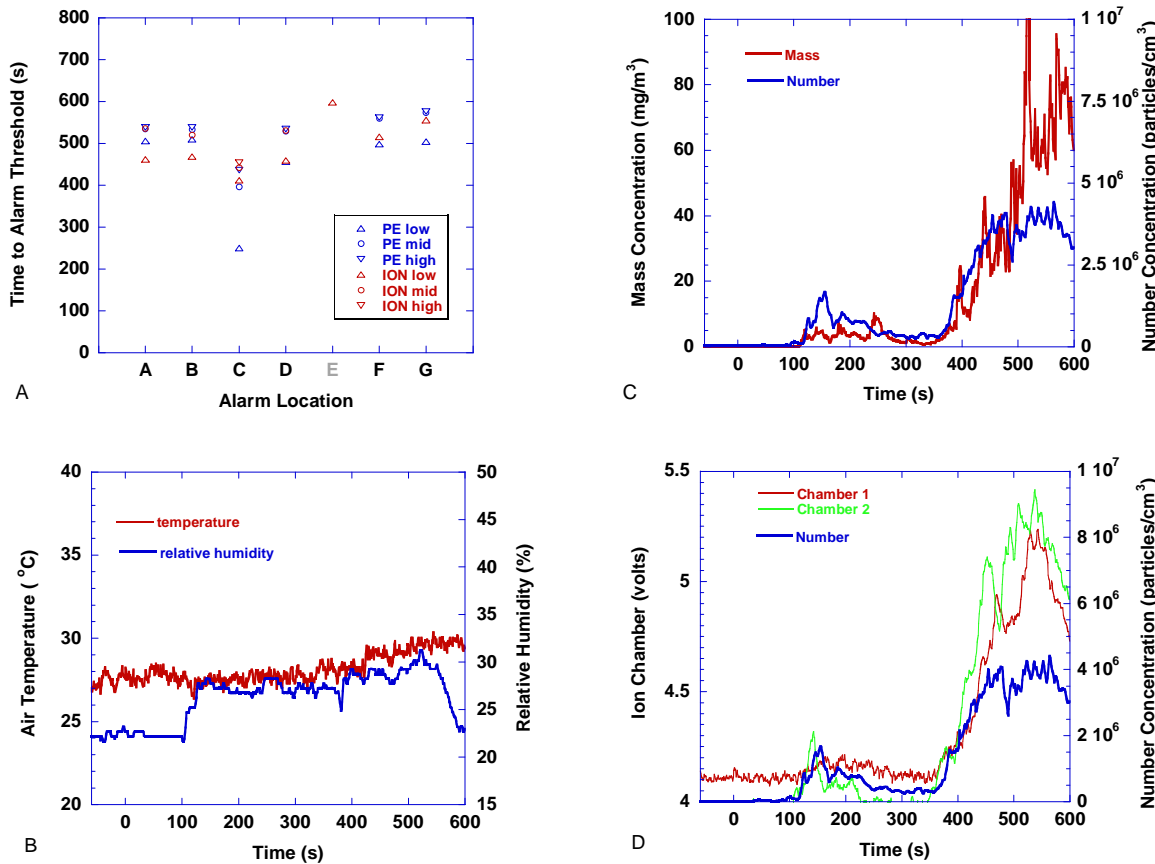


Figure 162. Frying hamburgers - three hamburgers in non-stick frying pan, floor fan off. Hamburgers in pan at $t=120 \text{ s}$

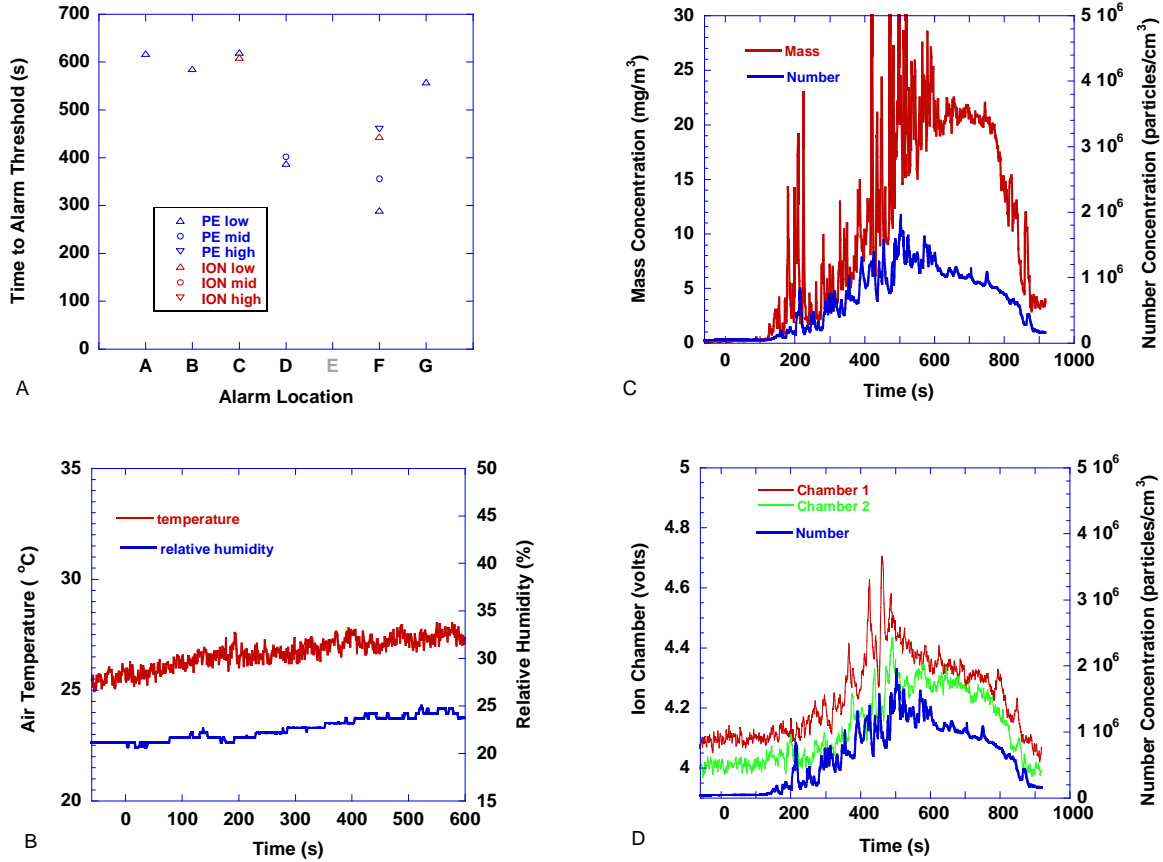


Figure 163. Frying hamburgers - three hamburgers in non-stick frying pan, floor fan on, living room window open. Hamburgers in pan at t=160 s

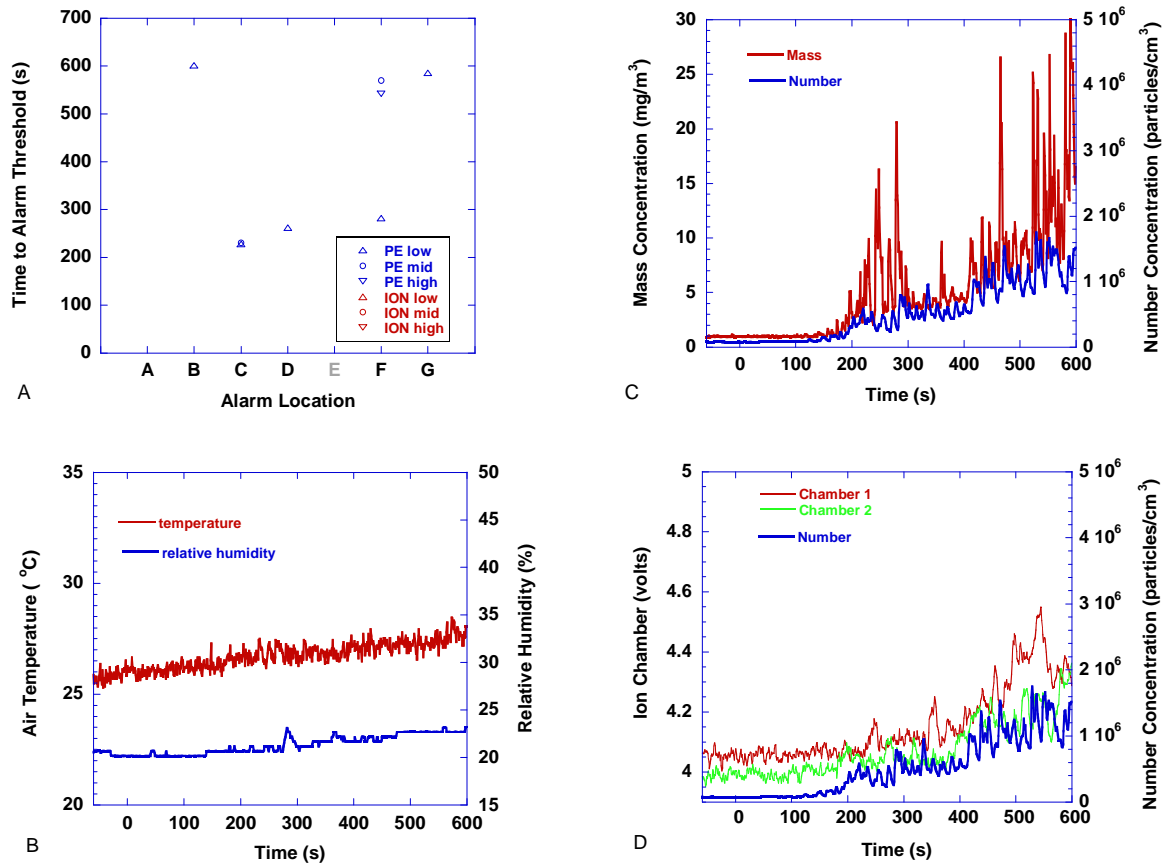


Figure 164. Frying hamburgers - three hamburgers in non-stick frying pan, floor fan on. Hamburgers in pan at t=150 s

The following generalizations describe the frying hamburgers tests:

- With no forced flow, photoelectric and ionization alarm thresholds were recorded at all locations with no clear preference as to which type reached a threshold first at the specified locations.
- The forced flow tests yielded significantly less ionization alarm thresholds.

6.3.5 Deep-frying Tortillas and French-fried Potatoes

Using the LP hot plate, 0.15 m diameter (6 in) corn tortillas were deep-fried in a large flat-bottom wok-style steel pan in corn oil approximately 50 mm in depth. The hot plate was set to the high setting. Six minutes after the burner was lit and the oil pre-heated, tortillas were added. A total of 10 tortillas were fried over a period of 10 min. Using the cast iron pan, 30 mm of vegetable oil was pre-heated on the large electric burner element for eight minutes. 454 g (1 lb) of frozen “French-fried” potatoes were added to the pan and cooked for 5 min to 6 min, removed and another 454 g of potatoes were added and cooked for an additional 5 min to 6 min, then removed.

Figure 165 shows the results for tortilla frying test with no forced air flow. Three locations reached ionization alarm threshold levels. The temperature rose 9 °C over the test period, while relative humidity rise reached a maximum of about 8 %. The mass concentration did not rise above 2 mg/m³ during the test. The number concentration peaked at about 6.5×10^6 particles/cm³. The ion chamber voltage rise follows the number concentration rise, with peak change in the voltages of 0.5 V and 0.6 V for chamber’s 1 and 2 respectively.

Figure 166 shows the results for deep frying French fried potatoes with no forced air flow. Only one ionization alarm threshold was recorded at the location closest to the source. The temperature increased 5 °C during the test period. The relative humidity initially dropped 2 % during the pre-heating stage, but showed a 10 % rise after each batch of potatoes were added to the hot oil. As the water was driven off the potatoes, the relative humidity would drop. The mass concentration showed two spikes of 3 mg/m³ and 1 mg/m³ soon after the potatoes were dropped into the hot oil. The number concentration peaked at about 3.5×10^6 particles/cm³. Ion chamber 2 voltage change peaked at 0.45 V, while chamber 1 voltage change peaked at 0.3 V.

The lack of sufficient aerosol mass concentration means it would be unlikely that these scenarios would produce any photoelectric alarms for any extended cooking time. Though, extended cooking times could produce aerosol levels sufficient to produce alarms in the more distant ionization alarms. Any spillage or spatter of hot oil on an electric heating element produces smoke and, some times, small short-lived flames, which would change the nature of the aerosol produced. Repeated spatter of the hot oil might produce enough smoke to reach the threshold for

photoelectric alarms; however one could argue that such a situation is potentially hazardous and an alarm sounding would not be characterized as a nuisance alarm.

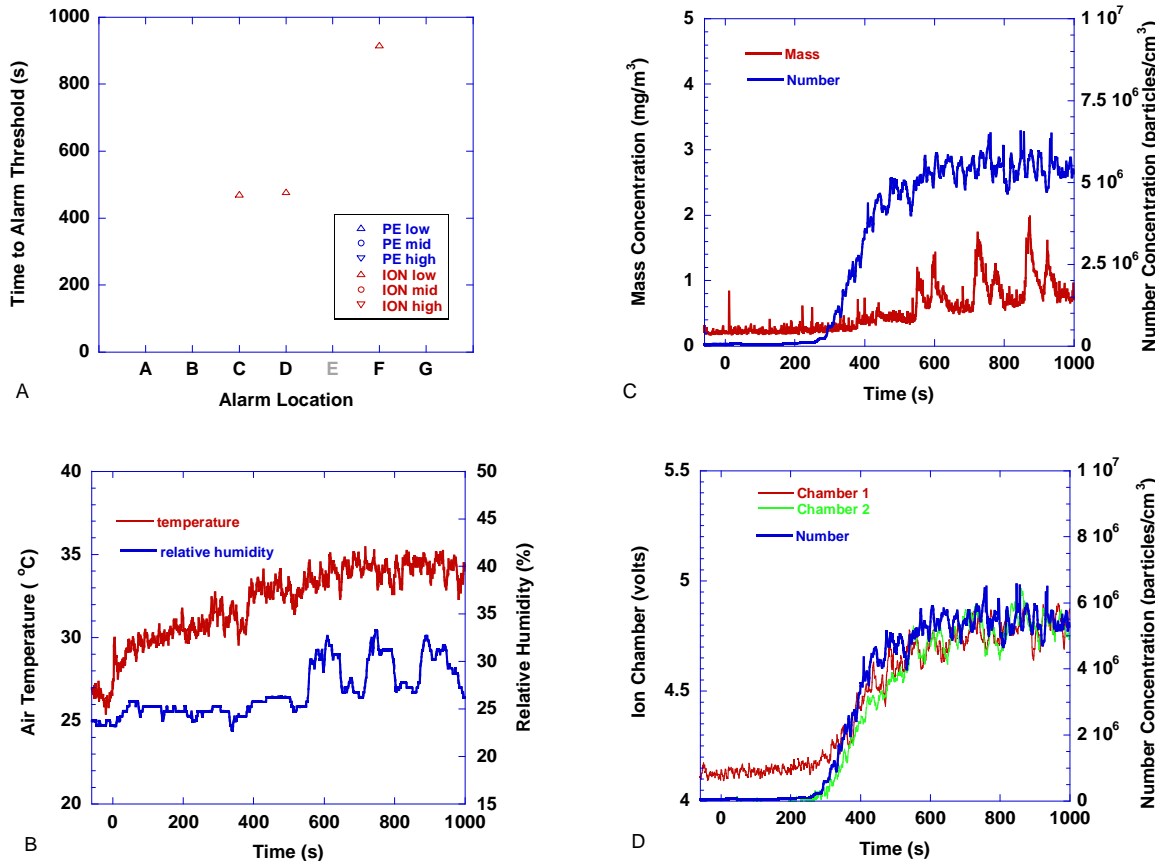


Figure 165. Deep-frying Tortillas scenario - steel wok, LPG hotplate, floor fan off, first tortillas in pan at t=360 s

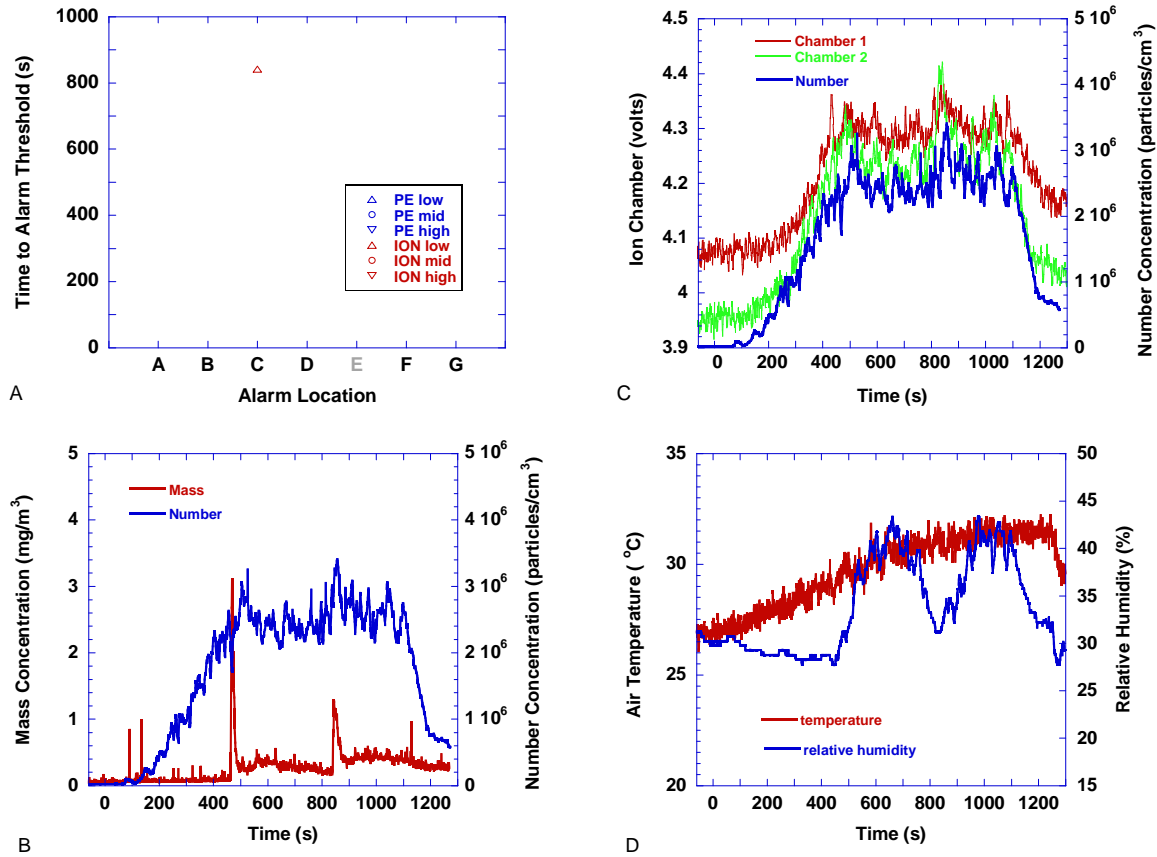


Figure 166. Deep-frying french fries scenario - steel wok, LPG hotplate, floor fan off, first french fries in pan at $t=360\text{ s}$

6.3.6 Broiled and Baked/Broiled Pizza

For the broiled pizza scenario, a small (158 g) frozen plain pizza was placed on a large metal “broiler” pan that was covered with aluminum foil, and placed in the oven. The broiler was set to high and the door opened to the broiling position. The pizza cooked for approximately 13 min then was removed. There was no forced flow for this test.

Figure 167 shows the results for broiling frozen pizza. While five locations reached ionization alarm thresholds, and only two locations reached photoelectric alarm thresholds, the first threshold reached was for the photoelectric alarm closest to the source. This was reached almost 300 s before the lowest ionization threshold was reached at that location. Interestingly, there was nothing evident in the Dustrak or CPC readings at the time the first photoelectric threshold was met. Temperature rise was on the order of 5 °C , though there was little change in the

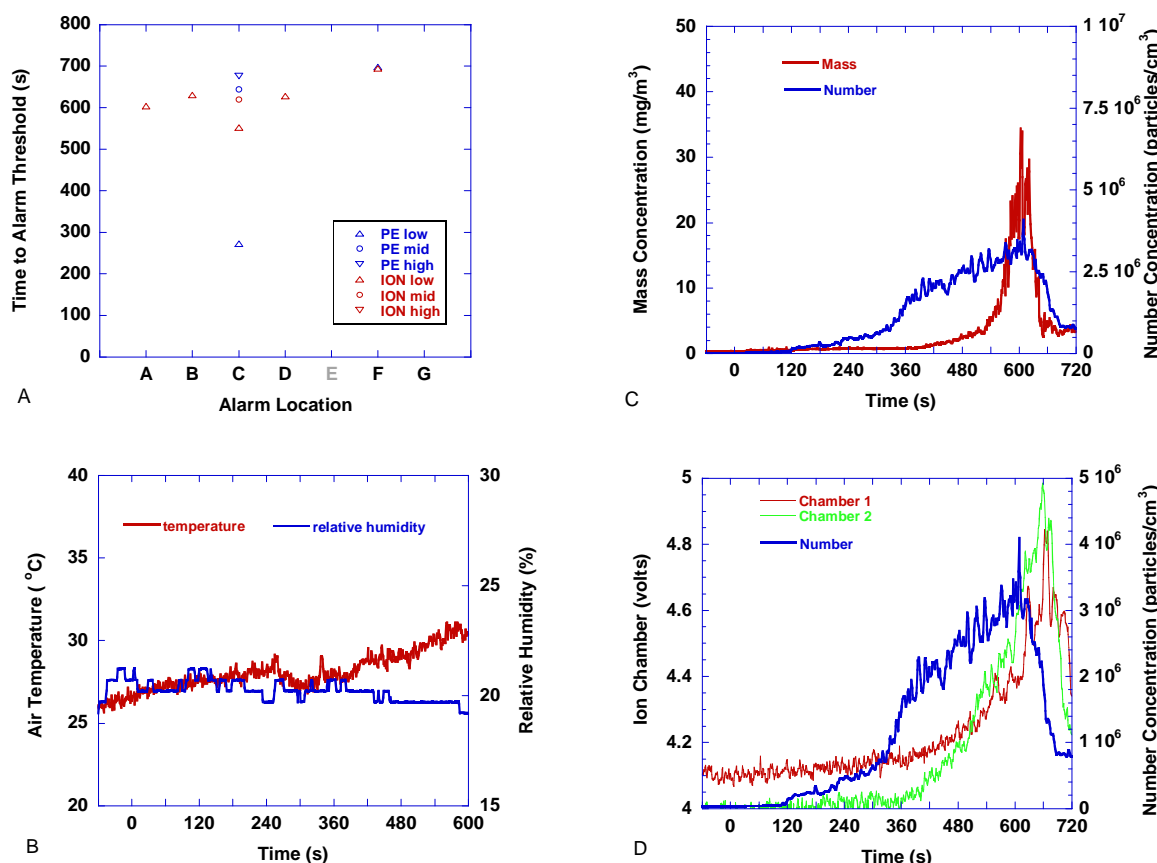


Figure 167. Broiling Pizza - one frozen pizza in oven set on broil, floor fan off. Oven on at t=0

relative humidity. The number concentration starts to rise at 120 s and peaks at 4×10^6 particles/cm³ just before 600 s. The mass concentration starts to rise at 400 s and reaches a peak of 30 mg/m³ at 600 s. The mass concentration increase is attributed to the browning of the cheese layer and small amounts of spatter hitting the broiler heating element. The ion chambers peaked at 600 s at voltage changes of approximately 0.7 V and 1.0 V for chamber 1 and 2 respectively. The voltage curve of chamber 2 does not follow the early rise in the number concentration suggesting that the aerosol produced early in the test was of a size too small to produce any significant ion chamber voltage change.

For the baked, then broiled pizza scenario, the oven was pre-heated to a setting of 176 °C (350 °F). At time t=0 the oven door was opened and one small frozen pizza on the broiler pan was placed in the oven. The pizza was baked for 630 s. During this time the oven door was opened once to visually check the pizza. After 630 s, the oven door was opened to the broil position, the broiler was turned to high, and the pizza was broiled for an additional 10 min. After broiling, the pizza was removed and the oven turned off. This scenario was repeated with the floor fan off and on. Typically, the pizzas were dark brown with some black, but deemed edible.

Figure 168 shows the results for the scenario with the floor fan off. All ionization alarm positions reached at least one threshold level, while only one position reached a photoelectric alarm threshold. The temperature showed two spikes in the baking phase, which were caused by the hot gases escaping the oven during the two periods the door was opened then closed. When the door was opened at the beginning of the broiling phase, the temperature jumped about 5 °C, then continued to rise another 3 °C over the next 600 s. The relative humidity dropped by about 5 % during the broiling phase. Three spikes in the number concentration on the order of (2 to 3 $\times 10^6$) particles/cm³ were observed in the number concentration at the three times the door was opened. By the end of the broiling phase, the number concentration had risen to 4×10^6 particles/cm³. The mass concentration started to climb at about 900 s and peaked at 6 mg/m³ by the end of the broiling phase. Both ion chambers tracked the early number concentration spikes and reached a voltage change of about 1 V for each chamber.

Figure 169 shows the results for the scenario with the floor fan on. During this test, only one ionization alarm reached a threshold value. Spikes in the air temperature were observed at the times the oven door was opened. The temperature rose 6 °C during the test, while the relative humidity fell from 30 % to 25 %. The number concentration also showed spikes when the oven door was opened, and it reached a peak of about 4×10^6 particles/cm³ by the end of the test. The mass concentration started to rise at about 1000 s and peaked with a value of nearly 5 mg/m³ at 1225 s. The ionization chambers followed the number concentration value and they reached peak values of about 0.5 V above their background levels.

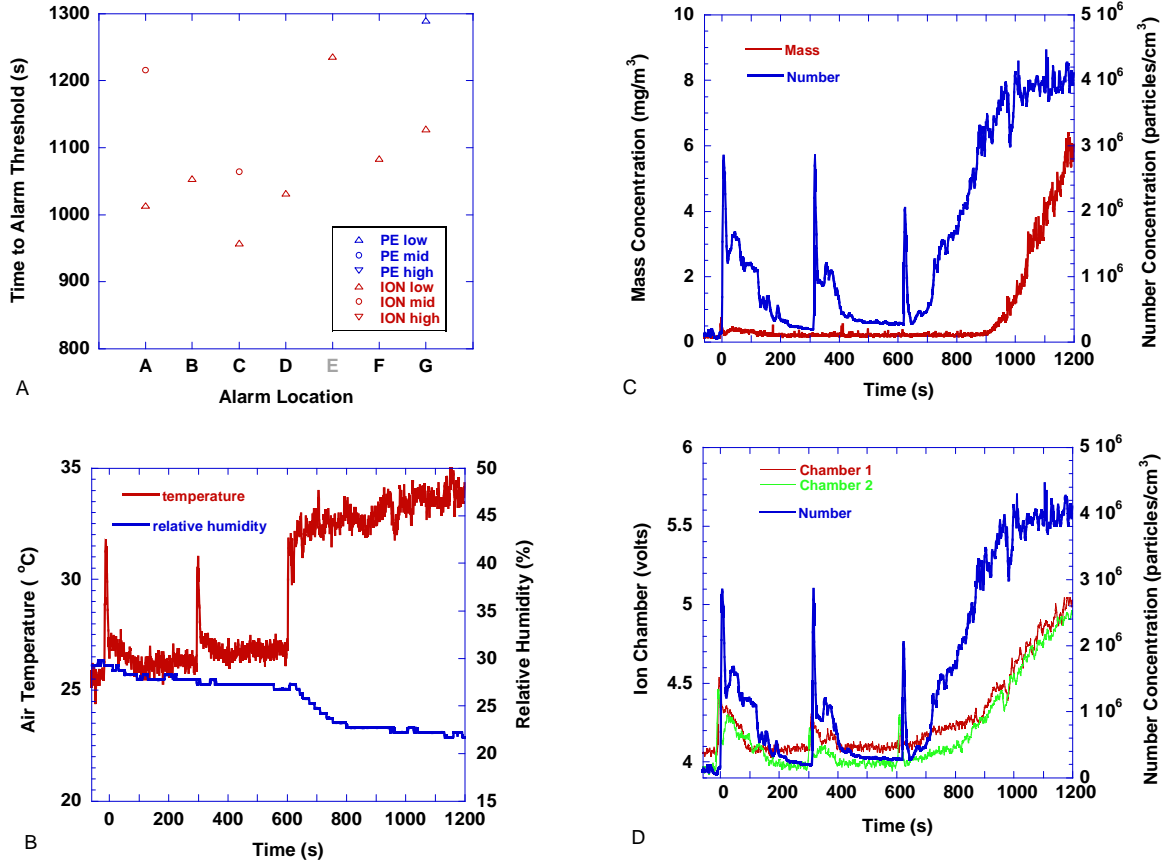


Figure 168. Bake/ broil pizza - one frozen pizza in oven set on bake and pre-heated to 350 °F, then set to broil 630 s later. Floor fan was off. Pizza in at t=0

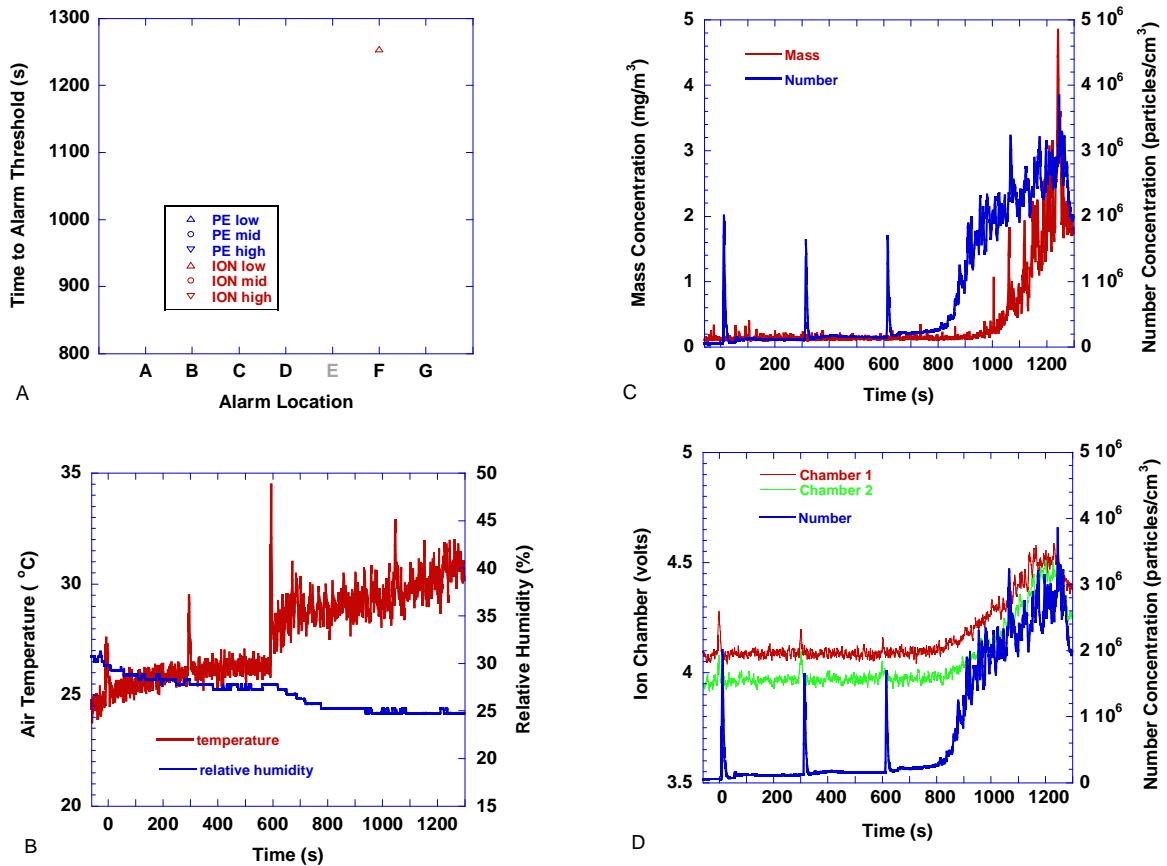


Figure 169. Bake/ broil pizza - one frozen pizza in oven set on bake and pre-heated to 350 °F, then set to broil 630 s later. Floor fan was on. Pizza in at t=0

The following generalizations characterize the broiling, and bake/broil scenarios:

- Every time the pre-heated oven was opened, a wave of heat and small particles spill out. Forced ventilation dilutes this source.
- Ionization alarm thresholds were reached more frequently than photoelectric alarms.
- Aerosol mass concentration is not significant until the cheese starts to brown on the pizzas.
- Forced flow significantly reduced the number of alarm thresholds reached.

6.3.7 Broiling Hamburgers

Four 110 g (quarter pound) frozen hamburgers were placed on an aluminum foil covered broiler pan and placed in the oven. With the oven door open to the broil position, the oven was set to high broil. After 10 min, the hamburgers were flipped, cooked for 5 to 6 min longer, then removed and the oven turned off.

Figure 170 shows the results for the case with the floor fan off. All ionization alarm locations reached alarm thresholds, while four out of six photoelectric alarms reached thresholds. Four ionization thresholds were reached before the hamburgers were flipped at 600 s. The air temperature started to rise at 200 s and climbed steadily to about 6 °C above the ambient temperature. The relative humidity did not change appreciably. The number concentration started to rise at about 200 s and reached a peak of about 4×10^6 particles/cm³ by the end of the test. The mass concentration started to rise at 500 s and reached a peak value of about 25 mg/m³ near the end of the test. The ionization chambers followed the number concentration and reached peaks about 1 V above the initial values.

Figure 171 shows the results for the case with the floor fan on. All of the ionization alarms reached thresholds, while five out of 6 photoelectric alarms reached thresholds. The air temperature climbed about 3 °C except for a short spike near the end of the test. The relative humidity remained at the initial value. The number concentration started to rise at 200 s and reached a peak at 800 s of nearly 5×10^6 particles/cm³. The mass concentration started to rise at about 400 s and between 800 s and 1000 s reached spiked to about 15 mg/m³. Ionization chamber 2, which is closer to the source, started to rise at about 200 s, while chamber 1 started to rise at about 300 s. Chamber 2 voltage showed two peaks at 600 s and 800 s corresponding to peaks in the number concentration. By the end of the test, chamber 1 voltage had rise by about 0.9 V and chamber 2 had risen by about 1.1 V.

The following generalizations characterize the broiling hamburger tests:

- More ionization alarm thresholds were reached than photoelectric thresholds.
- The forced airflow case saw more photoelectric alarm locations reaching thresholds than the no forced flow case.
- Number concentration in both tests started to increase 200 s before an appreciable rise in the mass concentration, suggesting smaller particles being produced in the early cooking stage.

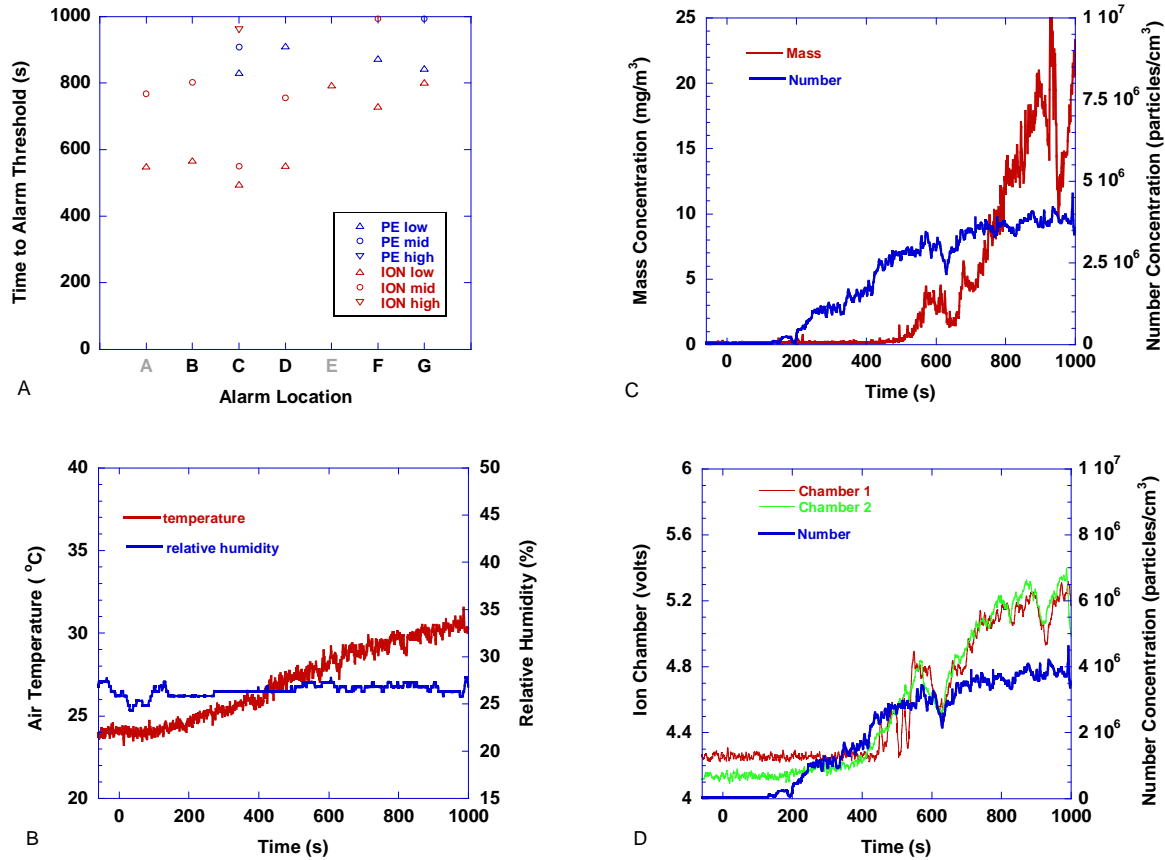


Figure 170. Broiling hamburgers - four hamburgers in oven set on broil, floor fan off. Oven on at t=0

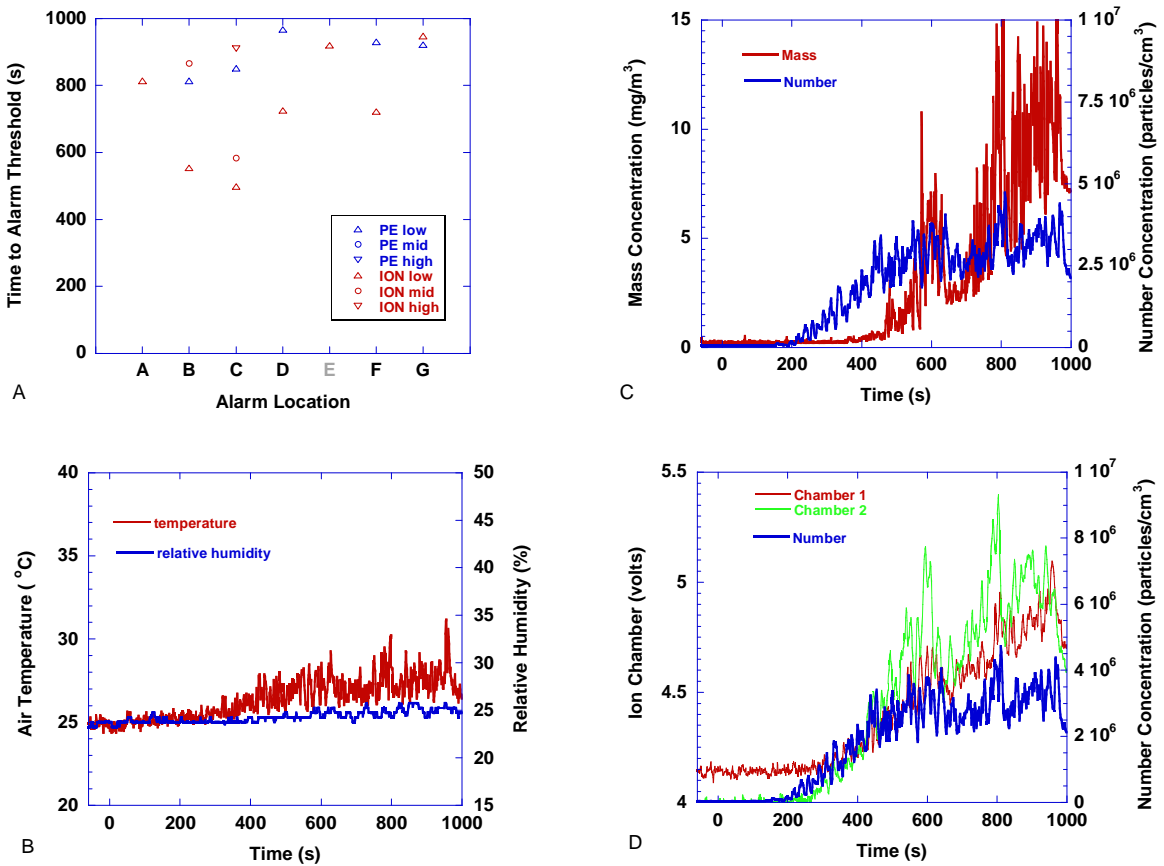


Figure 171. Broiling hamburgers - four hamburgers in oven set on broil, floor fan on. Oven on at t=0

6.3.8 Boiling Spaghetti Pasta

In a “two quart” non-stick pot of boiling water, between 1/3 and 2/3 of a 454 g (1 lb) package of dry spaghetti pasta was cooked for 10 min to 13 min. The water-filled pot was placed on the large electric burner element. The burner was set on high and, after the water began to boil, the pasta was added. In one variation, a tight-fitting lid was placed on the pot with the intention of causing the boiling water to spill over.

Figure 172 shows the results for the case with 1/3 package of spaghetti. A single ionization alarm threshold was reached at the location nearest to the source. The air temperature rose about 5 °C during the course of the test. The relative humidity rose from an initial value of 17 % to

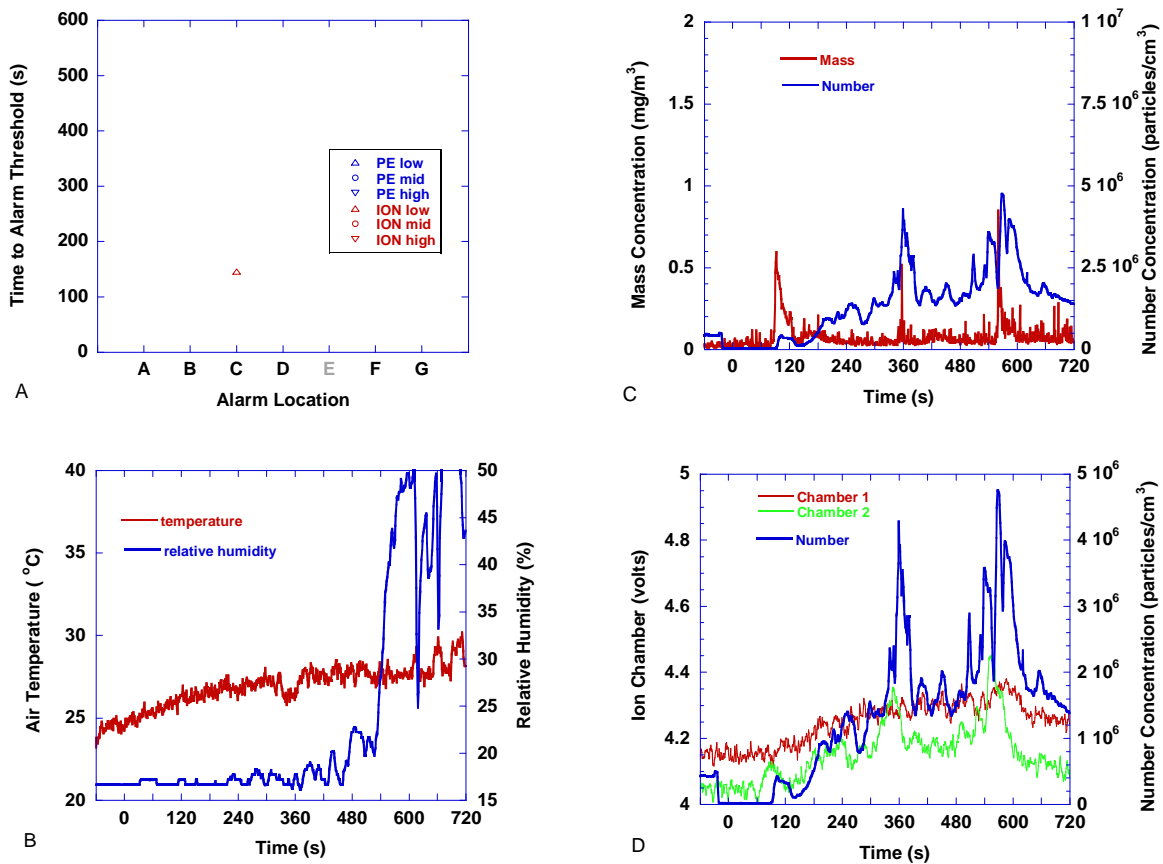


Figure 172. Boiling spaghetti pasta - 1/3 package (150 g), floor fan off.
Pasta placed in pot at t=360 s

over 50 % during the test. The number concentration started to climb at 120 s reaching a peak of 4×10^6 particles/cm³ when the pasta was added, followed by another peak of 5×10^6 particles/cm³ at 560 s. The mass concentration shows a spike at 100 s possibly due to material on the burner element being driven off. There was a spike at 360 s when the pasta was added, and again a spike at 560 s; all spikes were below 1 mg/m³. Ionization chamber 2 followed the number concentration trend, peaking at 360 s and 560 s, with a maximum value of 0.4 V above the initial value. Chamber 1 increased about 0.2 V above its initial value.

Figure 173 shows the results for the case with 2/3 of a package of pasta. Only one ionization threshold was met at the location closest to the source, before the pasta was added. The temperature and relative humidity trends were the same as observed in the test above. The number concentration started to rise at about 180 s, reaching a plateau at 360 s of 1.5×10^6 particles/cm³, then spiking to a value of 3.7×10^6 particles/cm³ at 610 s. The mass concentration

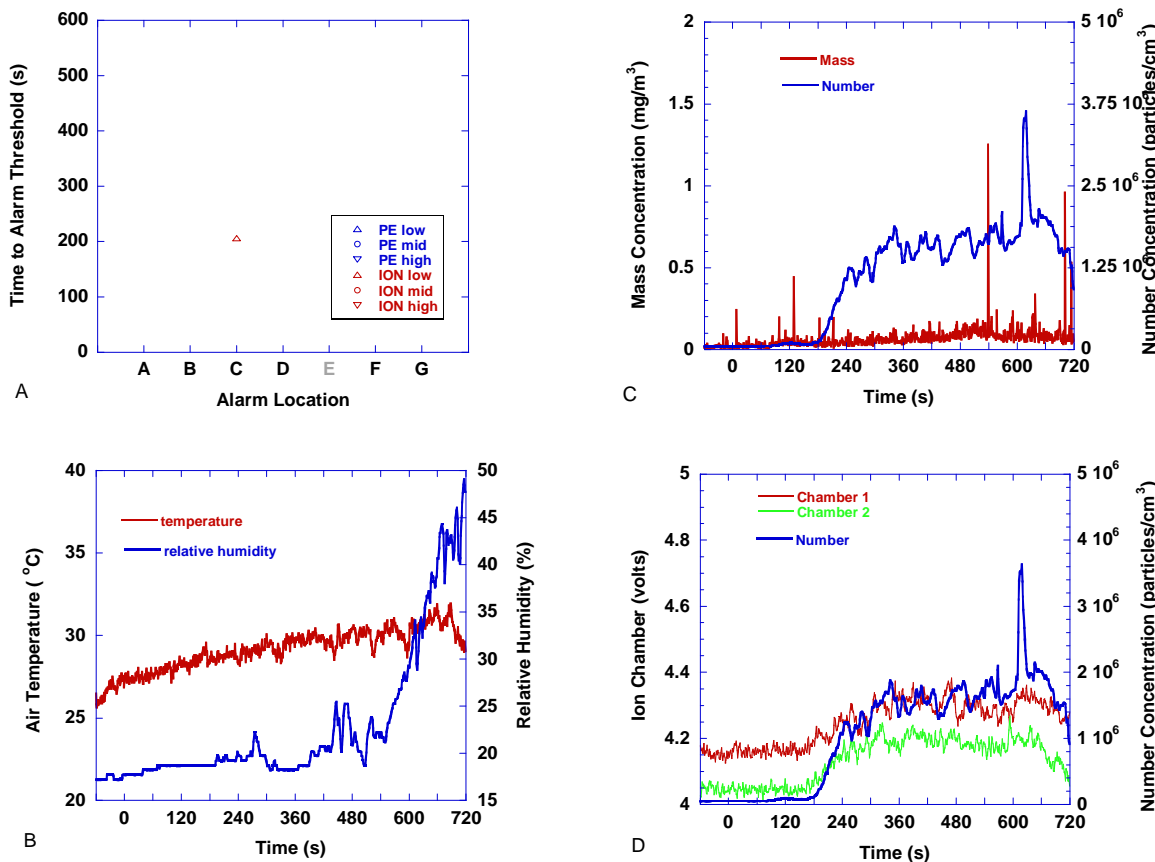


Figure 173. Boiling spaghetti pasta - 2/3 package (300 g), floor fan off.
Pasta placed in pot at $t=450$ s

showed only one spike greater than 1 mg/m^3 at 540 s. The ionization chambers followed the number concentration trend (except for the spike at 610 s.) Chamber 1 and 2 increased approximately 0.1 V and 0.2 V above their initial values, respectively.

Figure 174 shows the results for the case with 1/2 of a package of pasta cooked with the lid on. Only one ionization alarm reached a threshold, the alarm located closest to the source, 120 s after the pasta was added. The number concentration started to rise at 100 s climbing to a average value of $2.5 \times 10^6 \text{ particles/cm}^3$ by 400 s. At 625 s the number concentration spiked to nearly $5 \times 10^6 \text{ particles/cm}^3$, then dropped to about $2 \times 10^6 \text{ particles/cm}^3$. This spike is attributed to boil-over of the pot. The mass concentration, though elevated to about 0.5 mg/m^3 initially, experienced only one peak above 1 mg/m^3 at 530 s. The lid was removed at 940 s. Its removal did not appear to change room conditions.

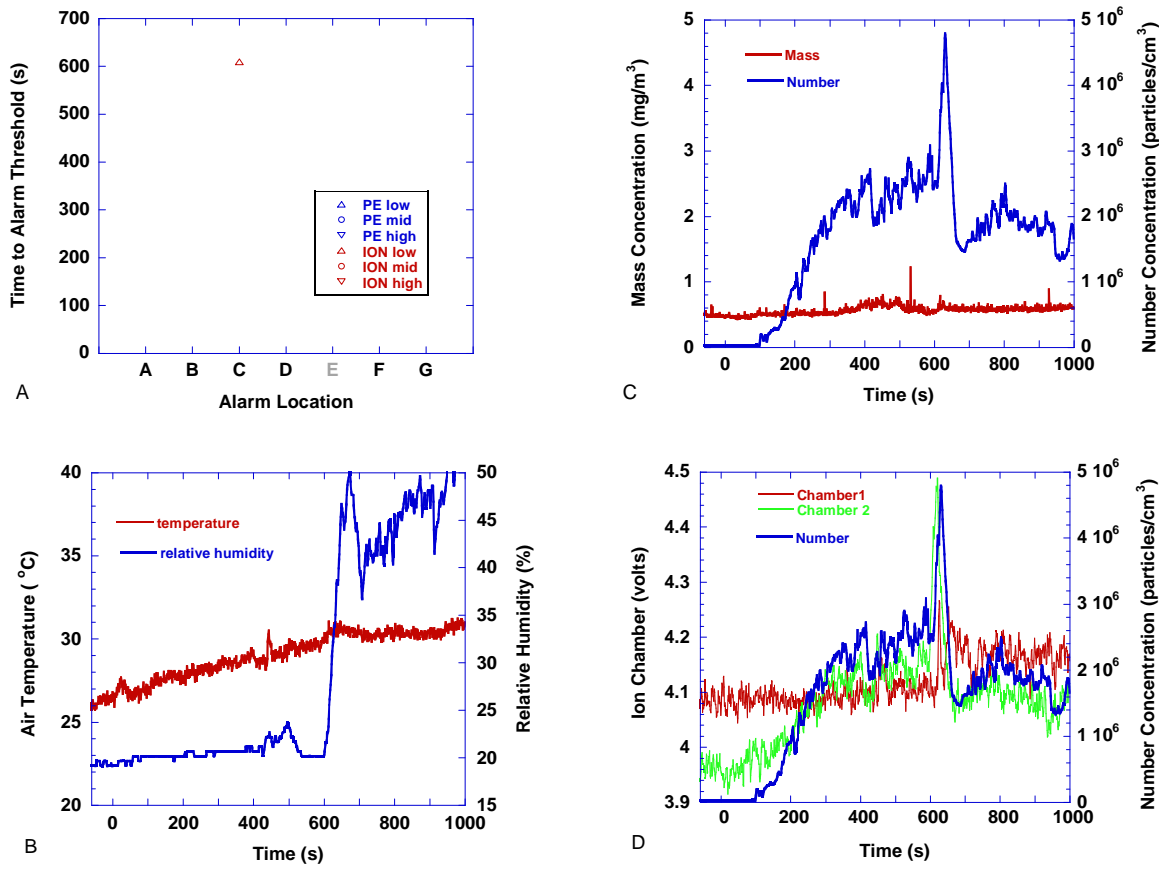


Figure 174. Boiling spaghetti pasta - 1/2 package (225 g), lid on, floor fan off.
Pasta placed in pot at $t=480$ s

Since only one alarm threshold was reached in each test, and all attributed to the alarm closest to the source, this scenario was not particularly challenging. However, the aerosol measurements do suggest that the electric heating element on a high setting produces aerosols. It is assumed that the cleanliness of the element and the pan surface in contact with it affect this aerosol production. In general, the boiling of the pasta in and of itself did not account for much aerosol production unless boil-over of the pot occurs, in which case the pasta water splashing on the hot surfaces appears to cause more aerosol formation.

6.3.9 Candle Burning

Four scented tea candles were placed on the counter top to the right of the stove and lit with a butane lighter. The candles burned for 15 min, then they were extinguished. There was no forced flow during this test.

Figure 175 shows the results for this test. No alarm thresholds were reached during this test. Since there was no forced airflow, the candle flames were laminar, with no flickering. Air temperature rose about 2 °C, and the relative humidity dropped by about 2 % during the test. The number concentration spiked at about 50 s to 5×10^5 particles/cm³, which is attributed to the butane lighter and the candle ignitions. Around 300 s the number concentration rose sharply for 1×10^5 particles/cm³ to 6×10^5 particles/cm³. This steep rise is most likely due to the ceiling jet

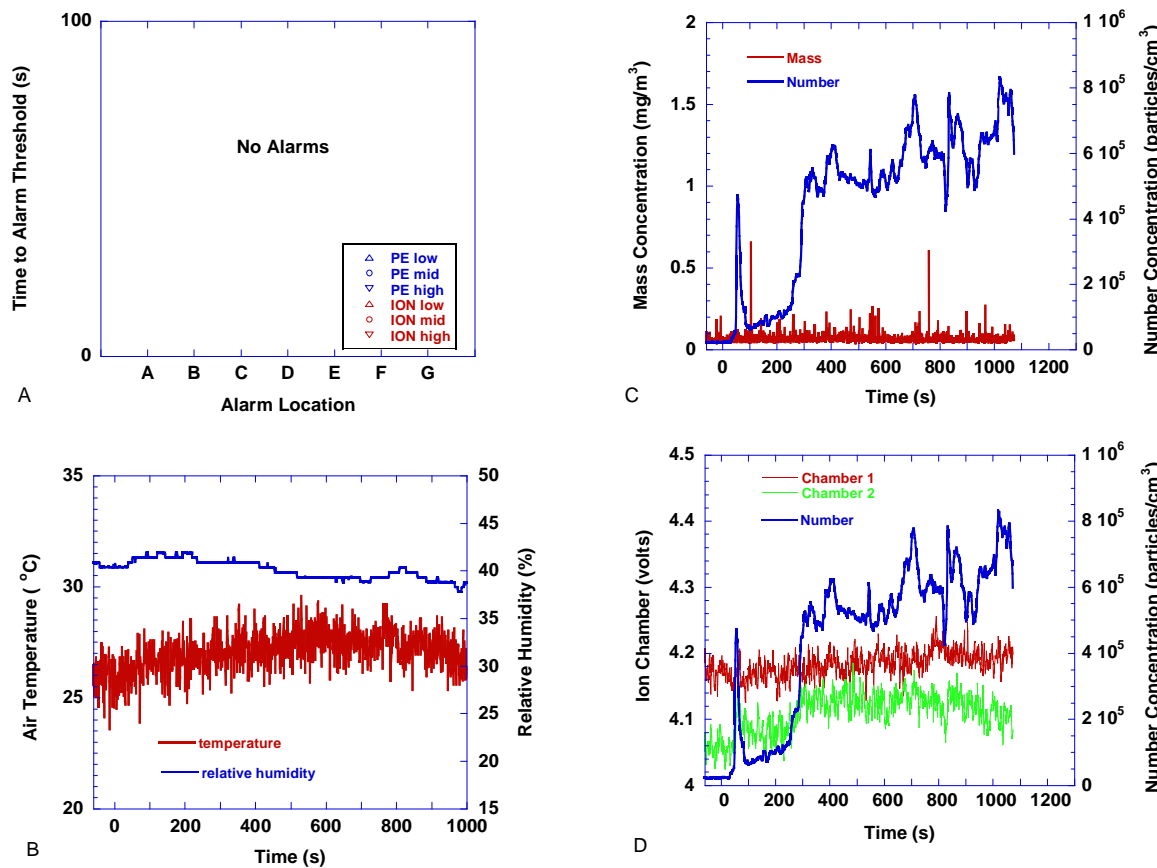


Figure 175. Candles burning - four tea candles burning on electric range top area.
Floor fan was off. Candles lit at t=0

from the plume formed by the burning candles reaching the aerosol sampling location. The number concentration peaked at about 8×10^5 particles/cm³ near the end of the test. No appreciable mass concentration was recorded; two spikes are attributed to local airborne dust or other background aerosol. Ionization chamber 2 voltage rose about 0.1 V above its initial value, while, chamber 1's voltage rose by a factor of 3 less.

Clearly, this scenario poses little threat for producing nuisance alarms. It is not clear if flickering candle flames or the presence of additives in the candles would produce enough aerosol to be a significant nuisance alarm threat.

6.3.10 Cigarette Smoking

Two persons seated in the kitchen area proceeded to smoke one cigarette each. In approximately 4 min, the smokers finished their cigarettes and exited the manufactured home, closing the door behind them. In both tests, there was no forced air flow.

Figures 176 and 177 show the results for these two tests. In the first test, no alarm thresholds were reached, while in the second test, the ionization alarm located nearest to the smokers did reach two thresholds near the end of the smoking period. Little change in air temperature or relative humidity was observed during both tests. The maximum number concentration reached was 1.45×10^5 particles/cm³ and 8.5×10^4 particles/cm³ for the first and second test. Mass concentration peaks of 2.5 mg/m^3 and 3 mg/m^3 were recorded in the first and second tests. Neither ionization chamber voltage changed significantly from the background mean values during both tests.

It is surprising that the ionization alarms were recorded during the second test, while no indications of a significant level of aerosol was recorded by the particle counter nor ionization chamber 2. The mass concentrations during both tests appear to be approaching threshold levels for photoelectric alarms, suggesting repeated smoking, or more smokers could produce threshold level values.

6.4 Controlled Incipient Fire Sources

The following incipient fire sources were performed to provide comparative results and put the nuisance alarm tests into context with the FE/DE tests. The cotton smolder and pyrolyzing wood blocks tests, are variants of EN 54 fire sensitivity test sources. The cotton smolder source was the same as used for the FE/DE tests discussed in Chapter 2. Thus, these data are mainly useful to determine the differences in detector response due to the layout of the building and resulting flow patterns during the tests. In addition, the data show the detector responses at various locations throughout the manufactured home.

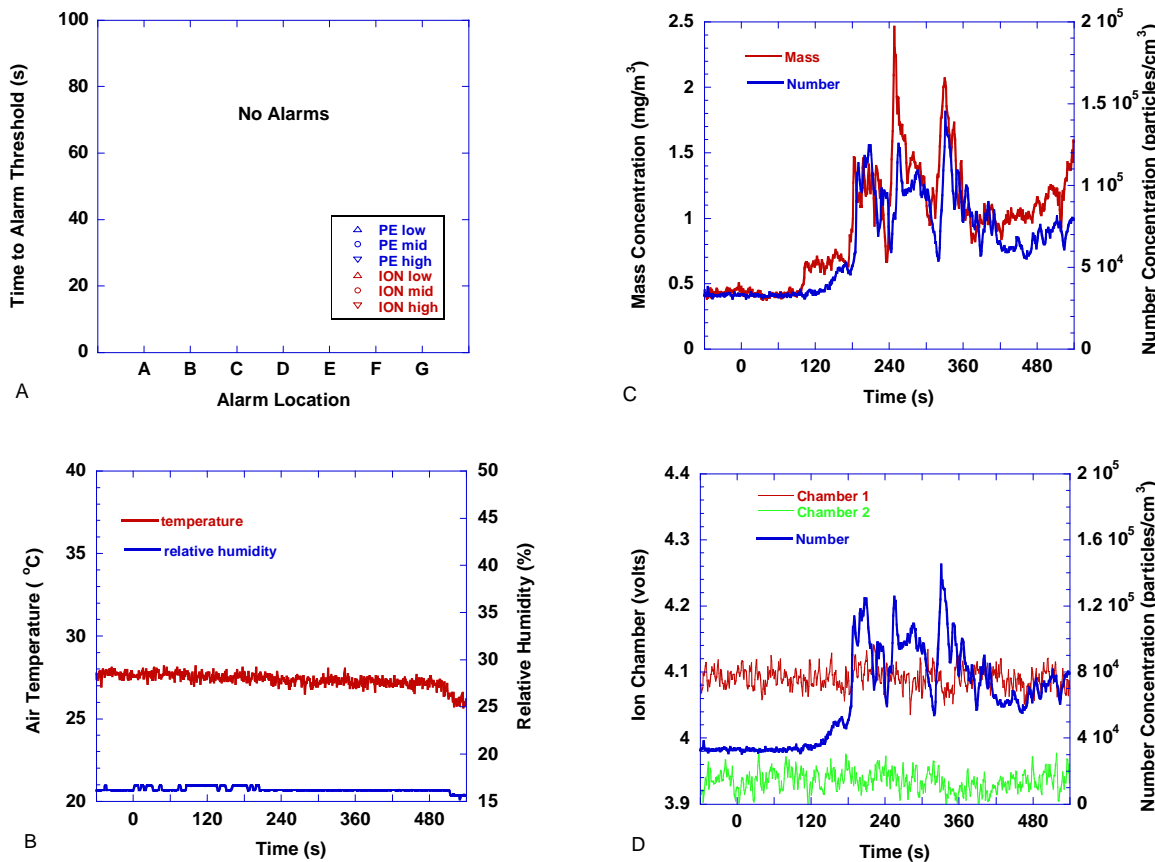


Figure 176. Cigarette smoking - two smokers smoking one cigarette each in kitchen area.
Floor fan was off. Cigarettes lit at t=0

6.4.1 Cotton Smolder

The staged wick ignition device was used to produce cotton smolder smoke. This is the same source used in the FE/DE to calibrate all of the modified analog output smoke alarms. 32 cotton wicks were placed in the staged wick ignition device, which was then set on the chair-burn load cell pan located in the living room area. After an initial 30 s delay, 8 sets of 4 wicks were ignited with a 12 s delay time between sets. The wicks smoldered for 30 min then the doors to the manufactured home were opened. The test was run with the floor fan off and repeated with the floor fan on.

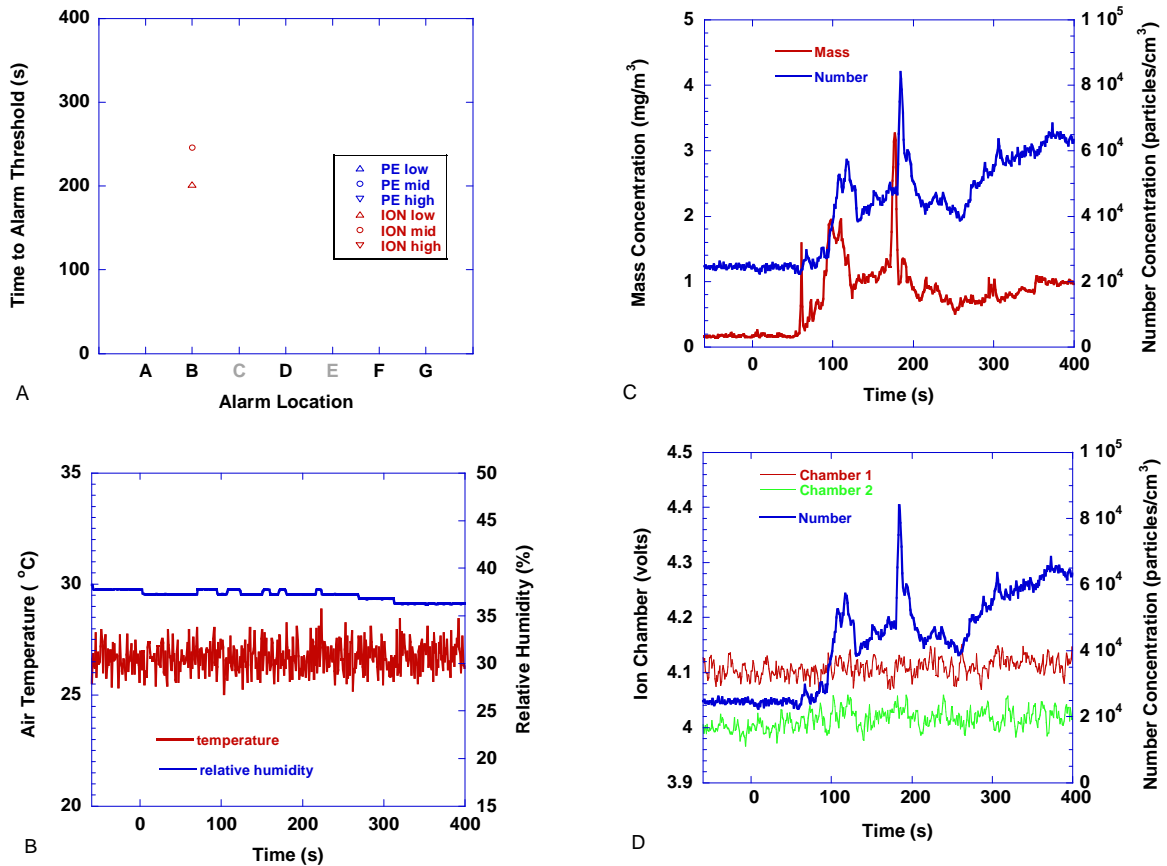


Figure 177. Cigarette smoking – two smokers smoking one cigarette each in kitchen area. Floor fan was off. Cigarettes lit at $t=0$

Figure 178 shows the results for the case with the floor fan off. All ionization alarms reached threshold levels, and all but one before 300 s. Five out of six photoelectric alarms reached threshold levels, the two closest to the source (location B) reached thresholds sooner. The air temperature rise was about 1°C , while the relative humidity dropped about 3%. The mass and number concentration both start to rise at 120 s and reach local peak values before 300 s of $30 \text{ mg}/\text{m}^3$ and $1.2 \times 10^6 \text{ particles}/\text{cm}^3$. The wick smoldering rate is highest soon after ignition. After a wick smolders away from its ignition coil smoldering proceeds at a steady rate reaching values of approximately $35 \text{ mg}/\text{m}^3$ and $1.25 \times 10^6 \text{ particles}/\text{cm}^3$. The early peaks in the number and mass concentrations are due the higher smoldering rates of the wicks soon after ignition. After dropping from the peak values, the number and mass concentration continued to climb for the duration of the test. The ionization chamber voltages followed the number concentration results,

realizing the early peak, then climbing for the remainder of the test. By the end of the test, the voltage change for each chamber was nearly 1 V.

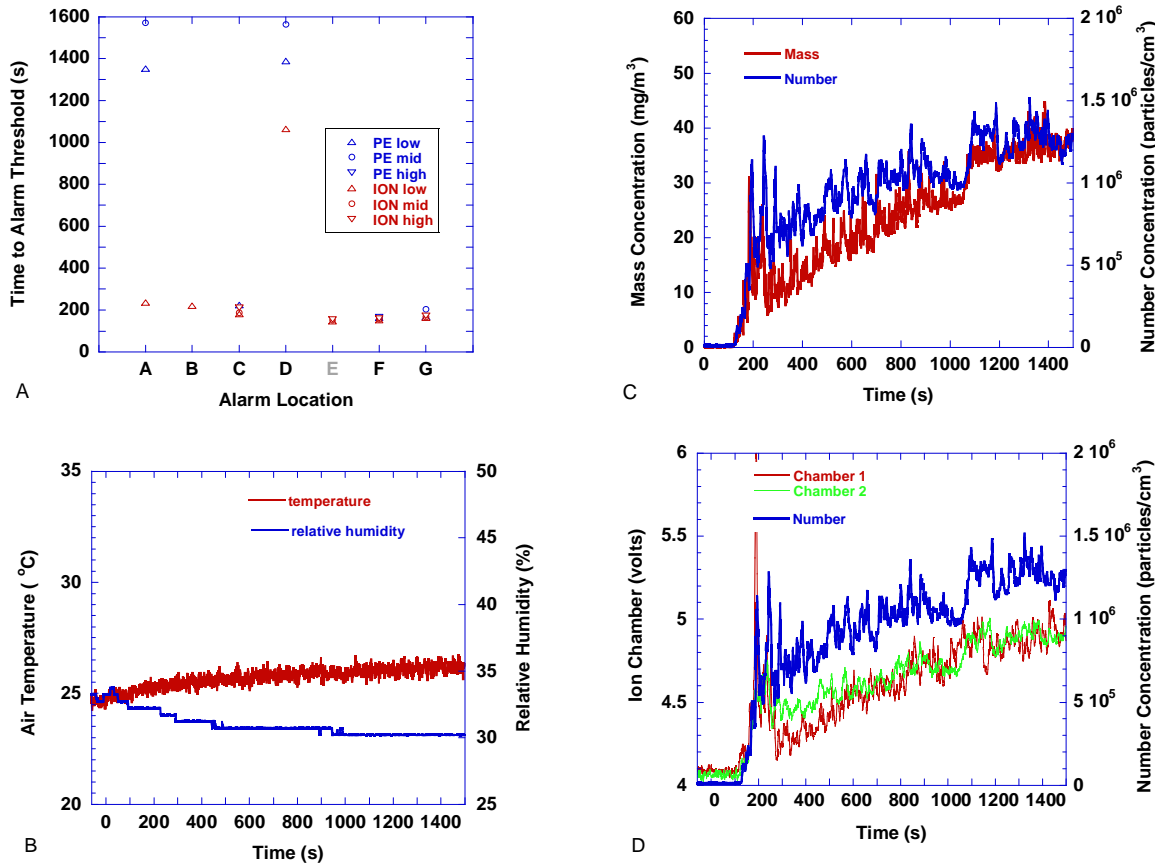


Figure 178. Smoldering cotton wicks – eight sets of four wicks were ignited with a 12 s delay using the staged wick ignition device, located on the living room floor at the chair burn location. Fan was off. Ignition sequence started at t=30 s

Figure 179 shows the results for the case with the floor fan on. Again, all ionization alarms reached threshold levels. There is clearly a relationship between the time to reach a threshold and the distance from the source; alarms closer to the source reach threshold levels first. Only three photoelectric alarms reached threshold levels, with the alarm closest to the source (F) reaching it first. The air temperature rose by about 2 °C and the relative humidity dropped by about 5 % during the test. Contrary to what was observed in the smoldering wick test without forced flow, there were no early peaks in the mass or number concentration. At 100 s the mass and number concentration start to rise. From 300 s to the end of the test, the mass concentration increased linearly to 36 mg/m³, while the number concentration increased towards an asymptote

of approximately 1.1×10^6 particles/cm³. Initially, the ionization chambers follow the number concentration trend, but from 800 s on they continue to climb while the number concentration starts to level off. This observation, along with the steady rise in the mass concentration suggests that the mean particle size was increasing during the test.

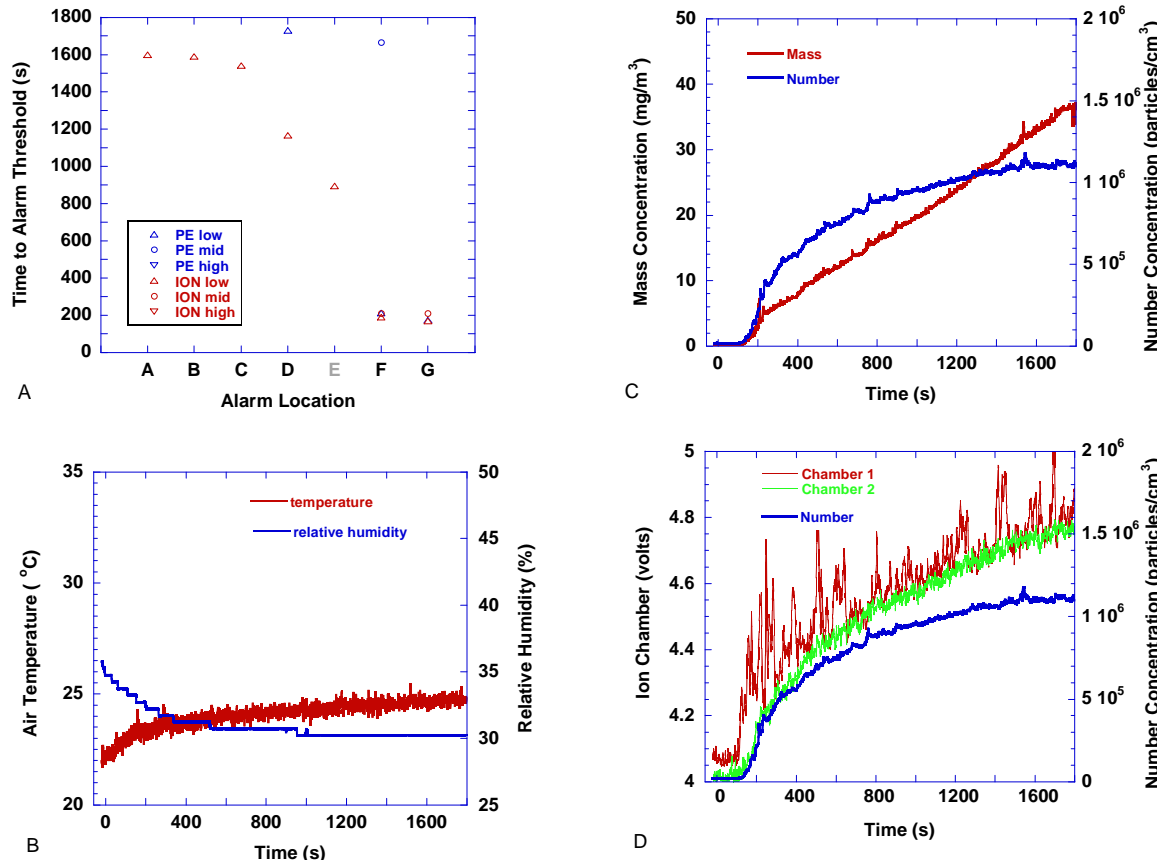


Figure 179. Smoldering cotton wicks -eight sets of four wicks were ignited with a 12 s delay using the staged wick ignition device, located on the living room floor at the chair burn location. Fan was on. Ignition sequence started at t=30 s

The following generalizations characterize the smoldering cotton scenarios:

- Ionization alarm thresholds were reached earlier and at more locations than photoelectric alarm thresholds.
- The mass and number concentration by the end of the test were nearly the same for both cases.

- A somewhat counterintuitive observation that in the case with the floor fan on, the time to reach a threshold level for ionization alarms was a strong function of the distance from the source, while in the case with the floor fan off, the time to reach ionization threshold levels occurred nearly simultaneously for six of seven alarms.

6.4.2 Wood Smolder

Eight 3.5 cm x 2.0 cm x 1.0 cm beech wood blocks were placed on a 750 W electric hot plate that was placed on the chair-burn load cell. Full power was applied to the hot plate. Within about 500 s, the blocks started to pyrolyze. After 20 min, the power to the hot plate was removed. The test was performed with the floor fan off and repeated with the floor fan on.

Figure 180 shows the results for the case with the floor fan off. All six photoelectric alarms reached threshold values, with the ones closer to the source tending to reach thresholds first. Four out of seven ionization alarms reached threshold values, and where three were collocated with photoelectric alarms, the ionization alarms took longer to reach threshold values. Only a very slight increase in air temperature, and decrease in relative humidity was observed. The number concentration started to rise at 550 s, while the mass concentration started to rise appreciably at 700 s. The number concentration peaked at about 1×10^6 particles/cm³ at 1350 s while the mass concentration reached a peak of about 65 mg/m³ at 1200 s. The ionization chambers followed the rise in number concentration, and reached voltage change peaks of 0.7 V.

Figure 181 shows the results for the case with the floor fan on. Five out of six photoelectric alarms reached threshold values, the one farthest from the source did not. Four out of seven ionization alarms reached threshold values, again, after photoelectric thresholds were met. Similar to the test above, only a very slight increase in air temperature, and decrease in relative humidity was observed. The number concentration started to rise at 500 s, peaking at 4×10^5 particles/cm³, while the mass concentration started to rise at 700 s, peaking at 38 mg/m³. Ionization chamber 1 started to rise noticeably at 800 s, and peaking at about 1 volt above the initial voltage at 1250 s. Chamber 2 started to rise at 1000 s and peaked 0.3 V above the initial voltage at 1500 s.

The following generalizations characterize the smoldering wood blocks tests:

- Photoelectric alarms reached thresholds earlier and at more locations than ionization alarms.
- The relatively high mass concentration and low number concentration levels suggest a mean particle size larger than the smoldering cotton source.

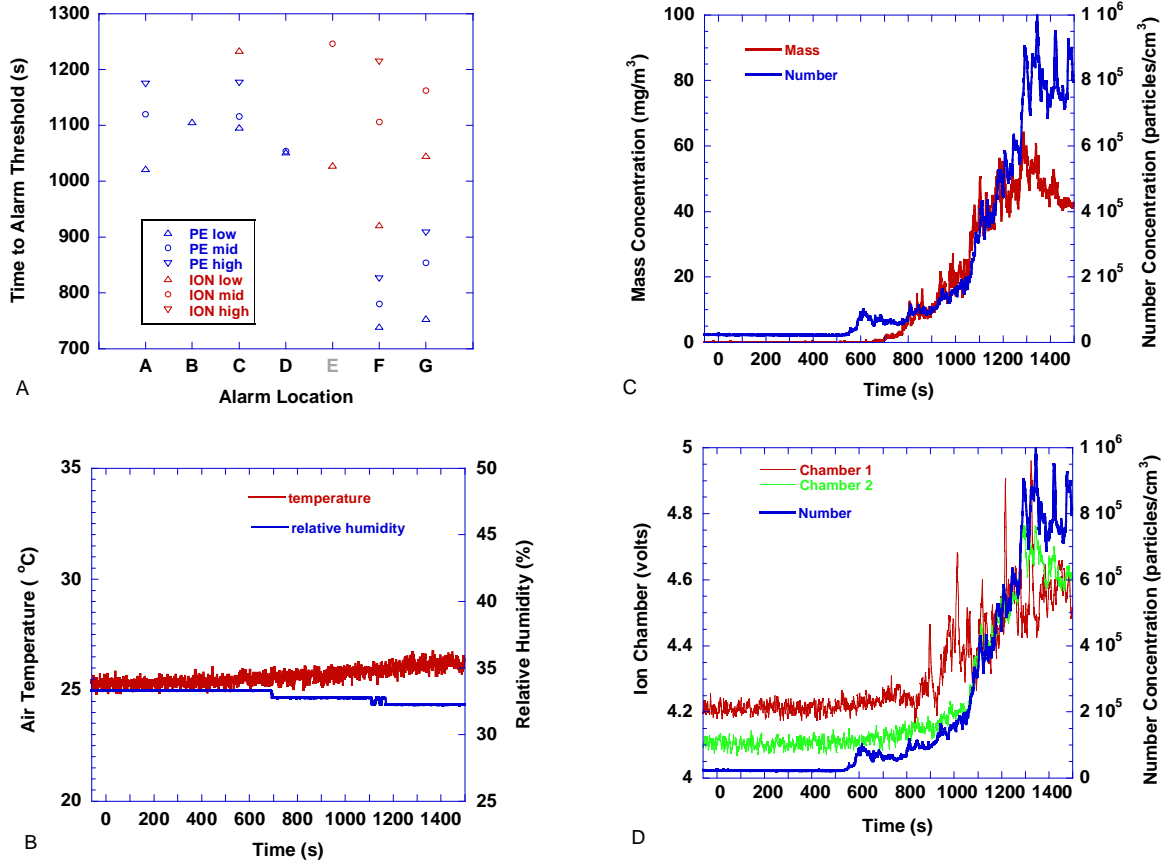


Figure 180. Smoldering wood blocks - eight beech wood blocks on an electric hotplate, located on the living room floor at the chair burn location. Fan was off. Power to hotplate on at t=0

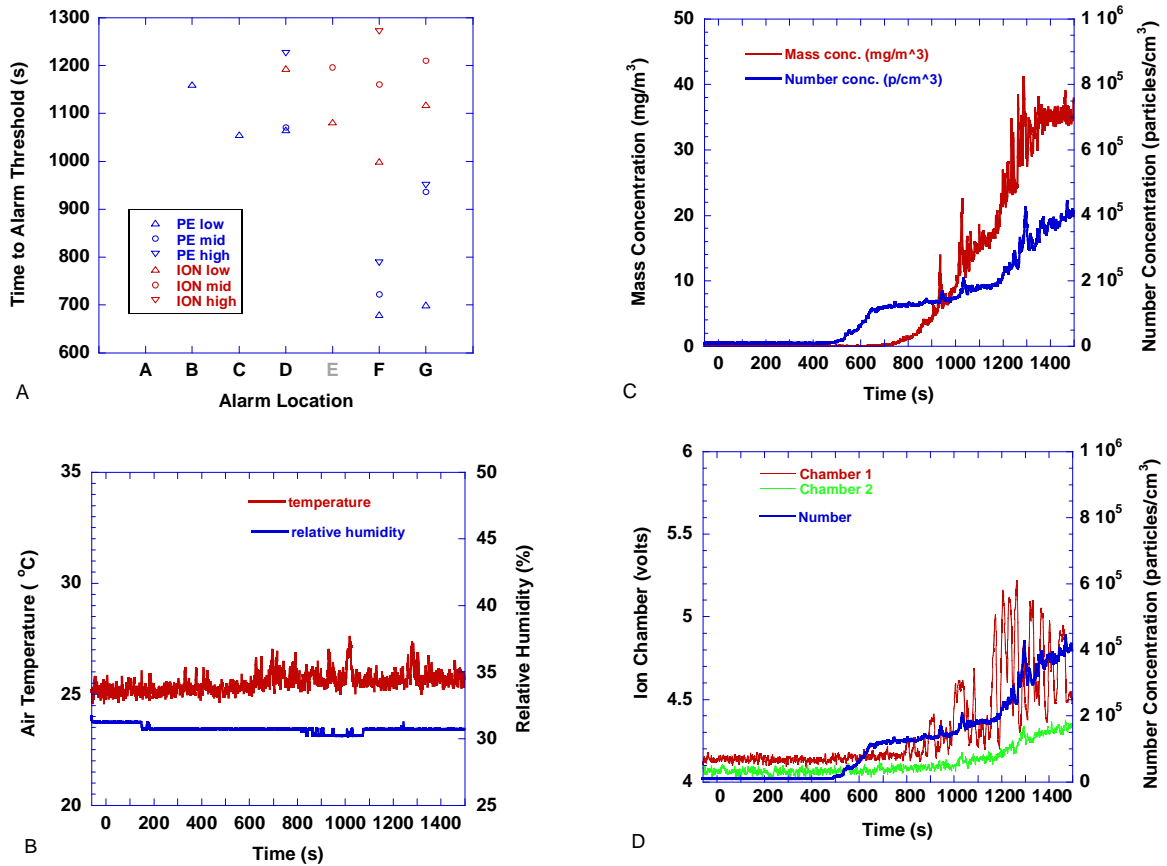


Figure 181. Smoldering wood blocks - eight beech wood blocks on an electric hotplate, located on the living room floor at the chair burn location. Fan was on. Power to hotplate on at t=0

6.4.3 Polyurethane Foam Smolder

Blocks of polyurethane foam, (approximately 8 cm x 8 cm x 10 cm) were removed from a chair cushion of the same type used in the smoldering chair fire scenario in the Home Smoke Alarm tests. A single block was used in each smolder test. A slit was made in the foam at the center of the 10 cm high block, and a nichrome heating wire (similar to the one used to ignite the chairs for the smoldering fire tests) was inserted. Electric power was applied to the wire to cause the foam block to smolder in the same manner as the fire tests discussed in section 3.3.2.

Smoldering was allowed to proceed for approximately 15 min. The test was repeated three times with the floor fan off and once with the floor fan on.

Figure 182 shows the results for the first test run with the floor fan off. Several photoelectric alarm thresholds were reached between 200 s and 400 s. Around 800 s all alarm thresholds were reached, this corresponded to a transition from smoldering to flaming of the foam block. The air temperature rose slightly until about 800 s where it rapidly rose by 10 °C following flaming of the foam. The flaming period was short lived due to the limited amount of material to burn, and the temperature dropped over the next 100 s. The relative humidity dropped by about 5 % during the test. The mass concentration started to rise at 100 s, and by 250 s reached a local peak of nearly 40 mg/m³. By 500 s it had dropped down to about 10 mg/m³, then started rising slowly again until 800 s when it rapidly shot up to a peak greater than 150 mg/m³. The number concentration started to rise at 100 s and by 300 s had reached a value of 1×10^5 particles/cm³, and remained steady until 800 s when it rapidly increased to a value of 4×10^6 particles/cm³. The ionization chambers showed an increase of 0.1 V from 100 s to 200 s. They remained unchanged until 800 s when they shot up rapidly by over 2 V.

Figure 183 shows the results for the second test run with the floor fan off. Two photoelectric alarms reached threshold values before 200 s, but no other alarms did. The block of foam initially smoldered vigorously, but as time went on, it apparently stopped. The test was stopped at 800 s. The air temperature rise was on the order of 2 °C, while the relative humidity dropped by about 5 %. The mass concentration started to rise at 100 s and reached a nominally steady value of 6 mg/m³ at 400 s. The number concentration started to rise at about 80 s and reached a maximum value of 9×10^4 particles/m³ by the end of the test. During the test, the increases in the ionization chambers voltages were 0.2 V and 0.05 V for chamber 1 and 2 respectively.

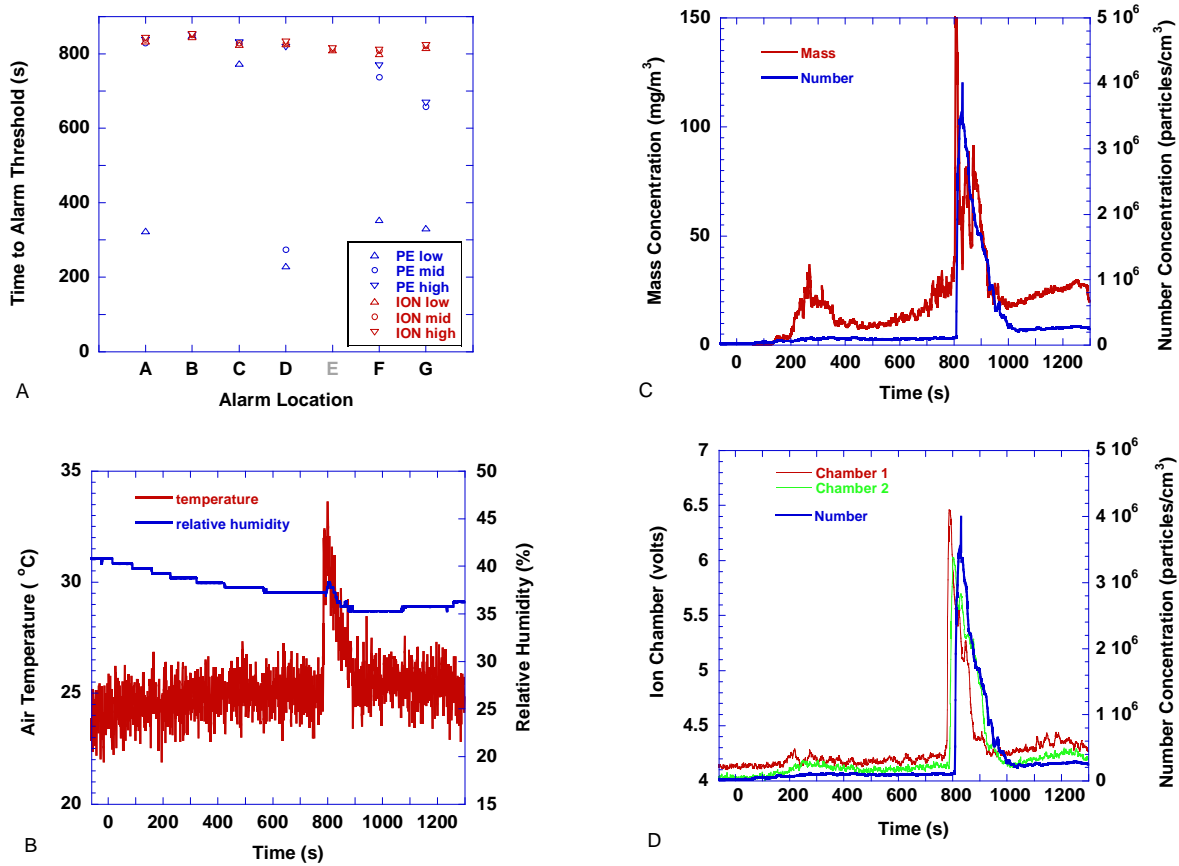


Figure 182. Smoldering foam - A polyurethane foam block, located on the living room floor at the chair burn location and ignited with an electrically powered nichrome wire heater imbedded in the block. Fan was off. Power to igniter on at $t=0$. Sample flamed at 798 s

Figure 184 shows the results for the third test run with the floor fan off. Three out of six photoelectric alarms reached threshold values, the three closest to the source. Air temperature rise was on the order of a couple of degrees Celsius, while the relative humidity dropped by about 5 % during the test. The mass concentration started to rise steadily at 100 s and reached a plateau of 13 mg/m^3 at 700 s. The number concentration started to increase around 50 s and reached a plateau of almost $6 \times 10^4 \text{ particles/cm}^3$ by 600 s. The spike in the mass concentration and number concentration just after the 600 s mark could be due to a transient flame inside the foam block. Flashing flames were observed in lab tests during smoldering of this chair foam. Sometimes the flashing led to sustained flaming, and sometimes not. Almost no change in either ionization chamber voltage was observed.

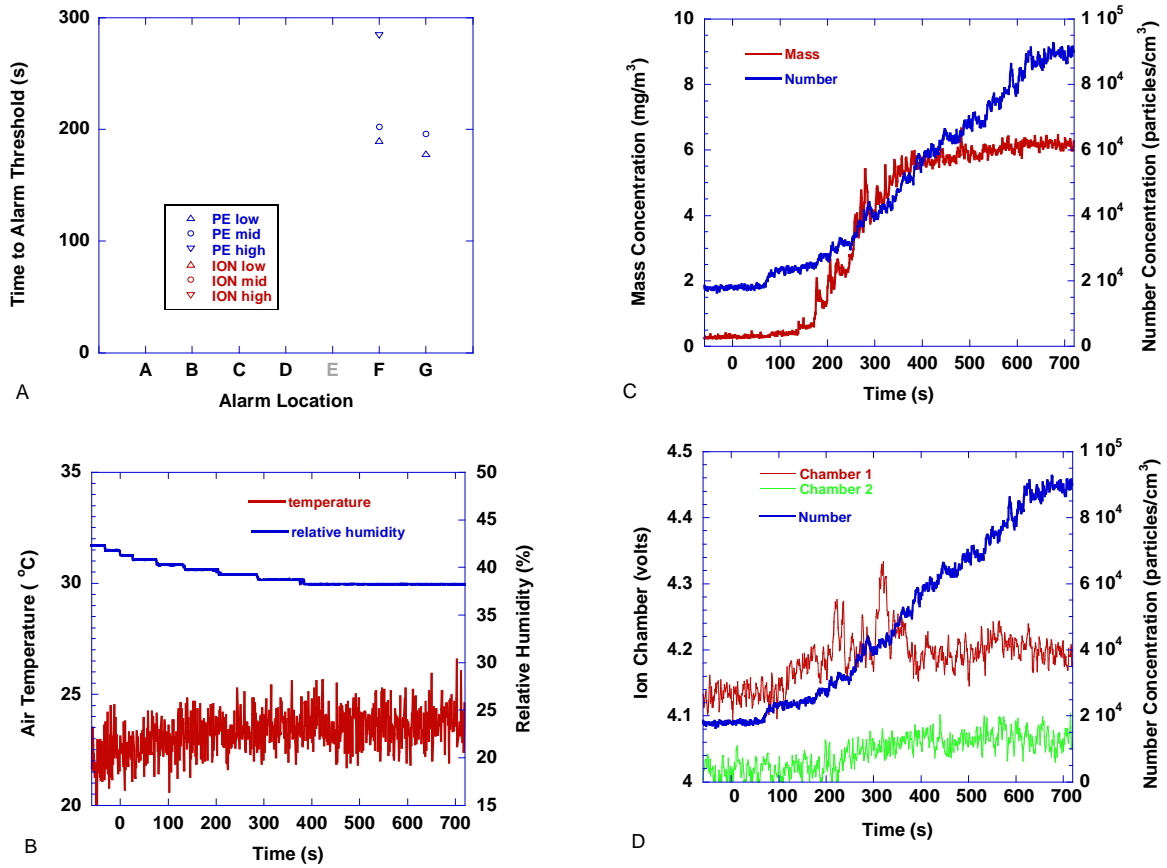


Figure 183. Smoldering foam - a polyurethane foam block, located on the living room floor at the chair burn location and ignited with an electrically powered nichrome wire heater imbedded in the block. Fan was off. Power to igniter on at t=0. Sample stopped smoldering

Figure 185 shows the results for the test run with the floor fan on. The three photoelectric alarms closest to the source reached threshold values, no other alarms did. Same as the last test, the air temperature rise was on the order of a couple of degrees Celsius, while the relative humidity dropped by about 5 %. The mass and number concentration both started to rise around 50 s. The mass concentration reached a peak of about 30 mg/m^3 at 260 s, while the number concentration reached a peak of $1.8 \times 10^5 \text{ particles/cm}^3$ at 360 s. By 500 s both mass and number concentration had leveled off to nearly steady values of 5 mg/m^3 and $1 \times 10^5 \text{ particles/cm}^3$ respectively. Ionization chambers reached peak values between 200 s and 300 s, with voltage rises of 0.15 V and 0.2 V for chambers 1 and 2 respectively.

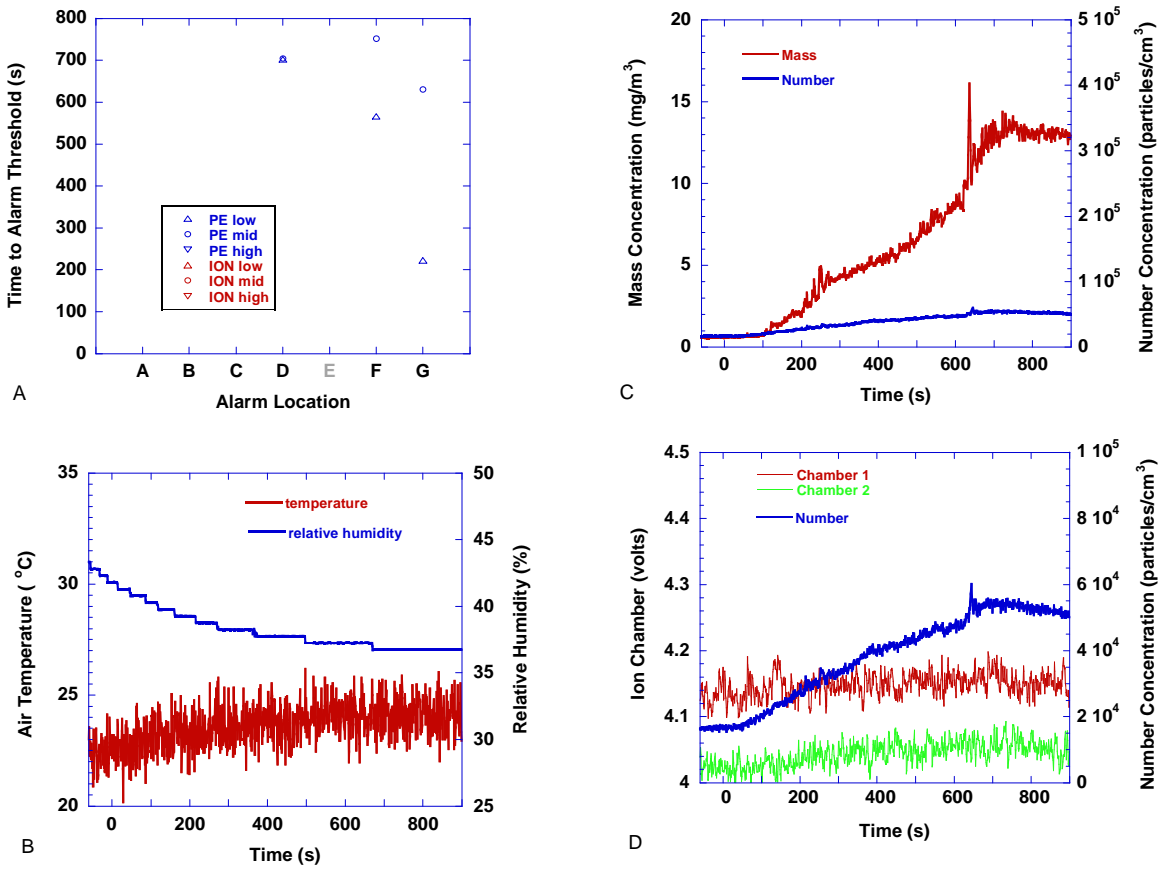


Figure 184. Smoldering foam - a polyurethane foam block, located on the living room floor at the chair burn location and ignited with an electrically powered nichrome wire heater imbedded in the block. Fan was on. Power to igniter on at t=0

The following generalizations characterize the smoldering foam tests:

- This test showed a lot of variation in terms of smoke production.
- The propensity was for photoelectric alarms to reach threshold values during smoldering, and all alarms to reach thresholds after transition to flaming.

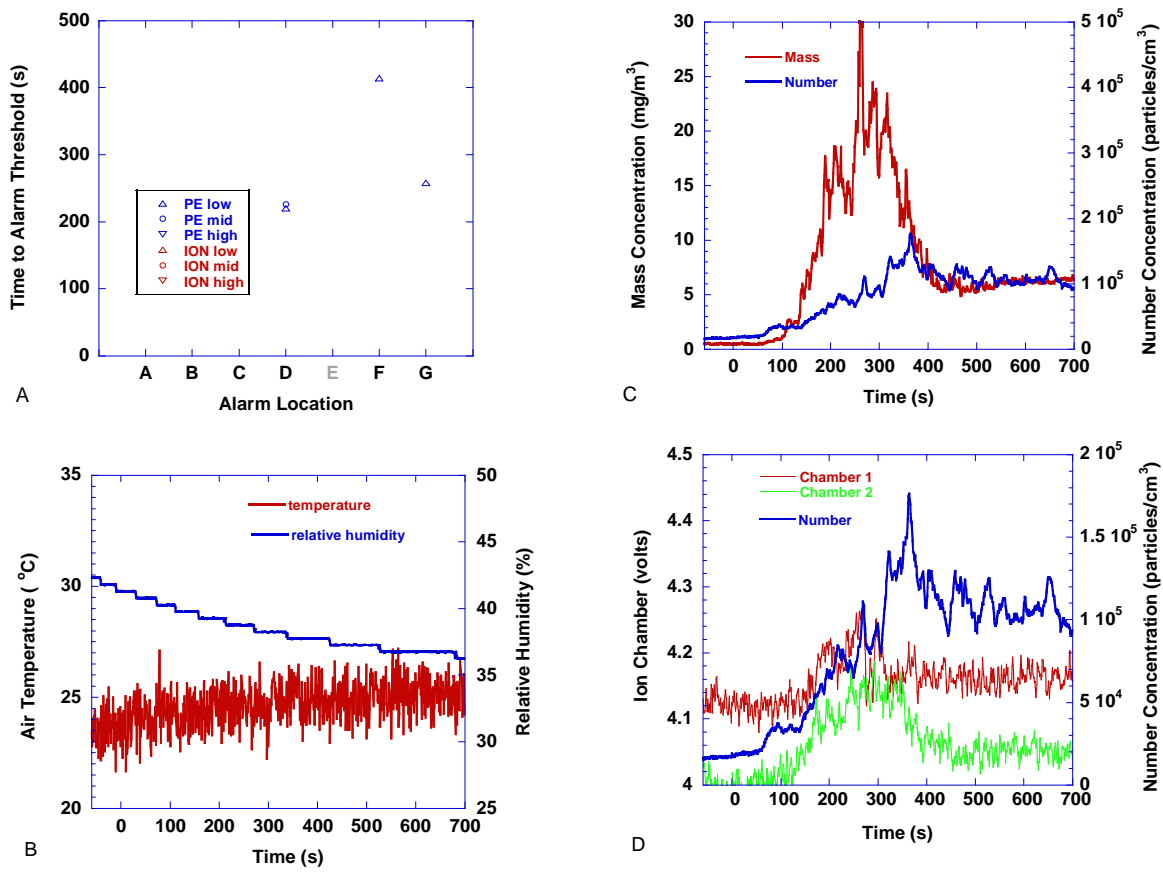


Figure 185. Smoldering foam - a polyurethane foam block, located on the living room floor at the chair burn location and ignited with an electrically powered nichrome wire heater imbedded in the block. Fan was on. Power to igniter on at $t=0$

The nuisance source test results performed here supported the two main conclusions drawn from the field studies on nuisance alarms, the type of alarm (ionization or photoelectric) and the location of the alarm (relative to the source) affect the frequency of nuisance alarms. Specifically, it was observed that the properties of the aerosol produced and its concentration affect whether either type of alarm threshold would be met. A relatively high number concentration of small particles is sufficient to produce nuisance alarms in ionization-type detectors, while not causing photoelectric-type alarms to activate. A high mass concentration of large particles can have the exact opposite outcome. In a quiescent environment only disturbed by a cooking heat source, cigarette, candle flame, or smoldering source, a distinct trend of an alarm's location relative to a source, and the propensity to reach an alarm threshold was observed. Forced flow conditions do not always follow that trend due to more rapid mixing, dilution and the directional nature of the flow relative to the source and the alarms.

6.5 FE/DE Emulation of Nuisance Sources

Several preliminary tests were performed in the FE/DE with the intent of reproducing similar environments observed in the manufactured home tests above. The tests included toasting bread, a burning candle, margarine and butter heated in a pan, smoldering cotton and wood blocks. The data collected included the air temperature and relative humidity inside the test section, laser light extinction, MIC current, carbon monoxide and carbon dioxide concentration, barometric pressure, flow velocity, and the output from two modified photo, ion, CO, thermistor units (D1 and D8, which were placed near the rear (location A) and front (location G) doors, respectively in the manufactured home; see figure 141 for locations)

The main objective of these tests was to demonstrate that important features of the selected scenarios could be reproduced in the FE/DE. Reproduction of perfect time histories of smoke and gas concentration, temperature and velocity at any detector location was not the goal. The tests were run at two different fan flows which produce flow velocities on the order of what was observed in the manufactured home test during no forced flow and forced flow tests (see section 6.3.1 for details of flow velocities). The results are presented below with a comparison to observations in the manufactured home tests.

6.5.1 Cotton Wick Calibration

Two calibration tests using the staged wick ignition source were performed. These tests were identical to the cotton wick calibration tests in section 5. The results are shown in figures 186 – 188. The electrochemical cell in D1 was not functioning properly and its results are not presented. Notice that the MIC signal fluctuated in clean air conditions as well as during steady smoke levels as shown in figure 187. This was caused by a problem in the picoammeter that was used to monitor the MIC and transmit a scaled voltage signal to the FE/DE data acquisition board. For this test and the FE/DE nuisance tests described below, this noisy MIC signal was present, and thus the MIC signal should be viewed as a relative indication of how a MIC would respond. Figure 186 shows repeated results for the photoelectric sensors compared to the laser light extinction. The sensor from unit D1 rose from an initial value of zero, while the sensor from unit D8 starts out at a value of about 5. An increase in the output for each of these sensors of about five would be the alarm threshold equivalent to 2.5 % obscuration. Figure 187 shows repeated results for the ionization sensors compared to the MIC output. For these sensors, a decrease of 25 from the initial level would be the equivalent of about 1 %/ft obscuration. Figure 188 shows the results for the CO sensor in unit D1 compared to the CO concentration from the gas analyzer for the repeated tests. The initial jump in the CO sensor response from zero to 10 was attributed to signal noise; this periodic noise was observed throughout the tests. The carbon monoxide results are presented below, but no further discussion of the results will be made here.

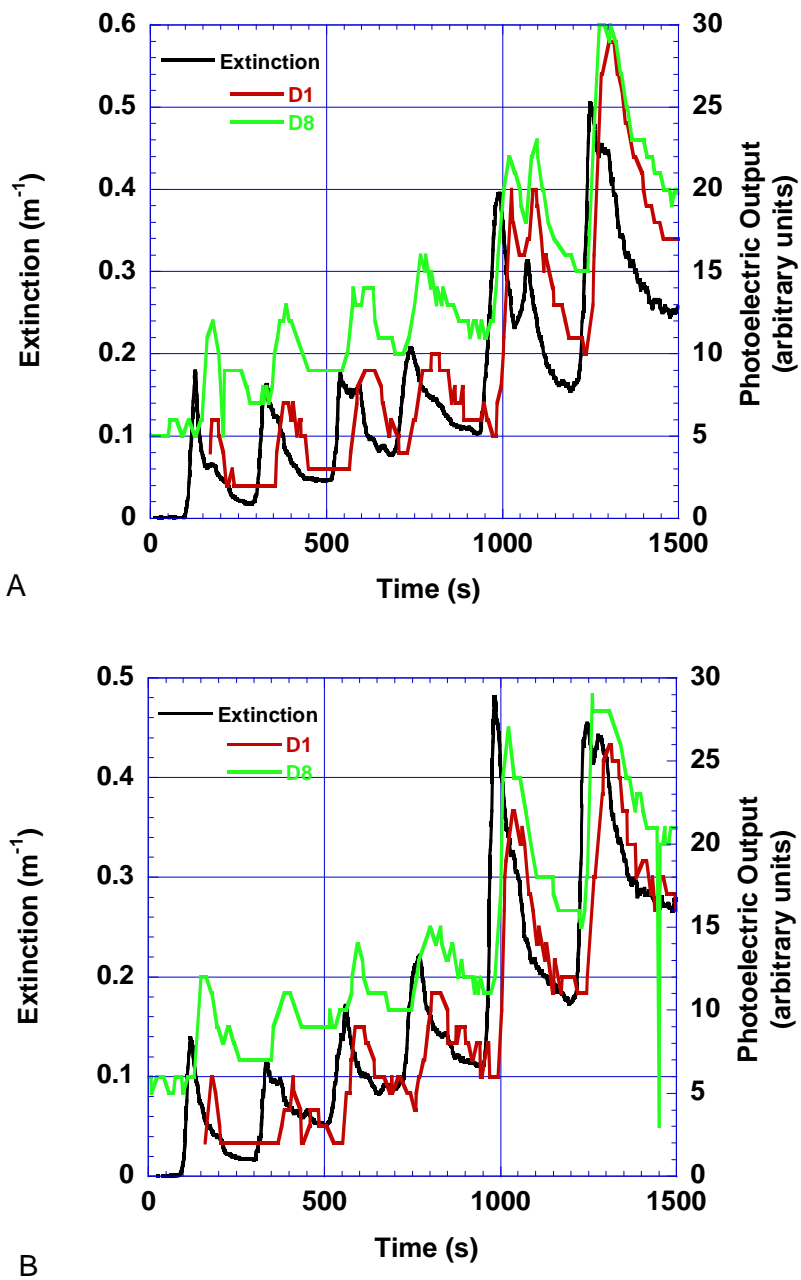


Figure 186. Photoelectric sensor response to cotton smolder smoke calibration test.
A and B indicate repeated tests

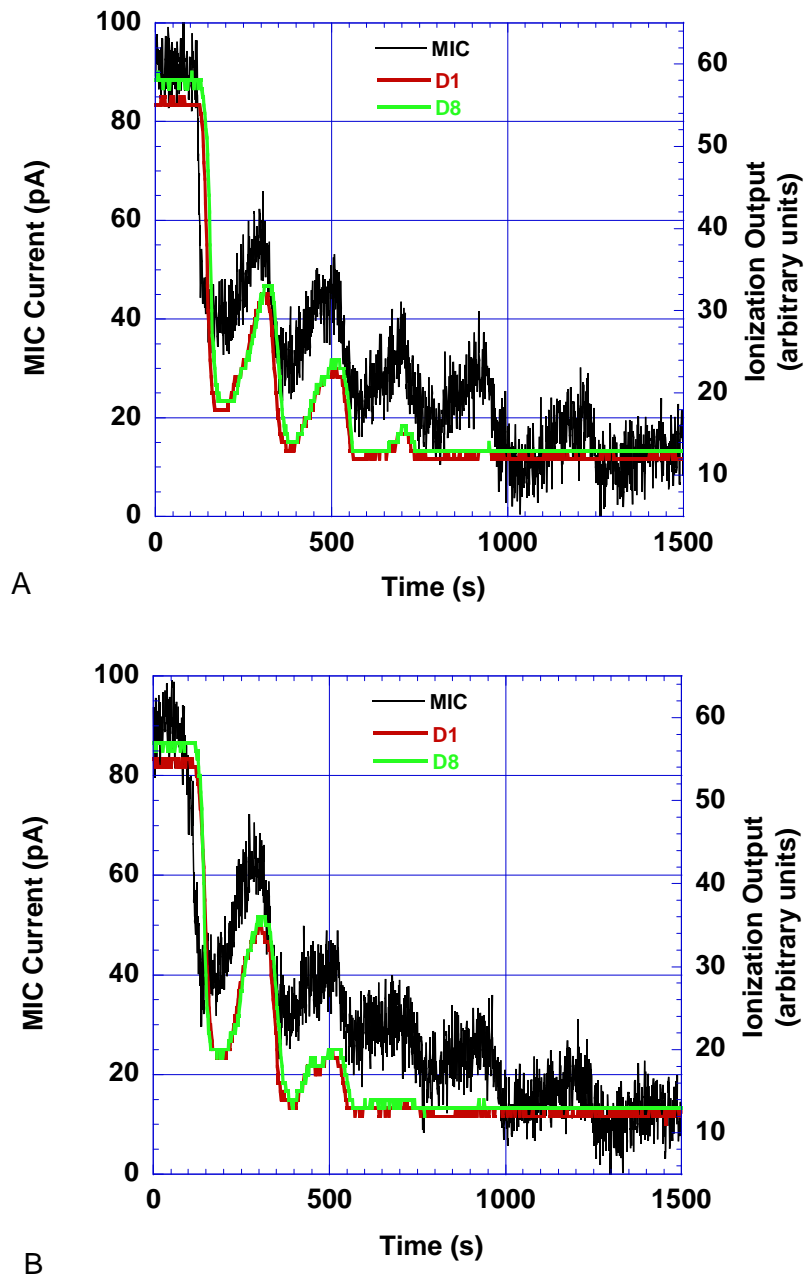


Figure 187. Ionization sensor response to cotton smolder smoke calibration test.
A and B indicate repeated tests

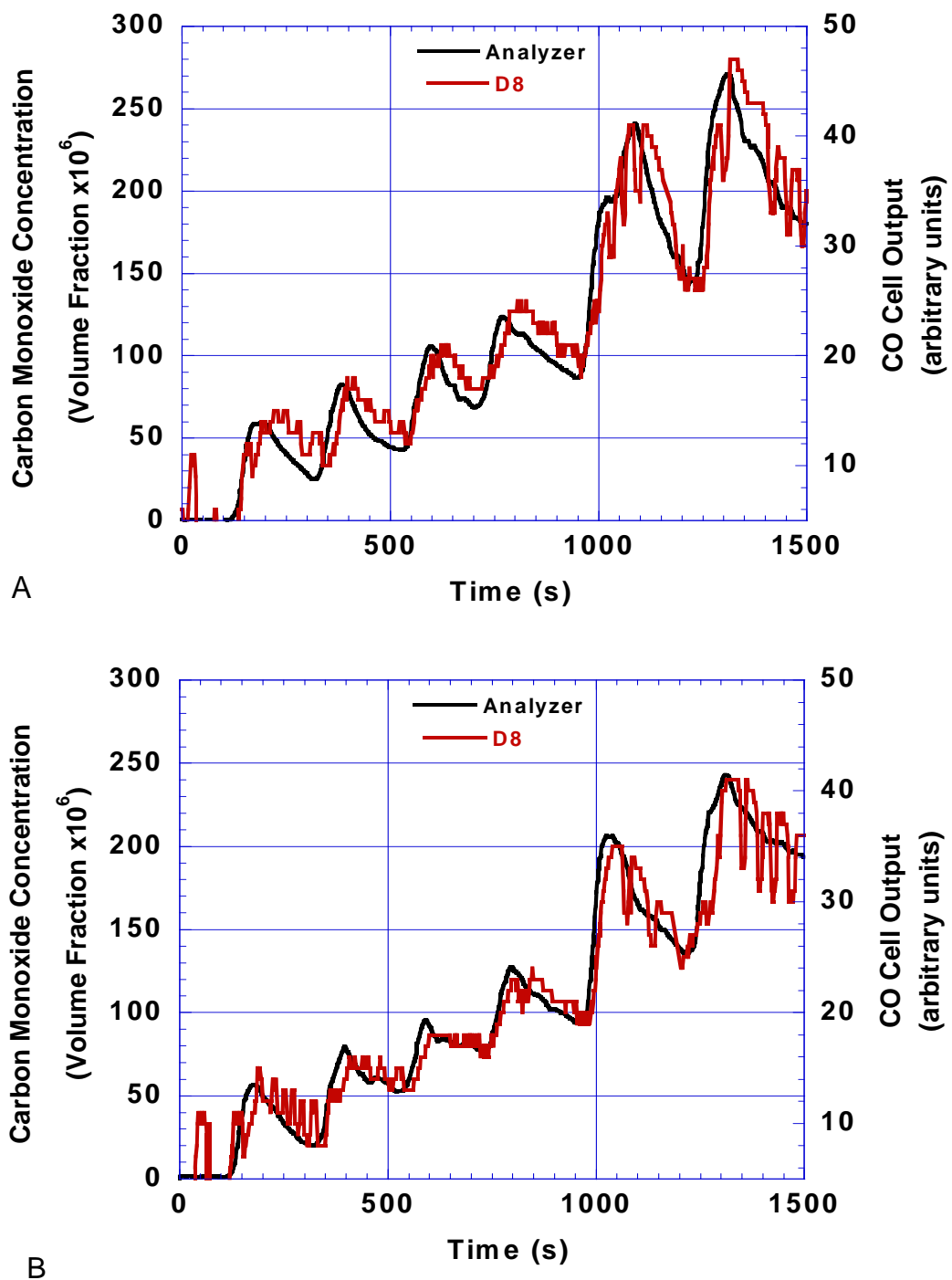


Figure 188. Electrochemical cell CO sensor response to cotton smolder smoke calibration test. A and B indicate repeated tests

6.5.2 Cotton Smolder Smoke Fire Scenario

The cotton smolder smoke scenario employed the same ignition sequence used in the manufactured home tests, but with half of the number of wicks (16). Tests were conducted at fan speeds of 7 Hz and 12 Hz, and each was repeated. The baffle plate was installed in the duct upstream of the test section to produce turbulent flow characteristics similar to those observed in the manufactured home tests. (The baffle plate was left in during all subsequent tests.)

Figures 189 and 190 show results for repeat runs at a fan speed of 7 Hz. The extinction was observed to peak at about 0.3 m^{-1} for the first test, and 0.5 m^{-1} for the second test. This difference is attributed to variation in the time to ignition for the two sets of wicks. At about 500 s the wicks were approaching a steady burning rate. The photoelectric and ionization sensor alarms reach threshold levels. Figure 191 and 192 show results for repeat runs at a fan speed of 12 Hz. Although the smoke concentration was lower due to the dilution with the higher duct flow, both photoelectric and ionization alarms reach threshold levels. The photoelectric sensor signal rise lags the rise in smoke concentration, and responds slower than the ionization sensor for all of these tests. This is partially due to smoke entry lag into the photoelectric sensor and an artifact from filtering the photoelectric sensor signals.

Both the FE/DE results and the manufactured home results for sensor units near the source achieve alarm threshold levels for both types of alarms during the ignition phase of the wicks when the peak amount of smoke was produced. The smoke concentration in the upper layer of the manufactured home continued to rise because it was a closed system.

6.5.3 Wood Smolder Smoke Fire Scenario

The generation of wood smolder smoke was identical to the method used in the manufactured home. Eight beech wood blocks were placed on the electric hot plate which was located at the bottom of the vertical rise in the duct. At time = 0 the heater was turned on. Figures 193 to 196 show the results for repeated tests at 7 Hz and 12 Hz fan flows.

The photoelectric sensors reach the alarm threshold levels slightly earlier than the ionization sensors. In the manufactured home tests, photoelectric alarm thresholds were reached earlier than the ionization alarm thresholds, but the time differential tended to be larger than what was observed in the FE/DE tests due to the inherently smaller volume of the FE/DE apparatus.

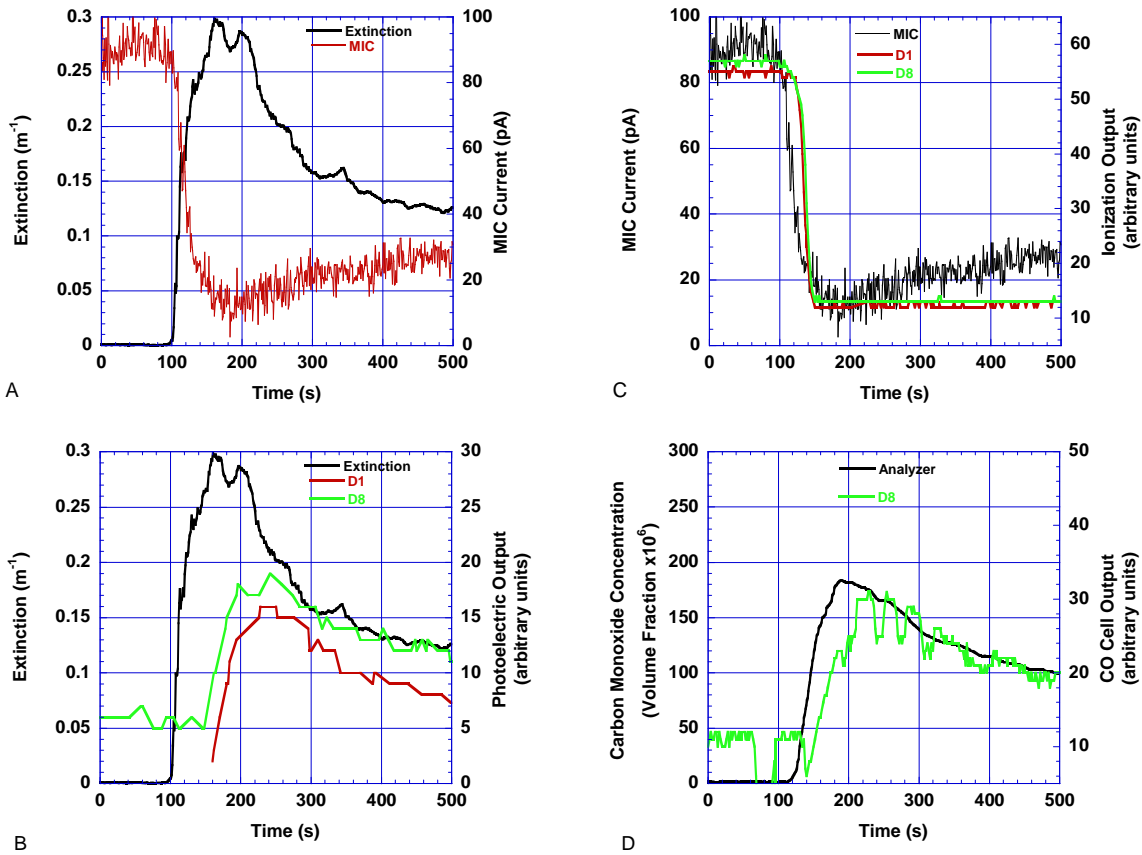


Figure 189. Smoldering cotton fire scenario, fan speed 7 Hz

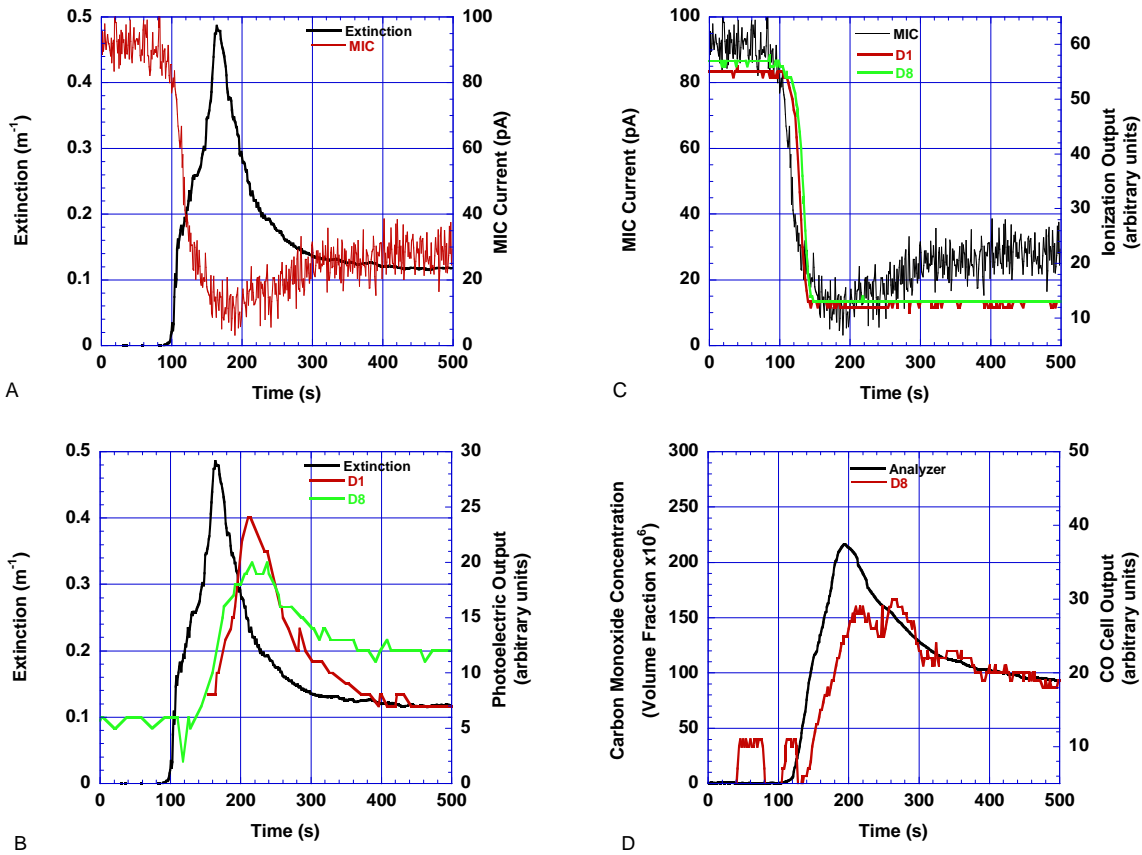


Figure 190. Smoldering cotton fire scenario, fan speed 7 Hz

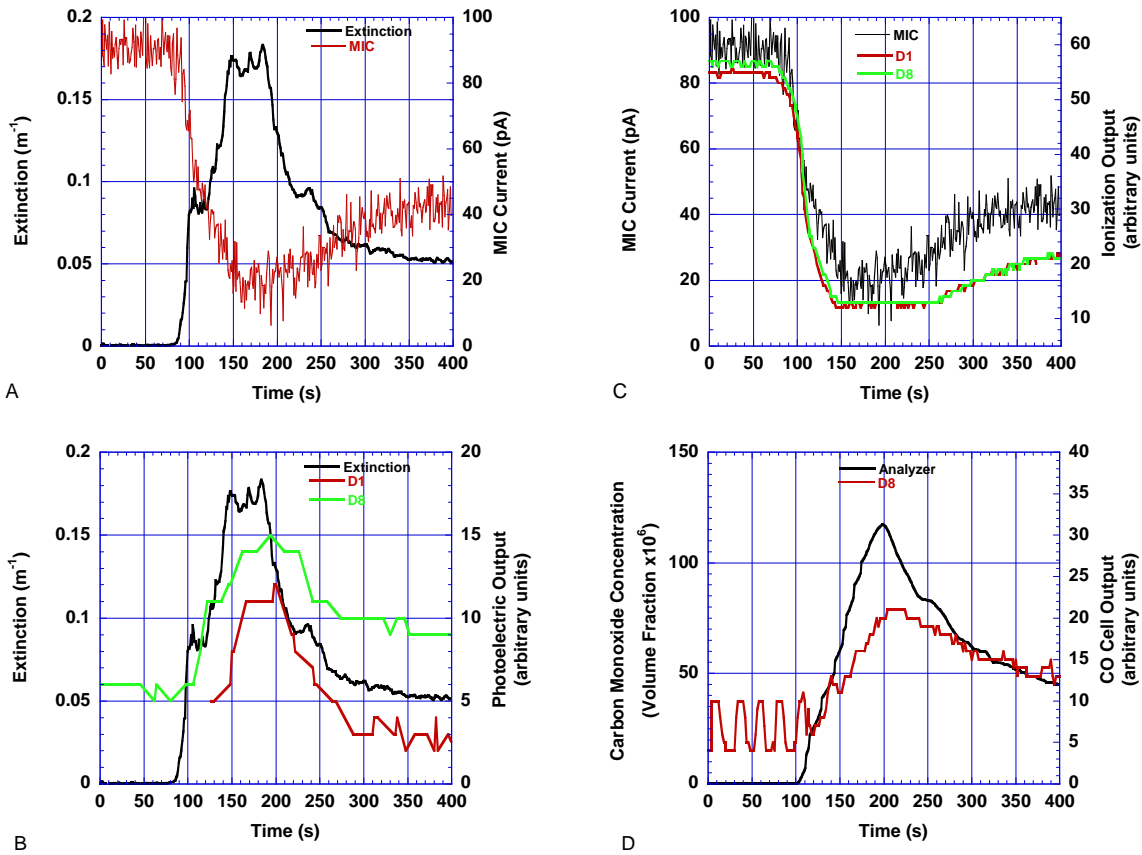


Figure 191. Smoldering cotton fire scenario, fan speed 12Hz

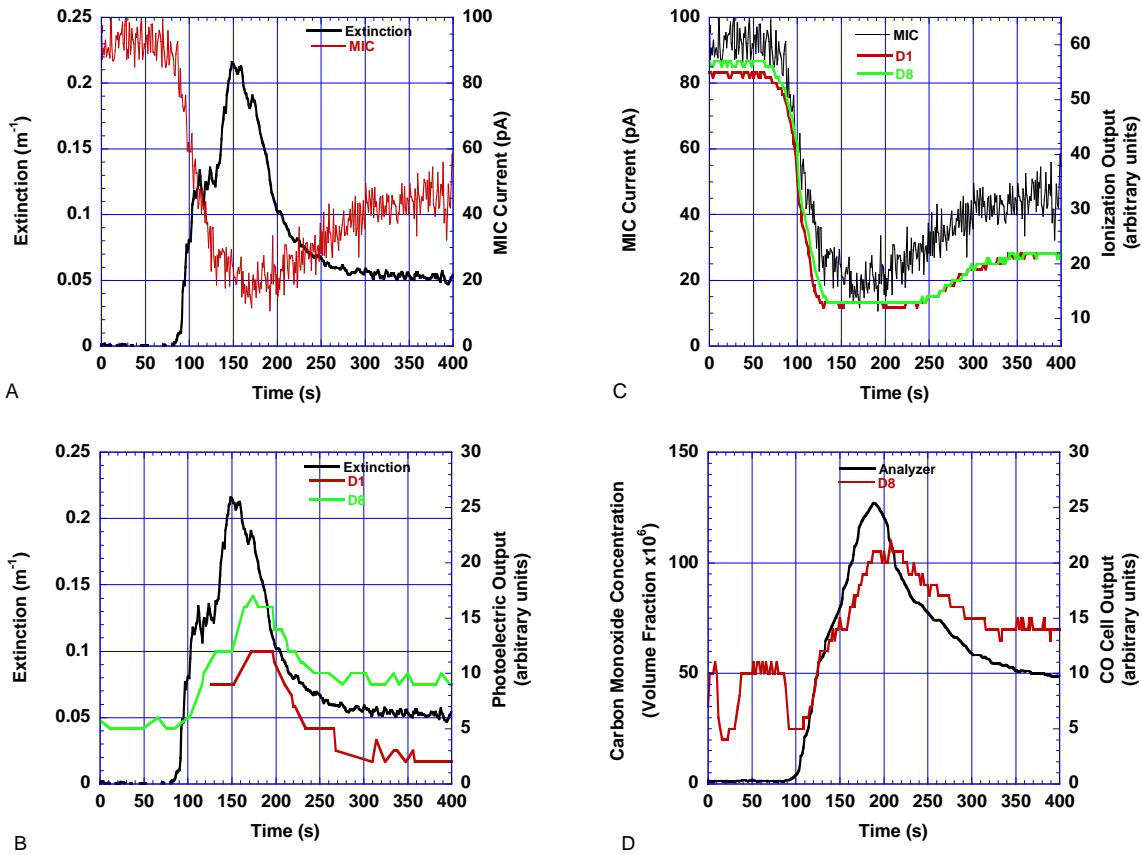


Figure 192. Smoldering cotton fire scenario, fan speed 12 Hz

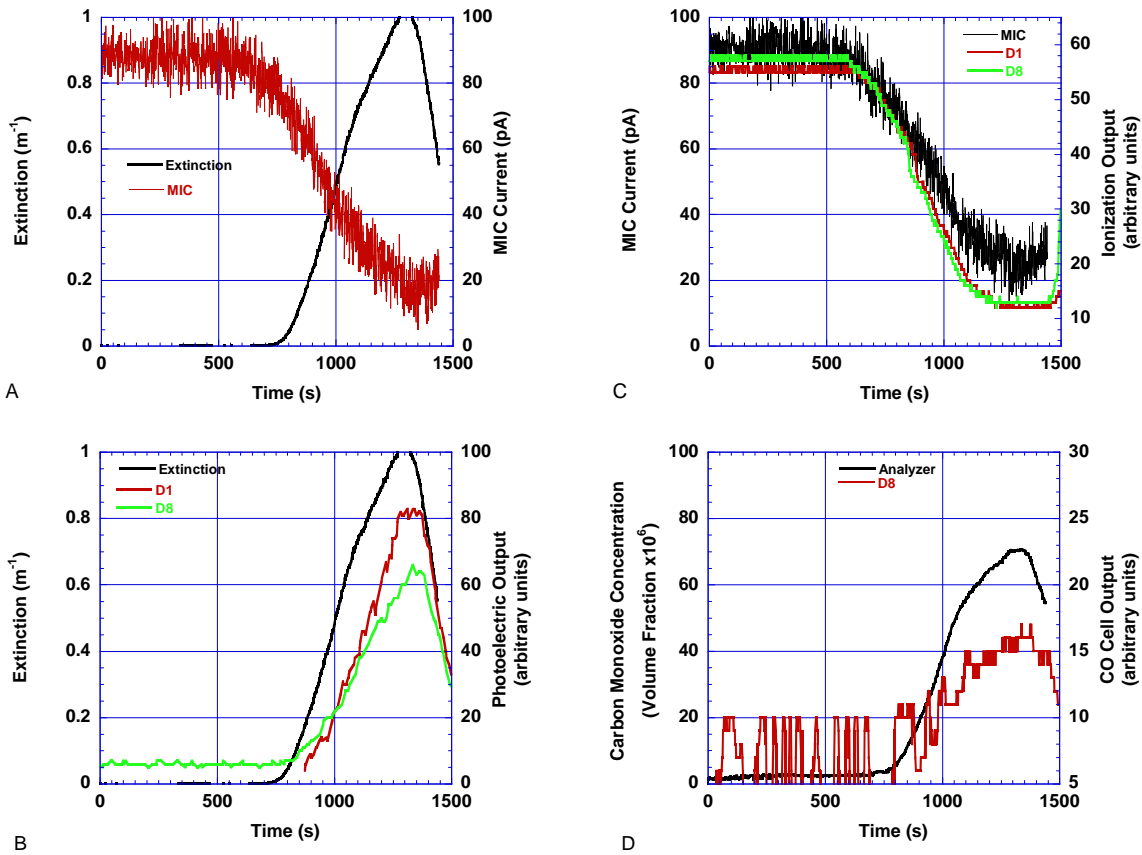


Figure 193. Smoldering wood fire scenario, fan speed 7 Hz

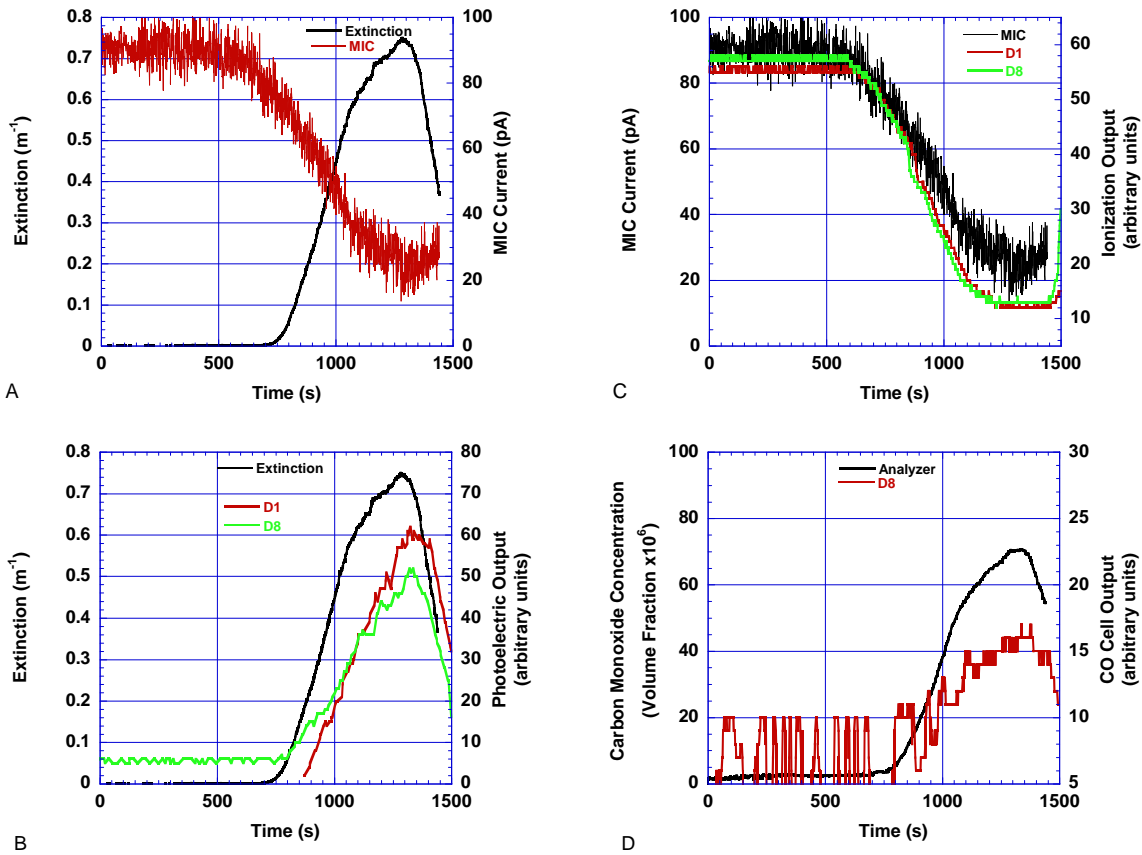


Figure 194. Smoldering wood fire scenario, fan speed 7 Hz

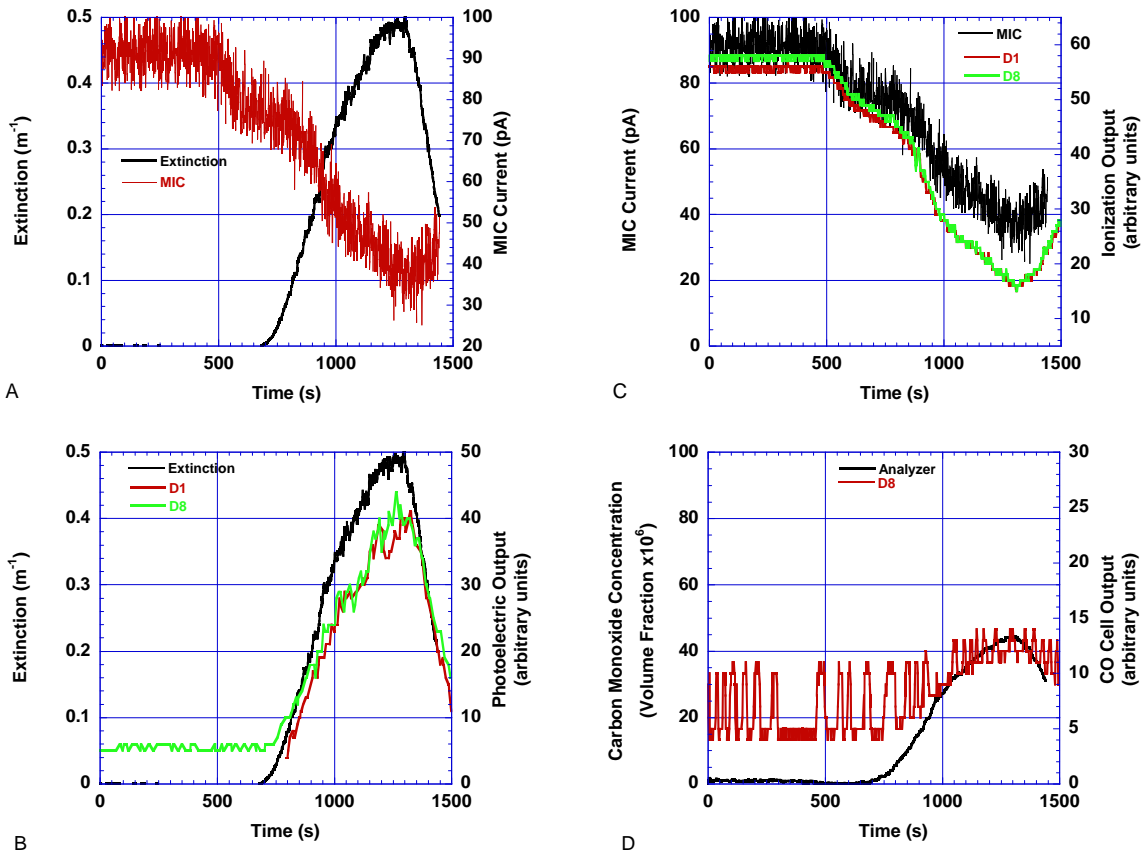


Figure 195. Smoldering wood fire scenario, fan speed 12 Hz

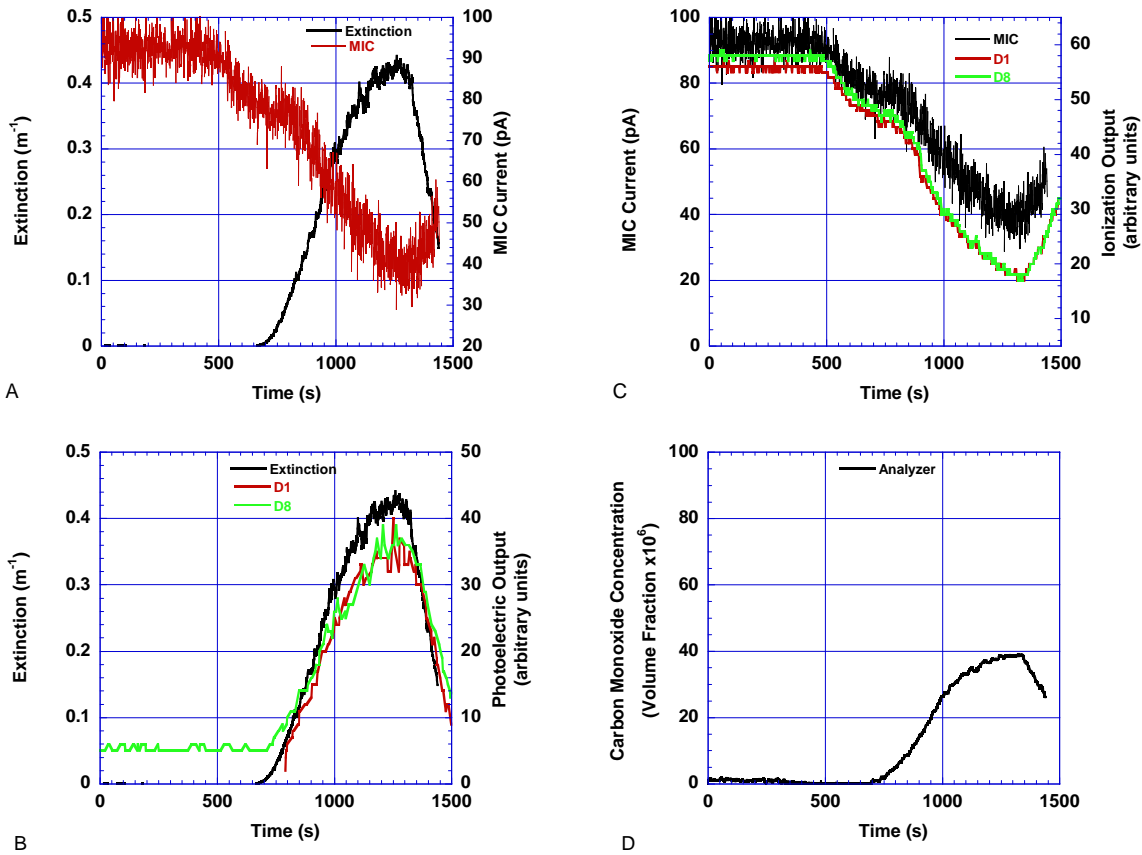


Figure 196. Smoldering wood fire scenario, fan speed 12 Hz

6.5.4 Candle Flame Nuisance Scenario

A single tea candle, the same brand used in the manufactured home tests, was placed in the FE/DE duct and lit. Figure 197 shows the results. This produced a slight decrease in the MIC output and in the ionization sensors, but not sufficient for an ionization alarm threshold. There was no observable light extinction. These observations mirror the manufactured home results, where no alarm thresholds were met. Only an increase in aerosol number concentration and a slight rise in the ionization chambers were evident.

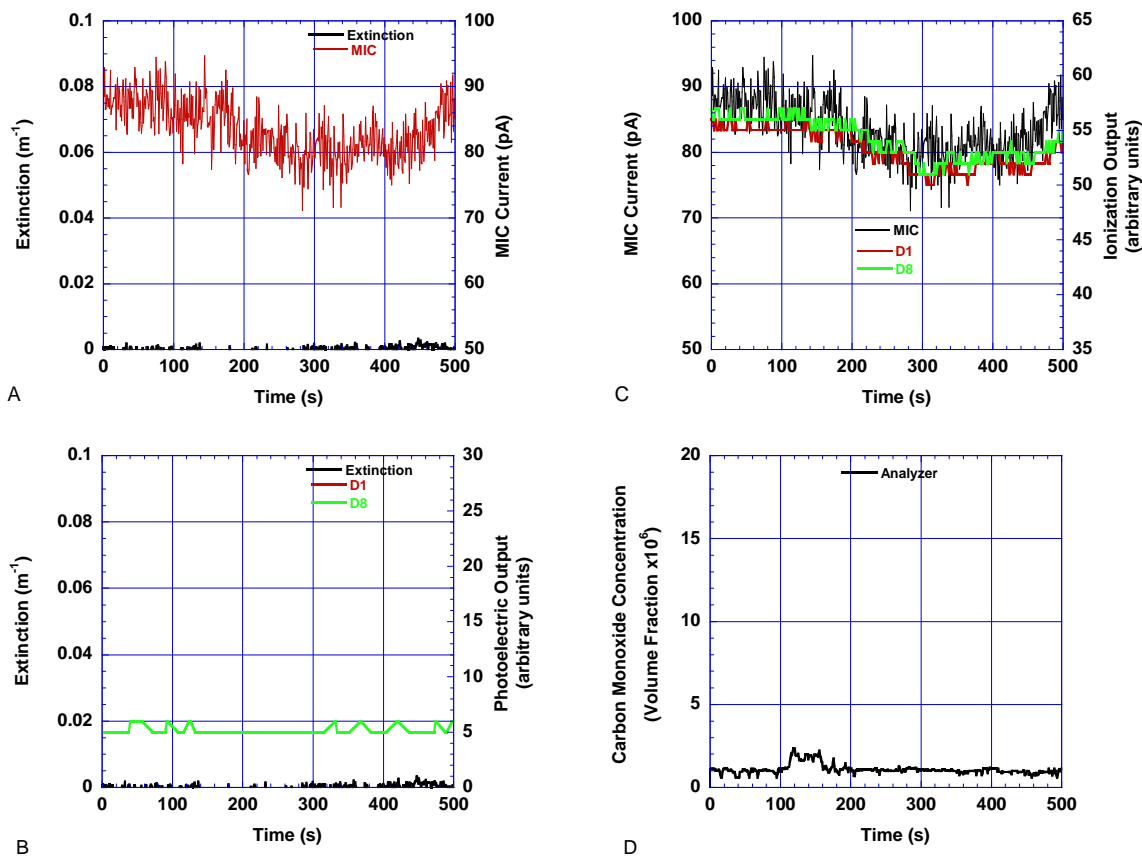


Figure 197. Candle flame , fan speed 7 Hz

6.5.5 Heated Margarine or Butter Nuisance Scenario

In these tests, a portable, thermostatically controlled, 15 cm diameter electric hotplate was used to heat either $\frac{1}{2}$ tablespoon of margarine or butter placed in a 15 cm diameter cast-iron frying pan. All tests were performed at a fan flow of 7 Hz.

Figures 198 to 200 show the results. No ionization alarm thresholds were reached during the margarine tests or the butter test. Photoelectric thresholds were reached during one margarine test and the butter test.

The FE/DE tests are somewhat different than the manufactured home tests in that the hot plate used in the FE/DE did not apparently heat up the cast-iron pan to temperatures reached on the cast-iron pan placed on the electric range. The thermostat in the portable hot plate does not let the temperature reach a level where the margarine or butter will smoke heavily.

6.5.6 Toasting Bread Nuisance Scenario

The same toaster and brand of bread that was used in the manufactured home tests was used in the FE/DE tests. The only difference was that one slice of bread was used in the FE/DE tests. For these tests, the toaster was turned on at 60 s and turned off at 300 s. Three tests at a fan speed of 7 Hz and two tests at 12 Hz were performed.

The results are shown in figures 201 to 205. Consistent with the manufactured home tests, both ionization and photoelectric alarm thresholds were reached, with the ionization alarms thresholds reached first. The delays between the extinction measurements and the photoelectric sensor signals were evident during all of the tests.

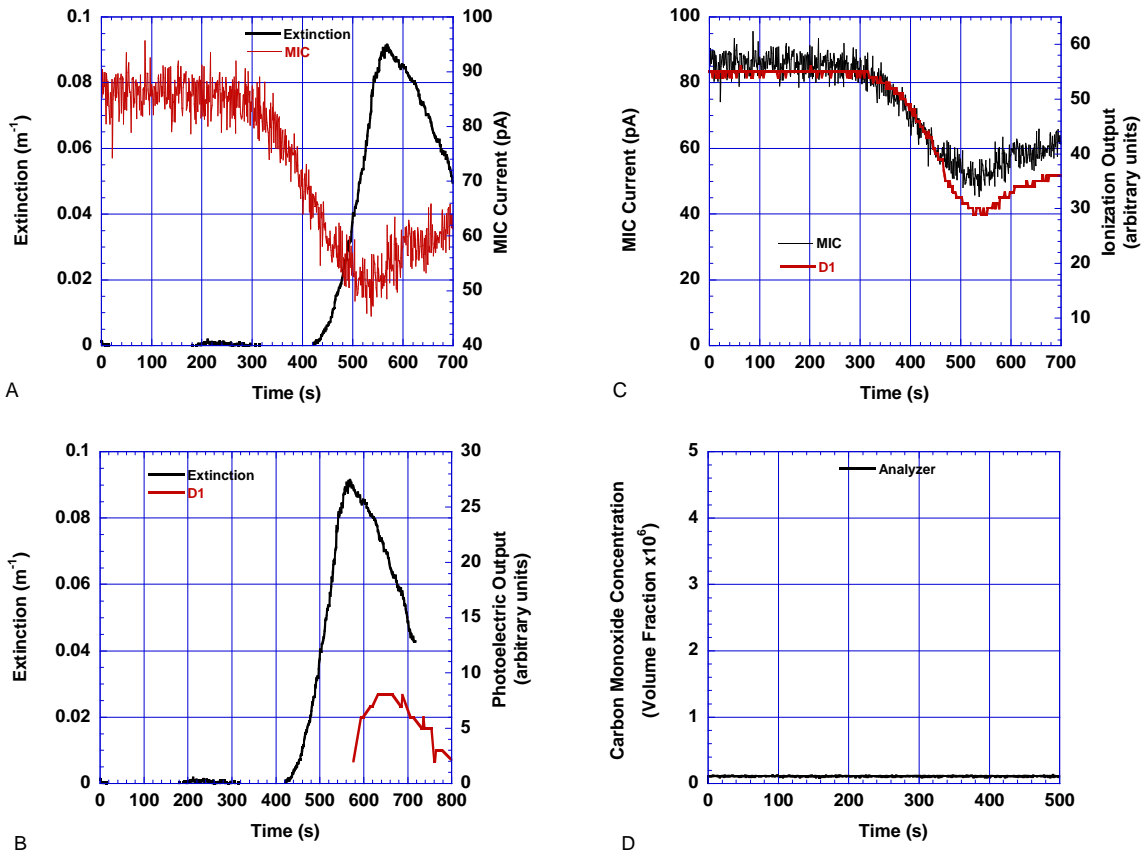


Figure 198. Margarine heated in a pan , fan speed 7 Hz

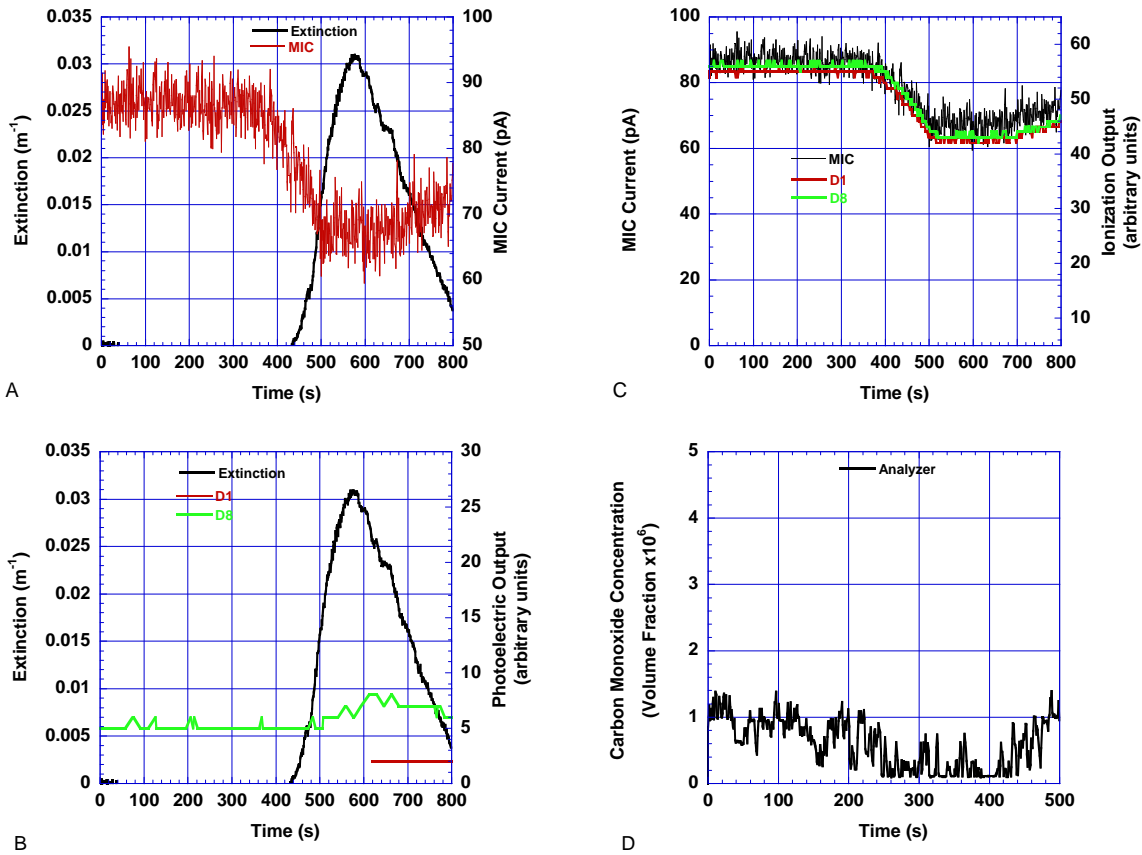


Figure 199. Margarine heated in a pan, fan speed 7 Hz

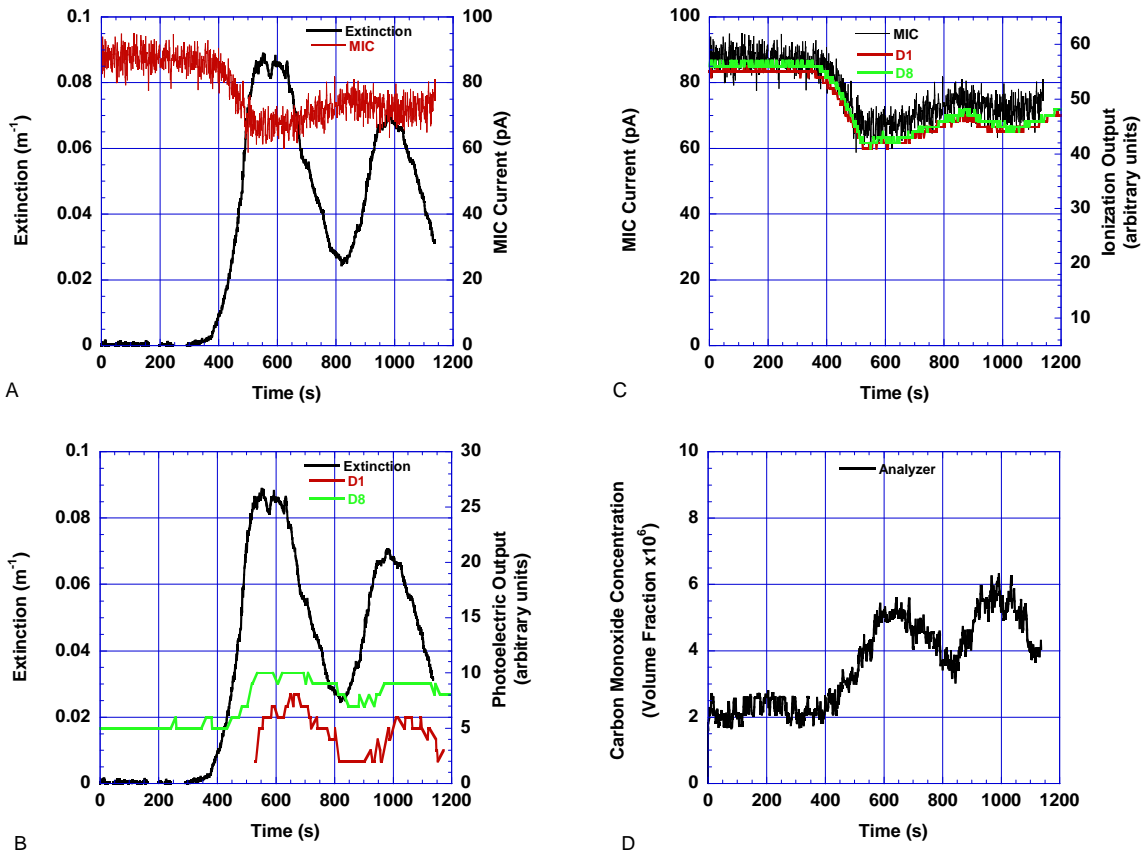


Figure 200. Butter heated in a pan, fan speed 7 Hz

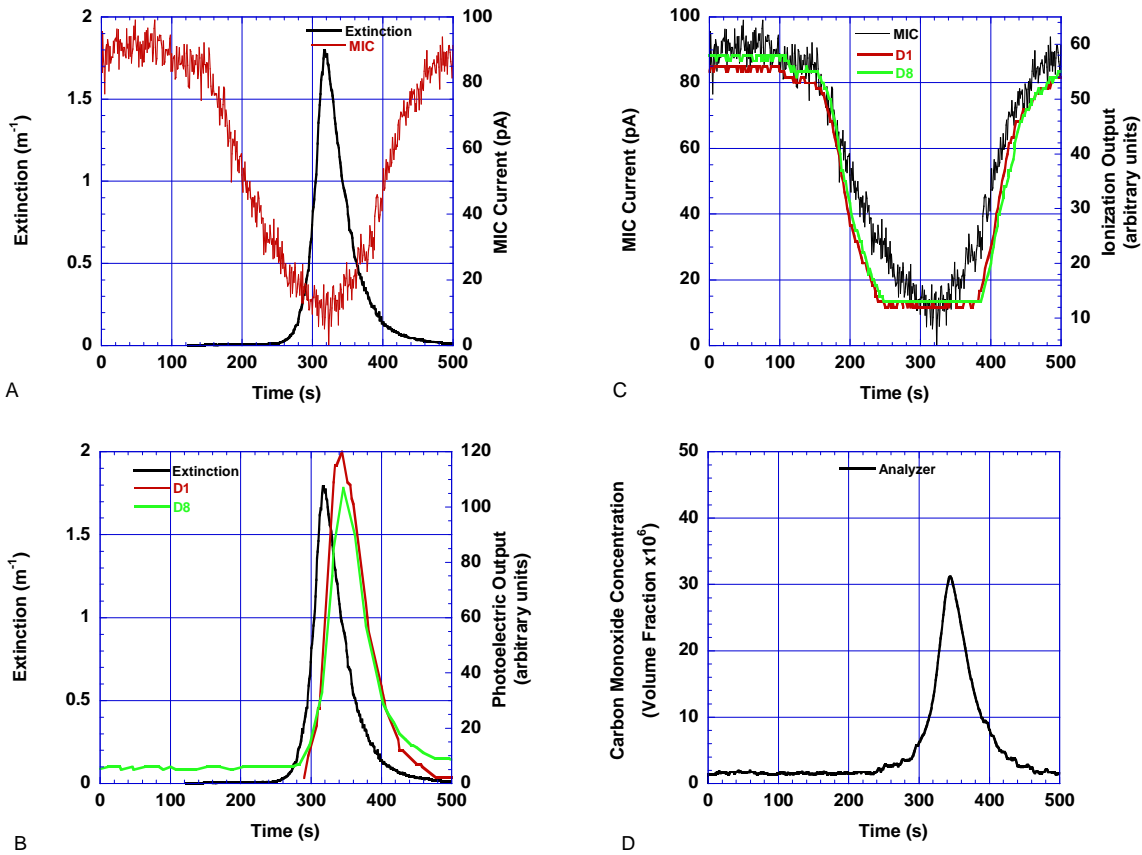


Figure 201. Bread in a toaster, fan speed 7 Hz

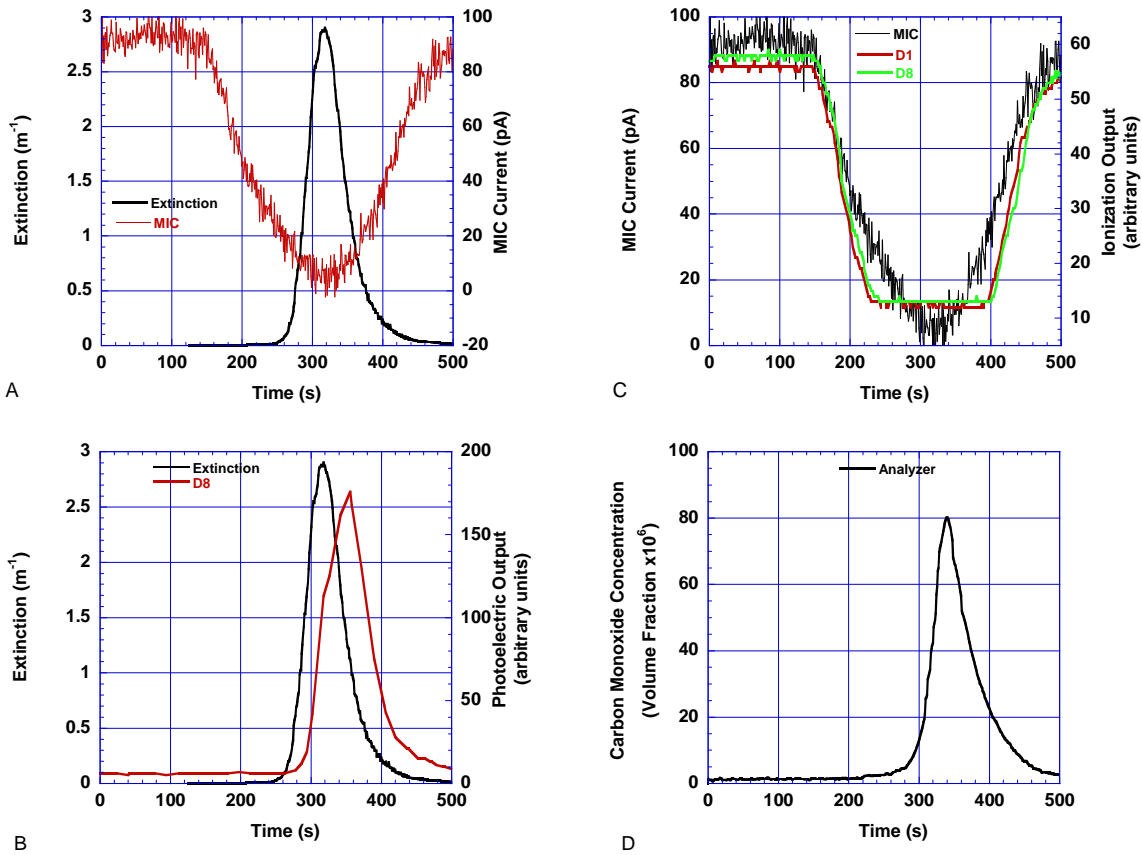


Figure 202. Bread in a toaster, fan speed 7 Hz

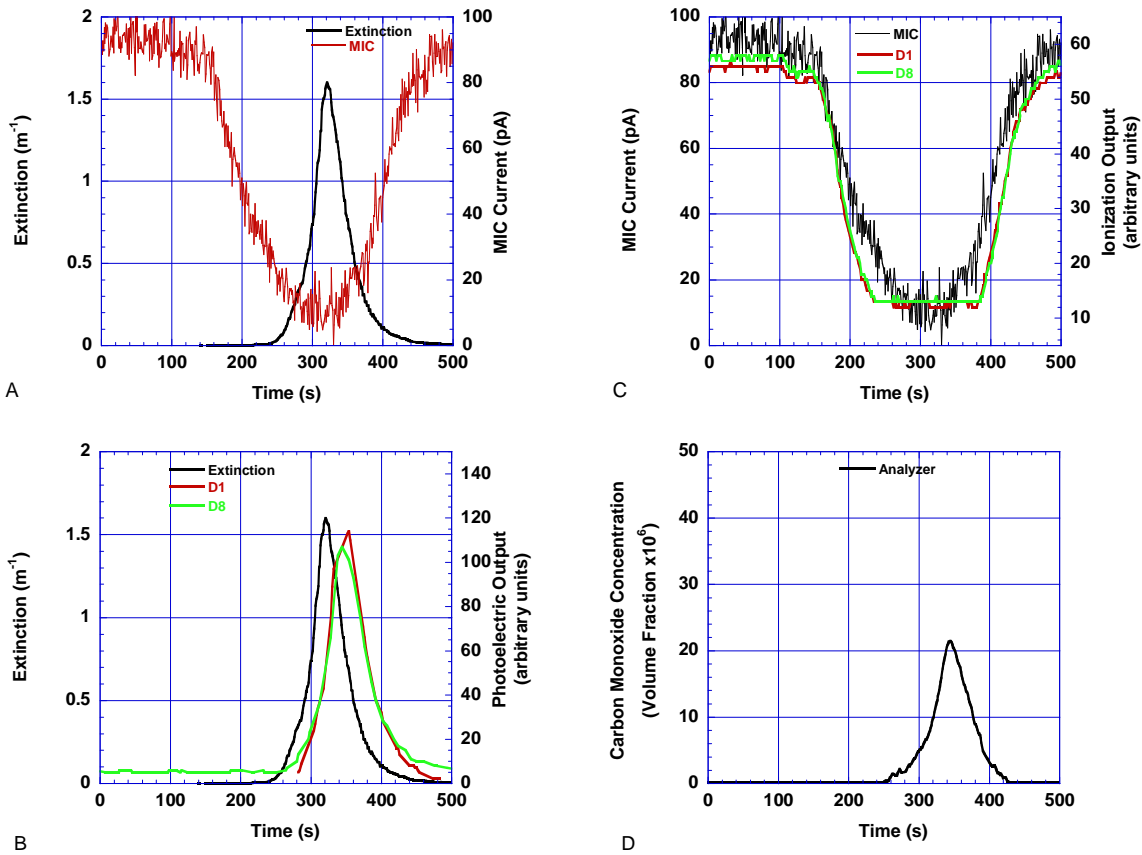


Figure 203. Bread in a toaster, fan speed 7 Hz

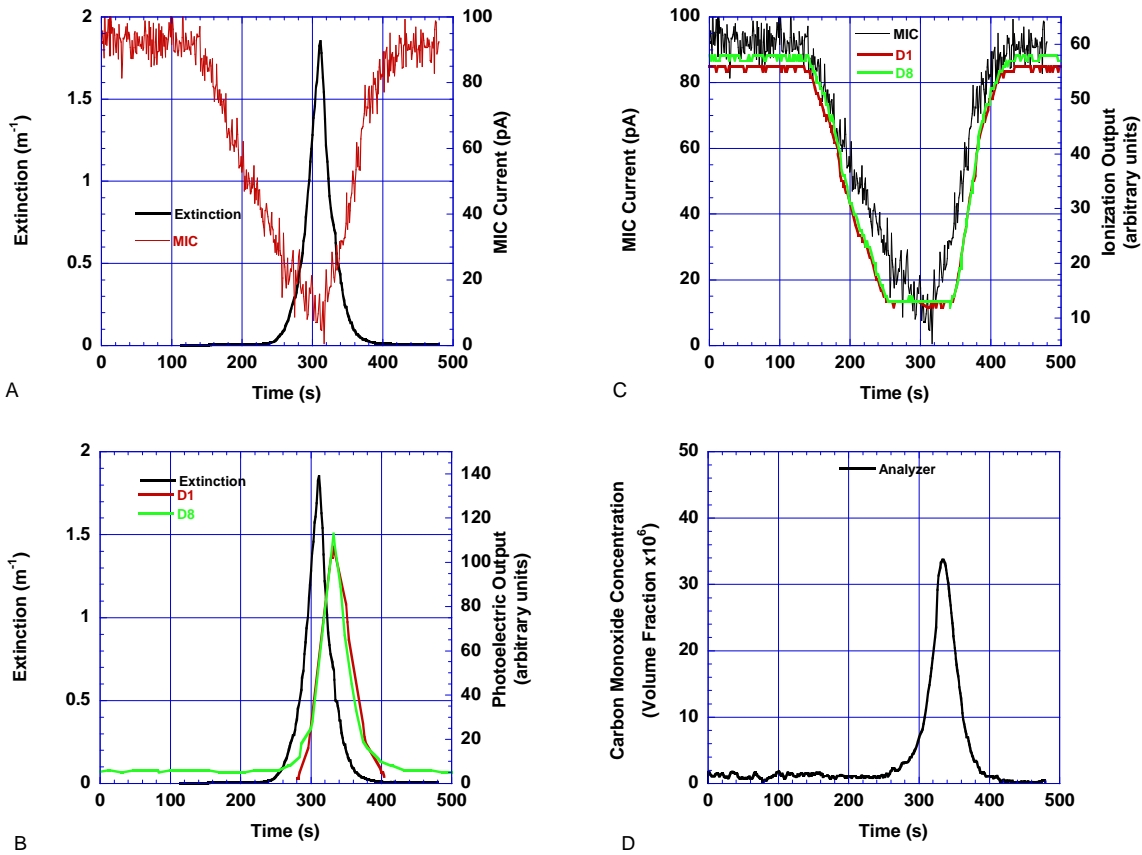


Figure 204. Bread in a toaster, fan speed 12 Hz

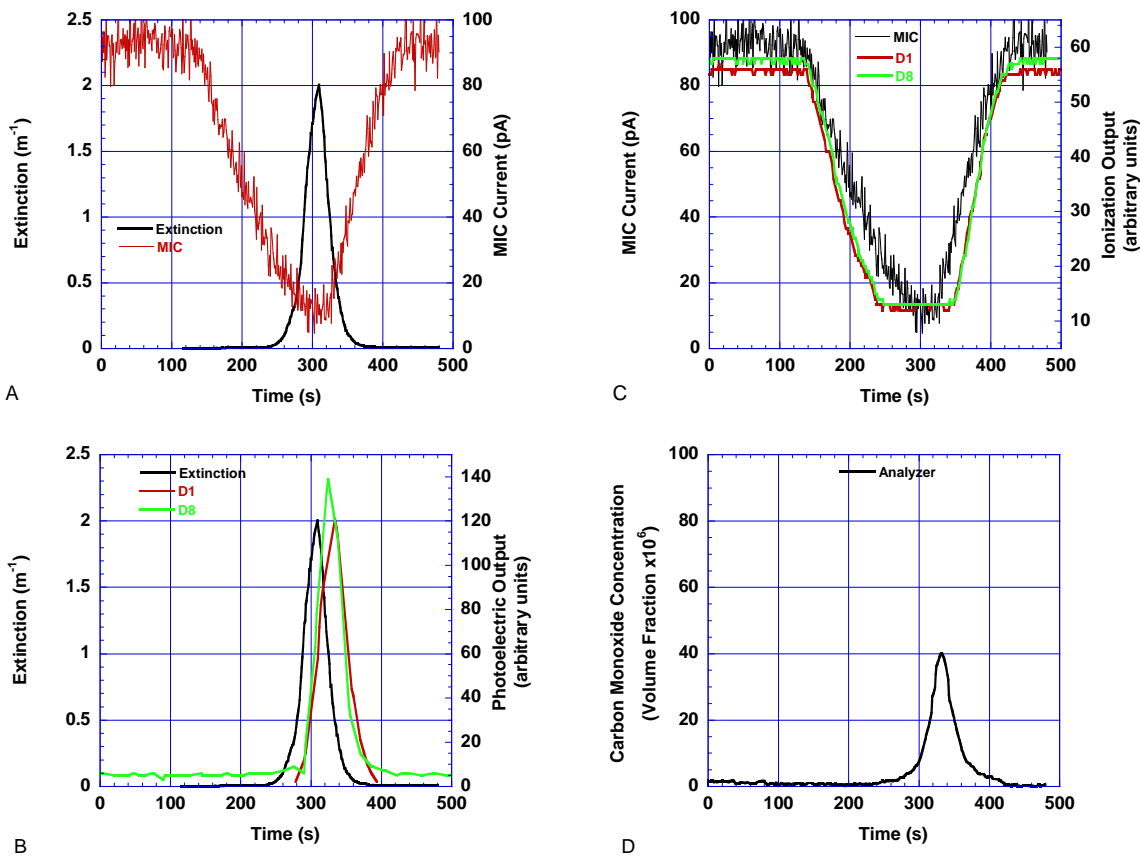


Figure 205. Bread in a toaster, fan speed 12 Hz

7 Discussion

In 1975, the Indiana Dunes study pioneered the idea of measuring the performance of home smoke alarms by the amount of escape time provided. Escape time is the time between the device alarm and the occurrence of untenable conditions at any point along the primary escape path – generally the corridors and stairs leading from the sleeping rooms to the egress door. While building codes require that sleeping rooms have a secondary exit, usually a window of sufficient size and within 6 m (20 ft) of grade [42], experience shows that these are rarely used to escape home fires. Thus, calculating the time between alarm activation and the onset of untenable conditions represents the performance metric most appropriate to evaluating the performance of smoke alarms in residences.

7.1 Smoke Alarm Activation Time

Smoke alarm requirements in building codes and standards require multiple devices depending on the size and arrangement of the dwelling. Thus, when determining the performance of smoke alarms, the escape time provided by any single device is not (necessarily) appropriate. Rather the escape time provided by the first of several devices at specific locations cited in the codes is the appropriate parameter to report.

For existing homes (and all homes, prior to 1993) smoke alarms are required outside the sleeping rooms and on each additional story of the home. This arrangement will be referred to as “every level” and represents the minimum arrangement allowed by code. In 1993 the National Fire Alarm Code (NFPA 72) was revised to require smoke alarms in every bedroom for new construction in addition to the every level locations, in order to improve audibility in bedrooms where occupants sleep with the door closed and to provide warning to the occupants of bedrooms with closed doors when the fire starts in that bedroom. We will refer to this arrangement as “every level + bedrooms.” The greatest escape times would be produced by a smoke alarm in the room of fire origin, but this would be guaranteed only if smoke alarms were required in every room – an arrangement that has never been required in any code. Thus the “every room” result represents the best possible performance that can be compared to “every level” as the minimum performance as a function of number and location.

Alarm times for heat alarms and residential sprinklers are always based on the activation of devices in the room of fire origin. NFPA 72 allows the use of heat alarms on an individual basis (for example, in locations where smoke alarms are not appropriate - in an attic). Similarly, some rooms - e.g., bathrooms, some closets - are not required to have sprinklers in a code-compliant home sprinkler system (NFPA 13D). All fires in these test series were in normally-occupied

spaces of the structures (living room, bedroom, or kitchen). Placement of heat alarms and residential sprinklers in these spaces is consistent with the appropriate codes.

Tables 23 and 24 shows a summary of alarm activation times for all of the tests. For each alarm technology and fire scenario, the average time to alarm is shown for typical alarm criteria (4.3 %/m for ionization alarms and 6.6 %/m for photoelectric alarms). For the manufactured home tests, each alarm time value is an average of available replicates. For the two-story home tests, only the flaming chair was replicated; all other data are single-test values.

Tables 23 and 24 also include alarm response times for three different alarm placement analyses described earlier: “Every Level,” “Every Level + Bedrooms,” and “Every Room.” For the “Every Level” placement, alarms in hallways of each structure are included. For the “Every Level + Bedrooms” placement, these alarms are supplemented with alarms included in all the bedrooms of the structure. Finally, the “Every Room” placement included every alarm in all rooms of the structure.

The “Every Level” alarm placement provides a comparison of different smoke alarms and fire scenarios. For flaming fires, the ionization alarms provided the first alarms for all flaming scenarios except the flaming mattress with the door closed in the two-story home (In this scenario, the sprinkler directly above the fire responded first, with alarms outside the room of fire origin following later since flow out of the room was limited to leakage around the door). Average time to first alarm for the all flaming fires range from 30 s to 3602 s, depending on the specific fire scenario, dwelling geometry, and alarm type. For smoldering fires, the photoelectric alarms provide shorter alarm times compared to other technologies. Average time to first alarm range from 1366 s to 4829 s, depending on the fire scenario, dwelling geometry, and alarm type. In all but one smoldering test, photoelectric alarms provided the first alarm (for the smoldering chair in the two-story home, the aspirated alarm uses photoelectric alarm technology and for the smoldering mattress in the two-story home, the photoelectric alarm in the dual alarm responds first). For the cooking oil tests, an ionization alarm responded first in the manufactured home while the photoelectric aspirated alarm responded first in the two-story home test.

Providing alarms in the bedrooms in addition to the “Every Level” alarm placement (the “Every Level + Bedroom” alarm placement) reduces the time to alarm for every fire scenario and most alarm technologies, providing an additional 3 s to 794 s of available egress time, depending on the specific fire scenario, dwelling geometry, and alarm type. Not surprisingly, alarm times for the bedroom fire scenarios were most affected by the additional alarms since alarms were now included for the room of fire origin. For all but one fire scenario, the same alarm technology was the first to respond in the “Every Level + Bedroom” alarm placement compared to the “Every Level” alarm placement. For this exception, one of the Dual Ion/Photo alarms in the bedroom in one test responded earlier than other alarms and moved the average alarm time downward. Other alarms responded shortly after this alarm.

In the “Every Room” alarm placement, all alarms in the structures were included in the calculations. For the photoelectric and ionization alarms, no additional reduction in alarm time was noted for the bedroom fire scenarios since the bedroom alarms were already included in the “Every Level + Bedroom” alarm placement. Some additional reduction in alarm times for flaming fire scenarios was expected due to placement of alarms in the room of fire origin for these scenarios.

Alarm placement had the greatest impact on reducing alarm time when alarms in the room of fire origin were included in the scenario. For bedroom fires, the greatest reduction was noted in the “Every Level + Bedrooms” placement scenario. For living room or kitchen fires, the reduction occurred in the “Every Room” placement. Few changes were noted for other alarm locations. In both test geometries, this is likely due to the simple geometries and initial alarm placement. For the manufactured home, the structure is essentially a single large compartment with bedrooms at either end of the structure. Thus, including additional alarms in the main compartment of the structure would be expected to have a minor impact on time to alarm. For the two-story home, there was no soffit between the living room and the stairwell to the upstairs level of the home. Thus, in most fires, alarms in the upstairs hallway of the home, included in the “Every Level” placement, were the first to alarm. Additional alarm locations in other location outside the room of fire origin thus had only a small impact on alarm time. For more complex geometries, the impact of alarm placement can be expected to be more pronounced.

Table. 23. Average time to alarm (in seconds) for several smoke alarms and fire scenarios in a manufactured home

Every Level Installation Criterion

Flaming	Photo	Ion	Dual Ion/Photo	Aspirated
Living Room	130	73	77	137
Bedroom	96	61	112	121
Bedroom (Door Closed)	619	172	114	643

Smoldering

Living Room	4615	4829	4605	4541
Bedroom	2622	3631	3354	2997
Bedroom (Door Closed)	3442	3428	3434	3446

Cooking

Kitchen	766	520	439	1172
---------	-----	-----	-----	------

Every Level + Bedrooms Installation Criterion

Flaming	Photo	Ion
Living Room	130	73
Bedroom	78	37
Bedroom (Door Closed)	84	34

Smoldering

Living Room	4615	4829
Bedroom	2179	3618
Bedroom (Door Closed)	2648	3402

Cooking

Kitchen	764	520
---------	-----	-----

Change from Every Level

Photo	Ion
--	--
-18	-25
-535	-138

--	--
-443	-13
-794	-26

-3	--
----	----

Change from Every Level + Bedrooms

Photo	Ion
-38	-45
--	--
--	--

-2063	-427
--	--
--	--

-73	-33
-----	-----

Table 24. Average time to alarm (in seconds) for several smoke alarms and fire scenarios in a two-story home

Every Level Installation Criterion

Flaming	Photo	Ion	Dual Ion/Photo	Aspirated
Living Room	107	70		
Bedroom	54	30		
Bedroom (Door Closed)	186	164		3602
Smoldering				
Living Room	1542	4824	1508	1424
Living w/AC	1366	4192	2030	2072
Cooking				
Kitchen	880	1554	898	858

Every Level + Bedrooms Installation Criterion

Flaming	Photo	Ion
Living Room	107	70
Bedroom	54	30
Bedroom (Door Closed)	186	164
Smoldering		
Living Room	1542	4824
Living w/AC	1338	4192
Cooking		
Kitchen	880	1554

Every Room Installation Criterion

Flaming	Photo	Ion
Living Room	107	70
Bedroom	54	30
Bedroom (Door Closed)	186	164
Smoldering		
Living Room	1542	4824
Living w/AC	1338	4192
Cooking		
Kitchen	880	1290

7.2 Tenability Times

For this report, the tenability time is when the first tenability limit is exceeded 1.5 m (5 ft) from the floor at any point along the primary escape path. It should be noted that the conditions at the instrument locations nearest to and in the same room as the fire were excluded since the codes are not designed to protect people intimate with the initial fire. The tolerance of people to fire conditions is a subject of considerable debate worldwide, because it has significant implications for public safety and for product liability. Deciding on appropriate tolerance limits is highly complex because of the broad variability among people and the need for conservatism to protect the more vulnerable portions of any population.

This topic has been the subject of current work by an international committee of experts working as ISO Technical Committee (TC) 92, subcommittee (SC) 3. This group has published a technical standard, ISO TS 13571 [26], that recommends limits of human tolerance to fire products. These limits are also consistent with the recommendations in the SFPE Handbook of Fire Protection Engineering [23]. Limits for elevated temperature and toxic gas species were taken from ISO TS 13571. For smoke obscuration, an optical density of 0.25 m^{-1} was used as a tenability criterion, a value typically used by the smoke alarm industry.

It should be noted that ISO TS 13571 is considered by most (including its principle authors) to be highly conservative, stating that the “*... values are intended to assure with high confidence that even vulnerable people will not be incapacitated, then killed.*” Thus, any observations based on analyses using these values may look much worse than what would be seen in actual use because tenability is based on the most susceptible of the population. The ISO TS 13571 values represent the best, international consensus so they were used for the primary analysis, but the data has been made available so that others can examine the impact of other limits.

7.3 Time Needed for Escape

As with the original Indiana Dunes tests this report does not select a value of time needed for escape since this is highly variable and is a function of the age and condition of the occupants, travel distances, behavior affecting pre-movement times, etc. An independent analysis of the Indiana Dunes data in 1975 [43] chose 3 min as an (arbitrary) reference number. A subsequent study funded by NIST at the University of Massachusetts (Amherst) [44] found average times needed to awaken sleeping occupants, phone the fire department, and evacuate all family members was about 50 s for families with children and nearly 70 seconds for the elderly.

This section will address escape times for best and worst case fire scenarios occurring in both the manufactured and 2-story homes. The evacuation of occupants in any occupancy consists of a

series of actions beginning with cues received from the fire situation to eventual movement out of the building or refuge within the space. This escape time analysis assumes that the initial cue is provided by the smoke alarm and that the occupants have received, recognized, and interpreted this and other cues of the fire situation. It is difficult to establish a quantitative result for escape time. Movement time has been monitored and recorded in a number of studies, and especially in residential cases, it is simple to obtain an occupant velocity for unimpeded flow (low density). Premovement times, on the other hand, are more difficult to obtain since these response times are not only dependent on the fire situation, but also on the layout of the house, time of day, placement of items in relation to occupants (such as clothes, phone, personal effects), position of occupants in relation to each other (i.e., are the children in the same room, hiding in a closet in the house), and the role of the person(s) in the house in times of emergency (i.e., will they investigate, gather others).

7.3.1 Movement Speed

Movement speeds are calculated using the maximum (unimpeded) exit flow speeds (table 3-14.4 in SFPE Handbook [45]). The population density of the space is low, therefore maximum speeds are considered to be possible. The maximum speed along a horizontal exit route is 1.2 m/s (235 ft/min). The stairs in the two-story home have 18 cm (7 in) risers and 28 cm (11 in) treads, which corresponds to a maximum travel speed of 0.95 m/s (187 ft/min). Stair travel speeds only apply to the two-story dwelling.

For elderly occupants, Ando [46] investigated unimpeded horizontal movement times and determined that travel speed for males and females was dependant upon age. A female around the age of 30, to signify a young occupant, would move at a velocity of 1.2 m/s (235 ft/min) and a female at the age of 70 years would move at approximately 0.75 m/s (148 ft/min). The younger occupant's speed agrees with the SFPE handbook's value for unimpeded movement over horizontal components. Proulx [47] performed a study of drilled-evacuation from four apartment buildings and summarized that occupants over 65 years old moved through the stairway at an unimpeded velocity of 0.43 m/s (85 ft/min).

7.3.2 Premovement Activities

Bryan [48], Wood [49], and Keating [50] have studied premovement actions of residential occupancies after the recognition phase has been completed. These actions (in no specific order) may be divided among the parental unit or taken on by a single person within the household and are the following: notifying others, getting dressed, calling the fire department, investigating, fighting the fire, and leaving. Wood states that the more serious a resident considers the fire to be, the more likely he/she is to leave the building immediately. Also, in his studies, he found that familiarity with the residence did not affect whether a person attempted to immediately exit the building or first retrieve personal items. In a 3 year study of Seattle residents, Keating found

that men were more likely to fight the fire, while women were more likely to request information (which could involve notifying others, the fire department, etc). However, since this study occurred more than 20 years ago, it is not clear that this trend would be presently observed.

Pearson and Joost [51]observed that premovement and movement times will be increased for those scenarios which include elderly occupants. They studied response times during the day and night of young adults in good health, elderly in good health, and elderly with arthritic impairments in a residential experimental facility. When comparing total egress times of all scenarios, the elderly subjects in good health took approximately 27 % longer and the arthritic subjects took 44 % longer than the young adult subjects to perform scenario behaviors and movements. Some response activities noted by Pearson and Joost were accompanied by estimated time. Again, these depend on the situation and are only included to give the reader some idea of the time taken to perform the activities shown in table 25 .

Table 25. Sample premovement activity time

Activity	Response Time (s) for young adults
Dressing - putting on robe	6 to 10
Calling fire department	15
Obtaining personal items (wallet, keys)	5 to 10
Awakening loved ones	5 to 10 per child

7.3.3 Escape Times

For both the two-story home and the manufactured home, several scenarios representing the shortest escape time, as well as a worst case were calculated. These calculated escape times represent reasonable lower and upper bounds, although shorter and longer escape times may be possible. The best case scenario for the manufactured home is an accidental fire where the occupants are located in the kitchen and begin evacuation immediately upon alarm activation. The worst case scenario includes an arthritic elderly couple asleep at the time of fire ignition. One child is present in each bedroom. It is important to note that there is no feedback between the fire and the occupants accounted for in this calculation. This may extend the escape time significantly.

In the manufactured home, a worst-case evacuation would involve one or both occupants walking from bedroom 2, through the kitchen, through the living room, into bedroom 1, then into bedroom 3, and finally out through the living room door. This is estimated to be 41 m (135 ft).

Distances are taken as straight lines (excluding obstacles) and are measured from the furthest corner in any room to the room door. A 41 m travel distance would take an elderly occupant approximately 55 s to traverse at 0.75 m/s. Prior to egress initiation, the occupants are assumed to dress, call the fire department, obtain personal items, and awaken both children. The cumulative response time (as opposed to the movement time) would be 55 s for a young adult family with 2 children to retrieve. For the elderly response times, multiplying 55 s by 1.44 gives a value of 80 s. Thus, the total escape time would be approximately (55 s + 80 s) or 135 s.

For the 2-story dwelling, movement of an elderly couple from the master bedroom, to bedroom 3, to bedroom 2, to the stairs, and out the front door totaled 33.7 m (110 ft) on horizontal surfaces and 5.8 m (19 ft) on the stairs. The movement time for the elderly arthritic couple with two young children present is 58 s. The premovement time for the two-story home would be identical to that of the manufactured home. Thus, the total worst case escape time for the two-story home is (58 + 80) or 138 s.

For the best case scenario, movement times in the manufactured home were calculated for the scenarios that would take the shortest amount of time to complete. This includes a young couple making dinner in the kitchen which results in an accidental grease fire. The distance to evacuate from the kitchen fire is approximately 2.7 m (9 ft.). The kitchen evacuation would take approximately 3 s to 5 s. Pre-movement time was assumed to be 0 s. In the two-story home, the young couple accidentally starts a fire. The distance to evacuate from the kitchen is approximately 11 m (36 ft). The kitchen evacuation would take approximately 10 s.

Additional scenarios are presented in table 26. The young family at night scenario is identical to the worst case scenario, except that the young family moves more quickly and takes less time performing premovement tasks. Additionally, the elderly couple in the kitchen would require a somewhat longer time than the young couple in order to evacuate the home from the kitchen. In conclusion, the manufactured home will require 5 s to 135 s of escape time in order to reasonably protect the occupants. The two-story home will require approximately 10 s to 140 s of escape time. Note that escape times are sensitive to building geometry and occupant behavior assumptions.

Table 26. Estimates of required escape times for best and worst case scenarios

Scenario		Premovement Time (s)		Movement Time (s)		Total Escape Time (s)	
		M. Home	Two-Story	M. Home	Two-Story	M. Home	Two-Story
Worst Case	Young family at night	55	55	35	35	90	90
	Elderly family at night	80	80	55	60	135	140
Best Case	Young couple in kitchen	- a	--	5	10	5	10
	Elderly couple in kitchen	--	--	10	15	10	15

a – best case scenarios neglect any premovement activity; actual escape times are likely to be longer than best case estimates

7.4 Smoke Alarm Performance

Table 27 and figures 206 to 208 present the average (for different alarm times of the same type and multiple tests of each scenario) available egress times for ion, photo, aspirated, and CO alarms as a function of installation requirement (every level, every level + bedrooms, and every room) and fire type (flaming, smoldering, and grease), for the manufactured home tests (tests SDC01 to SDC15 and SDC30 to SDC41). Table 28 includes equivalent results for the two-story home. For heat alarms and sprinklers, only a single location in the room of fire origin was included in the tests. Escape times are calculated as the time to the first alarm activation (for that type of alarm) minus the time to untenable conditions. Negative numbers thus indicate that tenability criteria were exceeded prior to alarm activation. Discussion in this section focuses on the manufactured home tests. Smoke alarm activation times and test tenability times for the two story tests were similar to comparable tests in the manufactured home and are available to facilitate similar analyses for this structure. Appendix B provides detailed data for alarm activation and test tenability.

Increasing alarm coverage from every level to every level plus bedrooms provides room of origin protection for mattress scenarios since the mattress was located in one of the bedrooms. For chair scenarios, this addition would not indicate an increase in protection for the current test series since chairs were never located in bedrooms in these tests.

On average, all of the alarm types provided positive available egress time for all manufactured home fire scenarios, with average available safe egress times ranging from 36 s to 2413 s. The alarms did not, however, provide positive available egress time in every test when the alarms were located only on every level but not in bedrooms. (In one manufactured home flaming mattress test with the doorway closed, the photoelectric alarm responded 22 s after the tenability limit was reached and in one two-story home smoldering chair test, the ionization alarm responded 54 s after the tenability limit was reached.) Ionization type smoke alarms typically provided the longest egress times for flaming (and grease) fires, and photoelectric smoke alarms typically provided the longest escape times for smoldering fires. Similar trends are seen for the two-story home tests, with ionization alarms providing the longest egress times for flaming fires.

As expected, alarm placement can effect the available safe egress time. For the manufactured home tests, including alarms in bedrooms in addition to those on every level increases average available safe egress time by from 3 s to nearly 800 s, depending upon fire scenario, alarm type, and alarm placement. Greater increases were noted for photoelectric (up to 794 s) or dual photoelectric / ionization alarms (up to 301 s) than for the ionization alarms (up to 138 s). No increase was seen for the aspirated photoelectric detector. This may be due to the periodic sampling of this detector. Additional increases were seen for the change from every level + bedrooms to every room. For the two-story home tests, the effect was far less pronounced. This was likely due to the interior design of the home. For fires downstairs, the upstairs hallway alarms were typically the first to respond since there was no soffit to impede smoke flow from the first floor into the stairwell to the alarms at the top of the stairs.

Table. 27. Available egress time (in seconds) for several different alarm technologies and fire scenarios in a manufactured home

Every Level Installation Criterion

Flaming	Photo	Ion	Dual Ion/Photo	Aspirated
Living Room	89	147	142	82
Bedroom	58	93	39	45
Bedroom (Door Closed)	876	1323	1808	852

Smoldering

Living Room	351	137	361	425
Bedroom	1382	120	362	731
Bedroom (Door Closed)	40	54	48	36

Cooking

Kitchen	592	838	899	187
---------	-----	-----	-----	-----

Every Level + Bedrooms Installation Criterion

Flaming	Photo	Ion
Living Room	89	147
Bedroom	76	118
Bedroom (Door Closed)	1411	1461

Smoldering

Living Room	351	137
Bedroom	1548	137
Bedroom (Door Closed)	834	80

Cooking

Kitchen	595	838
---------	-----	-----

Change from Every Level^a

Photo	Ion
18	25

167	17
794	26

3	
---	--

Change from Every Level + Bedrooms^a

Photo	Ion
38	45

2063	427

73	33
----	----

a – blank entry means no change compared to previous installation criterion for this alarm type

Table 28. Available egress time (in seconds) for several different alarm technologies and fire scenarios in a two-story home

Every Level Installation Criterion^a

Flaming	Photo	Ion	Dual Ion/Photo	Aspirated
Living Room	108	152		
Living Room (Replicate)	134	172		
Living Room (Fully-Furnished)	144	172		
Bedroom	350	374		
Bedroom (Door Closed)	3416	3438		
Smoldering				
Living Room	3298	16	3332	3416
Living Room (Air Conditioning)	2773	-54	2108	2066
Cooking				
Kitchen	952	278	934	974

Every Level + Bedrooms Installation Criterion^a

Flaming	Photo	Ion
Living Room	108	152
Living Room (Replicate)	134	172
Living Room (Fully-Furnished)	144	172
Bedroom	350	374
Bedroom (Door Closed)	3416	3438
Smoldering		
Living Room	3298	16
Living Room (Air Conditioning)	2800	-54
Cooking		
Kitchen	952	278

Every Room Installation Criterion^a

Flaming	Photo	Ion
Living Room	108	152
Living Room (Replicate)	134	172
Living Room (Fully-Furnished)	144	172
Bedroom	350	374
Bedroom (Door Closed)	3416	3438
Smoldering		
Living Room	3298	16
Living Room (Air Conditioning)	2800	-54
Cooking		
Kitchen	952	542

a – blank entry means no alarm of this type was included for this test type

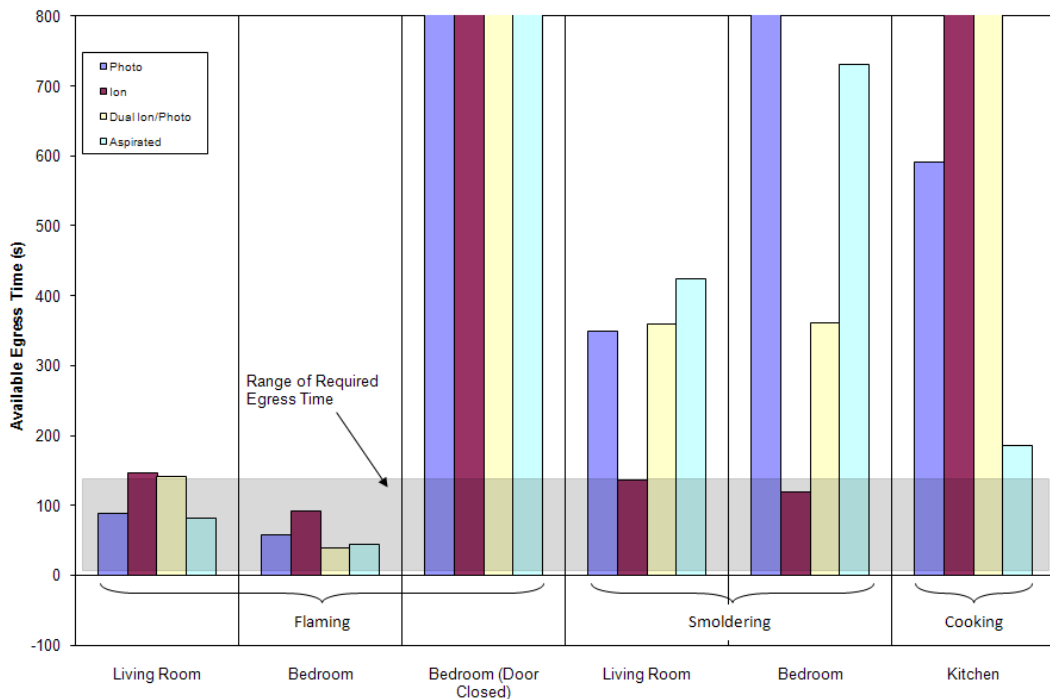


Figure 206. Average available egress time for several different alarm and fire types with alarms on every level for manufactured home tests

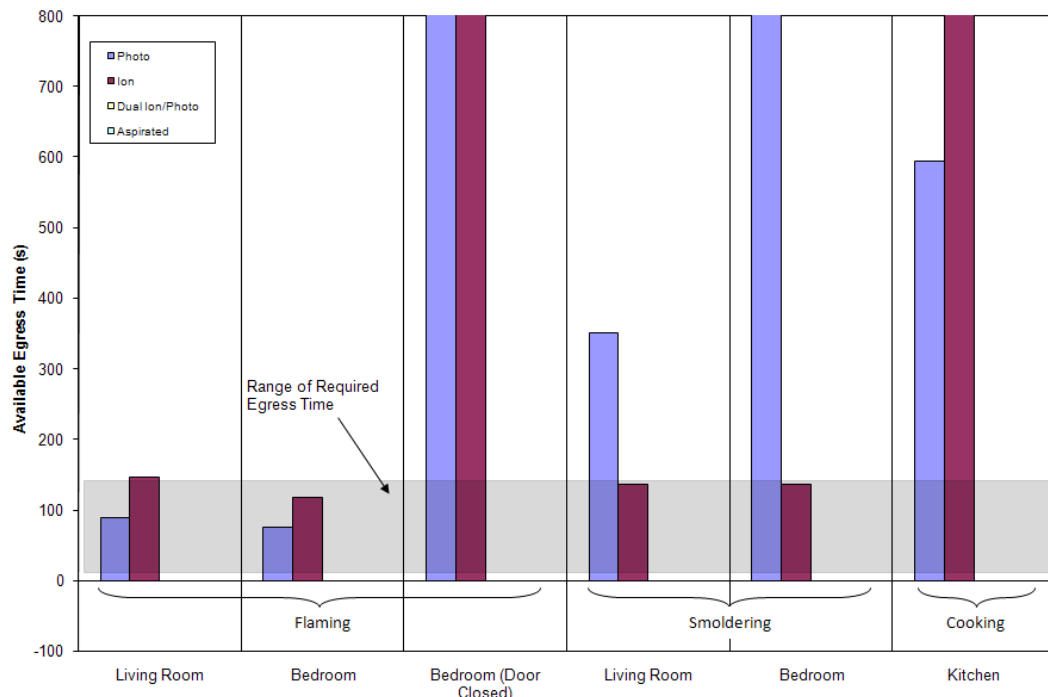


Figure 207. Average available egress time for several different alarm and fire types with alarms on every level + bedrooms for manufactured home tests

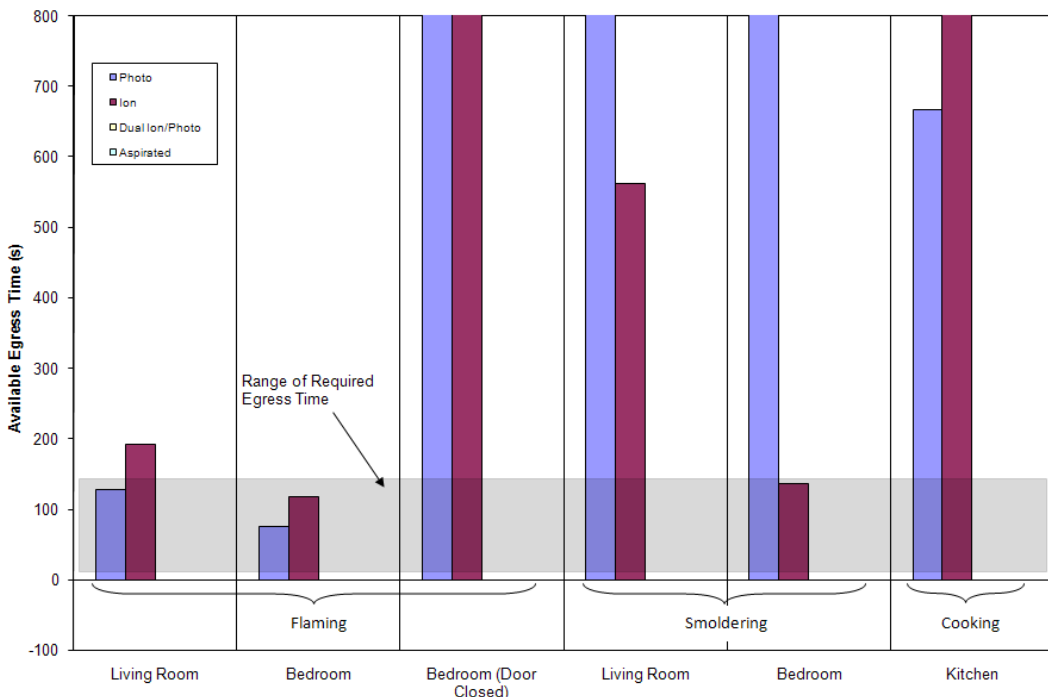


Figure 208. Average available egress time for several different alarm and fire types with alarms in every room for manufactured home tests

It is important to note that there is uncertainty in the estimates of available egress time as noted in section 5.7. For some of the tests, these times were relatively short and in some cases overlapped estimates of the time needed for egress from the buildings. For the most complex egress scenarios (with occupants asleep in all of the bedrooms) with the most sensitive populations (elderly adults with young children requiring egress assistance), the flaming fire scenarios may not provide sufficient time for escape regardless of the alarm technology. Thus, available escape time would be sufficient only if households follow the advice of fire safety educators, including sleeping with doors closed while using interconnected smoke alarms to provide audible alarm in each bedroom, and pre-planning and practicing escape so as to minimize pre-movement and movement times during egress.

7.5 Other Alarm Technologies

Additional fire detection technologies were included in the test fires to provide a point of comparison with the smoke alarms and to provide data for future analysis of fire alarms that may include multiple sensor technologies and complex algorithms to better predict accidental fires and thus reduce false alarms. For residential applications in the U.S. and Canada, carbon monoxide alarms, heat alarms, and residential sprinklers are used in concert with smoke alarms. Table 29 shows average alarm times for these technologies for the different fire scenarios in the

manufactured home. For each alarm technology and fire scenario, the time to alarm is shown for typical alarm criteria (50 ppm for CO alarms; heat alarms and tell-tale sprinklers were determined from an audible alarm and measured pressure drop, respectively). For the manufactured home tests, each alarm time value is an average of available replicates. Individual calculations for all of the alarms in all of the tests is included as Appendix B.

7.5.1 Carbon Monoxide Alarms

The carbon monoxide alarms responded to all fire scenarios, but particularly for scenarios which would be expected to produce significant quantities of carbon monoxide during the combustion process, i.e., smoldering mattress, smoldering chair, and door-closed flaming chair (which smoldered after the room of origin became oxygen limited). Alarm times ranged from 683 s to 3548 s, depending upon fire scenario and alarm placement.

7.5.2 Heat Alarms

Since nearly all of the tests in this study were limited to the very early stages of fire growth, heat alarms typically responded near the end of the tests and after the transition to flaming for smoldering tests. For flaming fires, alarm times ranged from 163 s to 1912 s.

Table. 29. Activation time (in seconds) for several different fire detection technologies and fire scenarios in a manufactured home.

Every Level Installation Criterion

	CO Alarm
Flaming	
Living Room	209
Bedroom	421
Bedroom (Door Closed)	683
Smoldering	
Living Room	3581
Bedroom	3188
Bedroom (Door Closed)	3458
Cooking	
Kitchen	1412

Every Level + Bedrooms Installation Criterion

	CO Alarm
Flaming	
Living Room	209
Bedroom	421
Bedroom (Door Closed)	683
Smoldering	
Living Room	3564
Bedroom	3188
Bedroom (Door Closed)	3458
Cooking	
Kitchen	1399

Every Room Installation Criterion (note a)

Flaming	CO Alarm	Heat Alarm	Tell-tale Sprinkler
Living Room	n.a.	163	246
Bedroom	n.a.	403	137
Bedroom (Door Closed)	n.a.	1912	126
Smoldering			
Living Room	n.a.	5992	5914
Bedroom	n.a.	3798	3983
Bedroom (Door Closed)	n.a.	n.a.	3414
Cooking			
Kitchen	n.a.	1362	1362

a – heat alarms and tell-tale sprinklers were included only in the room of fire origin

n.a. – no additional alarm included of this type

7.5.3 Tell-tale Sprinklers

The purpose of residential sprinklers is to improve protection against injury, life loss, and property protection. In particular, the design is expected to prevent flashover in the room of fire origin and to improve the chance for occupants to escape or be evacuated [52]. In the tests presented in this report, only the very early stages of a fire were studied, up to the point of incapacitation for occupants. Tell-tale sprinklers were included in the room of fire origin to provide a point of comparison between smoke alarms and sprinkler activation. For flaming fires, response time ranged from 126 s to 246 s. For smoldering fires, response occurred shortly after the transition to flaming.

7.6 Comparison with Earlier Tests

In the original 1975 study [1], over 20 detectors of various generic types and nominal sensitivities were exposed to 40 fires in two actual residences. The fire types included flaming and smoldering chairs and mattresses in the family room, basement, and bedroom, as well as JP-4 in a 20 cm (8 in) pan in the kitchen. The detector types included ionization, photoelectric, dual gate (combination ionization and resistance bridge), and rate-of-rise heat detectors. Each location included both a high sensitivity (one percent per foot obscuration) and a low sensitivity (two percent per foot obscuration) detector.

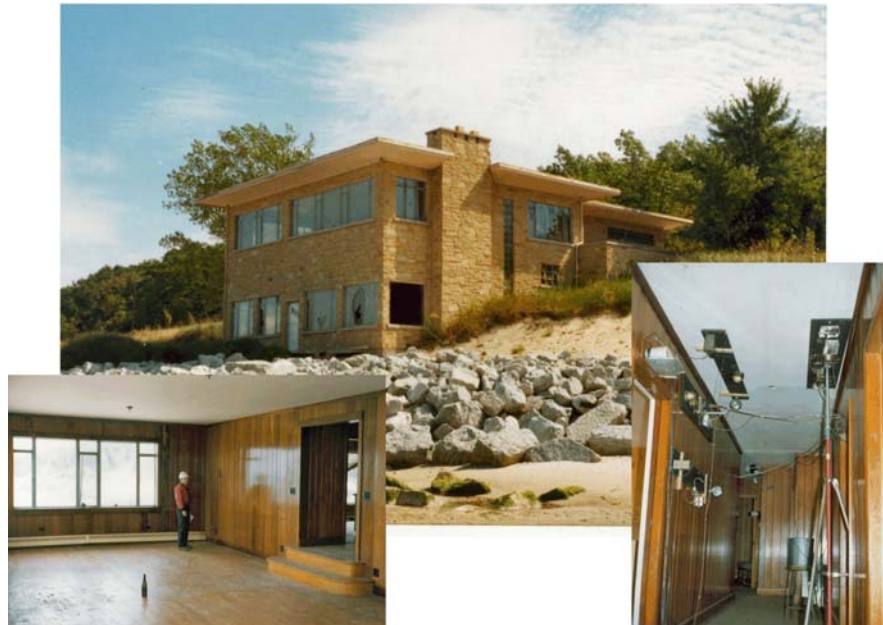


Figure 209. Test structure, sample interior room, and instrumentation in original 1975 Indiana Dunes Experiments

The two test sites were a two-story brick structure with a basement and a single-story brick residence with basement. Instrumentation for both sites included thermocouple arrays, white light beam obscuration measurements, and equipment to monitor oxygen, carbon monoxide, and carbon dioxide. The instrumentation was placed in the room of origin, representative bedrooms, and along the egress path.

Escape times in the current study for the ion type alarms for smoldering fires and for both ionization and photoelectric alarms for flaming fires were positive but somewhat short when compared to the performance of similar smoke alarms in the 1975 test series. Table 30 shows a comparison between the two test series.

These differences appear to be not so much because the alarms are activating more slowly, but rather because the tenability limits are being exceeded much faster. For flaming fires, alarm activation was somewhat shorter in the current tests than in the 1975 tests, and time to untenable conditions was dramatically faster in the current tests. This may be attributed partially to the different ISO tenability criteria compared to simpler limits in the 1975 study, and also due to significantly faster fire development observed in the upholstered furniture and mattresses used in these tests. Table 31 shows a comparison of tenability criteria used in the two studies. For the temperature and smoke obscuration criteria, values used in the current study are similar or slightly higher than those used in the 1975 study. For CO concentration, the range for the FED-based model used in the current study includes the value used in the 1975 study, but is also quite a wide range, depending on duration of the fire. For nearly all tests, the temperature or smoke criteria was met prior to the CO criterion.

A comparison of the fire growth in the two tests can be seen by comparing the temperatures near the ceiling for the tests from the two studies. For this comparison,

Table 30. Comparison of alarm times and times to untenable conditions for 1975 and current studies

		1975 Tests	Current Tests
Alarm Times	Flaming	146 ± 93	47 ± 35
	Smoldering	1931 ± 1103	2042 ± 876
Tenability Times	Flaming	1036 ± 374	177 ± 69
	Smoldering	4419 ± 1790	2148 ± 1023

Table 31. Comparison of tenability criteria used in the 1975 and current studies

	1975 Study	Current Study
Temperature	$T \geq 66^{\circ}\text{C}$	$T \geq 88^{\circ}\text{C}^a$
Gas Concentration	$\text{CO} \geq 0.04\% \text{ volume fraction}$	$\text{CO} \geq 0.02 - 0.3^b\% \text{ volume fraction}$
Smoke Obscuration	$\text{O.D.} \geq 0.23 \text{ m}^{-1}$	$\text{O.D.} \geq 0.25 \text{ m}^{-1}$

a – value for flaming fires calculated from ISO TS 13571 equation for convected heat

b – range of average values calculated from ISO TS 13571 equation for asphyxiant gases with tenability times for flaming fires and smoldering fires

Table 32. Comparison of fire growth rates in the 1975 and current studies

	Time to 65°C near burn room ceiling (s)	
	1975 Study	Current Study
Flaming	969 ± 527	131 ± 40
Smoldering	4893 ± 2236	4332 ± 1893

the time for the temperature near the ceiling to reach 65 °C was used as an indication of the rate of fire growth (table 32). Average time for flaming fires was significantly longer in the 1975 tests than in the current study – 969 s versus 131 s. Average times for smoldering fires in the current test series were comparable to those observed in the 1975 tests. It is important to note, however, that the smoldering fire scenarios are very difficult to reproduce experimentally, and that times in the present study has an uncertainty (based upon one standard deviation) which overlaps the uncertainty in the 1975 study. Therefore, caution should be exhibited in drawing conclusions based upon comparisons of smoldering tenability times between the two studies.

While the 1975 study also used actual upholstered furniture and mattresses, these were purchased from a (charity) resale shop from donated articles. Such items purchased in 1975 would have been new in the early 1960s or even late 1950s and represented materials and constructions of that period. The chairs used in the present study were purchased from a furniture rental store and, while used, were only a year or two old. The mattresses were purchased new. Thus, the materials were certainly significantly different. Fire development in the current tests showed generally similar timing in growth of heat release rate to other recent studies for upholstered furniture [53] and mattresses [54].

In the upholstered furniture study, a set of upholstered chairs was constructed from five different fabric/foam combinations and subjected to a variety of ignition sources suggested by fire statistics. In the study, an effort was made to choose from across the spectrum of typical residential materials although no statistical justification for the particular materials was made. Time to peak heat release rates in excess of those necessary to lead to untenable conditions in structures in the current study ranged from about 150 s to nearly 1000 s. It is estimated that a comparable value for chairs in the current study is about 300 s. For mattresses, time to incapacitation using similar criteria to the current study ranged from 240 s to 1150 s, depending upon the mattress. It is important to note that this study included reduced flammability designs not currently on the market. Thus, the materials used in the current study should not be dramatically different than other currently available materials. Still, it is important to note that while both the 1975 study and the current study attempted to use a representative sample of available and important furnishings, each study included only a small fraction of those available in the marketplace.

Conversely, alarms in the current study were, on average, of similar sensitivity compared to the alarms in the 1975 study. In the current study, the sensitivity of the unmodified smoke alarms were discussed in section 2.6. The average sensitivity measured for all alarms tested was $1.54\text{ %}/\text{ft} \pm 0.45\text{ %}/\text{ft}$. In the 1975 study, the average of all alarms tested was $1.91\text{ %}/\text{ft} \pm 0.73\text{ %}/\text{ft}$. While the average for the 1975 tests is higher, the uncertainty in the data overlaps.

7.7 Nuisance Alarms

Nuisance alarms in residential settings from typical cooking activities, smoking or candle flames are affected by the properties of the aerosol produced and its concentration, the location of an alarm relative to the source, and the air flow that transports smoke to an alarm. This is not surprising, as the same observations have been made in the fire tests here and other studies. This study provides a detailed set of data that can be used to address several issues involving nuisance alarms and reinforces current suggested practices including the following:

- Clearly, the advice that alarms not be installed close to cooking appliances if at all possible is valid. These results show that homeowners who are able to move the location of an alarm that frequently experiences nuisance alarms would do well to maximize its distance from cooking appliances while keeping it in the area to be protected.
- It was observed that ionization alarms had a propensity to alarm when exposed to nuisance aerosols produced in the early stages of some cooking activities, prior to noticeable smoke production. This phenomenon could be particularly vexing to homeowners who experience such nuisance alarms.
- This data set could be used to assess the efficacy of employing an alarm with its sensitivity set to a level near the least sensitive limit allowable, relative to a more sensitive alarm.
- This study can be used to assess the benefits in terms of reduction of nuisance alarms from a typical ionization alarm with the use of a dual photoelectric/ionization sensor alarm that would maintain better overall sensitivity to a variety of fire sources (flaming and smoldering). Combined with the fire test series data, a basis for the sensitivity level settings on each alarm sensor could be proposed that is tied to test data.
- The so-called “hush” button or any other function that decreases sensitivity through human intervention to silence alarms for a fixed time period requires that a sensitivity adjustment and time period be specified. This data set could be used to assess the effectiveness of a sensitivity adjustment for a specific time period before resetting to the base sensitivity relative to these nuisance scenarios. The data could also be used to compare such a feature to other proposed strategies designed to reduce nuisance alarms.
- Carbon monoxide electrochemical cells at all alarm locations gathered data on the level of carbon monoxide produced during the tests and transported to the alarms. These data in conjunction with the complete fire test series data could be used to verify combined smoke/CO alarm algorithms.

The FE/DE nuisance source tests captured salient features of some of the manufactured home tests. Clearly more work needs to be done to produce a set of tests and the performance criteria that covers a significant range of residential nuisance sources, and would assure a benefit in terms of nuisance alarm reduction. This work is part of ongoing research with the FE/DE at NIST.

8 Summary

The data developed in this study include measurement of the output of a number of alarm devices for a range of fire scenarios and residences. In addition, temperature, smoke obscuration, and gas concentrations throughout the structures were monitored during this test series. A summary of the major efforts of this study relative to the original 11 goals presented in section 1.3 are discussed below. Specific conclusions are included in section 9.

1. Evaluate the performance of current smoke-alarm technology

Current smoke alarm technology includes two operating principles – the ionization-type sensor and the photoelectric (scattering) sensor. The project included examples of current products containing each of the sensor designs currently being sold in the U.S. market so that the results would be representative of the full range of product performance expected.

Smoke alarms of either the ionization type or the photoelectric type consistently provided positive escape times. In some cases the escape time provided was relatively short and may overlap with a range of estimates of the time necessary for occupant egress.. Consistent with prior findings, ionization type alarms provided somewhat better response to flaming fires than photoelectric alarms, and photoelectric alarms provided (often) considerably faster response to smoldering fires than ionization type alarms.

In many cases, available escape time would be sufficient only if households follow the advice of fire safety educators, including sleeping with doors closed while using interconnected smoke alarms to provide audible alarm in each bedroom, and pre-planning and practicing escape so as to minimize pre-movement and movement times during egress.

2. Test conditions representative of current fatal residential fires

To ensure that the room sizes and arrangements, materials of construction, and ventilation conditions were representative of actual dwellings, all tests were conducted in real dwelling units. First, a manufactured home was procured and delivered to the NIST site for use in both fire tests and nuisance alarm tests. The floor plan selected was a three bedroom, two bath arrangement with a master suite at one end and the other bedrooms at the other end. This size and arrangement represents not only manufactured homes but also apartments and condominiums of about 100 m² (or about 1000 ft²). A second test site was a three bedroom, two-story, brick home, 139 m² (1490 ft²) in size.

Careful choice of test scenarios helps insure the representativeness of the study. Important factors included the room of fire origin, ignition source and first item ignited, and the ventilation conditions that affected the fire development and combustion chemistry. A review of recent fire statistics was conducted to select the most important fire scenarios representative of fatal and non-fatal fires in the U. S. In addition to the scenarios themselves, the test matrix considered the need to perform sufficient replicates to allow estimates of experimental uncertainty and repeatability.

3. Evaluate the efficacy of current requirements for number and location of smoke alarms

The experimental design provided data on the performance of alarms in various installation arrangements. Groups of alarms were located in the room of fire origin, at least one bedroom, and in a central location on every level. Thus, by considering the alarm times of devices in various locations against tenability times for any test it was possible to determine the escape time provided by various installation arrangements including every room, every level with or without every bedroom, and single detectors. Since both ionization and photoelectric types were included at each location the performance by sensor type is also quantified.

Smoke alarms of either type installed on every level generally provided positive escape times for different fire types and locations. Adding smoke alarms in bedrooms increased the escape time provided, especially for smoldering fires. In addition, occupants of bedrooms sleeping with the door closed would benefit from improved audibility of alarms within the room. This provides data for evaluating whether bedroom smoke alarms should be required in existing homes as they have been in new homes since 1993. It is important to note that the available safe egress times may overlap with the range of estimates of necessary egress time for the residences studied. Some of this is due to conservative tenability criteria based on incapacitation of the most vulnerable occupants that was used for the current study. Use of tenability criteria based on incapacitation or death of healthy individuals would certainly increase the available safe egress time.

Escape times in this study were systematically shorter than those found in a similar study conducted in the 1970s. This is related to some combination of faster fire development times for today's products that provide the main fuel sources for fires, such as upholstered furniture and mattresses, different criteria for time to untenable conditions, and improved understanding of the speed and range of threats to tenability. Still, it is important to note that while both studies attempted to use a representative sample of available and important furnishings, each study included only a small fraction of those available in the marketplace. Since there may be significant differences in the burning behavior between items of furniture, general conclusions are beyond the scope of this study and may warrant additional research.

4. Develop standard nuisance alarm sources to be included in the test program

Smoke alarms are susceptible to alarming when exposed to non-fire aerosols. In residential settings, this typically involves cooking activities or transient, high humidity conditions (i.e., “shower steam”). The approach taken was to define a set of nuisance scenarios, replicate the events that cause nuisance alarms, and quantify the important variables. Translating the results to a set of nuisance source conditions reproducible in a suitable test-bed (i.e., a test room or the fire emulator/detector evaluator) would allow for more comprehensive detector performance testing. Preliminary tests were performed in the FE/DE with this in mind. Programming realistic and reproducible fire and nuisance conditions in the FE/DE is an ongoing research project at NIST.

Experiments conducted with common nuisance sources produced data that should be useful in the development of new performance requirements for conditions that should not activate smoke alarms. Since the data include analog signal levels and duration for each of the sensor types they should be useful in evaluating a range of approaches to nuisance alarm reduction from reducing alarm threshold for a specified time (“hush” feature) to decision algorithms and multi-sensor arrays.

5. Examine other fire detection technologies in combination with smoke alarms

The program included mechanically aspirated (system-type) photoelectric smoke detectors, residential CO alarms, heat alarms, and tell-tale residential sprinklers in the tests along with currently available residential smoke alarms. Activation times for these devices will facilitate future analysis and development of fire detection devices using inputs from multiple sensors.

6. Obtain data on the potential for improvements in performance by new technologies

Simple alarm times for currently available smoke alarms are not sufficient to identify potential performance improvements so analog sensor data were recorded for both the fire performance and nuisance alarm testing. Additional instrumentation was selected and located to supplement the analog sensor data and allow better quantification of results. Examples included thermocouple measurements of temperatures and temperature gradients, smoke and gas species concentrations in several locations, and convective flow velocities in the ceiling layer at the level of the sensors.

7. Include fuel items that incorporate materials and constructions representative of current residential furnishings

Fuel (combustible) items were selected as generically appropriate to the room of origin and fire scenario identified from NFIRS analysis and typical of materials and constructions in common

use today. Specifically, upholstered chairs were used for living room fires and mattresses for bedroom fires that were purchased from local, retail sources. No modifications were made and no accelerants were used to enhance or retard the burning behavior of the items. Cooking oil used in kitchen fires was also a normal commercial product that was not modified in any way.

8. Fully characterize test detectors and alarms in a consistent manner to facilitate comparisons

All detectors (smoke, heat, and CO) were characterized in NIST's FE/DE apparatus under similar conditions using an appropriate source. This allowed direct calibration of all devices in a comparable way and a means to verify the performance of sensors in combination or utilizing algorithms that may be suggested by the results of this study.

9. Utilize fire models to extend the applicability of the test arrangements and maximize the test instrumentation

Modeling, using NIST's CFAST and FDS models, was performed prior to testing to evaluate the impacts of the selected fuels and fire scenarios on the instrumentation and test structures and to assist in identifying the most appropriate instrument locations.

10. Make All of the Data Collected as Widely Accessible as Possible

Clearly the best method of (global) dissemination of the test data was to employ the Internet. Thus, a public web site was established (<http://smokealarm.nist.gov/>) on which the detailed results of tests were published as NIST Reports of Tests. This publication vehicle exists as a means to quickly disseminate test data that is factual in nature – no observations or conclusions were included. Thus the web site contains floor plans of the test sites showing instrument locations, details of the fuels and test conditions, and test data in electronic form.

11. Provide Opportunities to Enhance Public Fire Safety Education

CPSC, USFA, NFPA, and others have significant efforts in public fire safety education. The information obtained in these tests will provide a basis for improving public fire safety messages and will quantify the protection provided by residential smoke alarms. The project data could be used to show the reduction in protection resulting from one or more devices being nonfunctional as a motivation for testing and maintenance by the homeowner. Video recording of all of the tests from multiple locations were made. These recordings will be made available as part of the information on the public web site for use in public safety announcements and educational materials.

Finally, a press day was held that resulted in stories carried on all the major news networks and on more than 75 local outlets from Maine to Hawaii.

9 Conclusions

1. The data developed in this study include measurement of temperature and smoke obscuration in addition to gas concentrations for a range of fire scenarios and residences. Measurement of the response of smoke alarms, CO alarms, heat alarms, and tell-tale sprinklers are also included. These data could be of significant value in developing appropriate algorithms for alarms that may include one or more sensor types.
2. Smoke alarms of either the ionization type or the photoelectric type consistently provided time for occupants to escape from most residential fires.
 - a. In many cases, available escape time would be sufficient only if households follow the advice of fire safety educators, including sleeping with doors closed while using interconnected smoke alarms to provide audible alarm in each bedroom, and pre-planning and practicing escape so as to reduce pre-movement and movement times.
 - b. Smoke alarms may not provide protection for people directly exposed to the initial fire development (so-called "intimate with ignition").
 - c. Consistent with prior findings, ionization type alarms provided somewhat better response to flaming fires than photoelectric alarms, and photoelectric alarms provided (often) considerably faster response to smoldering fires than ionization type alarms.
 - d. Smoke alarms of either type installed on every level generally provided positive escape times for different fire types and locations. Adding smoke alarms in bedrooms increased the escape time provided, especially for smoldering fires. It is important to note that the available safe egress times may overlap with the range of estimates of necessary egress time for the residences studied. Some of this is due to conservative tenability criteria based on incapacitation of the most vulnerable occupants that was used for the current study.
 - e. Escape times in this study were systematically shorter than those found in a similar study conducted in the 1970's. This is related to some combination of different criteria for time to untenable conditions, improved understanding of the speed and range of threats to tenability, and faster fire development times for today's products that provide the main fuel sources for fires, such as upholstered

furniture and mattresses. It is important to note that while both the 1975 study and the current study attempted to use a representative sample of available and important furnishings, each study included only a small fraction of those available in the marketplace. Still, this study is consistent with other recent studies of furniture and mattresses even though there may be significant differences in the burning behavior between items of furniture.

- f. A mechanically aspirated (system-type) photoelectric smoke detector included in the study consistently responded after the other photoelectric smoke alarms, even for smoldering fires where convective flow rates are low and smoke entry might be an issue. Since only one such alarm was included in the study, more general conclusions cannot be drawn.
 - g. Residential sprinklers activated well after the smoke alarms and after the heat alarms in all of the scenarios. While these sprinklers have an outstanding record of saving lives and property, the later activation time implies that residential sprinkler installations should always include smoke alarms (as currently required in NFPA 13D and 13R) to provide greater escape times for those capable of escaping.
4. Experiments conducted with common nuisance sources produced data that should be useful in the development of new performance requirements for conditions that should not activate smoke alarms. Since the data includes analog signal levels and duration for each of the sensor types they should be useful in evaluating a range of approaches to nuisance alarm reduction from reducing alarm threshold for a specified time (“hush” feature) to decision algorithms and multi-sensor arrays.

10 References

- [1] Bukowski, R. W., Waterman, T. E., and Christian, W. J. "Detector Sensitivity and Siting Requirements for Dwellings: A Report of the NBS 'Indiana Dunes Tests.'" NFPA No. SPP-43. Nat. Fire Prot. Assn., Quincy, MA, 1975.
- [2] McGuire, J. H. and Ruscoe, B. E., The Value of a Fire Detector in the Home, Fire Study No. 9 of the Division of Building Research, National Research Council of Canada, Ottawa, 1962
- [3] Hall, J. R., Jr., U. S. Experience with Smoke Detectors and Other Fire Detectors, Who Has Them? How Well Do They Work? When Don't They Work? National Fire Protection Association, 1996.
- [4] U.S. Consumer Product Safety Commission; U.S. Fire Administration; National Fire Protection Association; Congressional Fire Services Institute. , "National Smoke Detector Project," U.S. Consumer Product Safety Commission, Washington, DC, 86 p. 1994.
- [5] Cleary, T. G., "Fire Emulator/Detector Evaluator: Design, Operation, and Performance. International Conference on Automatic Fire Detection "AUBE '01", 12th. Proceedings. National Institute of Standards and Technology. March 25-28, 2001, Gaithersburg, MD, Beall, K.; Grosshandler, W. L.; Luck, H., Editors, National Institute of Standards and Technology, Gaithersburg, MD NIST SP 965; February 2001. 312-323 pp, 2001.
- [6] Smith, Charles, "Smoke Detector Operability Survey: Report on Findings", U.S. Consumer Product Safety Commission, October, 1994
- [7] Bukowski, R. W., "Investigation of the Effects of Heating and Air Conditioning on the Performance of Smoke Detectors in Mobile Home. Final Report."National Bureau of Standards, Gaithersburg, MD, NBSIR 79-1915; 179 p. 1979.
- [8] Milke, J. A.; and McAvoy, T. J., "Analysis of Signature Patterns for Discriminating Fire Detection With Multiple Sensors. Fire Technology, Vol. 31, No. 2, 120-136, May 1995.
- [9] Gottuk, D.; Rose-Pehrsson, S.; Shaffer, R.; and Williams, F. "Early Warning Fire Detection via Probabilistic Neural Networks and Multi-Sensor Arrays." Proceedings of Research and Practice: Bridging the Gap. Fire Suppression and Detection Research Application Symposium. Proceedings. Fire Protection Research Foundation. February 23-25, 2000, Orlando, FL, 365-369

- [10] "Saving Lives, Saving Money, Automatic Sprinkler A 10 Year Study, A detailed history of the effects of the automatic sprinkler code in Scottsdale, AZ," available from the Home Fire Sprinkler Coalition, <http://www.homefiresprinkler.org>, 2003.
- [11] Peacock, R. D., Averill, J. A., Bukowski, R. D., and Reneke, P. A., "Home Smoke Alarm Project: Manufactured Home Tests," Natl. Inst. Stand. Technol., Report of Test FR 4016, 2001.
- [12] Averill, J. A., Peacock, R. D., Bukowski, R. W., and Reneke, P. A., "Home Smoke Alarm Project: Two-Story Home Tests," Natl. Inst. Stand. Technol., Report of Test FR 4017, 2002.
- [13] Babrauskas, V., Peacock, R. D., Janssens, M., and Bathos, N. E., "Standardization and Presentation of Fire Data: The FDMS," Fire and Materials, Vol. 15, pp. 85-92, 1991.
- [14] "Standard for Safety Single and Multiple Station Smoke Alarms, UL 217," Underwriters Laboratories Inc., Northbrook, IL.
- [15] Cleary, T. G., "Home Smoke Alarm Project: Alarm Response Calibration," Natl. Inst. Stand. Technol., Report of Test FR 4019, 2003.
- [16] Helsper, C., Fissan, H., Muggli, J., and Scheidweiler, A., "Verification of Ionization Chamber Theory," Fire Technology, Vol. 19, No.. 1, pp. 14-21, 1983.
- [17] Hosemann, J., P., "Über Verfahren zur bestimmung der Korngrossenverteilung hochkonzentrierter Polydispersionen von dielektrischen Miepartikeln," Ph.D. thesis, Aachen, 1970.
- [18] Smith, L., U. S. Consumer Product Safety Commission, private communication, June 1999.
- [19] "NFPA 101, Life Safety Code, 2003 Edition," Volume 6 of the National Fire Codes, Natl. Fire Protection Association, Quincy, MA (2003).
- [20] "SFPE Engineering Guide to Performance-Based Fire Protection Analysis and Design of Buildings," NFPA No. SFPE-00, Natl. Fire Protection Association, Quincy, MA (2000).
- [21] Peacock, R. D. and Babrauskas, V. "Analysis of Large-scale Fire Test Data." Fire Safety Journal 17, pp. 387 – 414, 1991.
- [22] Peacock, R. D., Bukowski, R. W., Reneke, P. A., Averill, J. D., and Markos, S. H., "Development of a Fire Hazard Assessment Method to Evaluate the Fire Safety of Passenger Trains." Proceedings of the Fire and Materials 2001 Conference, January 22-24, San Francisco, Interscience Communications, London, pp 67-78.

- [23] The SFPE Handbook of Fire Protection Engineering, 2nd Ed. P. J. DiNenno, Editor. Natl. Fire Prot. Assoc., Quincy, MA, 1995.
- [24] Peacock, R. D., Averill, J. A., Bukowski, R. W., and Reneke, P. A., "Home Smoke Alarm Project, Manufactured Home Tests," NIST Fire Research Report of Test FR4016, Natl. Inst. Stand. Technol., <http://smokealarm.nist.gov/Series1.htm>, June 2002.
- [25] Averill, J. A., Peacock, R. D., Bukowski, R. W., and Reneke, P. A., "Home Smoke Alarm Project, Two-Story Home Tests," NIST Fire Research Report of Test FR4017, Natl. Inst. Stand. Technol., <http://smokealarm.nist.gov/Series2.htm>, June 2002.
- [26] Life threat from fire – Guidance on the estimation for time available for escape using fire data, Proposed Technical Specification, ISO/TS 13571, International Organization for Standardization. 2002.
- [27] "NFPA 72, National Fire Alarm Code, 1999 Edition," Volume 5 of the National Fire Codes, Natl. Fire Protection Association, Quincy, MA (2002).
- [28] "NFPA 101, Life Safety Code, 2000 Edition," Volume 6 of the National Fire Codes, Natl. Fire Protection Association, Quincy, MA (2002).
- [29] Mulholland, G. W., and Liu, B. H., "Response of Smoke Detectors to Monodisperse Aerosols," Journal of Research of the National Bureau of Standards, Vol. 85, No. 3, pp. 223-238, May-June, 1980.
- [30] Litton, C. D., "A Mathematical Model for Ionization-type Smoke Detectors and the Reduced Source Approximation," Fire Technology, Vol. 13, pp. 226-273, 1977.
- [31] Mulholland, G. W., and Croarkin, C., "Specific Extinction Coefficient of Flame Generated Smoke," Fire and Materials, Vol. 24, pp. 227-230, 2000.
- [32] Cleary, T.G., "Measurements of the Size Distribution and Aerodynamic Properties of Soot," MS Thesis, University of Maryland, 1989.
- [33] Cleary, T.G., Weinert, D.W., and Mulholland, G.W., "Moment Method for Obtaining Particle Size Measures of Test Smokes", Natl. Inst. Stand. Technol., NISTIR 7050, 2003.
- [34] Shapiro, Julie, (Smoke Detector Operability Survey: Engineering Laboratory Analysis", U.S. Consumer Product Safety Commission, October, 1994.
- [35] Gottuk, D.T., Peatross, M.J., Roby, R.J., and Beyler, C.L., "Advanced Fire Detection Using Multi-signature Alarm Algorithms", Proceedings of the 11th Int. Conf. on Automatic Fire Detection (AUBE '99), March 16-18, 1999, Duisburg, Germany, Ed. Luck, H., pp. 237-246, 1999.

- [36] Ishii, H., Ono, T., Yamauchi, Y., Ohtani, S., "Fire Detection System by Multi-layered Neural Network with Delay Circuit", Proceedings of the 4th International Symposium on Fire Safety Science, July 13-17, 1994, Ottawa, Canada, Ed. T. Kashiwagi, pp. 761-772, 1994.
- [37] Cleary, T., and Ono, T., "Enhanced Residential Fire Detection by Combining Smoke and Carbon Monoxide Sensors", Proceedings of the 12th Int. Conf. on Automatic Fire Detection (AUBE '01), March 26-38, 2001, Gaithersburg, MD, Eds., Beall, K., Grosshander, W., and Luck, H., pp. 346-357, 2001.
- [38] Meacham, B.J., "The Use of Artificial Intelligence Techniques for Signal Discrimination in Fire Detection Systems", J. of Fire Prot., Engr., Vol. 6, No. 3, pp 125-136, 1994.
- [39] UL 268: Standard for Smoke Detectors for Fire Protective Signaling Systems, 4th ed., Underwriters Laboratories Inc., Northbrook, IL, 1996.
- [40] EN 54: Components of Automatic Fire Detection Systems, Part 9, Fire Sensitivity Test, European Committee for Standardization, Brussels, 1982.
- [41] Cleary, T. G., "Home Smoke Alarm Project: Alarm Response to Nuisance Sources," Natl. Inst. Stand. Technol., Report of Test FR 4020, 2003.
- [42] see, for example, International Building Code 2000, International Code Council, Falls Church, VA, 2000.
- [43] Wilson, R. "Computer Analysis of Data on Fire Detectors Available for Purchase in Massachusetts." Data From the National Bureau of Standards Indiana Dunes Tests Record, Firepro, Inc., Wellesley Hills, MA, National Bureau of Standards, Gaithersburg, MD, 11 p. January 28, 1976.
- [44] Nober, E. H.; Peirce, H.; Well, A. D.; Johnson, C. C.; Clifton, C. "Waking Effectiveness of Household Smoke and Fire Detection Devices. Fire Journal, Vol. 75, No. 4, 86-91, 130, July 1981.
- [45] Nelson, Harold E. and Mowrer, F. W. "Emergency Movement." In *The SFPE Handbook of Fire Protection Engineering, 3rd Edition*. National Fire Protection Association, Quincy, MA (2002).
- [46] Ando, K., Ota, H., and Oki, T. "Forecasting The Flow of People." *Railway Research Review* (45) pp. 8-14, 1988.
- [47] Proulx, G. "Evacuation Time and Movement in Apartment Buildings." National Research Council of Canada, Ottawa, Ontario, *Fire Safety Journal*, Vol. 24, No. 3, 229-246, 1995.

- [48] Bryan, J. L. "Project People - A Study of Human Response in Fire Incidents." Maryland University, College Park. Alena Enterprises of Canada. *Fire Retardents: Proceedings of 1977 International Symposium on Flammability and Fire Retardants*. May 19-20, 1977, Washington, DC, Technomic Publishing Co., Inc., Westport, CT, Bhatnagar, V.M., Editor, 103-127 pp, 1979.
- [49] Wood, P. G. "Survey of Behavior in Fires." Surrey Univ., Guildford, England, Fires and Human Behavior, John Wiley and Sons, New York, Canter, D., Editor(s), 83-95 p., 1980.
- [50] Keating, J. P. and E. L. Loftus. "Post Fire Interviews: Development and Field Validation of the Behavioral Sequence Interview Technique." Final Report. Natl Bur. Stand. (U. S.), NBS GCR 84-477, October 1984.
- [51] Pearson, R. G., and Joost, M. G. "Egress Behavior Response Time of Handicapped and Elderly Subjects to Simulated Residential Fire Situations." Natl Bur. Stand. (U. S.), NBS GCR 83-429, 1983.
- [52] NFPA 13R: Installation of Sprinkler Systems in One- and Two-Family Dwellings and Manufactured Homes, 1999 Edition, 2002 National Fire Codes. National Fire Protection Association, Quincy, MA, 2002.
- [53] Cleary, T. G., Ohlemiller, T. J., and Villa, K. M., "The Influence of Ignition Source on the Flaming Fire Hazard of Upholstered Furniture." Natl. Inst. Stand. Technol., NISTIR 4847, 1992.
- [54] Ohlemiller, T. J., and Gann, R. G., "Estimating Reduced Fire Risk Resulting From an Improved Mattress Flammability Standard." Natl. Inst. Stand. Technol., Tech. Note 1446, 2002.

Appendix A

Alarm Activation and Time to Untenable Conditions During Tests of Residential Smoke Alarms Included in the Study

Calculated Alarm Times

For each alarm included in each test of the program, data are included that identify the alarm, its inclusion within several alarm placement scenarios, calibration data for the alarm, and estimated alarm times for different assumed alarm thresholds. Columns in the data include

Key – the alarm type as “Alarm” for an analog-modified alarm, “Dalarm” for an unmodified alarm, “Sprinkler” for a tell-tale residential sprinkler, or COalarm for a carbon monoxide alarm.

Position – the room where the alarm was located

Level, level + br, all – identifies whether the alarm was included in an alarm placement scenario of “Every Level”, “Every Level + Bedrooms”, or “Every Room” as described in chapter 7 of the report.

dual – the alarm was part of a dual sensor alarm

name – specific alarm identification as detailed in section 2.5

label – a short alarm identification included in test data spreadsheets for this alarm

units – recording units for the measurement as recorded by the data acquisition system during the test, V or mV

m0, m1 – calibration constants for the alarm as detailed in table 1.

ave – average steady-state clear-air alarm output calculated as a average value prior to ignition, V or mV consistent with “units” column

low, mid, high – estimated alarm times for low, medium and high alarm threshold values, s

last data column (unlabelled) – end of test measured from ignition, s

Individual Alarms

Individual Alarms

Individual Alarms

Individual Alarms

Individual Alarms

Individual Alarms

Individual Alarms

Individual Alarms

Individual Alarms

Individual Alarms

Individual Alarms

Individual Alarms

Individual Alarms

Individual Alarms

Individual Alarms

Individual Alarms

Individual Alarms

Individual Alarms

Calculated Times to Untenable Conditions

Tenability Times

	A	B	C	D	E	F	G	H	I	J	K	L	M	N	O	P	
1		1	2	3	4	5	6	7	8	9	10	11	12	13	14		
2																	
3	Series	Manufactured Home Series #1															
4																	
5	Test	SDC01	Smoldering Chair in Living Room														
6																	
7	Time		1														
8																	
9	ISO Gas FED = 0.3																
10			CO2	CO2 Offset	CO2 Base	CO	CO Offset	HCN	HCN Offset	ASET	Final Value	Minimum		Outside Room of Origin			
11	Master Bedroom (A)	FEDG	GASA_3	0.070961	0.06	GASA_1	0.008282	-	-		0.238	4447	(ISO Gas)	6277	(Smoke)		
12	Utility Hallway (C)	FEDG	GASC_3	0.066902	0.06	GASC_1	0.000505	-	-		0.256						
13	Front Door Hallway (F)	FEDG	GASF_3	0.064811	0.06	GASF_1	0	-	-		0.065						
14	Burn Room (BEK)	FEDG	GASB_3	1.0265	0.06	GASB_1	0.076412	-	-	4447	0.300						
15																	
16	NIST Gas FED = 0.3																
17			CO2	CO2 Offset	CO2 Base	CO	CO Offset	HCN	HCN Offset	ASET	Final Value						
18	Master Bedroom (A)	FEDGN	GASA_3	0.070961	0.06	GASA_1	0.008282	-	-		0.000						
19	Utility Hallway (C)	FEDGN	GASC_3	0.066902	0.06	GASC_1	0.000505	-	-		0.000						
20	Front Door Hallway (F)	FEDGN	GASF_3	0.064811	0.06	GASF_1	0	-	-		0.000						
21	Burn Room (BEK)	FEDGN	GASB_3	1.0265	0.06	GASB_1	0.076412	-	-		0.000						
22																	
23	ISO Convected Heat = 0.3																
24			Temperature														
25	Master Bedroom (A)	FEDH	TCA_4							ASET	Final Value						
26	Burn Room Bedroom (B)	FEDH	TCB_4								0.145						
27	Utility Hallway (C)	FEDH	TCC_4								0.177						
28	Hallway Outside Burn Room Bedroom (D)	FEDH	TCD_4								0.155						
29	Living Room (E)	FEDH	TCE_4								0.162						
30	Front Door Hallway (F)	FEDH	TCF_4								0.172						
31	Closed Bedroom (G)	FEDH	TCG								0.171						
32											0.114						
33	Smoke Obscuration = 0.25 m-1																
34			OD														
35	Master Bedroom (A)	Smoke	SMA_4							ASET	Final Value						
36	Burn Room Bedroom (B)	Smoke	SMB_4								6277	0.255					
37	Utility Hallway (C)	Smoke	SMC_4									0.127					
38	Hallway Outside Burn Room Bedroom (D)	Smoke	SMD_4									5397	0.250				
39	Living Room (E)	Smoke	SME_4										0.078				
40	Front Door Hallway (F)	Smoke	SMF_4										6172	0.267			
41	Closed Bedroom (G)	Smoke	SMG											6012	0.257		
42															0.000		



National Research
Council Canada

Conseil national
de recherches Canada

NRC-CNR

FTIR Gas Measurement in Home Smoke Alarm Tests

Research Report 107

Date of Issue: September 2002

Authors: Joseph Z. Su
Malgosia Kanabus-Kaminska

Published by
Institute for Research in Construction
National Research Council Canada
Ottawa, Canada
K1A 0R6

FTIR GAS MEASUREMENT IN HOME SMOKE ALARM TESTS

By

Joseph Z. Su and Malgosia Kanabus-Kaminska

Fire Risk Management Program
Institute for Research in Construction
National Research Council of Canada

ABSTRACT

The National Research Council of Canada performed Fourier Transform Infrared (FTIR) gas measurements during fire detection experiments (Tests 1–14) in a manufactured home, as part of a joint study with several U.S. organisations and federal agencies to evaluate current requirements and technology of residential smoke detectors. The objectives were to identify toxic species (such as HCl, HCN, NO_x, HBr and HF) produced from test fires and to quantify their concentrations for use in determination of the onset of untenable conditions.

Fire scenarios included flaming and smouldering fires of a mattress in a bedroom, upholstered chair in the living area and cooking oil fires. The size, growth rate and duration of the test fires were closely controlled to create small, slow smouldering fires (1 to 2 hours) and short flaming fires (3 minutes or less). While these test fires provided the greatest challenge for smoke detectors to detect the fires early before becoming fully developed ones, the experiments were terminated well before reaching conditions that would produce a significant amount of toxic species.

FTIR spectra collected during all these tests show spectral features from CO, CO₂ and water vapour. FTIR spectra collected during the chair and mattress smouldering and cooking oil fires also show absorption characteristic of volatile hydrocarbon compounds. There was no apparent absorption from chemical species such as HCl, NO_x, HBr and HF in the FTIR spectra. These chemical species were below the minimum detection limit of the FTIR spectrometer in this full-scale experimental set-up. HCN was only detected in Test 14 with an under-ventilated condition and its maximum concentration was 60 ppm. Carbon monoxide and carbon dioxide were primary gas products produced in these fire detection tests.

TABLE OF CONTENTS

1.0	INTRODUCTION	1
2.0	EXPERIMENTS	2
3.0	RESULTS AND DISCUSSION	8
3.1	Smouldering Chair (Tests 1 and 11).....	8
3.2	Flaming Chair (Tests 2 and 10)	8
3.3	Smouldering Mattress (Tests 3, 4, 6 and 8).....	9
3.4	Flaming Mattress (Tests 5, 7, 9 and 14).....	9
3.5	Cooking Oil Fire (Tests 12 and 13).....	10
3.6	Primary Gas Products (CO and CO ₂).....	11
3.7	Secondary Gas Products	11
4.0	CONCLUSIONS	25
5.0	ACKNOWLEDGEMENTS	25
6.0	REFERENCES	25

LIST OF FIGURES

Figure 1.	Manufactured home and FTIR measurement system	4
Figure 2.	Plan view of a manufactured home, fire locations and FTIR gas sampling locations.....	5
Figure 3.	Upholstered chairs before and after smouldering and flaming fire tests	6
Figure 4.	Twin-size mattresses before and after smouldering and flaming fire tests	7
Figure 5.	4-min average of FTIR spectra for fire location after first smoke alarm (Test 1)	12
Figure 6.	4-min average of FTIR spectra for fire location (Test 1)	12
Figure 7.	4-min average of FTIR spectra for the master bedroom (Test 1)	12
Figure 8.	4-min average of FTIR spectra for the master bedroom (Test 1)	13
Figure 9.	2-min average of spectra from fire location before water discharge in Test 2.....	13
Figure 10.	1-min average of spectra at peak smoke obscuration in the master bedroom (Test 2).....	13
Figure 11.	Average of spectra for fire location in the last 4 minutes of mattress smouldering (Test 4).....	14
Figure 12.	Average spectrum for the fire room during peak smoke obscuration in Test 6 with mattress smouldering	14
Figure 13.	1-min average of spectra for the fire room after first smoke alarm in Test 8 with mattress smouldering	14
Figure 14.	Average of spectra for the fire room during the 50-s flaming in Test 4	15
Figure 15.	Average of spectra for the fire room during the 60-s flaming in Test 6	15

Figure 16. Average of spectra for the fire room during the 100-s flaming in Test 8	15
Figure 17. 1-min average of spectra for the fire room during suppression in Test 4.....	16
Figure 18. 4-min average of spectra for the master bedroom during/after suppression (Test 4).....	16
Figure 19. 2-min average of the spectra for the fire room during mattress flaming (Test 5)....	16
Figure 20. 3-min average of the spectra for the fire room during mattress flaming (Test 7)....	17
Figure 21. 2-min average of the spectra for the fire room during mattress flaming (Test 9)....	17
Figure 22. 2-min average of the spectra for the fire room after fire extinguishment (Test 9)....	17
Figure 23. Average of the spectra for the fire room during the last 30 s of mattress smouldering (Test 14)	18
Figure 24. 30-s average of the spectra for the fire room after mattress flaming (Test 14)	18
Figure 25. 90-s average of the spectra for the fire room after water spray (Test 14)	18
Figure 26. 60-s average of the spectra for the fire room after all doors opened (Test 14)	19
Figure 27. Average of spectra for last 2 minutes of cooking-oil heating (Test 13)	20
Figure 28. Average of spectra for last 2 minutes of cooking oil flaming (Test 13).....	20
Figure 29. 2-min average of spectra after cooking-oil fire extinguishment (Test 13)	20
Figure 30. Carbon dioxide concentration in master bedroom from FTIR and NDIR measurements for flaming chair (Test 2).....	21
Figure 31. Carbon dioxide concentration in master bedroom from FTIR and NDIR measurements for smouldering chair (Test 11).....	21
Figure 32. Carbon dioxide concentration in fire room from FTIR and NDIR measurements for flaming mattress (Test 5)	22
Figure 33. Carbon dioxide concentration in fire room from FTIR and NDIR measurements for smouldering mattress (Test 6)	22
Figure 34. Carbon dioxide concentration in master bedroom from FTIR and NDIR measurements for cooking oil fire (Test 12)	23
Figure 35. Carbon monoxide concentration in fire room from FTIR and NDIR measurements for flaming mattress (Test 5).....	23
Figure 36. Carbon monoxide concentration in fire room from FTIR and NDIR measurements for smouldering mattress (Test 6).....	24
Figure 37. Carbon monoxide concentration in master bedroom from FTIR and NDIR measurements for flaming chair (Test 10).....	24

FTIR GAS MEASUREMENT IN HOME SMOKE ALARM TESTS

by

Joseph Z. Su and Malgosia Kanabus-Kaminska

Fire Risk Management Program
Institute for Research in Construction
National Research Council of Canada

1.0 INTRODUCTION

Smoke alarms are important and cost-effective fire protection devices in residential dwellings, providing fire detection and evacuation warnings for occupants in case of fires. Between 1985 and 1995, Canada's death rate in fires declined by more than 40 per cent, much of this decline is attributed to the use of residential smoke alarms and the enforcement of relevant codes and standards. This is also the case in the United States where the fire death rate has declined by approximately 50% since 1975.

In spite of this, the fire protection community has an ongoing task to maximize the benefit of current smoke detector technologies and develop new technologies in order to improve residential fire safety. As a contributor, the National Research Council of Canada (NRC) joined forces with several U.S. organizations and federal agencies to evaluate the current state of residential smoke detector requirements (known as the Dunes II Tests). This experimental program, commissioned by the U.S. Fire Administration and U.S. Consumer Product Safety Commission and executed by the National Institute of Standards and Technology (NIST), are another systematic evaluation of residential smoke detector technologies, 25 years after the first Indiana Dunes Tests [1].

The research involved 2 series of full-scale fire detection experiments. Series 1 experiments were conducted in a manufactured home at a NIST test site [2]. Series 2 experiments were conducted in a two-storey single house in Kinston, North Carolina [3]. The research program began in October 2000 and is completed in September 2002. The research aimed to determine the response of smoke, heat, and carbon monoxide detectors to modern residential fires and the available egress time before the onset of untenable conditions. General information on the research program is on the web site <http://smokealarm.nist.gov/>.

Inhalation of toxic smoke generated by fires has been the major cause of fire fatalities. NRC's role in this important testing program has been to provide expertise in performing Fourier Transform Infrared (FTIR) measurement and analysis of smoke and toxic gases (such as HCl, HCN, NO_x, HBr and HF) during fire detection experiments and to participate in the project steering committee. The objectives were to identify and quantify the concentrations of harmful species produced from test fires and to provide data for use in determination of the onset of untenable conditions.

NRC participated in, and performed the FTIR gas measurement during Series 1 experiments in the manufactured home at the NIST site (Tests 1–14 in May and June 2001). The results of the FTIR measurement and data analysis for toxic gases are documented in this report.

2.0 EXPERIMENTS

Experimental details of detector placement, instrumentation for various measurements (temperature, heat release rate, mass loss rate, smoke properties, response of various detectors, etc.) and test conditions are described in the NIST report [2]. The following sections only address matters that directly relate to the FTIR gas measurement.

Figure 1 shows a manufactured home and FTIR measurement system that were used in full-scale fire detection experiments. This was a 900-square-foot one-storey house with 3 bedrooms, a bathroom, a kitchen, and a living area. Figure 2 shows a plan view of the test house, fire locations, and FTIR measurement points.

Fire scenarios included flaming and smouldering fires of a twin-size mattress in the end bedroom and an upholstered chair in the living area. Figures 3-4 show chair and mattress fuel packages and ignition sources used in the experiments. The flaming fire was started using an electric match that was inserted into a fold of the upholstered chair or mattress. The smouldering fire was started using an electric nichrome-wire loop (3.8-cm or 10-cm diameter) that was inserted into the polyurethane foam of the chair or mattress. An autotransformer was used to regulate the electric current to the smouldering loop in order to control the heat. Fire scenarios also included cooking oil fires, ignited by heating corn oil (500 mL) on a gas burner. These fuel packages were representative of common household items that were often first ignited in real fire incidents. In each experiment, the electric power to the ignition source or the gas burner was turned on 3 minutes after the start of the test.

NRC performed FTIR gas measurements during 14 full-scale fire detection experiments (8 experiments with fire origin in the end bedroom, 4 experiments with fire origin in the living area and 2 experiments with fire origin in the kitchen). Four gas sampling ports were located along the centre line of the house as shown in Figure 2. These included a ceiling sampling port (2.4 m above floor) in each of the 3 rooms of fire origin, and a target sampling port in the remote master bedroom at 1.5 m above floor (0.6 m from the end wall).

Each experiment involved a ceiling sampling port in the room of fire origin and the target sampling port for the gas measurement. Gas samples were drawn by pumps from the ceiling sampling port in the room of fire origin and the target sampling port in the master bedroom through two gas sampling lines to 2 FTIR spectrometers, respectively. Pyrex cylindrical gas cells (one with 10-cm pathlength and 110-mL volume, the other with 100-cm pathlength and 120-mL volume) with KBr optics were used for the FTIR spectrometers. The gas samples flowed through the gas cells at a flow rate of 9 L/min. To prevent the condensation of sample gases, the sampling lines and gas cells were heated (the temperature setting was 93°C for the line to the fire room and 121°C for the line to the master bedroom). The infrared light that emitted from the spectrometer passed through the gas cell. The FTIR spectrometers scanned the gas samples over a wide frequency range of 400 to 4500 cm⁻¹ at a 1-cm⁻¹ resolution.

Chemical compounds that give rise to a permanent or oscillating dipole moment can absorb the infrared light at unique characteristic frequencies, which serve as their "fingerprints". Species, such as HCl, HCN, NO_x, HBr and HF, absorb the infrared light and leave "fingerprints" at their characteristic frequencies in the infrared spectrum. The magnitude of the absorption of each species at its characteristic frequencies is a function of its concentration. With calibration of the FTIR spectrometers using standard gases at known concentrations, the concentration of each species produced during fire experiments can be quantified.

Table 1 shows a matrix of the FTIR measurement during the fire experiments. The bathroom window was partially open (33 cm x 20 cm opening) to make up air in the house. All exterior doors and other windows were closed during each experiment. The master bedroom door was always open. The doors of the smallest bedroom and the bathroom were always closed. The end bedroom door was open unless otherwise specified.

TABLE 1

FTIR Measurement during Tests in Manufactured Home (May and June, 2001)

	Test 1	Test 2	Test 3	Test 4	Test 5
Fire Origin	Living Area	Living Area	End Bedroom	End Bedroom	End Bedroom
Fuel	Upholstered Chair	Upholstered Chair	Mattress	Mattress	Mattress
Burning Mode	Smouldering	Flaming	Smouldering	Smouldering	Flaming
Burst to Flame at	2 h 8 min	3 min	no flame	58 min	3½ min
FTIR Gas Sampling	2 h 11 min	15 min	1 h 33 min	1 h 10 min	14 min

	Test 6	Test 7	Test 8	Test 9	Test 10
Fire Origin	End Bedroom	End Bedroom	End Bedroom	End Bedroom (Door Closed)	Living Area
Fuel	Mattress	Mattress	Mattress	Mattress	Upholstered Chair
Burning Mode	Smouldering	Flaming	Smouldering	Flaming	Flaming
Burst to Flame at	1 h 42 min	3½ min	1 h 4 min	3 min	7½ min (2 nd ignition)
FTIR Gas Sampling	1 h 52 min	15 min	1 h 11 min	25 min	15 min

	Test 11	Test 12	Test 13	Test 14	
Fire Origin	Living Area	Kitchen	Kitchen	End Bedroom (Door Closed)	
Fuel	Upholstered Chair	Cooking Oil	Cooking Oil	Mattress	
Burning Mode	Smouldering	Flaming	Flaming	Smouldering / Flaming	
Burst to Flame at	1 h 13 min	26 min	25 min	1 h	
FTIR Gas Sampling	1 h 20 min	33 min	36 min	1 h 14 min	

Note: the electric power to the ignition source or the gas burner was turned on 3 min after start of a test.



Figure 1. Manufactured home and FTIR measurement system

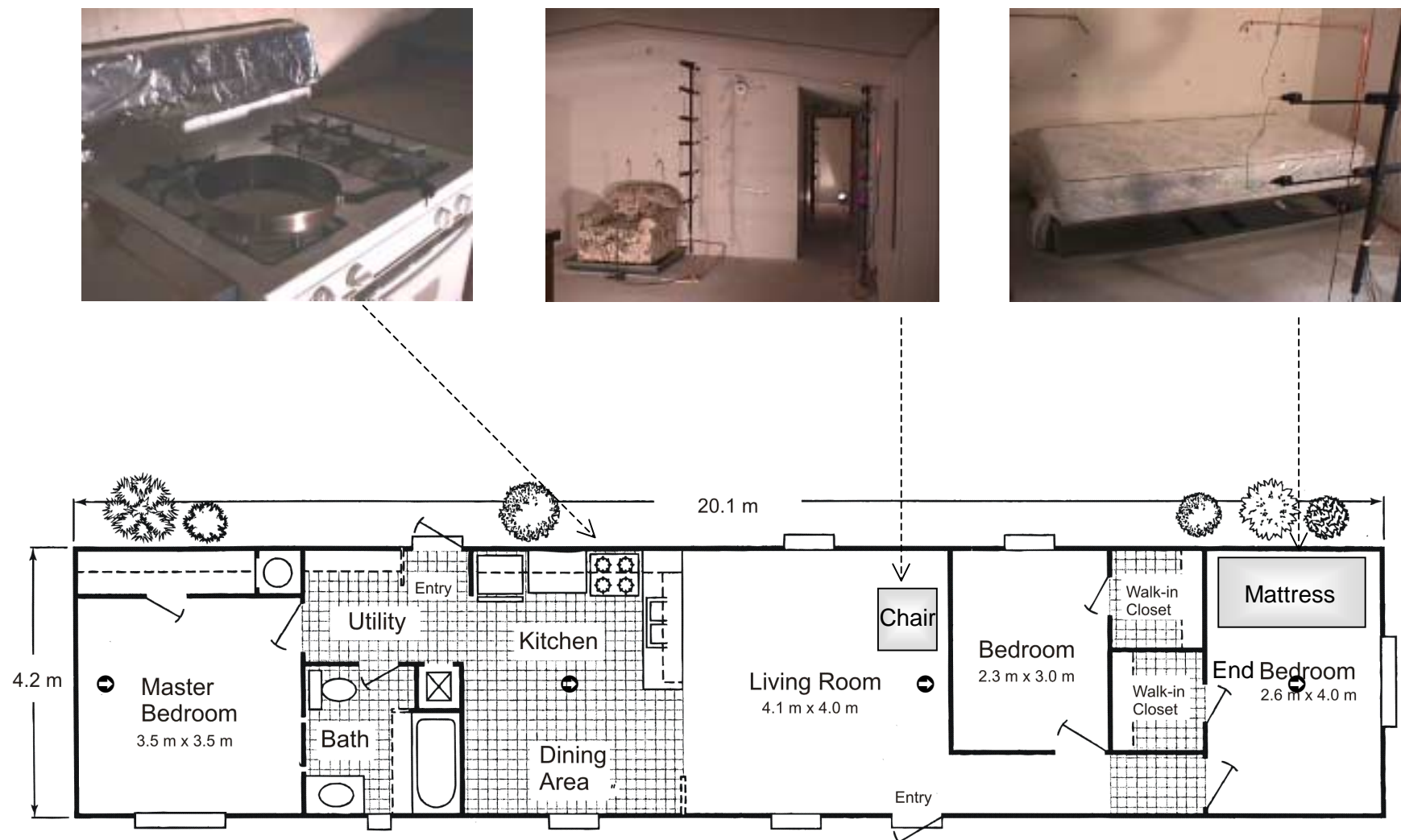


Figure 2. Plan view of a manufactured home (floor plan courtesy of NIST), fire locations (chair, mattress, kitchen stove) and FTIR gas sampling locations (◎)



Figure 3. Upholstered chairs before and after smoldering (1st row) and flaming (2nd row) fire tests



Figure 4. Twin-size mattresses before and after smoldering (1st row) and flaming (2nd row) fire tests

3.0 RESULTS AND DISCUSSION

A total of 50,000 frames of FTIR spectra (approximately 2 gigabytes) was collected during Tests 1-14 and analyzed in various ways to determine gas components in smoke. Final analysis results are presented as follows along with representative spectroscopic information.

3.1 Smouldering Chair (Tests 1 and 11)

In Tests 1 and 11, an upholstered chair was used as the fuel package to create a smouldering fire in the living area. The smouldering fire was controlled to develop very slowly. The ceiling temperature rise at the living area was 3°C or less during the smouldering period.

Figure 5 shows an FTIR spectrum after the first smoke alarm was actuated (57 min after energizing the ignitor) during Test 1, which is a 4-min average of the spectra from 56 to 60 min for the fire location. Figure 6 shows another average spectrum from the fire location and Figure 7 shows an average spectrum for the master bedroom for the following 4 minutes.

In Test 1, most of other detectors were actuated at least 87 min after energizing the ignitor. Figure 8 shows a 4-min average spectrum for the master bedroom (around 104 min) when the smoke obscuration, concentrations of CO₂ and CO and analog outputs of various detectors in the master bedroom were at peak values.

These spectra are representative of all spectra collected in Tests 1 and 11 during the smouldering chair fire, showing absorption from CO, CO₂ and water vapour as well as an absorption band around 3000 cm⁻¹. This absorption band around 3000 cm⁻¹ is characteristic of C-H stretching of volatile hydrocarbon compounds.

3.2 Flaming Chair (Tests 2 and 10)

In Tests 2 and 10, an upholstered chair was used as the fuel package to create a flaming fire in the living area. The first smoke alarm was actuated 24 s and 44 s after the ignition in Test 2 and Test 10, respectively; activation of many other detectors followed. Approximately 3 minutes after flaming, experimental conditions met the criteria for terminating the test (set by NIST) and water was discharged on the fire. The tests were ended with fire suppression and ventilation. Before the fire suppression, the ceiling temperature of the living area reached 125°C in Test 2 and 500°C in Test 10.

Figure 9 shows a 2-min average of the spectra from the fire location before the water discharge in Test 2. Figure 10 shows a 1-min average of the spectra from the master bedroom when the smoke obscuration and CO₂ concentration in the master bedroom were at peak values in the same test.

These spectra are representative of all spectra collected in Tests 2 and 10 during the flaming chair fire. The spectra show absorption only from CO, CO₂ and water vapour.

3.3 Smouldering Mattress (Tests 3, 4, 6 and 8)

In Tests 3, 4, 6 and 8, a twin-size mattress was used as the fuel package to create a smouldering fire in the end bedroom. During the smouldering period (90, 55, 99 and 61 min long, respectively), the change of temperatures in the house was very small in these tests; the maximum temperature rise was approximately 2°C in the room of fire origin.

Figures 11-13 are a few of representative spectra during mattress smouldering. Figure 11 shows an FTIR spectrum in Test 4, which is an average of the spectra from the fire location during the last 4 minutes (51 to 55 min from energizing the ignitor) of smouldering. Figure 12 is an average of the spectra from the fire room during a peak period of smoke obscuration when the first smoke alarm actuated (3443 s after energizing the ignitor) in Test 6. Figure 13 is a 1-min average of the spectra from the fire room when the first smoke alarm actuated (1950 s after energizing the ignitor) in Test 8. These spectra show absorption from water vapour, CO, CO₂ and an absorption band around 3000 cm⁻¹ due to C–H stretching of volatile hydrocarbon compounds.

The mattress smouldering changed to flaming 55, 99 and 61 minutes after energizing the ignitor in Tests 4, 6 and 8, respectively. Figure 14 shows an average of the spectra from the fire room during the 50-second-long flaming in Test 4. Figure 15 shows an average of the spectra from the fire room during the 60-second-long flaming in Test 6. Figure 16 shows an average of the spectra from the fire room during the 100-second-long flaming in Test 8. These spectra also show CO and CO₂ absorption as well as absorption from water vapour and C–H stretching of volatile hydrocarbon compounds.

Once the mattress started flaming, the ceiling temperature in the fire room rose quickly. The transition from smouldering to flaming was the criterion for terminating the tests (set by NIST). Water was discharged to suppress the fire (flaming only lasted for approximately 50-100 s in these mattress smouldering tests). Figure 17 shows a 1-min average of the spectra from the fire room during the fire suppression in Test 4. Figure 18 shows a 4-min average of the spectra from the master bedroom during and after the fire suppression in Test 4 when the smoke obscuration and analog output of various detectors were at peak values in the master bedroom.

The spectra shown in Figures 11-18 are representative of all spectra collected in Tests 3, 4, 6 and 8. Other than CO, CO₂, water and C–H stretching of volatile hydrocarbon compounds, there was no distinct absorption from any other chemical species in the FTIR spectra.

3.4 Flaming Mattress (Tests 5, 7, 9 and 14)

In Tests 5, 7, 9 and 14, a twin-size mattress was used as the fuel package to create a flaming fire in the end bedroom. Note that the fire-room door was closed in Tests 9 and 14.

In Tests 5 and 7, the first smoke alarm actuated 32 s and 43 s after the ignition, respectively. Activation of many other detectors followed. Approximately 3 minutes after ignition, experimental conditions met the criteria for terminating the tests (set by NIST) and water was discharged to the fire. The test was ended with fire suppression and ventilation. Before the fire suppression, the ceiling temperature of the fire room reached 180°C in Test 5

and 500°C in Test 7. Figure 19 shows a 2-min average of the spectra from the fire location during the flaming period in Test 5. Figure 20 shows a 3-min average of the spectra from the fire room during the flaming period in Test 7. The spectra show absorption pattern only from CO, CO₂ and water vapour.

Test 9 was similar to Tests 5 and 7. But, the fire room door was closed in Test 9. The first smoke alarm actuated 30 s after the ignition. Experimental conditions met the criteria for terminating the test approximately 3 minutes after ignition; water was discharged to extinguish the fire. Before the fire suppression, the ceiling temperature of the fire room reached 340°C. Figure 21 shows a 2-min average of the spectra from the fire room during mattress flaming. Figure 22 shows a 2-min average of the spectra from the fire room after fire extinguishment. The spectrum shows absorption only from CO₂, CO and water vapour.

Test 14 was similar to Test 9 with the fire-room door being closed. However, the mattress smouldered for 3400 s. The first smoke alarm in the fire room was actuated 2648 s after energizing the ignitor. Figure 23 shows a 30-s average of the spectra from the fire room during the last 30 seconds of mattress smouldering. The mattress fire became a flaming one approximately 3400 s after energizing the ignitor. Figure 24 shows a 30-s average of the spectra from the fire room during flaming. Approximately 1 minute after flaming, experimental conditions met the criteria for terminating the test and water was discharged to extinguish the fire (the ceiling temperature of the fire room reached 380°C before the fire suppression). Figure 25 shows a 1.5-min average of the spectra from the fire room after water spray. The fire room door was kept closed for another 9 minutes. Then, the doors of the fire room, front and back entrances were opened to allow smoke moving from the fire room to other parts of the house and outside. Figure 26 shows a 1-min average of the spectra from the fire room after all the doors were opened.

Figures 19-26 are representative of all spectra collected in Tests 5, 7, 9 and 14 during the flaming mattress fire. These spectra show absorption mainly from CO, CO₂ and water vapour. Prior to mattress flaming in Test 14, the spectra indicate weak absorption band around 3000 cm⁻¹ due to C-H stretching of volatile hydrocarbon compounds released during pyrolysis of the mattress. Since this test was conducted with an under-ventilated condition, the spectra did show absorption from HCN. The HCN concentration was at a maximum of 60 ppm, which was determined from the 1-min average spectra immediately after spraying water on the fire.

3.5 Cooking Oil Fire (Tests 12 and 13)

In Tests 12 and 13, corn oil (500 mL) in a cooking pan was heated on a gas burner until flaming. The propane stove was turned on 3 minutes after the start of the test. Smoke started to be produced (smouldering mode). The first smoke alarm actuated 9 to 10 minutes after heating the oil in these two tests. The cooking oil reached 382-387°C and auto-ignited 22-23 minutes after being heated in these two tests. In Test 12, the cooking oil flamed for 2.5 minutes and was manually extinguished. In Test 13, the cooking oil flamed for 5 minutes and then self-extinguished. Before the fire extinguishment, the ceiling temperature in the living area was 121°C in Test 12 and 118°C in Test 13; the ceiling temperature in the master bedroom was 59°C in Test 12 and 55°C in Test 13.

Figures 27-29 show 2-min average of the spectra from the kitchen area at different stages of Test 13. Figure 27 shows a 2-min average of the spectra from the kitchen area during the last 2 minutes of heating (before flaming). Figure 28 shows a 2-min average of the spectra

from the kitchen area during the last 2 minutes of flaming. Figure 29 shows a 2-min average of the spectra from the kitchen area after fire self-extinguishment. The spectra show absorption from CO, CO₂, water vapour and an absorption band around 3000 cm⁻¹ due to C–H stretching of volatile hydrocarbon compounds. These spectral features are representative of all spectra collected in Tests 12 and 13 with the cooking oil fire.

3.6 Primary Gas Products (CO and CO₂)

CO and CO₂ are primary gas products produced in the fire detection tests. The FTIR spectrometer was calibrated on site for CO₂ at concentrations of 1089 ppm, 5123 ppm and 2.01% and for CO at concentrations of 216 ppm and 1031 ppm. The transport time of the gas sample in the sampling lines was 10 ± 2 s, which was determined by aspirating the 2.01% CO₂ calibration gas through the sampling lines.

Figures 30-37 show typical CO and CO₂ concentrations from the FTIR analysis. Results from the FTIR measurement are consistent with those measured by NIST using the nondispersive infrared (NDIR) gas analyzers. For smouldering fires, most of the concentration rise happened after transition to flaming, similar to other parameters measured by NIST.

3.7 Secondary Gas Products

The main objectives of the FTIR measurement were to identify secondary gas products from the test fires. In addition to CO and CO₂, the FTIR measurement showed absorption around 3000 cm⁻¹, characteristic of C–H stretching of volatile hydrocarbon compounds from the chair and mattress smouldering as well as cooking oil fires. There was no apparent absorption from chemical species such as HCl, NO_x, HBr and HF in the FTIR spectra. In other words, these chemical species were below the minimum detection limit (MDL) of the FTIR spectrometer in this full-scale experimental set-up. HCN was only detected in Test 14 with an under-ventilated condition and its maximum concentration was 60 ppm.

The MDL depended not only on the quality of FTIR spectrometer's infrared source/detector and optical stability but also on operation parameters such as gas cell, number of scans and spectral resolution, as well as gas sampling systems used in the experiments. The MDL under this full-scale experimental set-up and operation conditions was estimated to be 30 ppm for HCN and HF, 50 ppm for HCl and NO₂, and 100 ppm for NO and HBr, based on previous calibration and data from similar gas sampling tests at NRC as well as library data from the FTIR spectrometer manufacturer.

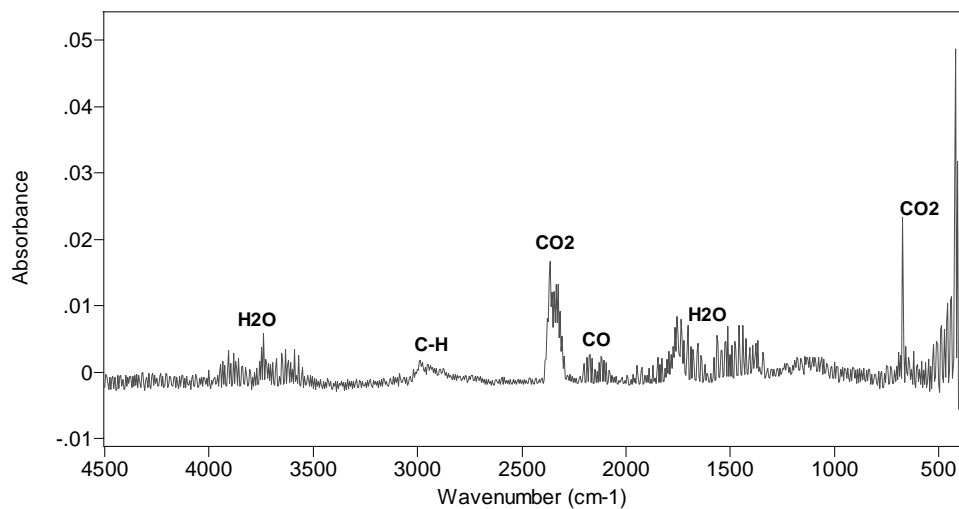


Figure 5. 4-min average of FTIR spectra for fire location after first smoke alarm (Test 1)

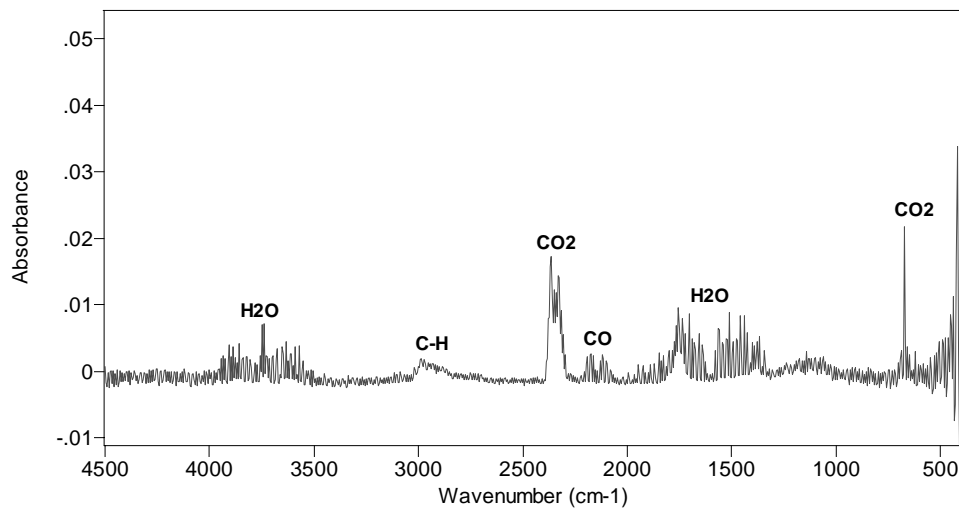


Figure 6. 4-min average of FTIR spectra (at 60 min) for fire location (Test 1)

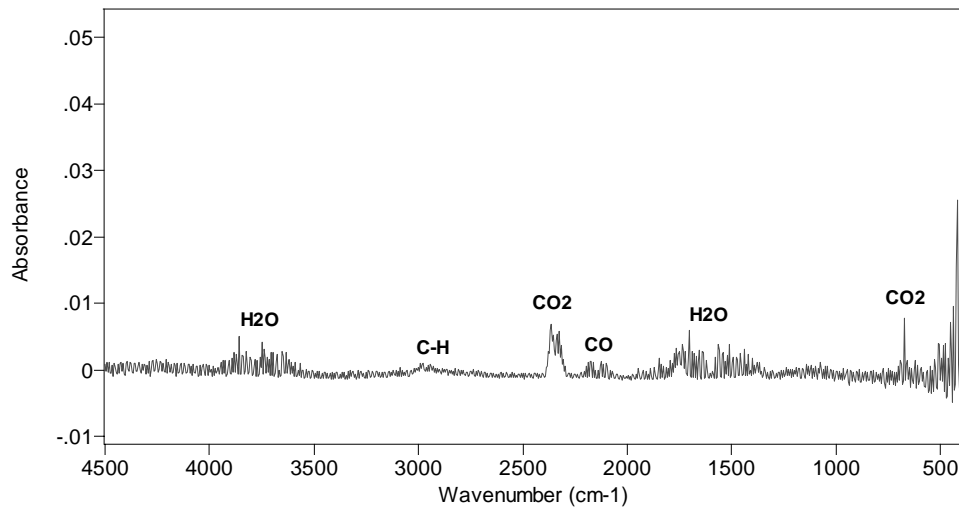


Figure 7. 4-min average of FTIR spectra (at 60 min) for master bedroom (Test 1)

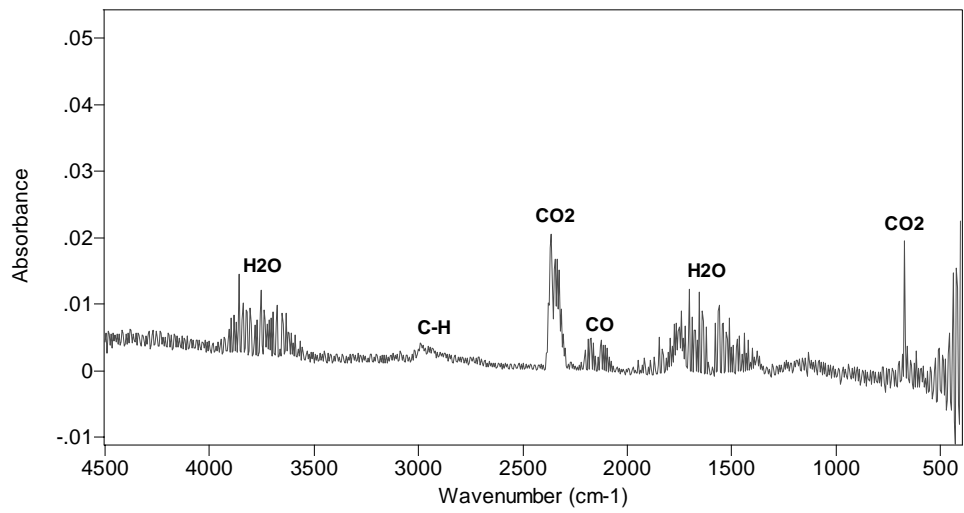


Figure 8. 4-min average of FTIR spectra (at 104 min) for master bedroom (Test 1)

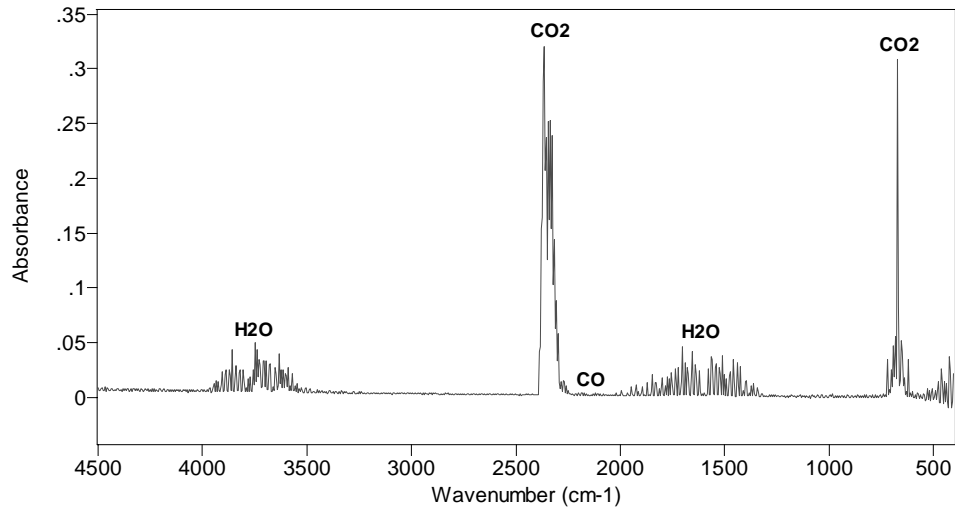


Figure 9. 2-min average of spectra from fire location before water discharge in Test 2

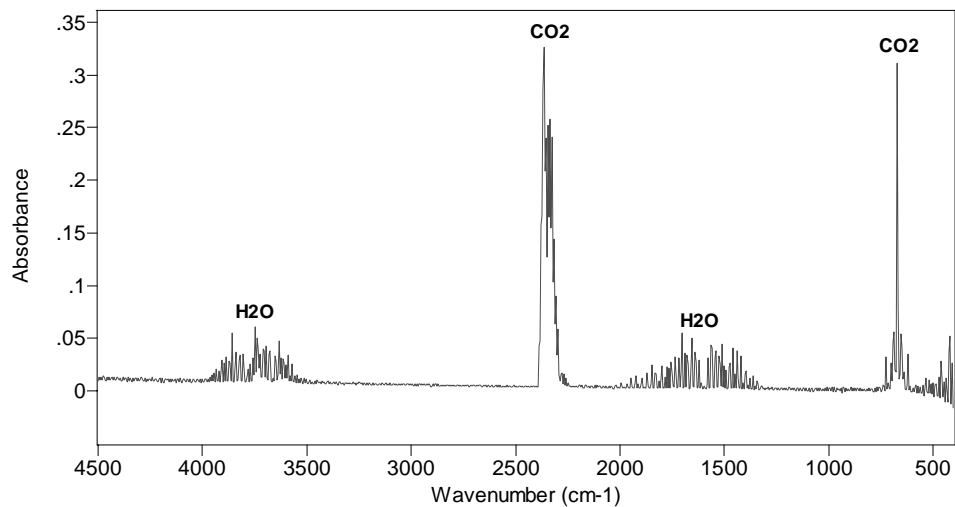


Figure 10. 1-min average of spectra at peak smoke obscuration in master bedroom (Test 2)

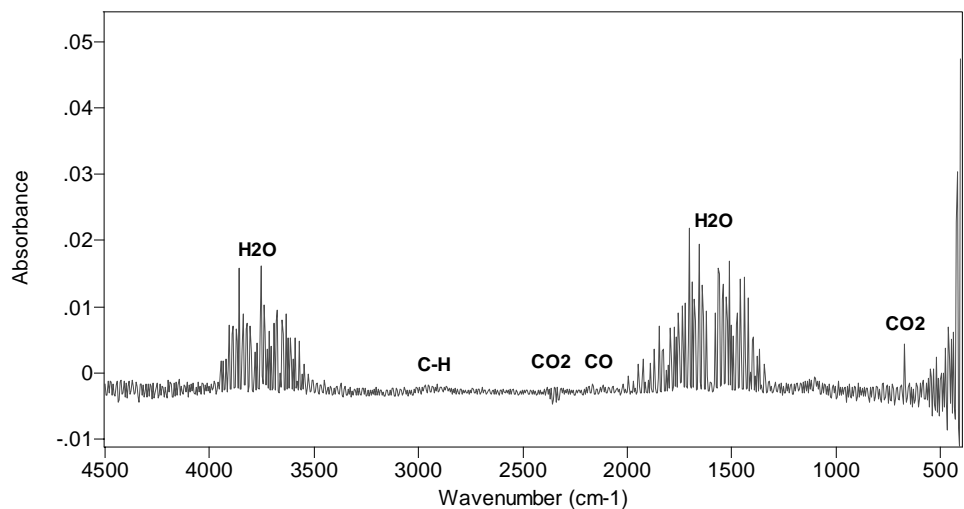


Figure 11. Average of spectra for fire location in last 4 minutes of mattress smouldering (Test 4)

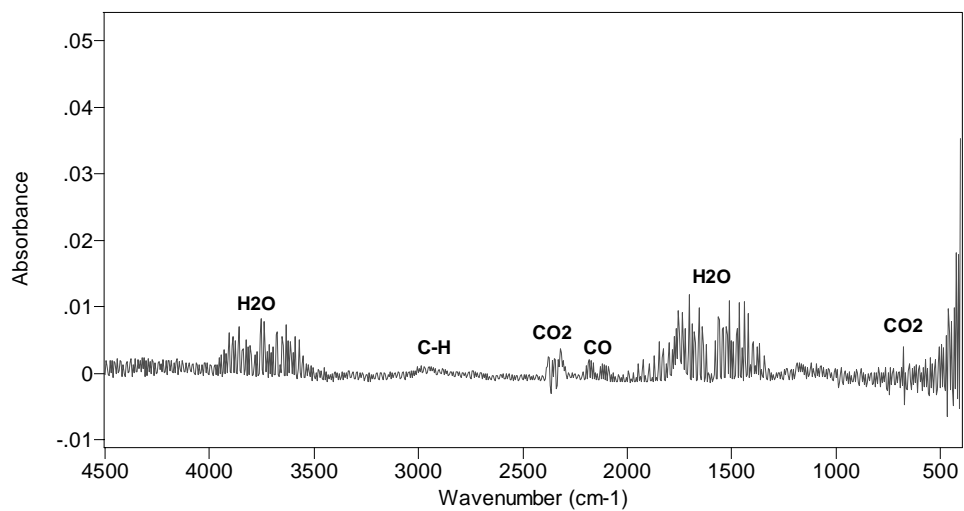


Figure 12. Average spectrum for fire room during peak smoke obscuration in Test 6 with mattress smouldering

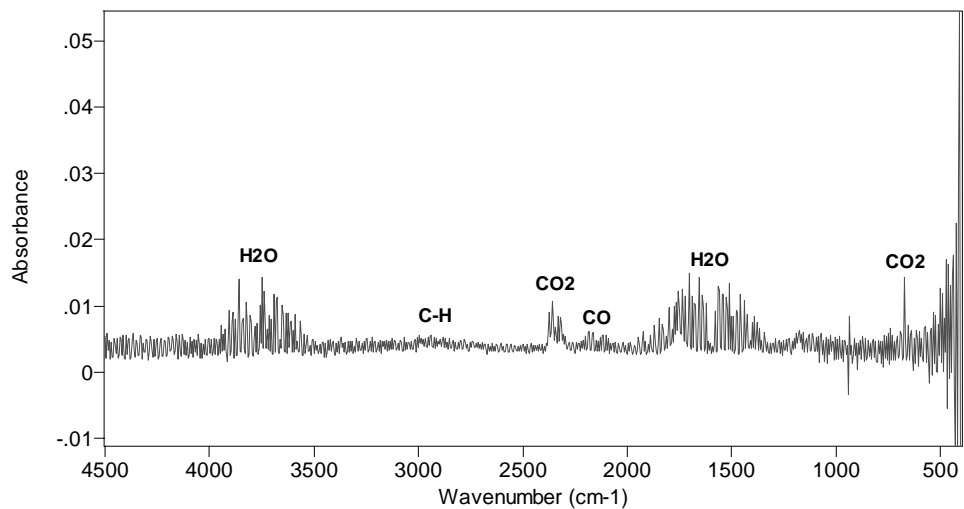


Figure 13. 1-min average of spectra for fire room after first smoke alarm in Test 8 with mattress smouldering

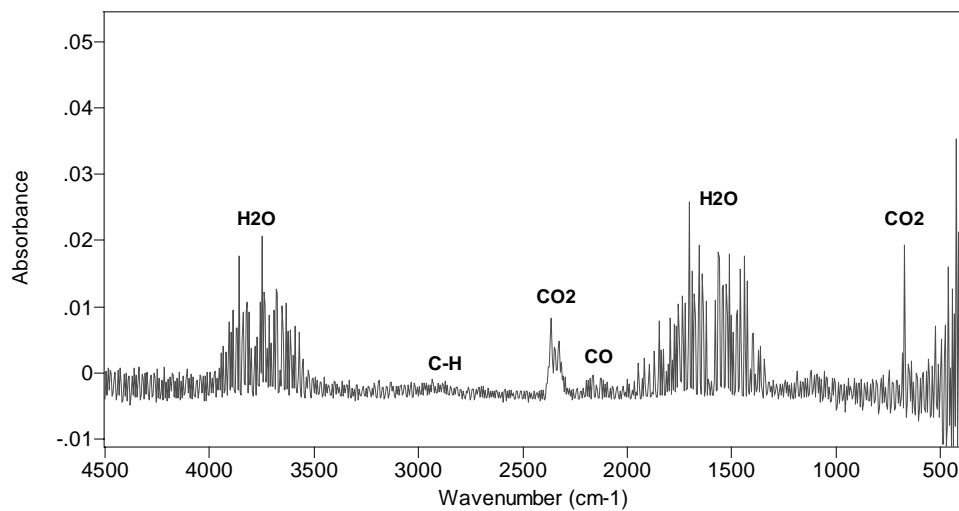


Figure 14. Average of spectra for fire room during the 50-s flaming in Test 4

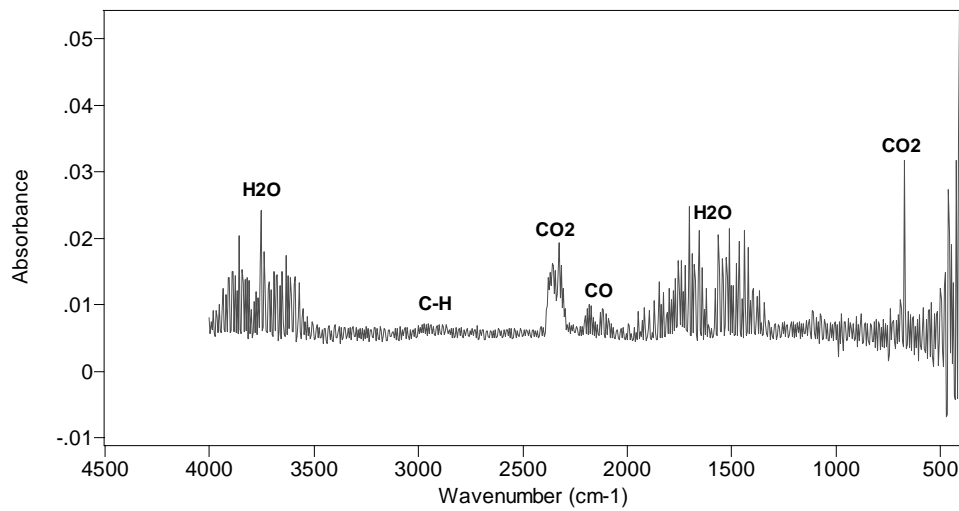


Figure 15. Average of spectra for fire room during the 60-s flaming in Test 6

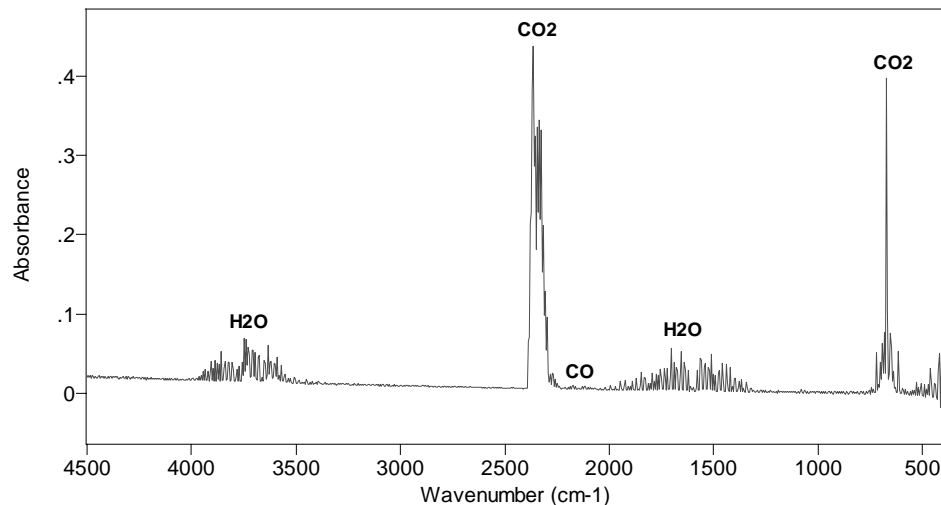


Figure 16. Average of spectra for fire room during the 100-s flaming in Test 8

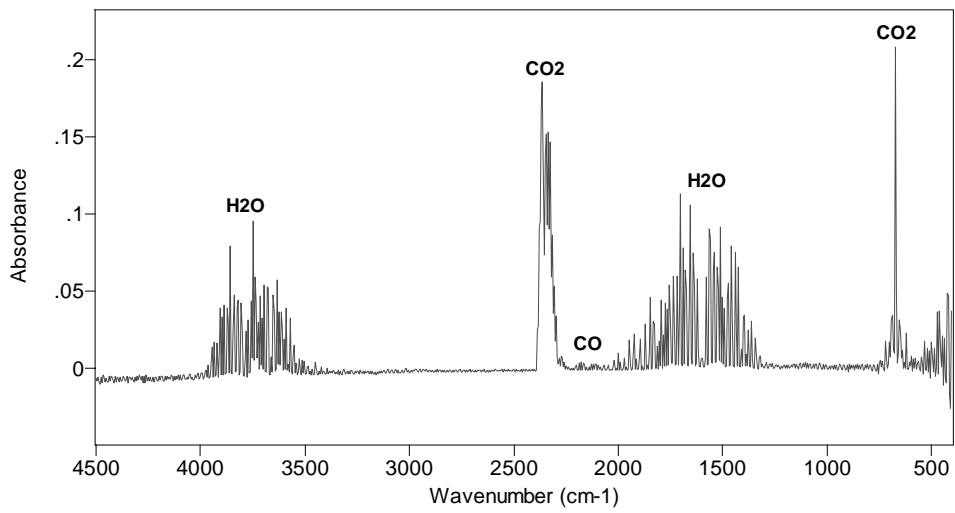


Figure 17. 1-min average of spectra for fire room during suppression in Test 4

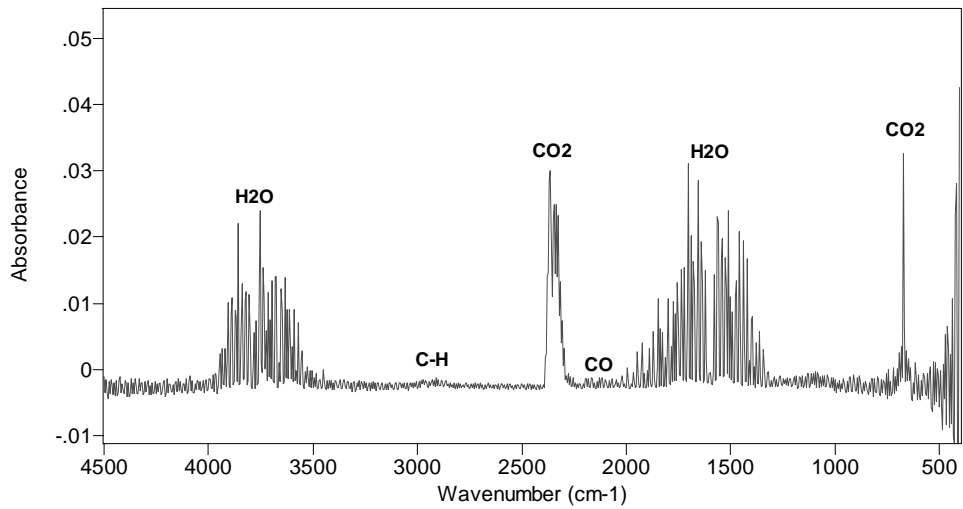


Figure 18. 4-min average of spectra for master bedroom during/after suppression (Test 4)

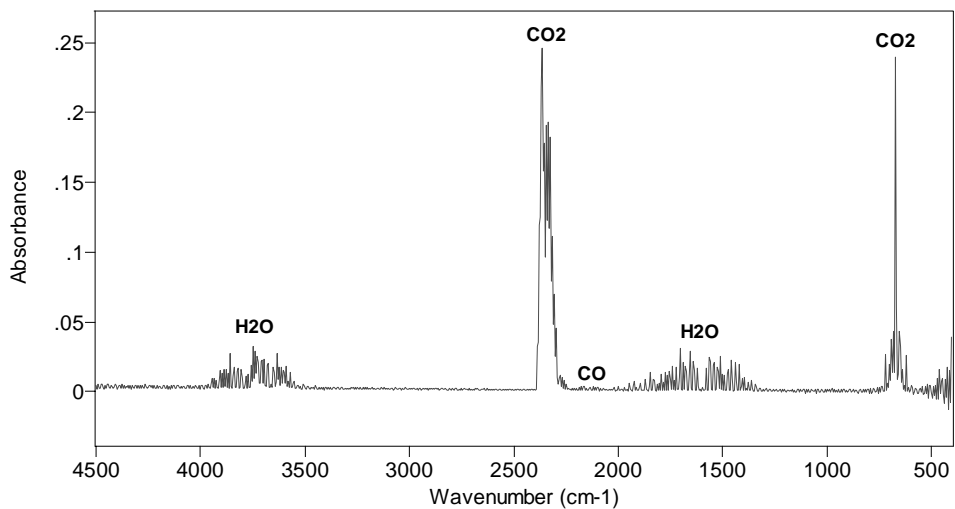


Figure 19. 2-min average of spectra for fire room during mattress flaming (Test 5)

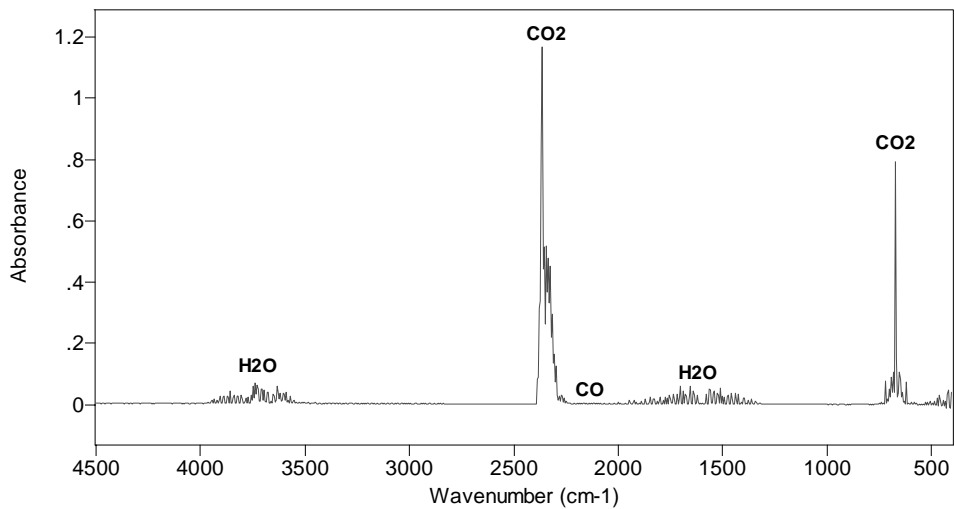


Figure 20. 3-min average of spectra for fire room during mattress flaming (Test 7)

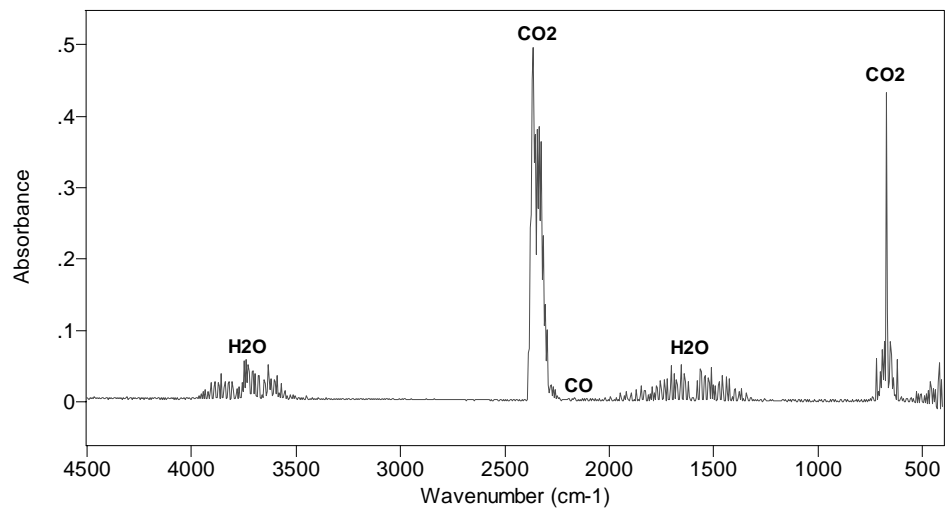


Figure 21. 2-min average of spectra for fire room during mattress flaming (Test 9)

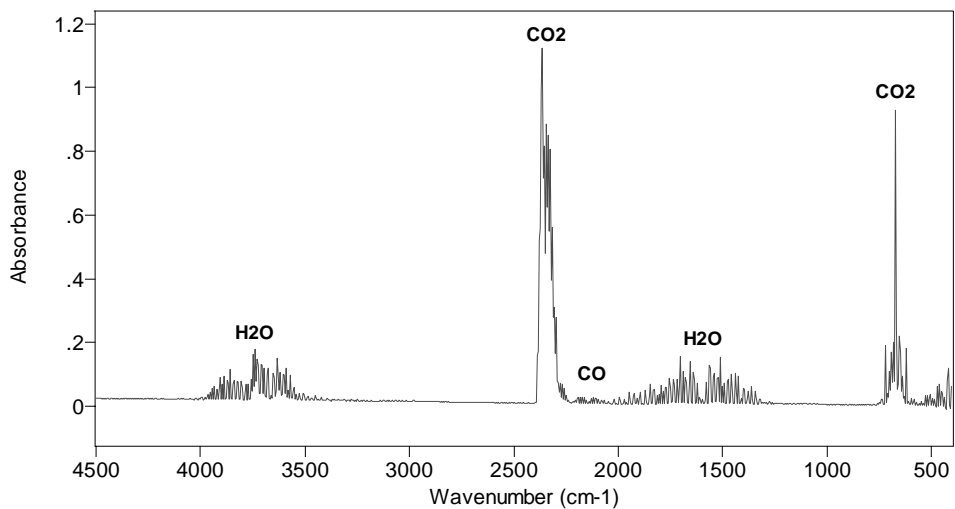


Figure 22. 2-min average of spectra for fire room after fire extinguishment (Test 9)

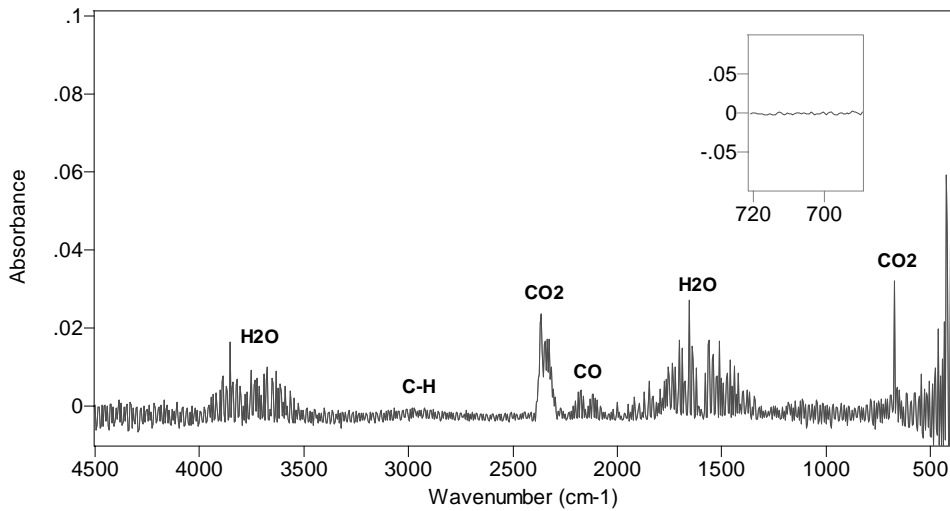


Figure 23. Average of spectra for fire room during the last 30 s of mattress smouldering (Test 14)

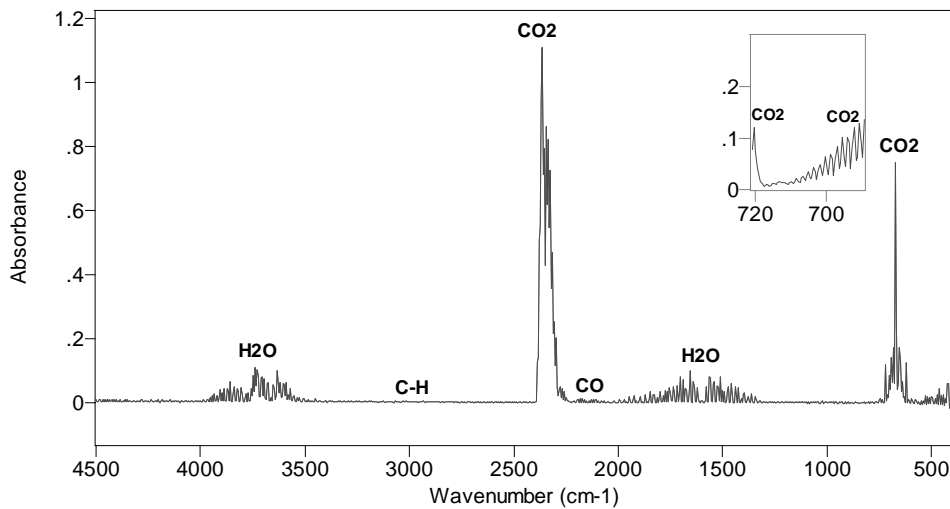


Figure 24. 30-s average of spectra for fire room after mattress flaming (Test 14)

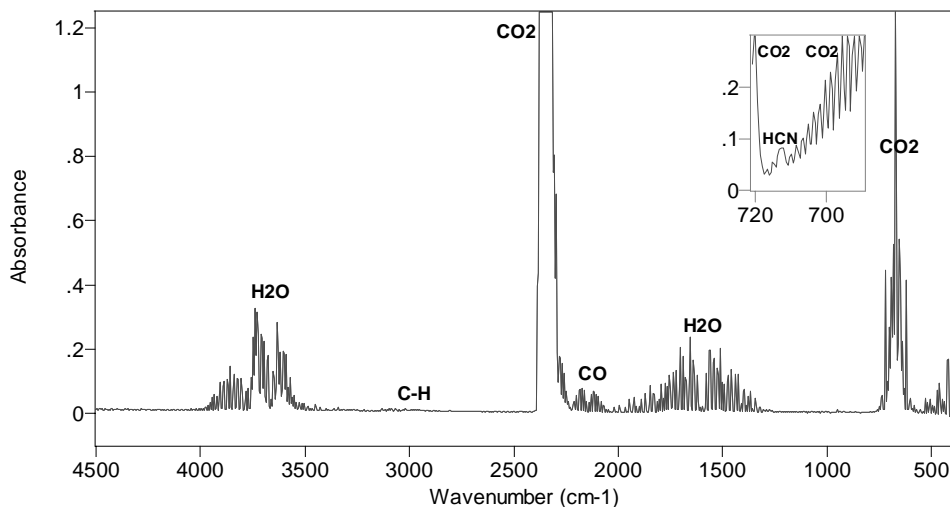


Figure 25. 90-s average of spectra for fire room after water spray (Test 14)

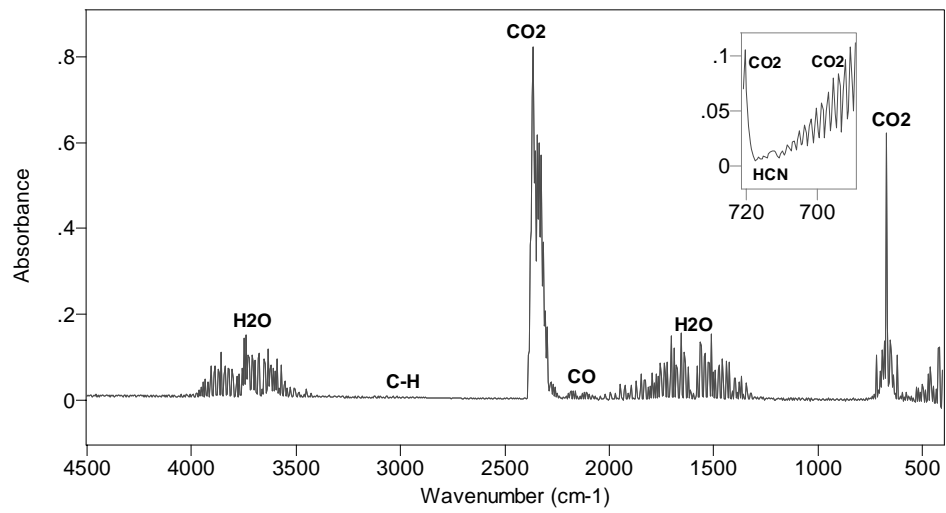


Figure 26. 60-s average of spectra for fire room after all doors opened (Test 14)

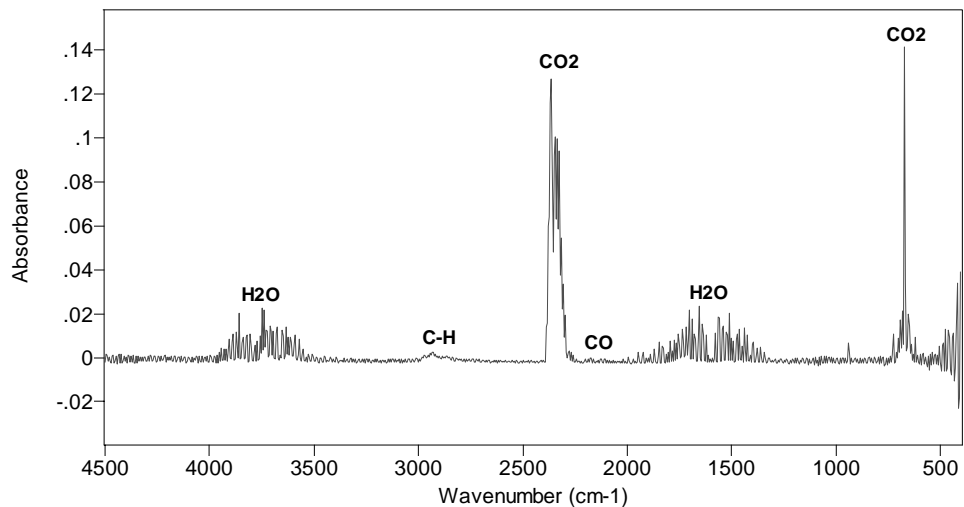


Figure 27. Average of spectra for last 2 minutes of cooking-oil heating (Test 13)

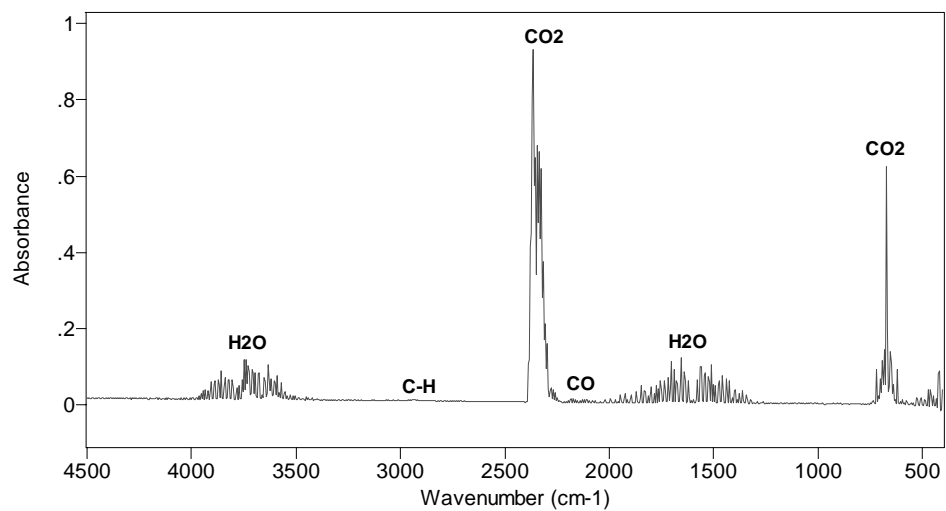
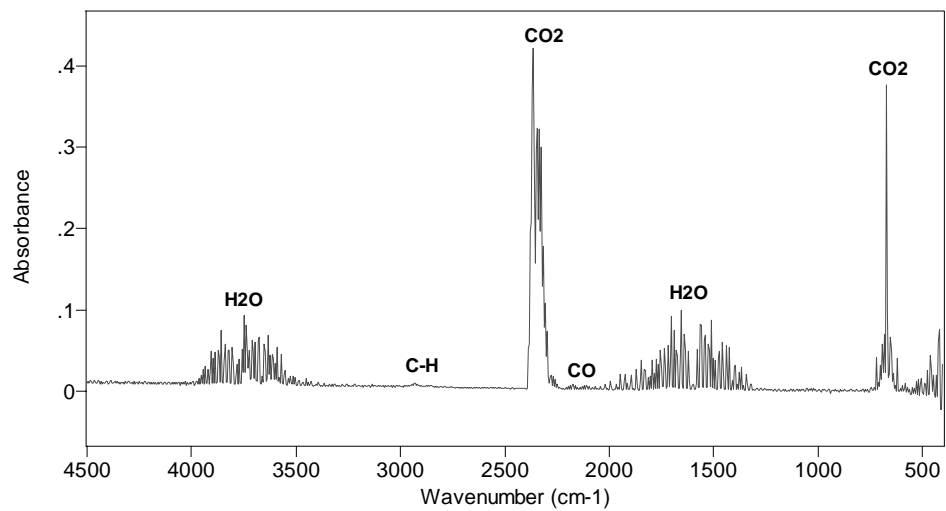


Figure 28. Average of spectra for last 2 minutes of cooking-oil flaming (Test 13)



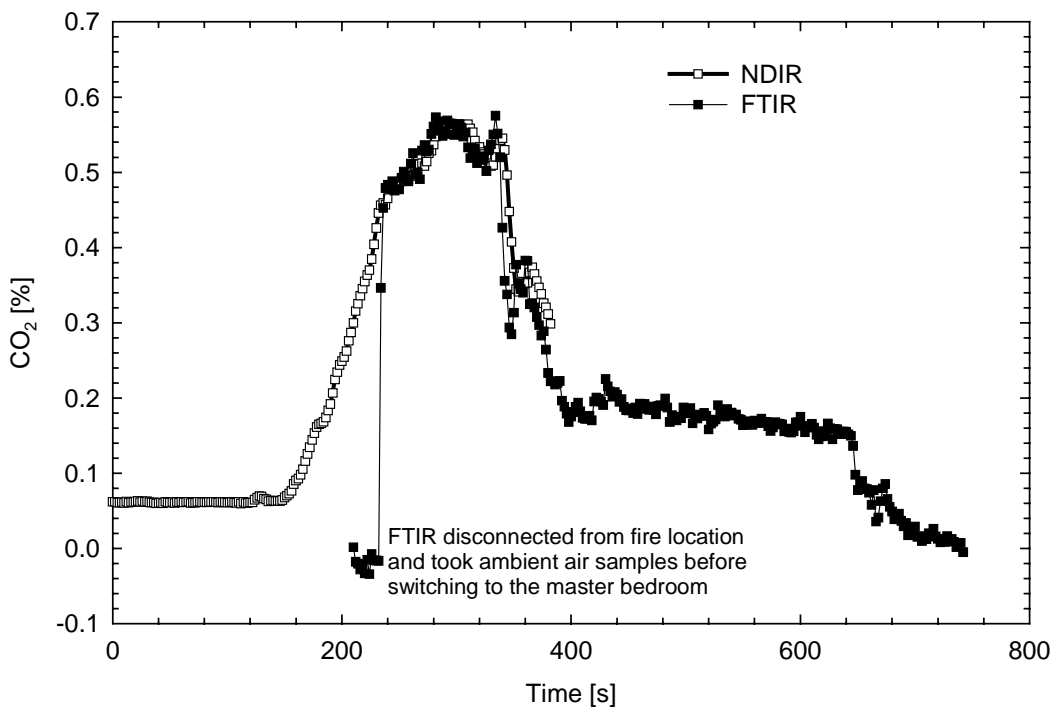


Figure 30. Carbon dioxide concentration in master bedroom from FTIR and NDIR measurements for flaming chair (Test 2)

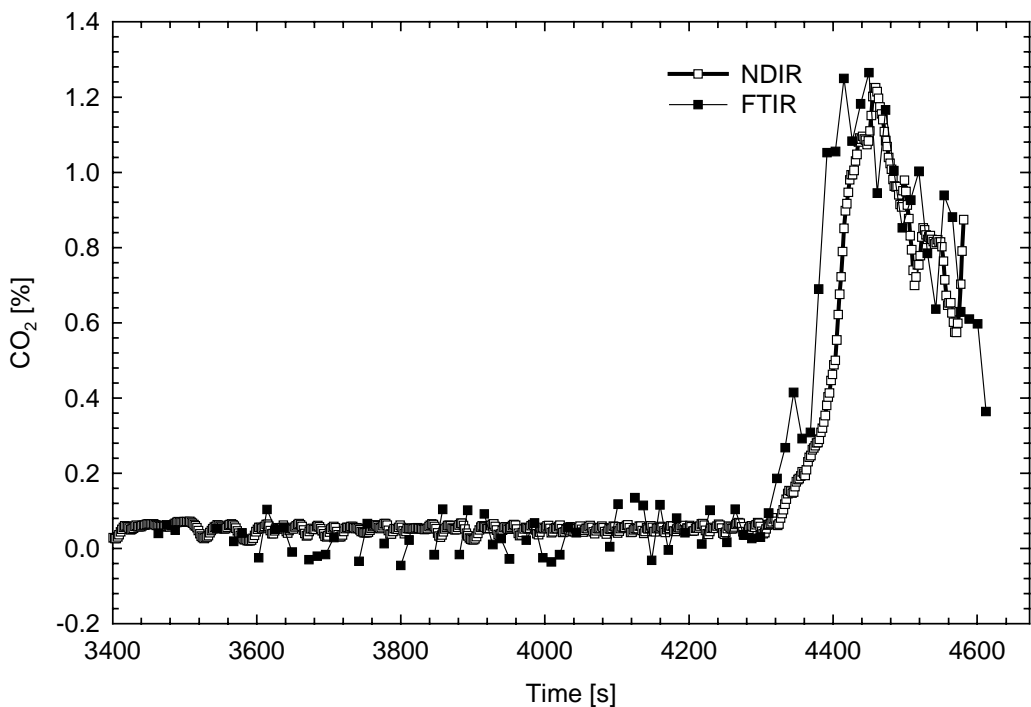


Figure 31. Carbon dioxide concentration in master bedroom from FTIR and NDIR measurements for smouldering chair (Test 11)

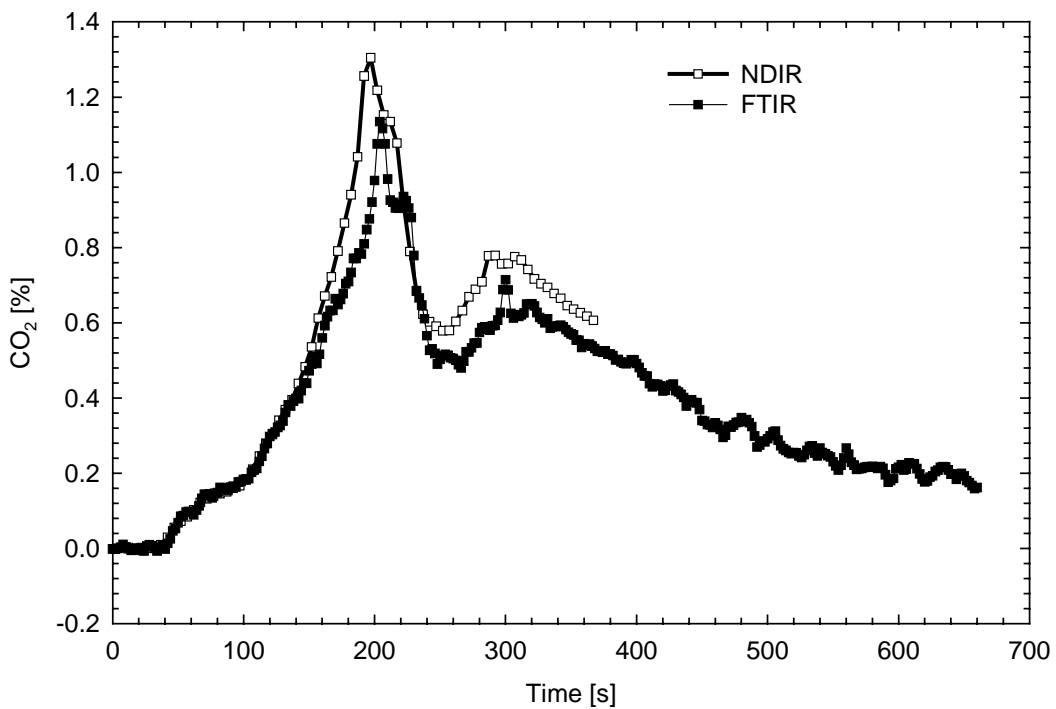


Figure 32. Carbon dioxide concentration in fire room from FTIR and NDIR measurements for flaming mattress (Test 5)

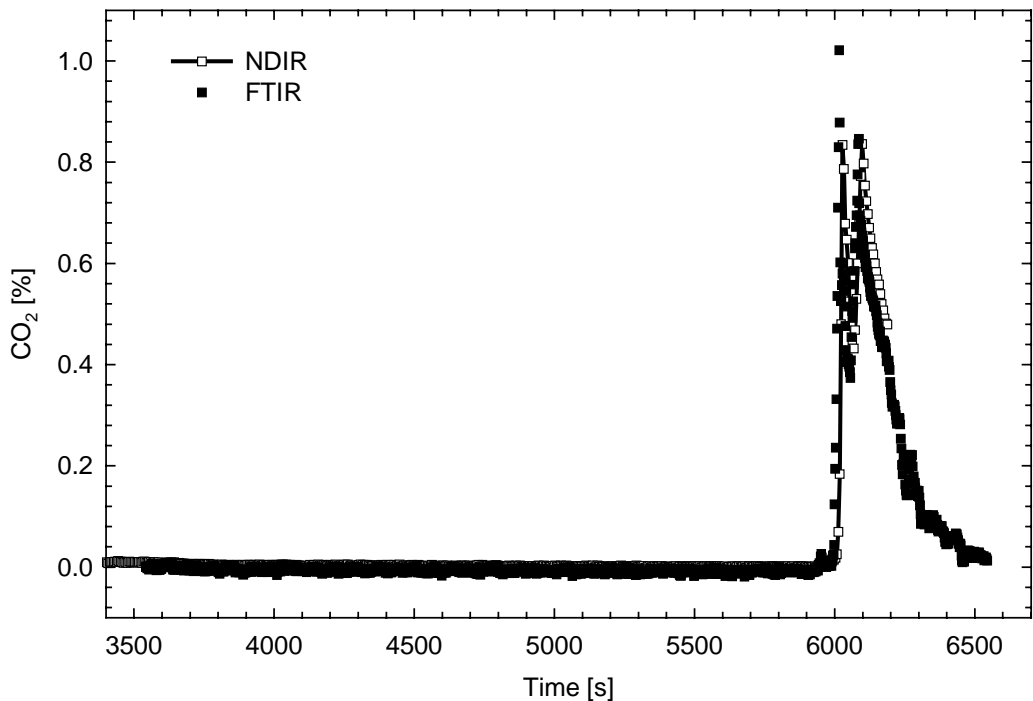


Figure 33. Carbon dioxide concentration in fire room from FTIR and NDIR measurements for smouldering mattress (Test 6)

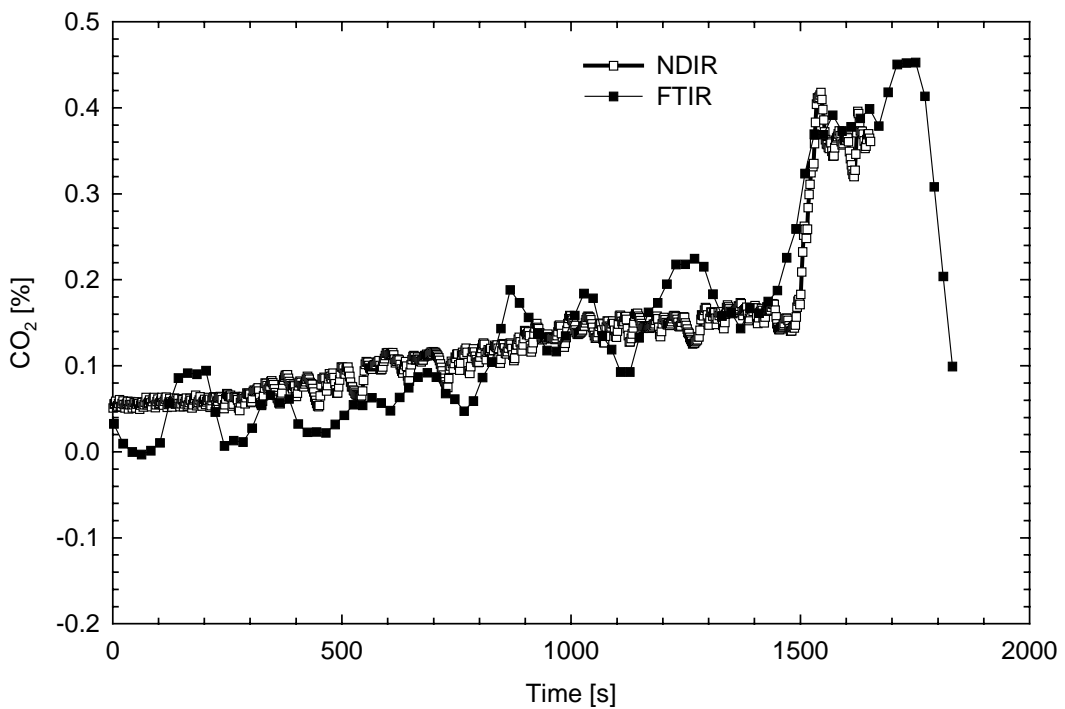


Figure 34. Carbon dioxide concentration in master bedroom from FTIR and NDIR measurements for cooking oil fire (Test 12)

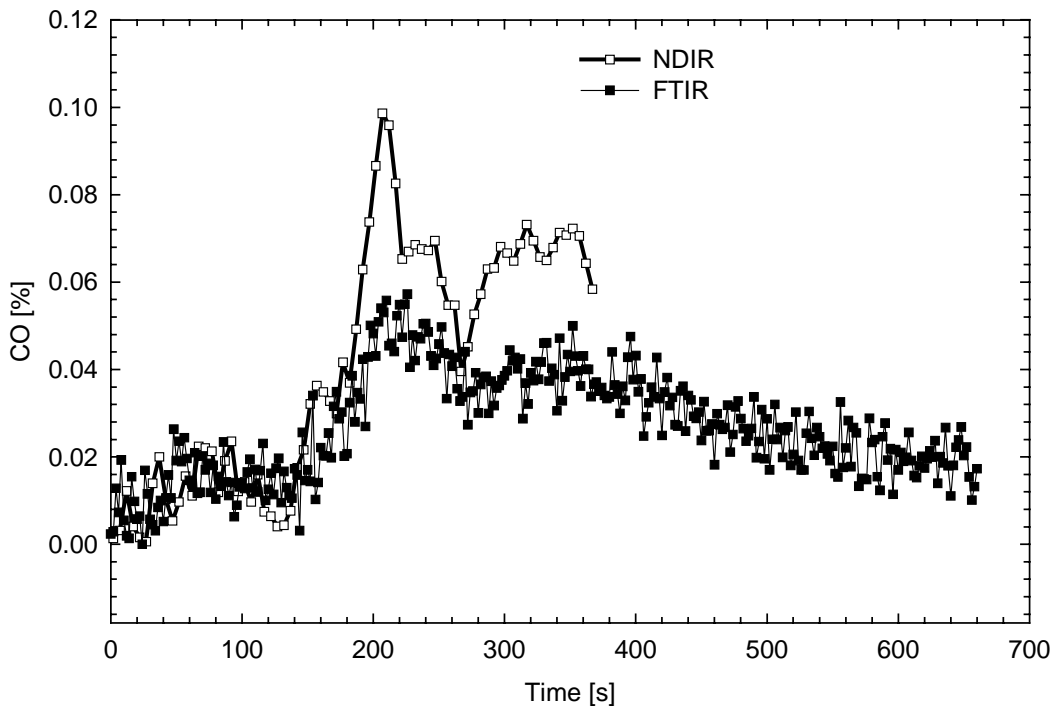


Figure 35. Carbon monoxide concentration in fire room from FTIR and NDIR measurements for flaming mattress (Test 5)

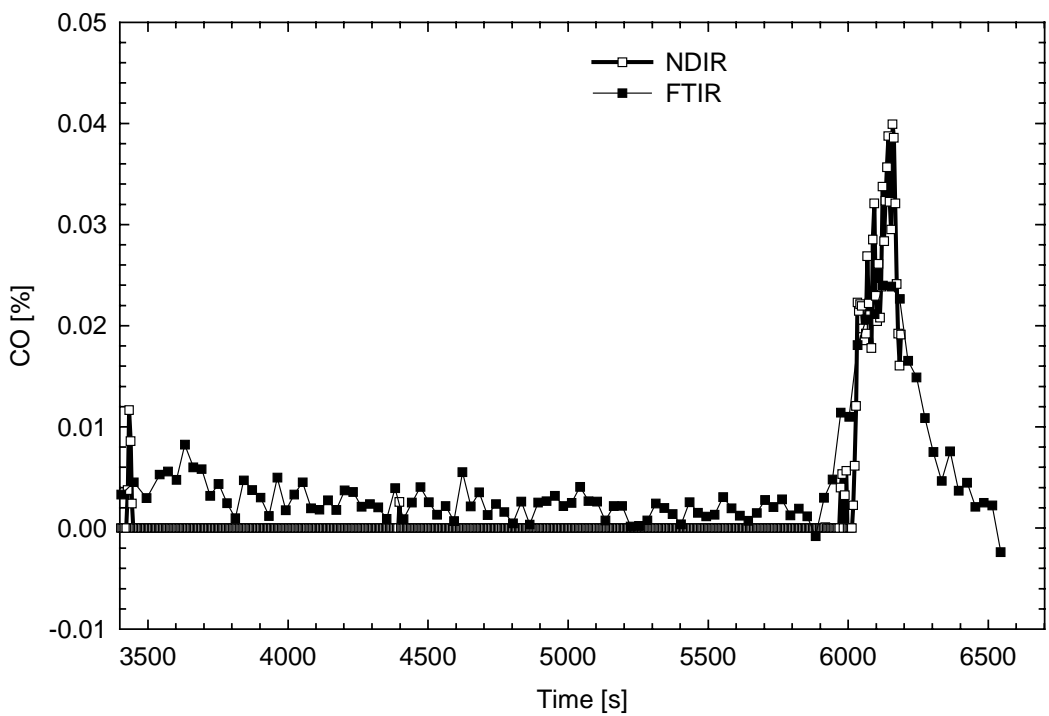


Figure 36. Carbon monoxide concentration in fire room from FTIR and NDIR measurements for smouldering mattress (Test 6)

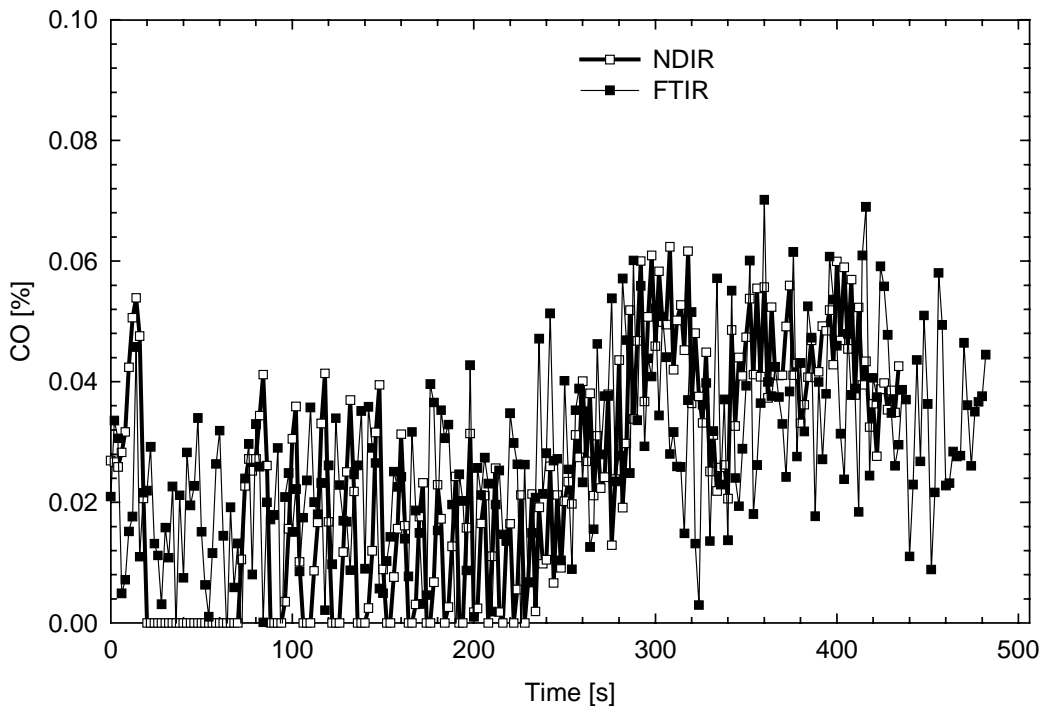


Figure 37. Carbon monoxide concentration in master bedroom from FTIR and NDIR measurements for flaming chair (Test 10)

4.0 CONCLUSIONS

The small, slow smouldering fires and short flaming fires provided the greatest challenge for the smoke detectors to detect the fires early before becoming fully developed ones. However, the experiments were terminated well before reaching conditions that would produce a significant amount of chemical species, such as HCl, HCN, NO_x, HBr and HF, above the minimum detection limit of the FTIR spectrometer in this full-scale experimental set-up. Carbon monoxide and carbon dioxide were primary gas products produced in Tests 1-14. There was no apparent absorption from chemical species such as HCl, NO_x, HBr and HF in the FTIR spectra. FTIR spectra collected during the chair and mattress smouldering and cooking oil fires show absorption in region characteristic of volatile hydrocarbon compounds. The FTIR measurement only detected absorption from HCN (60 ppm at maximum) during Test 14 with an under-ventilated condition.

5.0 ACKNOWLEDGEMENTS

NRC acknowledges financial contributions from the Canadian Fire Alarm Association and Health Canada. NRC also acknowledges supports from NIST, in particular, Mr. Richard W. Bukowski, Mr. Nelson P. Bryner, Dr. Marc R. Nyden and the testing crew for logistic and experimental support.

6.0 REFERENCES

1. Bukowski, R. W., Waterman, T. E., and Christian, W. J., "Detector Sensitivity and Siting Requirements for Dwellings: A Report of the NBS 'Indiana Dunes Tests.'" NFPA No. SPP-43. Nat. Fire Prot. Assn., Quincy, MA, 1975.
2. Peacock, R.D., Averill, J.D., Bukowski, R.W., and Reneke, P.A., "Home Smoke Alarm Project, Manufactured Home Tests," NIST Report of Test FR 4016, Fire Research Division, Building and Fire Research Laboratory, National Institute of Standards and Technology, Gaithersburg, MD, June, 2002.
3. Averill, J.D., Peacock, R.D., Bukowski, R.W., and Reneke, P.A., "Home Smoke Alarm Project, Two-Story Home Tests," NIST Report of Test FR 4017, Fire Research Division, Building and Fire Research Laboratory, National Institute of Standards and Technology, Gaithersburg, MD, June, 2002.